CHAPTER - I
INTRODUCTION

1.0 General

Along the Indo-Gangetic planes, the Indian subcontinent has vast deposits of silty sands on the banks of perennial Himalayan rivers namely Indus, Ghaggar, Barinadi, Yammuna & Ganga, where the river sands are obtained with varied proportions of non plastic silts. The authors have diverse experiences with the soil exploration of these deposits for structural foundations. As per soil classification systems, the sand and silt are coarse and fine grained granular materials. These are obtained in abundance as geological deposits in the earth crust. They occur with varied surface textures and shapes ranging from angular to spherical with moisture in void space. In modern times, some of the granular industrial byproducts deposited as structural fill with common range of specific gravity, unit weight and grain characteristics are often classified for sizes as sand and silts [Trivedi and Sud; (2002)]. Over the past fifty years there were intensive attempts to characterize sandy soils without fines [Brinch Hasen (1970); deBeer (1965); Feda (1961); Meyerholf (1965); Vesic (1973)]. However, there were scanty efforts to map the engineering behavior of silty sands. The authors observed that silty sands are largely found in earth's crest in a low to medium density states with varied moisture. This material supports structural rafts and deep foundations for multistoried buildings, underground excavations, tunnels and pipelines. There is a need to characterize this granular media as an engineering material.

There is a better understanding of the anticipated behavior of clean sand under undrained monotonic loading in terms of its initial state of stress, void ratio and state parameters. There is a mixed opinion in the literature on the role of fines on stress strain behavior of silty sand [Pitman et al. (1994); Vaid (1994); Zlatovis and Ishihara (1995)]. The natural sands contain varying amount of fines, whereas the current knowledge of its engineering behavior is primarily based on clean sands [Thevanayagam et al. (1996 a, b)]. It is difficult to ascertain the behavior of silty sand as contractile. The stress strain behavior of silty sand needs further explanation. The factor that controls the behavior of confined silty sands is a matter to be investigated. Further, the presence of fines in sand has an influence on the bearing capacity. The problem of bearing capacity of shallow foundations on granular soil has been studied for many years [deBeer (1965); Feda (1961); Brinch Hasen (1970); Meyerholf (1965); Oner (1972); Vesic (1973); Zadroga (1994)]. However, an accurate solution capable of predicting

the peak load carrying capacity for a wide range of soil relative densities, effective stress conditions, and foundation shapes within a practical context remains elusive owing to the presence of fines.

The structural measures for foundations are widely used in weak soil conditions to support the column loads. Sometimes the excavation needs to be braced during foundation construction. One of the available solutions is to use side supports to the excavation during construction. Due to the problems associated with the removal these supports, they are provided as a part of the permanent structure. Accordingly it consists of two parts; it is to deal with the structural analysis of the footing if the side supports are used as an end supports for the foundation [Sawwaf and Nazer (2005)]. Secondly, the effect of these supports on the lateral movement of the soil underneath the foundation is to be investigated as the effect of lateral confinement on the bearing capacity of the silty sands. While there are several solutions for the first problem, such as isolating the foundation from the side supports, but the effect of lateral confinement by these side supports on the foundation behavior is not well understood.

The decreasing availability of good construction sites has led to increased use of sites with marginal soil properties. In view of this, the requirement for in situ treatment of foundation soil to improve its bearing capacity and reduce the settlement has raised markedly. The soil confinement is one such method of improving the bearing capacity and reducing the settlement of the footings on silty sands. The more recent advancement in this field is to provide the confinement to the soil by using metal cells. This novel technique of soil confinement has not received much attention in foundation applications. In the Metropolitan cities all around the world, structures are constructed in a close proximity due to the non-availability of the land. The presence of structures around the footing under consideration simulates a condition similar to the existence of a skirt as considered in the present problem. The findings of our research are essentially to provide the lateral confinement by physical means and to extend its application to the buildings/ structures erected close to each other in the vicinity. If there are similar structures erected besides the central footing the effect implies confinement and the improvement in the bearing capacity. The settlement can be interpreted using a similar model as used by the author. The lateral confinement of soil is not really a direct means of soil improvement.

By using a ring beam or a skirt as soil improvement technique has been investigated by many researchers. They used the ring beam under circular foundation [Mahiyar and Patel (2000),

Martin (2001)]. They have noticed a significant improvement in the footing response due to the ring beam resistance to lateral displacement of soil underneath the footing. Boushehrian and Hataf (2003), Laman and Yildiz (2003) experimentally investigated the ultimate bearing capacity of ring foundations supported by a sand bed with and without geogrid reinforcement. The results proved that the ultimate bearing capacity values can be improved up to three times that of the unreinforced case. Ranjan and Rao (1985) improved the soil by using granular piles surrounded with skirts. They found out that the granular skirted pile foundations have a lot of potentiality for structures which are sensitive to settlement and are subjected to heavy loads. Ortiz (2001) inserted a discontinuous vertical skirt dowels around existing foundation. A marked increase 20 % in the bearing capacity and a reduction of settlement were observed.

It is a structural effect of the lateral confinement which really reduces the settlement of foundations on granular soils. The lateral confinement is applied as cylindrical rings (just as a laboratory/experimental tools) below the footing. It results in to added stiffness of the soil which was referred as soil improvement. When the footing is loaded, such a cell resists the lateral displacements of soil underneath the footing and confines the soil leading to a significant decrease in the vertical settlement. It results into added stiffness of the soil.

In order to investigate the effect of confinement on bearing capacity and settlement of circular footings, the cylindrical cells of different diameters and heights were instrumented in the laboratory using 0.94mm thick mild steel plate. The cells were open at both the ends. It was modeled as a circular footing supported on a silty soil, which is surrounded by a mild steel cell having the same soil outside. The tests were performed without cells (un–confined case) below the footing and also with the cells (confined case).

1.1 Scope of the Present Work

A survey of the available literature indicates that relatively less experimental and analytical data is available regarding the effect of confinement on the bearing capacity and settlement characteristics of circular footings of different sizes for silty sands. The problem of bearing capacity of shallow foundations on granular soil has been studied for many years; however, an accurate solution capable of predicting peak load carrying capacity for a wide range of soil relative densities, effective stress conditions and foundation shapes within a practical context remained elusive owing to the presence of fines.

In view of the above observations, investigations have been carried out on model footings to study the effect of fines and confinement on various parameters like bearing capacity,

settlement and failure pattern of confined silty sands. Initially tests were conducted on clean sand and then on sand with varying proportions of fines in order to know the effect of fines on bearing capacity and settlement characteristics of clean sand.

Tests were also performed for confined and unconfined cases in order to know the effect of confinement on bearing capacity and settlement characteristics of silty sands.

Model footings of different sizes used were circular in cross-section, made rough at the base by pasting the sand paper of uniform grade. The footings have been tested in a mild steel tank having reaction frame for load application. The tank has been filled with poorly graded dry Ghaggar clean sand which is maintained at a uniform density by raining it from a height through a pouring device. Load on the footings have been applied in increments by hydraulic jacks calibrated through proving rings. Settlement of footings have been recorded at every load increment by sensitive dial gauges. Pressure-settlement curves have been plotted. Based on the results, the optimum ratios of d/D and h/D are recommended which give higher values of improvement factor and smaller values of settlement reduction factor.

1.2 Organization of the Thesis

This thesis consists of six chapters. Chapter-I deals with the introduction. Chapter-II contains the literature review. All the available literature on the topic has been critically reviewed. Literature review is divided into two sections. Section one deals with the review of the effect of fines on the behavior of clean sand. Section two incorporates the review on effect of confinement on bearing capacity and settlement characteristics of different soils.

Chapter III deals with the development of model testing programme. It includes details of the preliminary tests conducted to determine physical and engineering properties of the soil used in investigation. Development of testing programme includes fabrication of test tank, model footings, loading device & pouring device and deciding about height of fall of sand in order to maintain a uniform density. Details of the procedure adopted to carry out the model studies have been given.

Interpretation of the model test data has been presented in Chapter IV. It includes development of non-dimensional factors for bearing capacity and settlement of confined and unconfined cases of silty sands. Conclusions and suggestions for further research have been given in Chapter V and Chapter VI respectively.

List of publication from the current work has been given after chapter VI.

List of references has been given at the end of the thesis.

CHAPTER-II
LITERATURE REVIEW

2.0 General

The natural sand contains varying amount of fines whereas the current knowledge of its engineering behavior is primarily based on clean sands [Thevanayagam et al. 1(996 a, b)].

Moreover, the presence of fines in sand has an influence on the bearing capacity. The problem of bearing capacity of shallow foundations on granular soils has been studied for many years [deBeer (1965); Feda (1961); Brinch Hasen (1970); Meyerholf (1965); Vesic (1973)].

However, an accurate solution capable of predicting the peak load carrying capacity for a wide range of soil properties and foundation shapes within the practical context remains elusive owing to the presence of fines.

Experimental investigations on the behavior of confined footings, till now have been generally devoted towards the use of multiple geocells. However, it has been observed that relatively greater number of these experimental investigations have been made towards the bearing capacity of sand and clay only. No studies are reported concerning the bearing capacity and settlement characteristics of confined silty sands.

A review of earlier investigations on the effect of confinement on bearing capacity is briefly reported. Some important experimental investigations of this aspect have also been supplemented in the review.

The literature review consists of two sections. Section one deals with the effect of fines on the behavior of clean sand and section two deals with the effect of confinement on the bearing pressure.

2.1 Effect of Fines

The role of non-plastic silt and its content on the stress–strain behavior of loose sand has been under discussion for a considerable amount of time. Over 40 years ago Terzaghi (1956) Hypothesized that silt particles could create a ‘‘metastable’’ particle structure that could explain the static liquefaction observed in the failure of large submarine slopes. Recent laboratory studies that have investigated the susceptibility of liquefaction appear to be divided regarding the effect of non-plastic silt content. During cyclic testing of tailings sand

Ishihara et al. (1980) found that the strength depended on consistency and that plastic fines have higher resistance to liquefaction than non-plastic ones. Kuerbis et al. (1988) observed that increasing the silt content up to 20% resulted in more dilative behavior in undrained triaxial tests on sand, when the experiments were performed at the same skeleton void ratio. Pitman et al. (1994) also concluded that when silt was added to Ottawa sand, it became less collapsible in undrained triaxial compression tests. Others found that nonplastic silt may increase the potential of liquefaction (Troncoso and Verdugo 1985; Sladen et al. 1985). Ishihara (1993) and Verdugo and Ishihara (1996) concluded that increasing the silt content increases the potential for sand to exist in nature in a contractive state that can induce the possibility of flow failure or liquefaction. Thevanayagam (1998) found that the presence of non-plastic silt may either increase or decrease the undrained shear strength depending on the inter granular void ratio. Historically, most actual cases of earthquake induced liquefaction were observed to occur in silty sands (Seed et al. 1991; Chaney and Pamukcu 1991; Yamamuro and Lade 1999). Especially susceptible appear to be mine tailings facilities, where the soil is usually hydraulically deposited into very loose states with very high silt content.

Both clean sands and sands containing silt have been shown to be liquefiable in the field (Mogami and Kubo 1953; Seed and Lee 1966; Youd and Bennett 1983) and in the laboratory (Lee and Seed 1967; Casagrande 1975; Koester 1994). Nonplastic silts, most notably mine tailings, have also been found to be susceptible to liquefaction (Okusa et al. 1980; Garga and McKay 1984). Numerous laboratory studies have been performed and have produced what appear to be conflicting results. Several studies have reported that increasing the silt content of a sand will either increase the sand's resistance to liquefaction (Chang et al. 1982; Dezfulian 1982; Amini and Qi 2000), or decrease the sand's resistance to liquefaction (Shen et al. 1977; Troncoso and Verdugo 1985; Vaid 1994; Lade and Yamamuro 1997; Yamamuro and Lade 1997; Zlatovic and Ishihara 1997).

Law and Ling (1992) & Koester (1994) have found that the sand's resistance to liquefaction will initially decrease as the silt content increases until some minimum resistance is reached, and then increase as the silt content continues to increase . Finally, several studies (Shen et al. 1977; Troncoso and Verdugo 1985; Kuerbis et al. 1988; Vaid 1994) have shown that the liquefaction resistance of a silty sand is more closely related to its sand skeleton void ratio than to its silt content.

The objective of this section is to present a literature review on the effect of fines on the engineering properties of sand. Research and subsequent literature on the subject is focused on the effect of non-plastic fines on the behavior of clean sand.

2.1.1 Minimum and Maximum Void Ratios

Burmister (1948); Tavenas and La Rochelle (1972) and Selig and Ladd (1973) reported that the concept of relative density has been subjected to some criticism. The criticism has been focused on difficulties in obtaining e_{max} and e_{min}, particularly for sands with more than 15% fines content. However, careful execution of a specific procedure to determine e_{max} and e_{min} does lead to a reasonably reproducible numbers (and a relative density reproducible to 65%). Additionally, important advantages are offered by the use of relative density, notably that relative density allows unification of the description of density or degree of compaction of granular soils with fines content ranging from 0 to 20% with respect to the densest and loosest possible states for these soils.

Kuerbis et al. (1988) found that the maximum and minimum void ratio of silty sand decreased as the silt content was increased from 0 to 20%. Similar results were observed by Lade and Yamamuro (1997) for Nevada and Ottawa sands mixed with nonplastic fines. For Ottawa sand mixed with Sil-Co-Sil. minimum and maximum void ratios were determined in this study according to ASTM D 4253 and ASTM D 4254. Minimum density was obtained by pouring sand into a standard compaction mould with a volume of 0.00283 m^3 using a thin-walled cylindrical tube. Maximum density was achieved by densifying the dry sand in a compaction mould of 0.00283 m^3 using an electromagnetic vertically vibrating table with a frequency of 60 Hz. A double amplitude of vertical vibration of 0.379 mm was found to be optimum for all gradations. Even though the ASTM recommended procedure is applicable for fines content up to 15%, no difficulties were found while using it for 20% silt content. Table 2.1 gives the maximum and minimum void ratios of clean and silty Ottawa sands as a function of silt content. It is clear that e_{max} and e_{min} of silty sands decreases with increase of fines content from 0 to 20%. The rate of decrease drops as the fines content approaches 20% and Kuerbis et al. (1988) and Lade and Yamamuro (1997) observed in their studies that e_{max} and e_{min} increases after the fines content exceeds about 25%. This pattern of decreasing e_{max} and e_{min} with increasing fines content is well explained by Lade and Yamamuro (1997). As fines are added to either a dense or loose sand matrix, most particles initially occupy the voids between the sand particles. This represents a reduction in void ratio with increase in the amount of fines. Some particles, however, end up between the surfaces of adjacent sand particles. Such particles would tend to cause an increase in void ratio as they do not occupy the natural void space left by the sand matrix and to push sand particles apart. Due to the methods of preparation of loose and dense samples, more particles are found between the

surfaces of adjacent sand particles in loose sands than in dense sands. Hence the larger drops in e_{min} than in e_{max} for a given increase in fines content have been observed as given in Table 2.1.

Table 2.1. Minimum and maximum void ratios for clean and silty Ottawa sands (Salgado et al. 2000)

Silt (%)	$\mathbf{e_{min}}$	$\mathbf{e_{max}}$
0	0.48	0.78
5	0.42	0.70
10	0.36	0.65
15	0.32	0.63
20	0.29	0.62

For a given overall void ratio, there is a fines content for which they completely (or almost completely) separate adjacent sand particles. An easy way to determine the fines content for which this happens is based on the concept of the skeleton void ratio e_{sk} given by Kuerbis et al. (1988), which is the void ratio of the silty sand calculated as if fines were voids

$$e_{sk} = \frac{(1+e)}{(1-f)} - 1 \qquad (2.1)$$

Where e = overall void ratio of soil; f = ratio of weight of fines to total weight of solids. Whenever e_{sk} is greater than the maximum void ratio $(e_{max})_{f=0}$ of clean sand, the sand matrix exists with a void ratio higher than it could achieve in the absence of fines. It means that the sand particles are, on average, not in contact and the mechanical behavior is no longer controlled by the sand matrix.

Kuerbis et al. (1988) observed the skeleton void ratio as a function of void ratio for 5, 10, 15, and 20% fines. For each gradation, a limit void ratio (and a corresponding limit relative density) can be defined. For Ottawa sand with e_{max} = 0.78, these relative densities are 3% for 5% fines, 17% for 10% fines, 38% for 15% fines and 59% for 20% fines. For relative densities lower than the limit relative density, the fines control and the behavior becomes that of a sandy silt or sandy clay depending upon the nature of the fines. For soils denser than the limit relative density, the behavior is that of sand, modified by the presence of fines.

2.1.2 Behavior of Clean Sand with Fines

Lade et al. (1998) observed that when clean sand is mixed with increasing amounts of non-plastic silt, the minimum and maximum void ratios as well as the range of void ratios change and highly unstable and compressible particle structures can be formed when gently deposited into loose configurations [Lade and Yamamuro (1997); Yamamuro and Lade (1997b)]. Sands with low silt content may form a particle structure that is shown in the schematic drawings in Fig. 2.1. The diagram on the left side of Fig. 2.1 shows silty sand deposited with very low input energy into a loose state. Both Terzaghi (1956) and Hanzawa (1980) have hypothesized that a metastable soil structure may explain the behavior of liquefiable silty sands. In the metastable soil structure, the void spaces between the larger grains are relatively unoccupied and the larger grains, which will make up the load-bearing skeleton, are held slightly apart by smaller silt particles near the contact points. The diagram on the right side of Fig. 2.1 shows how the applied shear and normal stresses affect this unstable particle structure. The silt particles that were separating the larger grains are forced into the void spaces. Initially, this collapse creates large contractive volumetric strains. This collapse can be observed during both consolidation and shearing. These qualitative attributes are observed to coincide with the volume change behavior in drained triaxial compression tests on loose silty sands whose specimens are prepared using dry depositional methods [Yamamuro and Lade (1997b), (1998)]. A large amount of contractive volumetric strain occurs at low pressures and low axial strains. It is also observed that the volumetric strains associated with the collapse were nearly identical between 25 and 100 kPa, indicating that the collapse is easily triggered. The particle structure shown in Fig. 2.1 also explains why silty sands exhibit increasing dilatancy with increase in confining pressure under undrained conditions. Once the collapse has occurred and the silt particles have been pushed into the void spaces, the larger load-bearing grains move into better contact resulting in increased dilation as the confining pressure is increased. This effect counterbalances the normally observed behavior in experiments on loose clean sands, whose specimens were prepared using dry depositional methods, for increased amounts of volumetric contraction with increasing confining pressures in loose sands.

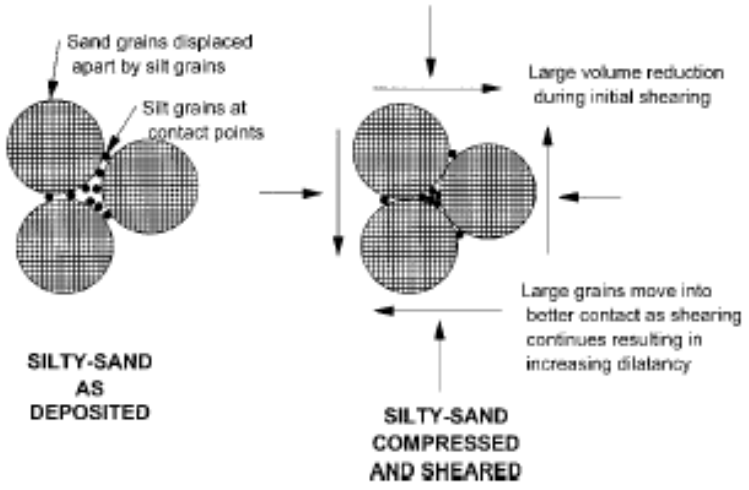

Fig. 2.1 Schematic diagrams illustrating hypothesized particle structures for loose sand with low silt content; diagram on left shows loose, compressible structure after deposition, while diagram on right shows structure after densification due to shearing [Yamamuro and Lade (1997)]

Many studies have indicated that in case of nonspherical binary particle (presence of only large and small particles) mixtures [Kuerbis et al. (1988); Pitman et al. (1994); Lade et al. (1998); Thevanayagam (1998)] the particle structure is different with the presence of large quantities of small particles as opposed to lower quantities. This is displayed in Fig. 2.2 where the void ratio is plotted against the fines content. The maximum density line is shown with the different binary particle structures at different silt contents. On the line segment between points A and B where the maximum density is increasing with the silt content, the fine particles fill the void spaces between the large grains until point B is reached. At this point the void spaces are almost completely filled. Between points B and C the larger particles become significantly displaced from each other by the large quantity of smaller particles until finally only small particles are present at point C. The maximum density decreases on this line segment. It is hypothesized that the particle structures at lower densities are somewhat similar to those at the maximum density lines. To achieve the maximum density a great deal of energy must be applied during the deposition process of silty sand.

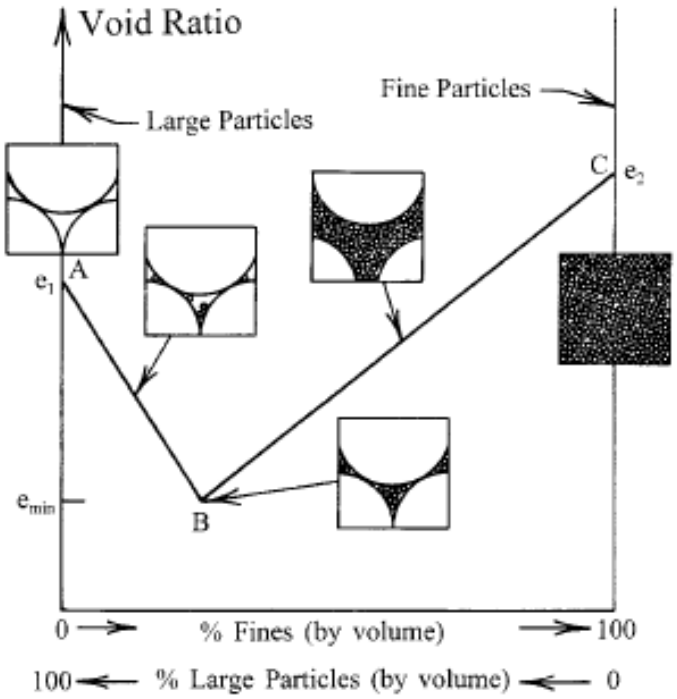

Fig.2.2. Different types of particle structures at different silt contents along maximum density line for binary mixtures [Yamamuro and Covert (2001)]

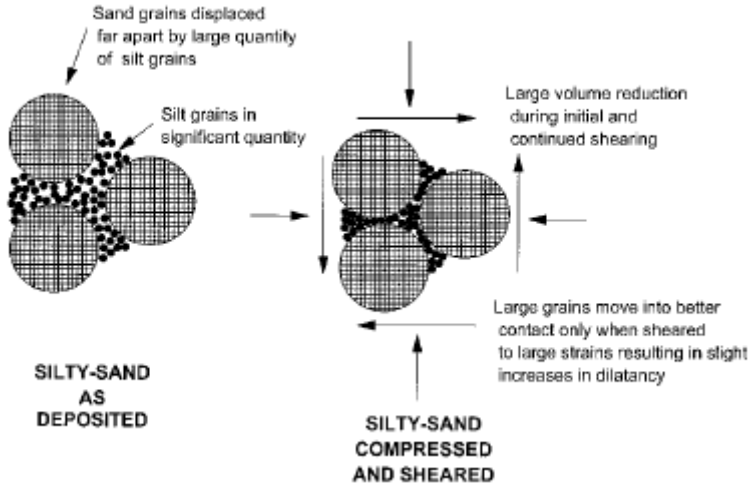

Fig. 2.3. Schematic diagrams illustrating hypothesized particle structures for loose sand with high silt content; diagram on left shows loose, compressible structure after deposition, while diagram on right shows structure after densification due to shearing [Yamamuro and Lade (1997)]

However, at low densities with low silt content, where there is a low-energy deposition process, it is hypothesized that the particle structure is as shown in Fig. 2.1. At low densities with high silt content, the resulting hypothesized particle structure is shown in Fig.2.3. The diagram on the left-hand side of Fig. 2.3 shows the particle structure as deposited with low

input energy. Notices that the larger sand grains are displaced a significant distance apart by the large quantity of loose silt particles. When the stresses are applied as shown in the diagram on the right side of Fig. 2.3, there is a large volume reduction. The amount of volume reduction is more related to the compressibility of the loose silt that is deposited between the larger sand grains. Full contact between the large grains may not be established resulting in the silt particles being part of the load-bearing skeleton. The deduced behavior is quite different than that hypothesized for loose sands with low silt content, as was shown in Fig. 2.1. One can summaries that the contractive nature of loose sands with high silt content may extend to larger strains because the volume change tendency is not solely based upon an unstable particle arrangement. The structure is highly compressible.

2.1.3 The Effects of Fine Content and Plasticity on Cyclic Resistance (Liquefaction)

Most of studies on sandy soils with fines indicate potential phenomenon of dilatancy under varied monotonic and cyclic boundary conditions. This is interesting to consider the cyclic resistance over and above the monotonic resistance in the literature review on behavior of sand in presence of fines.

Both clean sands and sands containing fines have been shown to be liquefiable in the field [Mogami and Kubo (1953); Robertson and Campenella (1985); and Holzer et al. (1989)] and in the laboratory [Lee and Seed (1967a); Chang et al. (1982); and Koester (1994)]. Additionally, non-plastic silts, most notably mine tailings, have also been found to be susceptible to liquefaction [Okusa et al. (1980); and Garga and McKay (1984)]. The main factors that are reviewed here are the effects of non-plastic fines content and the effects of plastic fines content and plasticity on the liquefaction resistance of sandy soils.

2.1.3.1 The Effects of Non-Plastic Fine Content

There is no clear consensus in the literature as to the effect which increasing non-plastic fines content has upon the liquefaction resistance of a sand. Both field and laboratory studies have been performed, and the results of these studies indicate that increasing the non-plastic fines content in a sand will either increase the liquefaction resistance of the sand, decrease the liquefaction resistance of the sand, or decreases the liquefaction resistance until some limiting fines content is reached, and then increases its resistance. To further complicate issues, some researchers have shown that the liquefaction resistance of silty sands is not a function of the silt content of the soil so much as it is a function of the soil's sand skeleton void ratio.

Field Studies

Field studies following major earthquakes have produced conflicting evidence as to the effects of silt on the liquefaction resistance of sands. Based upon case histories of actual soil

behavior during earthquakes, there is evidence that soils with greater fines contents are less likely to liquefy in a seismic event. Okashi (1970) observed that during the 1964 Nigata earthquake in Japan, sands were more likely to liquefy if they had fines content of less than 10 percent. Additionally, Fei (1991) reports that for the 1976 Tangshan earthquake in China the liquefaction resistance of silty soils increased with increasing fines content. Finally, Tokimatsu and Yoshimi (1983) found in a study of 17 worldwide earthquakes that 50 percent of the liquefied soil had fines contents of less than 5 percent. They also found that sands with fines contents greater than 10 percent had a greater liquefaction resistance than clean sands at the same SPT blow count. While some research has shown that an increase in fines content results in an increase in liquefaction resistance, other research has shown the opposite effect. Tronsco and Verdugo (1985) report that mine tailings dams constructed of soils with higher silt contents are more likely to liquefy than similar dams constructed of sands with lower silt contents. Chang et al. (1982) note that case studies reveal that most liquefaction resulting from earthquakes has occurred in silty sands and sandy silts. Okusa, et al. (1980), and Garga and McKay (1984) each report cases of mine tailings dams constructed with up to one hundred percent silt-sized particle liquefying during earthquakes in Chile and Japan. All of the fines involved were either silts of low plasticity or non-plastic silts.

Field based methods for determining liquefaction susceptibility, such as methods based on SPT blow counts or CPT measurements, must account for the presence of fines in the soil (Tatsuoka et al, 1980). Seed et al (1985) modified the cyclic stress ratio (CSR) versus normalized SPT blow count curves originally proposed by Seed and Idriss (1971) to account for the increase in liquefaction resistance provided by an increased fines content. The revised chart provides a series of curves for 5 percent, 15 percent, and 35 percent fines. These curves indicate that, for a given blowcount, a larger CSR it required to liquefy a soil with higher fines content.

Laboratory Studies

As previously noted, there is a great discrepancy in the literature as to the effects which increasing the non-plastic, i.e. silty, fines content has upon the liquefaction resistance of a sandy soil.

Several investigators have found that the cyclic resistance of a sandy soil increases with increasing silt content. For specimens prepared to a constant gross void ratio, Chang et al. (1982) found that after a small initial drop, cyclic resistance increased dramatically with increasing silt content. The cyclic resistance increased nearly linearly with silt content until a

silt content of 60 percent was reached, increasing to a cyclic resistance between 50 and 60 percent greater than that of the clean sand. Similarly, Dezfulian (1982) reported a trend of increasing cyclic resistance with increasing silt content. Both studies used silts with either some small level of plasticity or a measurable clay fraction.

This trend of increasing cyclic strength with increasing fines content can be seen in the data for a sand tested at different fines contents by Chang et al (1982). Numerous authors have reported a decrease in cyclic resistance with increasing silt content. Shen et al. (1977), Tronsco and Verdugo (1985), and Vaid (1994) have all reported this trend for specimens prepared either to a constant gross void ratio or a constant dry density. The decreases in cyclic resistance were marked, decreasing as much as 60 percent from their clean sand values for an increase in silt content of 30 percent (Tronsco and Verdugo, 1985).

Rather than a simple decrease in cyclic resistance with increasing fines contents, several investigators have reported that the cyclic resistance of the sand first decreased as the fines content increased and then increased after crossing some threshold fines content.

Koester (1994) and Law and Ling (1992) found that for specimens prepared to a constant gross void ratio, as silt content increased the cyclic resistance of the soil decreased until some limiting silt content was reached, at which point the cyclic resistance began increasing. Koester (1994) reported a decrease in cyclic resistance to less than onequarter of the clean sand cyclic resistance at a silt content of 20 percent, followed by an increase in cyclic resistance to 32 percent of the clean sand value at a silt content of 60 percent. Unlike Chang et al. (1982), and Dezfulian (1982), neither of these studies reported increases in cyclic resistance to levels greater than those determined for the clean sand. Several studies have shown that cyclic resistance is more closely related to sand skeleton void ratio than it is to gross void ratio, gross relative density, or fines content. Finn, et al.(1994) found that at the same gross void ratio, the cyclic strength of a sand decreases with increasing fines content. They also found that at the same sand skeleton void ratio, cyclic strength remains constant with increasing fine content, as long as the fines can be accommodated in the void spaces created by the sand skeleton. Not all soils however, exhibit a constant cyclic resistance with a constant sand skeleton void ratio. Shen et al. (1977), Kuerbis et al. (1988), and Vaid (1994) have shown that for specimens prepared to constant sand skeleton void ratios, the cyclic resistance of a sand does not remain constant, but increases with increasing silt content.

Clearly, based upon the conflicting evidence presented in the literature, the fines content of a sandy soil does not alone provide a definitive measure of its liquefaction potential.

2.1.3.2 The Effects of Plastic Fines Content and Plasticity and Plasticity Based Cyclic Resistance (Liquefaction) Criteria

There is general agreement in the literature as to the effect which the quantity and plasticity of the fine-grained material has on the liquefaction resistance of a sandy soil. There is agreement that whether the fine grained material is silt or clay, or more importantly, whether it behaves plastically or non-plastically, tends to make an important, consistent difference in the cyclic strength of the soil. The majority of studies have shown that the presence of plastic fines tend to increase the liquefaction resistance of a soil.

Field Studies

The effect of clay content on the liquefaction resistance of sandy soils has also been clearly established in field studies. Seed et al. (1983) concluded that if a soil has a clay content greater than 20 percent it will not liquefy. A study of worldwide earthquakes by Tokimatsu and Yoshimi (1983) came to the same conclusion.

Laboratory Studies

Several laboratory studies have shown a strong correlation between an increased plasticity of the fine-grained portion of the soil and the increased liquefaction resistance of that soil. Ishihara and Koseki (1989) found that while there was no clear correlation between either clay content or fines content and liquefaction resistance, increasing plasticity index consistently increased liquefaction resistance. Yasuda et al. (1994) also found that increasing plasticity index increased liquefaction resistance. Only Koester (1994) provides evidence that would appear to indicate that soil plasticity is not a controlling factor in liquefaction resistance in soils with plastic fines. He found that while at a given void ratio, fine type and plasticity play a minor role in liquefaction resistance, they exert far less influence than the percentage of fines in the soil.

Table 2.2 Summary of literature review on the effects of fines on the cyclic (liquefaction) resistance of sandy soils

YEAR	INVESTIGATOR	FINDINGS
1953	Mogami and Kubo	For loam with a PI of 34 percent, shear strength during vibration decreases with increasing acceleration of vibration
1961	Florin and Ivanov	All cohesionless materials can liquefy
1967	Lee and Seed	For a compacted silt with a PI of 9, cyclic strength increases with: A) Increasing density B) Increasing confining pressure C) Increasing consolidation stress ratio
1968	Lee and Fitton	1) At constant confining stress and relative density, fine silty sands have the lowest cyclic strength 2) Grain size has more effect on cyclic strength than grain shape or grain size distribution 3) Peak pore pressure response decreases with increasing grain size 4) For granular soils, cyclic strength decreases with decreasing grain size 5) In silt and clay, cyclic strength increases with decreasing grain size 6) Clayey fines may improve cyclic strength considerably, while silty fines may tend to decrease the cyclic strength
1971	Seed and Idriss	Very fine sands, with D_{50} approximately equal to 0.08 mm, are most susceptible to liquefaction
1974	Lee and Albaisa	The relationship between pore pressure ratio and the ratio of the cycle to the number of cycles required for 100 percent pore pressure ratio forms a small band for a given sand over a large range of densities and confining stresses
1977	Ishihara et al.	For soil with 0 to 100 percent fines, fines with PI of 20 1) As percent fines increases, cyclic strength increases 3) For a given fines content, cyclic strength increases as OCR increases. Difference increases with increasing fines content
1977	Shen et al.	For samples prepared to a constant dry density: 1) As fines content increases, cyclic resistance decreases 2) For a constant sand skeleton void ratio, cyclic resistance increases
1980	Okusa et al	Mine tailings with greater than 90 percent fines, but no plasticity, liquefied during the 1978 Izu-Oshima-Kinkai Earthquake in Japan. 1) Liquefied material was sub-rounded silt with grain to grain contact with some clay attached to larger particle faces. 2) Non-liquefied material was silt-sized particles wrapped in clay with no grain to grain contact.
1980	Tatsuoka et al	Must account for effect of grain size on blow count. Failure to do this leads to an overly conservative analysis

		for fine or silty sands
1982	Dezfulian	For undisturbed specimens of silty and clayey sands at various densities, cyclic resistance increases with increasing fines content.
1982	Chang et al	1) Case studies reveal that most liquefaction events have occurred in silty sands and sandy silts 2)The effect of gradation is less than the effect of mean grain size 3) Cyclic strength of a silty sand decreases from 0 to 10 percent silt content then increases to a silt content of 60 percent where it levels off. 4) At 10 percent silt content, sand grain to grain contact still prevails 5) Above 60 percent silt content, sand grains are merely floating in the silt matrix 6) As the number of cycles to failure increases, the effects of D_{50} and C_u become less important to cyclic resistance 7) For clean sands, cyclic strength increases with increasing D_{50} 8) Fine sands more susceptible to liquefaction than coarse sands 9) Differences in permeability due to differences in silt content lead to differences in pore pressure development
1984	EL Hosri, Biarez, and Hicher	Cyclic strength of silty clay increases with decreasing void ratio and increasing relative density.
1984	Garga and McKay	Isotropically and anisotropically consolidated cyclic triaxial tests on undisturbed remolded samples of 33 mine tailings materials. Materials had from 0 to 100 percent fines, but negligible plasticity. All results were adjusted to 50 percent Dr :1) Undisturbed samples had higher cyclic strength than remolded samples 2) Non-tailings sands were stronger and coarser (fewer fines). 3) Cyclic strength increases with increasingmconsolidation ratio 4) In isotropically consolidated tests, soils with D_{50} between 0.1 and 0.3 mm has lowest cyclic strength
1985	Robertson and Campanella	1) Liquefaction resistance increases with decreasing D_{50} below a D_{50} less than approximately 0.25 mm 2) Cyclic stress ratio to cause liquefaction versus cone tip penetration is a function of grain size. Separate curves for $D_{50} < 0.15$ mm and $D_{50} > 0.25$ mm.
1985	Tronsco and Verdugo	1) Tailings dams with low silt content are more resistant to liquefaction than dams with higher silt contents. Possibly because increasing silt content decreases permeability and thus pore pressure dissipation. 2) At a constant void ratio of approximately 0.9: A) As silt content increases, soil becomes more compressive, less dilative. B) For a given shear strain, shear modulus, G, decreases as

		silt content increases. C) Cyclic strength increases by 270 percent as silt content decreases from 30 percent to 0 percent. This effect is more noticeable in the 0 to 15 percent range than in the 22 to 30 percent range.
1988	Kuerbis et al	1) At constant silt content, resistance increases as void ratio decreases 2) At constant void ratio, resistance decreases a silt content increases
1989	Holzer et al	During Imperial Valley earthquake of 1979 liquefaction occurred in silts with as little as 7 percent sand and up to 10 percent clay
1989	Ishihara and Koseki	There is no clear correlation between either clay content or fines content and cyclic strength. PI correlates well. As PI increases, cyclic strength increases.
1992	Law and Ling	For specimens prepared to a constant gross void ratio, as silt content increased, the cyclic resistance of a soil decreased until some limiting silt content was reached, at which point the cyclic resistance began increasing
1994	Koester	Based on results of 500 undrained cyclic triaxial tests on samples with a sand skeleton void ratio corresponding to a relative density of 50 percent: 1) Lowest cyclic strength occurs at 20 to 26 percent fines 2) Fine type (i.e. plasticity) is less important than percentage. 3) Cyclic strength decreases with increasing fines content to approximately 20 percent fines, then increases. Cyclic strength was still lower at 60 percent fines than at 12 percent fines. 4) Lowest lower bound strength occurred for well graded sands at 20 to 30 percent fines 5) Residual strength of sand with 20 percent silt is very low 6) Post-liquefaction monotonic loading leads to a dilative response. 7) Liquefaction becomes inevitable at a pore pressure ratio of 70 percent for clean sands and 80 percent for sands with fines. Once this threshold pore pressure ratio is reached strain occurs more rapidly in sands with fines than in clean sands.
1994	Singh	1) At 50 percent relative density sands with 10, 20, or 30 percent silt have slightly lower resistances to liquefaction than clean sand at the same relative density. 2) At constant void ratio, cyclic strength increases with increasing silt content. This may be due to increasing relative density as more silt is added at a constant void ratio.
1994	Vaid	1) In compression, sand exhibits increasing dilatancy with increasing silt content 2) In extension, sand exhibits only slightly increasing

		contractiveness with increasing silt content 3) Silty sands are liquefiable only in extension not in compression 4) At constant silt content, resistance increases as void ratio decreases 5) At constant void ratio, resistance increases as silt content decreases 6) At constant sand skeleton void ratio, resistance increases slightly as silt content increases.
1994	Yasuda et al	1) As fines percentage increases, cyclic strength increases slightly 2) As clay percentage increases, cyclic strength increases slightly 3) As PI increases, cyclic strength increases 4) Undisturbed "aged" samples of silty sand are stronger than remolded samples 5) Strength gain with time is more rapid for silty sands than for clean sands 5) Increase in SPT blowcounts from 1 year and 50 years after fill placement is most significant if soil contains more than 40 percent fines

2.1.4 Shear Strength

Pitman et al. (1994), Zlatovic and Ishihara (1995) and Thevanayagam et al. (1996a) have reported that as fines content increases, initially the steady state strength at same void ratio decreases followed by an increase in shear strength with a further increase in fine content beyond about 30%.A similar behavior has also been observed for the cyclic behavior of silty sands [Vaid (1994) and Singh (1994)].

Thevanayagam (1998) have studied the concept of intergranular void ratio (e_s), intergranular relative density (D_{rs}) and interfine void ratio (e_f).It is assumed that up to a certain fines content the finer grains do not actively participate in the transfer of contact frictional forces or their contribution is secondary. It is further assumed that the specific gravities of the finer grains and coarser grains are the same. Then, for a unit volume of solids containing both sized grains at a fines content (FC, as a percentage of the total weight of the solids), the volume of fines is FC/100 and the volume of coarser grains is (1-FC/100).Accordingly ,the intergranular (coarse grains) void ratio e_s is defined as the void ratio of the original coarser-grains matrix structure if the fines were removed from there (Fig 2.4).The apparent volume of voids in the coarser-grain matrix and the volume of coarser grain solids are then (e+FC/100) and (1-FC/100) [Fig 2.4c], respectively, where e is the global void ratio of the silty sand.

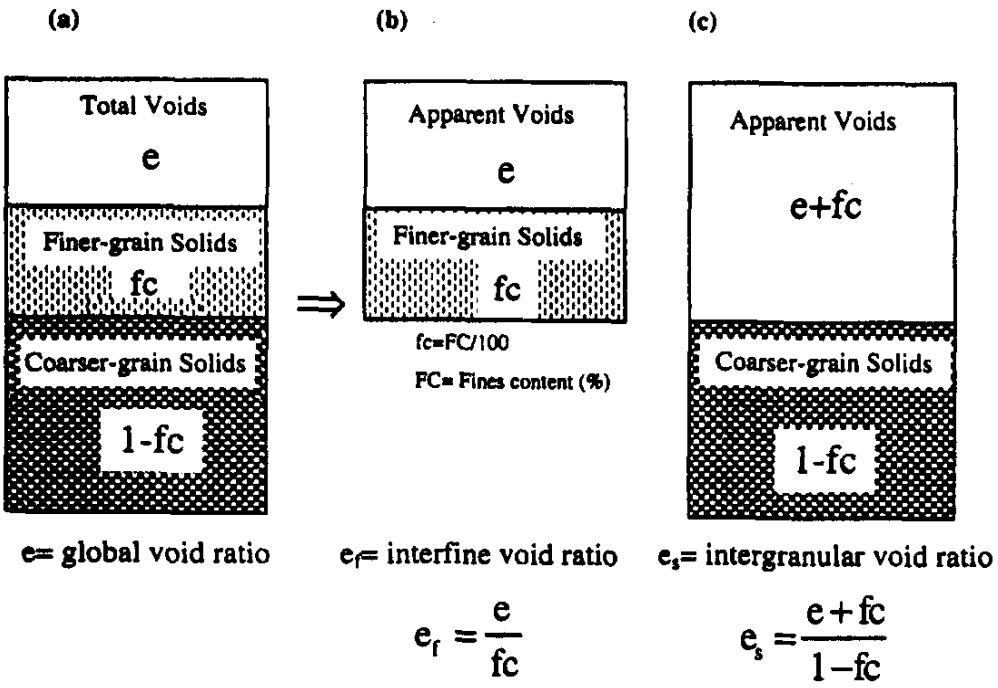

Fig. 2.4 Systematic diagrams: (a) Silty sand; (b) Silt matrix; (c) Sand matrix [Thevanayagam (1998)]

According to Thevanayagam (1998), intergrannular void ratio (e_s) may be defined as

$$e_s = \frac{\left(e + \frac{FC}{100}\right)}{\left(1 - \frac{FC}{100}\right)}$$

The intergranular void ratio e_s is considered to be an index of active coarser granular frictional contacts that sustain the normal and shear forces. The corresponding intergranular relative density D_{rs} is defined as

$$D_{rs} = \frac{e_{\max,HS} - e_s}{e_{\max,HS} - e_{\min,HS}}$$

If the fines content is increased significantly, the soil may be completely governed by the contacts along the fines whereas the coarser grains float within the fines. The presence of coarser grains has no effect on the force chain, except perhaps serving as a medium of contact between the many finer grains around it. Since it is not a void, nor does its volume affect the nature of the force chain in the finer grains, the volume of the coarser grains can be safely ignored. Contrary to the earlier case where the finer grains were considered to be voids, in the case the coarser grains are considered to be zero volume (Fig 2.4b). The silty sand may

behave in a similar way as that of the host finer-grained silt at an interfine void ratio (e_f) defined as

$$e_f = \frac{e}{\left(\frac{FC}{100}\right)}$$

The behavior of the silty sand/sandy silt in this category is anticipated to resemble with that of the 100% finer-grained (host) silt at a void ratio e_f and the relevant confining stress.

Thevanayagam (1998) examined the effect of fines and the confining stress on large strain undrained shear strength of silty sands in triaxial compression test. He also presented the hypothesis on the mechanism causing the low and confining stress dependent upon shear strength of silty sands.

Experimental data on silty sands indicate that the large strain undrained shear strength is dependent on intergranular void ratio or intergranular relative density .The shear strength of a dense silty sand specimen at an intergranular void ratio e_s (less than $e_{max,HS}$) is approximately the same as that of the host sand at a void ratio equal to e_s. When $e_s > e_{max,HS}$, the shear strength of a silty sand is low and is dependent on the initial confining stress .At higher fines content greater than about 30%, the silty sand may behave in a similar manner as that of the host fine grained soil at an equivalent void ratio of e_f, unless the density of the silty sand is very high.

2.2 Effect of Geocell

2.2.1 General

The decreasing availability of good construction sites has led to increased use of sites with marginal soil properties. In view of this, the requirement of in situ treatment of foundation soil to improve its bearing capacity has risen markedly. The soil reinforcement is one method of treatment. The more recent advancement in this field is to provide three-dimensional confinement to the soil by using geocells. The geocell foundation mattress consists of series of interlocking cells constructed from polymer grid reinforcement, which contains and confines the soil within its pockets. A review of literature suggests that this novel technique of geocell reinforcement though successfully applied in some areas of geotechnical engineering, has not received much attention in foundation applications.

2.2.2 Geocell Systems and Applications

The development of the concept of the reinforcement of soil by cellular confinement is credited to the United States Army Corps of Engineers who developed the concept for the stabilization of granular materials such as beach sand under vehicle loading. This initial work performed at the U.S. Army Engineer Waterways Experimental Station led to the development of commercially available geocell systems.

The requirement for in situ treatment of foundation soil to improve its bearing capacity and reduce the settlement has raised markedly. The soil confinement is one such method of improving the bearing capacity and reducing the settlement of the footings resting on silty sands. It is a structural measure to reduce settlement of foundations on granular soils using lateral confinement. The lateral confinement is applied as cylindrical rings known either as geo-cells of plastic sheets or metallic rings confining the soil below the footing. It results in to added stiffness of the soil.

2.2.3 Laboratory Studies on Geocell Reinforcement

2.2.3.1 Laboratory Studies on Geocells

Several laboratory studies on the reinforcing effect of geocell mattresses have been carried out over the last two to three decades. These studies were aimed at a wide variety of applications and the experimental procedures and setups differ considerably.

Table 2.2 provides a summary of the relevant literature discussed in this section.

Rea and Mitchell (1978) reported on laboratory tests to investigate the reinforcement of sand, using paper grid cells. Their study investigated the influence of the ratio of the diameter of the loading area to the cell width, the ratio of cell width to cell height and the subgrade stiffness. A mattress of square paper grid cells with a membrane thickness of 0.2 mm and a cell height of 51 mm was filled with uniform fine quartz sand at its maximum density of 16.8 kN/m^3. The sand had a mean particle size of 0.36 mm and a coefficient of uniformity (C_u) of 1.45. Failure of the reinforced soil was sudden and well-defined and in some cases the cells burst open from the bottom along the glued junctions.

Mhaiskar and Mandal (1992, 1996) investigated the efficiency of a geocell mattress over soft clay. The influence of the width and height of the geocells, the strength of the geocell membranes and the relative density of the fill material were investigated. Geocells of needle punched nonwoven and of woven slit film were used in the study. Mumbra sand with a

minimum density of 16.05 kN/m^3, a maximum density of 18.1 kN/m^3 and C_u of 4.6 was used as a fill material. Tests were performed with the fill at a relative density of 15% and at 80%.

Table 2.3 Summary of literature survey

Researchers	**Geocell type**	**Application**	**Parameters investigated**
Rea and Mitchell (1978)	Square paper grid	Reinforcement of sand	Ratio of load width to cell width, cell aspect ratio, subgrade stiffness
Mhaiskar and Mandal (1992, 1996)	Needle punched woven and nonwoven slit film	Geocell mattress over soft clay	Cell aspect ratio, strength of geocell membrane, density of fill
Krishnaswamy et al. (2000)	Diamond and chevron patterned geogrid geocells	Embankment on geocell reinforce-ment over soft clay	Effect of mattress reinforcement
Dash et al. (2001)	Geogrid geocells	Strip footing supported by sand bed reinforced with geocell mattress	Geocell Pattern mattress size and aspect ratio, depth of mattress, tensile strength of geogrids density of sand
Dash et al. (2003)	Geogrid geocells	Circular footings on geocell reinforced sand over soft clay	Width and height of geocell mattress, and the addition of planar reinforcement layers and geogrids layer underneath geocell mattress.
Mandal and Manjunath (1995)	Bamboo and geogrid	Strip footing supported on reinforced soil	Distance of placement of reinforcement from center of footing, length of reinforcement
Sawwaf and Nazer (2005)	Open at both end and made up of UPVC	Circular footing supported on confined sand	Cell diameter, cell height, embedded depth of footing
Singh et al.(2008)	Cell made up of milsd steel sheet	Square footing supported on confined sand	Cell width, cell height
Emersleben and Meyer (2008)	Geogrid	Circular plate resting on geogrid reinforced dry sand	Cell diameter, cell height

Krishnaswamy et al. (2000) reported on the laboratory model tests of embankments on a geocell reinforced layer over soft clay. Diamond and chevron patterned geocells made of uniaxial and biaxial geogrids were used to construct the embankment foundation over the soft clay. The geocells were filled with a clayey sand and clay. The embankment was loaded until failure occurred.

Dash et al. (2001) reported on laboratory tests of a strip footing supported by a sand bed reinforced with a geocell mattress. The parameters varied in this study included the pattern of the geocell formation, the size, the height and width of the geocell mattress, the depth to the top of the geocell mattress, the tensile stiffness of the geogrids used to form the cell walls and the relative density of the sand fill. The geocells were filled with a dry river sand with a C_u of 2.32, C_c of 1.03 and an effective particle size of 0.22 mm. The minimum and maximum dry

unit mass were 1450 kg/m^3 and 1760 kg/m^3. The model footing tests were performed at relative densities of 30 to 70%.

In a subsequent study Dash et al. (2003) performed model studies on a circular footing supported on geocell reinforced sand underlain by soft clay. The width and height of the geocell reinforced mattress was varied in the study. The effect of the addition of a geogrids layer underneath the geocell mattress and the effect of planar reinforcement layers were also investigated. A soft natural silty clay with 60% fines passing the 75 μm sieve was used at the base of the test setup. The sand overlaying the clay was poorly graded sand with a C_u of 2.22, C_c of 1.05 and an effective particle size (D_{10}) of 0.36 mm. The density of the sand was kept constant at 1703 kg/m^3 corresponding to a density of 70%.

Sawwaf and Nazer (2005) have conducted the model tests on model circular footings to investigate the effect of confinement on ultimate bearing capacity. The aim of the study was to model and investigate the effect of soil confinement by piles on the behavior of soil foundation system. Authors have also studied the idea of improving the footing response by using confining cylinders around each individual footing. The sand used in this research is medium-to-coarse sand, washed, dried and sorted by particle size. It is composed of rounded-to sub rounded particles. The specific gravity of the soil particles was determined by the gas jar method. Three tests were carried out producing an average value of 2.654. The maximum and the minimum dry densities of sand were found to be 19.95 and 16.34 kN/m^3 and the corresponding values of the minimum and the maximum void ratios are 0.305 and 0.593 respectively. The effective size (D_{10}), uniformity coefficient (C_u) and coefficient of curvature (C_c) for the sand were 0.152 mm, 4.071 and 0.771, respectively.

Initially, the behavior of the footing supported on the unconfined conditions was determined and then compared with that of confined soil to investigate the effect of cell height (h), cell diameter (d) and the embedded depth (z) for cases when the foundation level is lower than the cell top.

The confining elements were made of unplasticized polyvinyl chloride (UPVC) cylinders with different diameters and heights. The used diameters were 50, 80, 100, 120, 150, and 200 mm. UPVC is produced from the polymerization of a vinyl chloride monomer with certain additives including heat stabilizers and lubricants. The interior and exterior surfaces of the cylinder were made very smooth. The thickness of the cylinder wall was 2.5 mm.

Mandal and Manjunath (1995) used geo-grid and bamboo sticks as vertical reinforcement elements and studied their effect on the bearing capacity of strip footings. Tests were performed on Mumbra sand with an effective grain size of 0.2mm, uniformity coefficient (C_u) of 4.6, angle of internal friction 38^0 and relative density 73%.The footing used was 100mm wide and was made up of well seasoned wood of 40mm thickness. The reinforcing elements were made of Nelton geo-grid strip 3mm thick and 100mm wide and bamboo sticks 6mm in diameter.

Singh et al. (2008) have studied the effect of confinement of a model square footing resting on Ganga sand under eccentric-inclined loads. Dry river sand with a C_u of 2.32, C_c of 1.03 and an effective particle size of 0.22 mm was used in the study. The minimum and maximum dry unit mass were 1450 kg/m^3 and 1760 kg/m^3 respectively. The model footing tests were performed at relative densities of 30 to 70%.Confining cells were made up of 10mm thick mild steel sheet.

Emersleben and Meyer (2008) reported on laboratory tests to investigate the effect of geo-cells. Geo-cells consisted of a series of interconnected single cells which were connected at their joints forming a honeycomb structure. The geo-cells were expanded and filled with the soil. The cell walls completely encased the infill material and provided an all around confinement to the soil. Study was carried out to evaluate the influence of cell height and cell diameter. Tests were performed on dry sand with maximum particle size 2mm, uniformity coefficient (Cu) 3.2 and coefficient of curvature (Cc) 1.03.The friction angle of the sand used was 38.9^0.

2.2.3.2 Inferences from Laboratory Tests on Geocells

Rea and Mitchell (1978) observed that the reinforcement resulted in stiffening of the reinforced layer giving a raft like action to the layer. A raft like action of the geocell reinforced layer is also observed by Cowland and Wong (1993) for geocell reinforced layer under an embankment over soft clay. Other researchers have mentioned the load spreading action of the reinforced layer and a subsequent reduction in the vertical stress in the layer underlying the geocell layer [Mhaiskar and Mandal, (1992); Bush et al. (1990)]. Dash et al. (2001) showed an increased performance on the footing over a buried geocell layer even with the geocell mattress width equal to the width of the footing. The geocell mattress transfers the footing load to a deeper depth through the geocell layer.

An increase in the bearing capacity of the geocell mattress with an increase in the ratio of cell height to cell width was observed by Rea and Mitchell (1978) and Mhaiskar and Mandal (1992). Dash et al. (2001) found that the load carrying capacity of the foundation bed increases with an increase in cell height to diameter ratio up to a ratio of 1.67, beyond which further improvements were marginal. The optimum ratio reported by Rea and Mitchell (1978) is around 2.25. Krishnaswamy et al. (2000) reported an optimum ratio of about 1 for geocell supported embankments constructed over soft clays. Dash et al. (2001) also noted that not only the aspect ratio of the cells but also the cell size (the cross sectional area of the cell compared to the loading area) had an influence on the performance of the geocell system. The increased load carrying capacity with decreasing pocket size is attributed to an overall increase in rigidity of the mattress and an increased confinement per unit volume of soil. A similar influence of the pocket size on the behavior of the geocell reinforced soil was observed by Rajagopal et al. (1999) while performing triaxial tests on geocell reinforced soil samples.

Increased relative density of the soil increased the strength and stiffness of the reinforced soil [Mhaiskar and Mandal (1992); Dash et al. (2001); Bathurst and Karpurapu (1993)]. Dash et al. (2001) attributed this to an increase in the soil-cell wall friction with a subsequent increase in the resistance to downward penetration of the sand as well as a higher dilation resulting in higher strains in the geocell layer. Higher strains were mobilized in the geocell layers due to the dilation of the sand. It was noted that this only occurred after a settlement of 15% of the footing width. Dash et al. (2001) used a non-dimensional factor, called the bearing capacity improvement factor (I_f), to compare results from different tests. This influence factor was defined as the ratio of footing pressure with the geocell reinforced soil at a given settlement to the pressure on un-reinforced soil at the same settlement. It was noted that I_f increases with increase in settlement at a more or less constant rate for soil at lower densities (D_r=30-40%). However, for soil at higher densities, the rate of increase of I_f is higher for higher settlements.

Mhaiskar and Mandal (1992) concluded that geotextiles with a high modulus are desirable for use in geocells as they result in a stiffer and stronger composite. A similar response was found by Dash et al. (2001) and Krishnaswamy et al. (2000) and is also shown by the theory proposed by Bathurst and Karpurapu (1993) and Rajagopal et al. (1999).Dash et al. (2001) reported an increase in load carrying capacity of the foundation bed when using a chevron pattern compared to a diamond pattern. They contributed this to a higher rigidity of the chevron-patterned geocell resulting from a larger number of joints for the same plan area of

geocell. Krishnaswamy et al. (2000), however, concluded that in the reinforcement of an embankment over soft clay, the performance of the chevron and diamond patterned geocells was the same.

Dash et al. (2001) had found an improvement in the load bearing capacity of the buried foundation mattresses with an increase in the mattress thickness up to a geocell height of twice the width of the footing beyond which the improvement is only marginal due to the local failure of the geocell wall taking place.

Rea and Mitchell (1978) interpreted the mechanism of reinforcement of the sand by the geocells in the following manner. Sand is confined and restricted against large lateral displacements until the tensile strength of the reinforcement is exceeded. The tension in the reinforcement gives compression in the sand contained within the cell, giving increased strength and stiffness to the sand in the regions beyond the edges of the loaded area. This conclusion is supported by the work of Mhaiskar and Mandal (1992) who stated that their experimental results showed the hoop stress to be a significant factor contributing towards the strength increase in the reinforced layer.

Table 2.3 summarizes the inferences from literature survey.

Qualitatively speaking the influence of different parameters on the performance of geocell reinforced soil seems to be similar across the wide variety of applications and geocell geometries. Quantitatively speaking, however, the influence of each parameter is dependent on the specific geometry of the application. This highlights the need for a more fundamental understanding of the interaction between the geocell membranes and fills material.

Mandal and Manjunath (1995) used a non-dimensional factor called the bearing capacity ratio (BCR) to compare the bearing capacity improvement. This factor is defined as the ratio of the footing ultimate bearing capacity with soil reinforcement to the footing ultimate bearing capacity without reinforcement.

The details of reinforcement pattern are shown in Fig 2.5. The results of test series are shown in Fig 2.6. It is apparent from the curves that reinforcement modified the stress-displacement behavior of the footing. It appears that these reinforcing elements resist the lateral displacement of soil underneath the footing and confine the sub-grade soil. They observed that vertical reinforcement located beyond a horizontal distance of two times the footing width has no appreciable effect on the bearing capacity of the footing-soil system as compared with at a distance of 0.5 *B (B* is the footing width)from the center of the footing.

They also studied the effect of the reinforcing length on the bearing capacity. They observed that as the reinforcing length increases, the bearing capacity also increases.

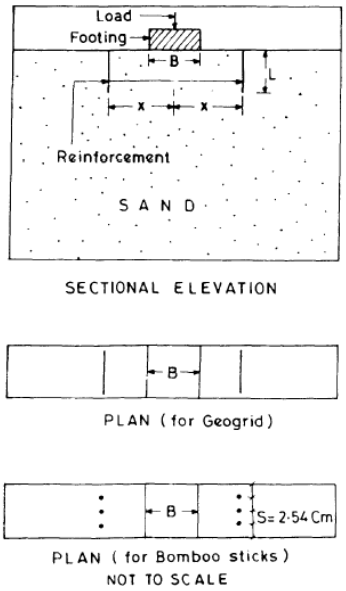

Fig. 2.5 Nomenclature and reinforcement pattern [Mandal and Manjunath (1995)

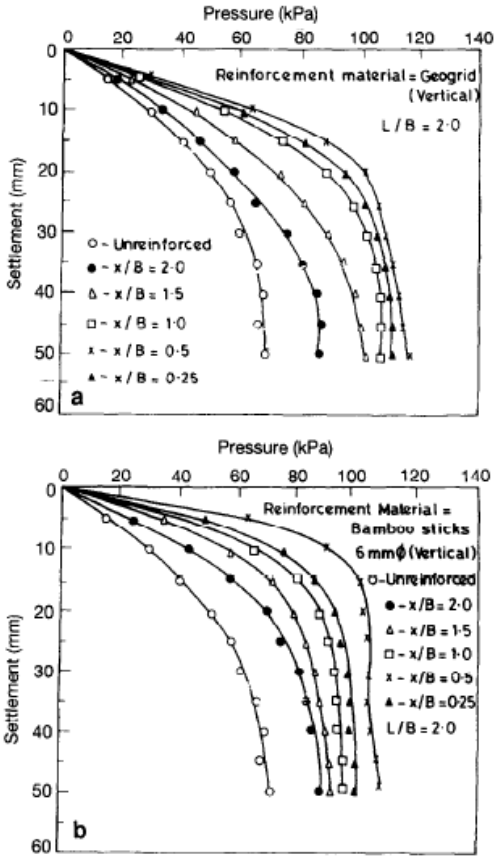

Fig.2.6 Relation between pressure and settlement for subgrades reinforced with (a) geo-grods and (b) bamboo sticks [Mandal and Manjunath (1995)]

Table 2.4 Inferences from literature survey

Parameter	**References**	**Inferences**
Geocell Reinforcement	Rea and Mitchell (1978) Cowland and Wong (1993), Mhaiskar and Mandal (1992), Bush et al. (1990),Dash et al. (2001)	Results in stiffening of reinforced layer Causes load spreading
Cell aspect ratio (h/w) i.e. ratio of cell height to cell width	Rea and Mitchell (1978), Mhaiskar and Mandal (1992) Krishnaswamy et al. (2000),Dash et al. (2001)	Increased bearing capacity with increased h/w ratio
Cell size	Dash et al. (2001),Rajagopal at al. (1999)	Smaller cell size- increased stiffness and load carrying capacity
Relative density of soil	Mhaiskar and Mandal (1992), Dash et al. (2001), Bathurst and Karpurapu (1993)	Increased relative density results in increased strength and stiffness of reinforced layer.
Membrane modulus	Mhaiskar and Mandal (1992), Dash et al. (2001), Krishnaswamy et al. (2000) Bathurst and Karpurapu (1993) Rajagopal et al. (1999)	Higher modulus results in stiffer and stronger reinforced layer.
Pattern	Dash et al. (2001) Krishnaswamy et al. (2000)	Chevron pattern leads to increased load carrying capacity compared to diamond pattern. Chevron and diamond pattern give similar response
Cell diameter and cell height	Sawwaf and Nazer (2005)	Improvement in BCR with increase in d/D ratio and maximum benefit could be achieved corresponding to d/D ratio of 1.33.Also increased cell height shows increase in bearing capacity.
Distance of placement of reinforcement and length of reinforcement	Mandal and Manjunath (1995)	Reinforcing element resists the lateral displacement of soil underneath the footing and confines the subgrade soil.
Footing depth relative to the cell top	Sawwaf and Nazer (2005)	No effect on the behavior of the model footing.
Cell width and height	Singh et al.(2008)	Bearing capacity increases with increase in B/b ratio and max corresponding to B/b=1.5.Increased cell height show increase in strength
Cell diameter and height	Emersleben and Meyer (2008)	Settlements can be reduced depending upon geo-cell diameter. Settlement decreases with increasing cell height.

Sawwaf and Nazer (2005) used a non-dimensional factor called the bearing capacity ratio (BCR) to compare bearing capacity improvement. This factor is defined as the ratio of the footing ultimate load with soil confinement to the footing ultimate load in tests without soil confinement.

It was observed that a significant increase in the bearing capacity of the model footing supported on confined sand with the increase of normalized cell diameter *d*/*D* until a specific value of *d*/*D* after which the bearing capacity ratio (BCR) decreases with an increase in the *d*/*D* ratio.

Increasing the cell heights results in a greater improvement in the bearing capacity ratio (BCR). This increase in cell height results in the enlargement in the surface area of the cell–model footing leading to a higher bearing capacity load. The slope of the bearing capacity ratio (BCR) versus *h*/*D* curves for *d*/*D* ratios of 0.67 and 2.67 are less than the comparable slopes for *d*/*D* ratios of 1.33 and 1.6.

Sawwaf and Nazer (2005) also reported that using soil confinement could result in an improvement in bearing capacity as high as 17 times more than that without soil confinement. It is clear that the best benefit of soil confinement could be obtained with a (*d*/*D*) ratio between 1.0 to 2.0 with the maximum improvement in the bearing capacity at a ratio of about 1.4 for different heights of confining cells.

It was also observed that varying the foundation depth relative to the cell top has no effect on the behavior of cell–model footing. The difference between the maximum BCR (11.53) and the minimum value (11.06) is 0.47 which is likely to be caused by the slight disturbances that occur in the sand beds while placing the footing within the cell.

Singh et al. (2008) reported that the soil confinement could result in the improvement in bearing capacity as high as 6.75 times more than that without soil confinement and best benefit of soil confinement could be obtained with a B/b (width of footing/width of cell) ratio between 1.0 to 2.0 with the maximum improvement in the bearing capacity at a B/b ratio of 1.5 for different heights of confining cells. It was also observed that increasing cell heights result in greater improvement in the bearing capacity.

Emersleben and Meyer (2008) reported on laboratory tests to investigate the effect of geo-cells. Geo-cells consist of a series of interconnected single cells which are connected at their joints and forming a honeycomb structure. The geo-cells were expanded and filled with soil. The cell walls completely encase the infill material and provide an all around confinement to

the soil. Studied was carried out to evaluate the influence of cell height and cell diameter. Tests were performed on dry sand with maximum particle size 2mm, coefficient of uniformity (Cu) was 3.2 and coefficient of curvature (Cc) was 1.03.The friction angle of the sand used was 38.9^0.

From experiments they found that highest settlements were measured for unconfined dry sand. If sand is reinforced by geo-cell, the settlement was reduced depending upon the geo-cell diameter. With decrease in cell diameter the settlement also decreases. The smallest settlements were measured for a cell diameter of 16cm.The difference between the geo-cell diameter of 160mm and 230 mm was marginal up to a load of $300kN/m^2$. At higher loads the measured settlements were higher for the geo-cell layer with a diameter of 23cm.The highest settlements were measured for a cell diameter of 30cm and settlements were similar to the un-reinforced sand and no significant benefit due to the geo-cell layer was observed.

They also studied the influence of geo-cell height on the load settlement behavior. It was found that measured settlements were decreasing with increase in cell height. The smallest settlements were measured for a cell height 20cm. The improvement of load settlement response due to an increase of the cell height from 15 cm to 20 cm is negligible. Similar results were observed by Dash et al. (2001) and Sitharam and Sireesh (2005).

Recently, using a ring beam or a skirt as soil improvement technique has been investigated by many researchers. They used the ring beam under circular foundation [Mahiyar and Patel (2000); Martin (2001) and Nasser M. Saleh et al. (2008)]. They have noticed a significant improvement in the footing response due to the ring beam resistance to lateral displacement of soil underneath the footing.

Boushehrian and Hataf (2003) and Laman and Yildiz (2003) experimentally investigated the ultimate bearing capacity of ring foundations supported by a sand bed with and without geogrid reinforcement. The results proved that the ultimate bearing capacity values can be improved up to three times that of the unreinforced case.

Rao and Narhari (1979) developed a skirted plug foundation and indicated that the provision of skirting to the soil plug is generally beneficial and can be applied when the settlement is restricted for a given load. Ranjan and Rao (1985) improved the soil by using granular piles surrounded with skirts. They found out that the granular skirted pile foundations have a lot of potentiality for structures which are sensitive to settlement and are subjected to heavy loads.

Ortiz (2001) inserted a discontinuous vertical skirt dowels around existing foundation. A marked increase of 20 % in the bearing capacity and a reduction of settlement were observed. Al-Aghbari and Zein (2004, 2006) carried out tests on strip and circular footing models resting on sand. Their results showed that the use of structural skirts improved the bearing capacity by a factor up to three.

Mahiyar and Patel (2000) have utilized the software package ANSYS to study the effect of using a skirt to prevent footing tilting due to eccentric loading. They provided a downward vertical projection to the footing at the edge near the eccentric load. They indicated that for a given value of eccentricity, the tilt can be reduced to almost zero by providing a vertical skirt.

Bransby and Randolph (1999) used the FEM to study the effect of vertical skirt under strip and circular foundation. Results indicated that the use of skirt with circular foundation gave better improvement than that obtained from strip foundation.

Gourvenec (2002, 2003) applied two and three dimensional finite element analysis to assess the behavior of strip and circular skirted foundations subjected to combined vertical, moment, and horizontal loading. The skirt enhanced vertical, horizontal, and moment load capacity compared to flat foundations.

Yun and Bransby (2003) carried out a series of centrifuge model tests to investigate the response of skirted foundation on loose sand under combined vertical, horizontal, and flexural loading. The tests showed that the horizontal capacity of the skirted foundation was increased to about 3-4 times that of plane foundation. They also suggested that the foundation failure mechanism changed from sliding to a rotational mode.

Appolonia et al. (1968) studied the effect of changing the angle of the skirt connected with the footing on the sand compressibility. They observed that the sand compressibility decreased rapidly as the angle of skirt increased from zero to 30˚ with the vertical, and attained nearly a constant value for angles between 30˚ and 45˚.

Giri (1994) constructed a laboratory model for skirted footing by assembling four plates around the periphery of footing subjected to vibrated eccentric load. Results indicated that increasing the inclination angle of the skirt has a remarkable increase in resonance frequency and a decrease in amplitude.

Madhav and Ghosh (1994) developed a mathematical model for the analysis of a reinforced foundation bed by incorporating the confinement effect of a single layer of reinforcement. It is quantified in terms of the average increase in confining pressure due to the reinforcement

from which modified shear stiffness of the granular soil surrounding the reinforcement are obtained. Parametric studies for plane strain conditions show that the confinement effect of reinforcement leads to an improved mechanical response over the unreinforced granular fill-soft soil foundation system.

Al-Aghbri and Mohamedzein (2004) has proposed a modified equation for skirted strip foundation on dense sand. A series of tests were performed on foundation models to study the factors that affect the bearing capacity of foundation with skirts. The authors have compared the results obtained from the propose equation with the results obtained from Terzaghi (1943), Meyerhof (1963), Hansen (1970) and Vesic (1973) bearing capacity equations for foundations without skirt. The comparison shows that the use of structural skirt can improve the bearing capacity by a factor 1.5 to 3.9 depending on the geometrical and structural properties of the skirt and foundation, soil characteristics and interface conditions of the soil-skirt-foundation system.

Tyagi (2007) investigated the improvement in bearing capacity using skirts but his results suffice to a numerical model which need an experimental verification.

Structural skirts fixed to the edges of the shallow foundations have been used for a considerable time in off shore structures and other situations where water scour may be the problem. **Bransby** and ***Randolph (1998), Watson and Randolph (1998)*** have provided valuable detailed consideration of their use in such applications. However, the use of such structural skirts in conjunction with conventional shallow structural foundations has not been used widely more over the improvement in the bearing capacity occurring from their use has not been investigated in detail.

CHAPTER-III
EXPERIMENTAL PROGRAMME

3.0 General

The organization and execution of the test programme involves the fabrication of apparatus suitable for the model study and carrying out a series of tests in order to have a record of observations.

In the present investigation, model tests have been conducted on circular footings having different diameters. Initially tests were conducted on circular footings without confinement and then for confined case to study their pressure-settlement characteristics. Effect of fines on bearing capacity and settlement has been observed and analysis has been done for different diameter footings. We used model footings of different sizes circular in cross-section. The footings were tested in a mild steel tank fitted with a reaction frame for load application. The tank was filled with dry sand which is maintained at a uniform density by raining it from a height through a pouring device. Load on the footings was applied in increments with the help of hydraulic jacks calibrated through proving rings. The settlement of the footings was recorded after every load increment with the help of deformation dial gauges. Pressure-settlement curves have been plotted.

3.1 Test Material

3.1.1 Ghaggar Sand and Fine Characteristics

Going through the preliminary survey reports of the geology of the area it was decided to obtain sand was from the banks of Ghaggar river. The author investigated specific gravity, grain size distribution, load bearing and settlement characteristics of the Ghaggar sand.

Locally available Ghaggar sand after washing has been used as the foundation bed and it is designated as clean sand. The non plastic fines passing through IS 75μ sieve were used. The fines were prepared in the laboratory. A number of soil samples were taken from a nearby area and then wet analysis was carried out to know the percentage of particles passing 75 μ sieves. After processing, soil was finalized for the preparation of fines having a maximum amount particles passing 75 μ. A wet analysis was carried out on the selected soil samples. The material passing through 75 μ was collected in a container and allowed to settle. The passing material is dried in an oven and thereafter pulverized. The pulverized material was again sieved though 75 μ sieve. Then a hydrometer analysis was carried out as per IS: 2720

[(Part 4)-1985] to know the amount of clay fraction. The amount of clay fraction was found insignificant.

3.2 Footings

The model circular footings with diameters of 0.45m, 0.30m, 0.15m and 0.1m made up of mild steel shown in Plate 1 have been used.

In order to simulate the roughness of actual foundation, the base of the model footing has been made rough by sand of uniform grade.

Plate 3.1 Photograph of footings used

3.3 Confining Cells

In order to investigate the effect of confinement on bearing capacity and settlement characteristics of circular footings, the cells were instrumented in the laboratory. The confining cells of different diameters and heights (Plate 3.2) were instrumented in the laboratory using 0.94 mm thick mild steel plates. The cells were open at both the ends. It was modeled as a circular footing supported on a silty soil which is surrounded by a mild steel cell having same soil outside.

Plate 3.2 Photograph showing confining cell of different diameters and heights

3.4 Characterization

This section contains the details of experimental programme on characterization of silty sands. This includes investigations on various physical and engineering properties of silty sands considered to be relevant to understand the engineering behavior of silty sands.A summary of tests is given in Table (3.1a).

3.4.1 X-ray Diffraction and Electron Microscopy

The X-ray diffraction analysis was carried out to investigate the mineralogical properties of sand and fines. The Ghaggar sand and fines were characterized for the identification of phases by x-ray diffractometer. The identification of specific crystalline mineral was based on Bragg's equation.

$$\lambda = 2d \sin 2\theta \qquad (3.1)$$

Here, λ is the wave length of X-ray specific to the Cu target element (=1.542 $\mathring{A}$) and d is the inter planner spacing. The test was conducted between $10^{\circ}$and 100° (2θ), at the rate of 2°/s using the CuK_{α} characteristic radiation of Cu target element. The inter planner spacing of respective peaks on the X-ray pattern were calculated from the corresponding 2θ angle. These peaks were associated with the characteristic minerals.

The morphology of clean sand and sand with fines was characterized by Scanning Electron Microscope (SEM).These tests were conducted at Indian Institute of Technology, Roorkee.

3.4.2 Grain Size Analysis

The grain size analysis was conducted to estimate the variation in grain size of clean sand and sand with varying proportions of fines. For silt, hydrometer analysis was performed. The grain size analysis was performed in conformity with IS-2720[(Part 4)1985] on samples of clean sand and sand with varying proportions of fines.

3.4.3 Specific Gravity

Specific gravity test was conducted on clean sand and sand with varying proportions of fines in accordance with IS-2720[(Part 3) Sec 2-1980]. It was observed during the tests that the de-aeration takes longer time in silty sands than in clean sands and to achieve the consistency of results, silty sands required de-aeration for not less than 15 minutes.

3.4.4 Shear Strength

The shear strength of clean sand and sand with varying proportions of fines was estimated using direct shear test (Plate 3.3). The shear tests were conducted on constant density in dry state on silty sands. These tests were conducted as per IS-2720 [(Part13) 1986].

Plate 3.3 Photograph showing direct shear test set up

A series of direct shear tests were performed on clean sand and on sands with varying fine content in order to know the effect of fines on the value of angle of internal friction. The samples were prepared by estimating the weight of sand and silt required for desired percentage of fine content. The weighed amount of silt and sand were then mixed properly. The shear box with soil specimen was fitted into position. The normal pressure of 50 kPa was then applied. After the required pressure was applied, the shear strain was applied. The shear strain was applied at a constant rate of 0.2mm/min on the upper half of the box till the

constant value of the proving ring is achieved. The process is to be repeated for the next higher value of normal pressure. By the same procedure two more samples were tested at a normal pressure of 100kPa and 150kPa for different samples of soil having different proportions of fines.

3.4.5 Relative Density

The relative density of sand has been computed as per Indian Standards for determination of density index for cohesionless soils in the apparatus shown in Plate 3.4.

Plate 3.4 Photograph showing relative density test set up

The minimum and maximum void ratios were determined according to IS: 2720 [(Part14)-1983]. Minimum density was obtained by pouring the sand into a standard mould with a volume of 0.003m^3 using a thin walled funnel. The maximum density was obtained by densifying the dry sand in a standard mould of 0.003m^3 using a motorized vertically vibrating table at a frequency of 3600 vibrations per minute, a vibrator with amplitude variable between 0.05 and 0.65 mm under 1.15 kN load. The loaded specimen was vibrated on vibrating table for 8 minutes. A constant relative density of (~52 percent) has been maintained throughout the test programme.

3.5 Model Plate Load Test

3.5.1 Test Set-up

The size of the tank was designed keeping in view the size of the footing to be tested and its zone of influence. For small scale plate load test, a tank of inner plan dimensions of 0.6m X

0.6m and a height of 0.6m was made up of 10mm thick mild steel sheet for a footings of diameter 100mm and 150mm as shown in Plate 3.5.For large scale plate load test, a tank of inner plan dimensions of 1.5m X 1.5m and a height of one meter was made up of 10mm thick mild steel sheet for footings of diameter 300mm and 450mm as shown in Plate 3.6.

Plate 3.5 Photograph of small scale plate load test (0.6m X 0.6m X 0.6m)

Plate 3.6 Photograph of large scale plate load test (1.5m X 1.5m X 1.0m)

The stiffeners supported the vertical plates so that no lateral movement of plate took place when the load was applied. Inside faces of tank have been marked with horizontal parallel bands at a depth interval of 10cm so as to serve as guide marks for depositing the sand layers.

3.5.2 Tank Filling Techniques

The placement and compaction of the fill material are important for any model study. The density of sand should be controlled and it should remain the same throughout the test programme. To obtain a uniform and reproducible density, the sand is deposited by rainfall

technique. Placement of sand by rainfall depends mainly upon the intensity of rain and the height of fall. The intensity of rain depends upon the size of holes and their spacing in the pouring device. For a given intensity of raining, increase in height of fall increases the density.

A box, 500mm long, 500mm wide and 50mm deep open at top made up of 0.5mm thick steel sheet was made to serve as a pouring device .It was having the perforations of 4mm diameter at 25mm centre to centre spacing in longitudinal as well as transverse direction. The dry sand was deposited in the tank in 100mm layers by spreading it in the pouring device and allowing it to fall freely. A 100mm fixed height of fall was adopted for deposition of sand to maintain a density of 16.6kN/m^3. The density was maintained constant throughout the experimental programme by removing the affected sand layers after each test and repeating the same procedure of sand filling as stated above.

3.5.3 Loading Arrangement and Measuring Devices

The loading system was designed to ensure that the application of load on the footing is vertical. The loading devices were such that there was no possibility of developing eccentric loading.

A reaction loading frame was specially designed and fabricated for applying load on the footings. The complete unit was fixed on two vertical channel sections stiffened at top and bottom (Plate 3.7). The loading frame was designed in such a way that its position can be adjusted at the required height.

The load on the footings was applied by hydraulic jacks calibrated through 10t capacity proving rings. The hydraulic jacks took reaction from the reaction frame. Any release of load due to the settlement of footing was compensated by operation of the jack. Steel ball was placed between the proving ring and the hydraulic jack to maintain verticality of loads.

The settlement of the footings was recorded after every load increment with the help of sensitive dial gauges with a least count of 0.01mm, mounted on magnetic stands fixed on independent datum bars.

Plate 3.7 Photograph of test tank showing different components.

3.5.4 Experimental Procedure

The Ghaggar sand was deposited in the tank in layers of 100mm by pouring it from a fixed 50mm height of fall to maintain a uniform density of 16.6kN/m^3 (Relative density = 50.77%). It was filled in the tank up to a desired height and leveled with a wooden straight edge. The model footings were placed over the leveled surface of sand with proving ring and hydraulic jack mounted on them. A summary of experimental programme is given in Table (3.1b).

Before the commencement of the load test, a seating load of 0.7 kN/m^2 was applied which was released before the start of actual test. This was done to ensure the proper contact of base of footing and soil and to account for any looseness due to disturbance of top soil. The load was applied in increments of approximately one-sixth of estimated failure load of an isolated footing. For each load increment deformations were recorded until deformation recorded per hour was less than 0.01mm (Plate 3.8). Any decrease in load due to settlement of footing was compensated by operating a jack. The load increments were given until failure of the deposit was marked by a large settlement at a constant load.

Table 3.1(a). A summary of tests for characterization

SN	Property	Name of the test	Variable parameter	No. of tests
1	Mineral	X-ray diffraction	FC=0 and 100%	02*
2	Particle size and shape	Electron microscopy	FC= 0,5,10,15,20,25 and 100%	07
3	Specific gravity	Pycnometer	FC= 0,5,10,15,20,25 and 100%	07*
4	Particle size distribution	Sieve analysis	FC= 0,5,10,15,20 and 25%	07
5		Hydrometer analysis	FC=100%	01*
6	Void ratio	Relative density	FC= 0,5,10,15,20,25 and 100%	07*
7	Angle of internal friction	Direct shear test	FC= 0,5,10,15,20,25 and 100%	07*
* Checks for reproducibility applied				

Table 3.1 (b). A summary of experimental programme

SN	D (m)	Confinement parameters	Variables	No. of tests*
A. Load tests without cellular confinement				
1	0.1, 0.15		FC=0, 5, 10,20 and 25%	12
	0.3, 0.45		FC=0, 5 and 10%	06
B. Load tests with cellular confinement				
2	0.1	d/D = 1.0, h/D =0.5, z/h = 0.0	FC=0, 5, 10,20 and 25%	05
3		d/D = 1.0, h/D =1.0, z/h = 0.0	FC=0, 5, 10,20 and 25%	05
4		d/D = 1.0, h/D =1.5, z/h = 0.0	FC=0, 5, 10,20 and 25%	05
5		d/D = 1.5, h/D =0.5, z/h = 0.0	FC=0, 5, 10,20 and 25%	05
6		d/D = 1.5, h/D =1.0, z/h = 0.0	FC=0, 5, 10,20 and 25%	05
7		d/D = 1.5, h/D =1.5, z/h = 0.0	FC=0, 5, 10,20 and 25%	05
8		d/D = 2.0, h/D =0.5, z/h = 0.0	FC=0, 5, 10,20 and 25%	05
9		d/D = 2.0, h/D =1.0, z/h = 0.0	FC=0, 5, 10,20 and 25%	05
10		d/D = 2.0, h/D =1.5, z/h = 0.0	FC=0, 5, 10,20 and 25%	05
11	0.15	d/D = 1.0, h/D =0.5, z/h = 0.0	FC=0, 5, 10,20 and 25%	05
12		d/D = 1.0, h/D =0.75, z/h = 0.0	FC=0, 5, 10,20 and 25%	05
13		d/D = 1.0, h/D =1.0, z/h = 0.0	FC=0, 5, 10,20 and 25%	05
14		d/D = 1.5, h/D =0.5, z/h = 0.0	FC=0, 5, 10,20 and 25%	05
15		d/D = 1.5, h/D =0.75, z/h = 0.0	FC=0, 5, 10,20 and 25%	05
16		d/D = 1.5, h/D =1.0, z/h = 0.0	FC=0, 5, 10,20 and 25%	05
17		d/D = 2.0, h/D =0.5, z/h = 0.0	FC=0, 5, 10,20 and 25%	05
18		d/D = 2.0, h/D =0.75, z/h = 0.0	FC=0, 5, 10,20 and 25%	05
19		d/D = 2.0, h/D =1.0, z/h = 0.0	FC=0, 5, 10,20 and 25%	05
21	0.3	d/D = 1.0, h/D=0.5, z/h = 0.0	FC=0, 5 and 10%	03
22		d/D = 1.5, h/D=0.5, z/h = 0.0	FC=0, 5 and 10%	03
23		d/D = 2.0, h/D=0.5, z/h = 0.0	FC=0, 5 and 10%	03
24	0.1	d/D = 1.0, h/D = 0.5, FC =10%	z/h =0.0, 0.2, 0.4, 0.6, 0.8	05
25		d/D = 2.0, h/D = 0.5, FC =10%	z/h =0.0, 0.2, 0.4, 0.6, 0.8	05
26	0.15	d/D=1.5, h/D = 0.5, FC =10%	z/h =0.0, 0.2, 0.4, 0.6, 0.8	05
* Checks for reproducibility applied				

All the tests were repeated twice and sometimes even more to check the reproducibility of the test results.

Plate 3.8 Photograph of dial gauges for measurement of settlement of a plate

CHAPTER - IV
RESULTS AND DISCUSSION

4.0 General

This chapter is divided into two sections. Section one deals with the analysis of the results of characterization. Section two deals with the analysis of the results of bearing capacity and settlement characteristics of circular footings on confined silty sands.

The focus of this section is to understand the engineering behavior of silty sands in relation to their physical and engineering characteristics. Attempts have been made in the subsequent sections to explain the load bearing and settlement characteristics of silty sands on the basis of physical and engineering characteristics.

4.1 Characterization

The various test results analyzed to characterize are dealt within this section. This includes the results of x-ray diffraction, electron microscopy, grain size analysis, specific gravity, relative density and shear strength.

4.1.1 X-ray Diffraction

The X-ray diffraction [Fig 4.1 (a) & (b)] shows the diffraction pattern of fine and clean sand respectively. The sand and fines selected for evaluation of their bearing capacity were characterized by various established techniques. X-ray diffraction study was carried out to identify the various phases present in sand and fines. X-ray diffraction of sand showed the existence of SiO_2 phase only .The fines contain $Al_3Si_3O_{10}(OH)_{10}$ phase alongwith SiO_2 phase. However, the volume fraction of $Al_3Si_3O_{10}(OH)_{10}$ is very less as compared to SiO_2 . In addition to this the X-ray diffraction of fines also shows the peak shifting at higher diffraction angle with peak broadening which clearly indicates that the fines are more disordered as compared to the sand.

Comparing the X-ray diffraction pattern of the clean sand and fines with natural soil of similar gradation it is understood that natural fill may contain peaks of clay minerals such as kaolinite, montmorillonite, illite or chlorite. The quartz, kaolinite, montmorillonite show their presence among the mass amorphous substance even at a very low percentage (2%). Heating these components beyond 500^0C in furnace may destroy layer spacing in the crystal structure of kaolinite but montmorillonite, illite, mica, vermiculite and chlorite retain their approximate

layer spacing. Therefore, they can be identified well in the x-ray diffraction pattern. A detailed treatment on identification and quantitative analysis of various soil mineral species may be found out in the works of MacEwan (1946), Brown (1961), McCalib (1966) and Klug and Alexander (1974).

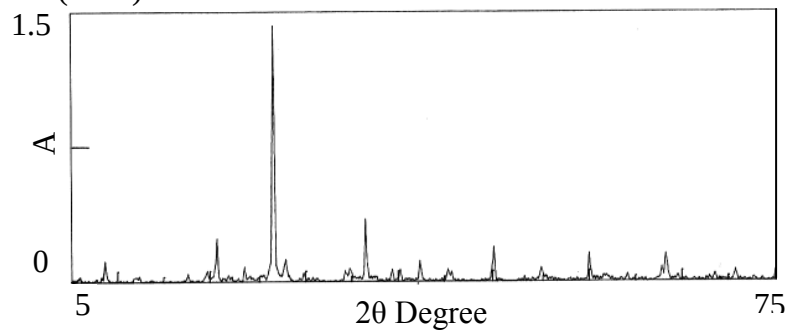

(a)

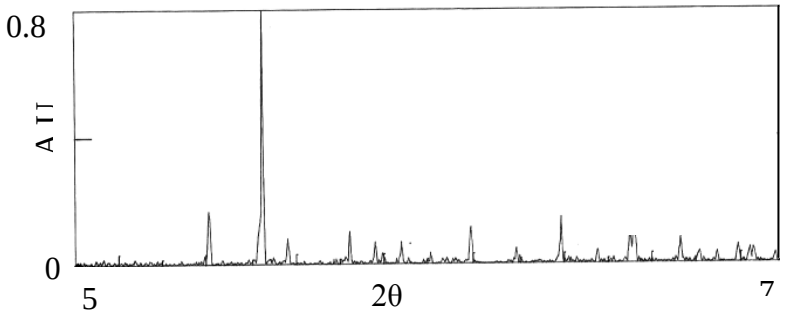

(b)

Fig. 4.1 X-ray diffraction pattern of: (a) Fines; (b) Clean sand

4.1.2 Electron Micrographs

A detailed micrographic investigation of clean sand and sand with varying amount of fines samples is presented in the Fig (4.2). Electron micrographs of clean sand samples suggest the presence of predominantly coarse grain particles. It also suggests that clean sand contains rounded and sub-rounded particles. It also suggests that clean sand samples contain very less amount of fines. The electron micrograph of silty sands indicates that as the fines are added to clean sand, the fines have tendency to adhere to the sides of sand particles. All the fines have tendency to form agglomerates. Agglomeration is the tendency of fines to stick together and appear as larger particle.

The structural features of clean sand have been presented in Fig (4.2) which has been taken at different magnifications. Fig. [4.2 (a)] represents the low magnification micrograph where sand particles of different sizes can be seen which varies from 80 micron to 600 micron size. The feature reveals that small sized particles are nearly spherical in nature and bigger size particles are faceted type. The higher magnification micrograph from Fig [4.2(a)] gives the

topological view on the sand particles. The flow patterns observed at the surface of the sand indicate that the formation of sand has occurred due to weathering action. The contours observed at the surface further indicate that the particle size itself gets reduced either by tumbling action which causes wear and tear.

Fig [4.2(b)] reveals the micrograph of fines. Here also similar morphology as in the case of sand is seen but the size of the particles is reduced to greater extent. The particle size varies from 1 micron to 75 micron. The interesting feature is that at some places smaller size particles get themselves sticked to bigger size particles. This is because of the fact that surface charges do build up and smaller size particles are being attached to that one. The particle coagulation in fines can also be seen.

The structural features of sand mixed with fines: Fig. [4.2(c)] to Fig [4.2(g)] represent the structural features of sand mixed with fines containing 5 to 25% at the interval of 5% fines respectively. Here also two different types of distribution can be seen. One is the coarse one which corresponds to sand particles and the other one to the fine particles. The important feature in case of 5% fines which is shown in Fig [4.2(c)] is that both conglomerates of particles are segregated. However, some fines can be seen in between sand particles. Fig [4.2(d)] represents the SEM micrograph of sand containing 10% fines. In this case the volume fraction of fine particles nearer to sand particles increases. As the amount of fines is increased from 10 to 15%, it is observed that fines occupy the available space as well as they are sticking to the surface of sand particles. One of the important structural features observed in 25% fines is particles of small size get themselves coagulated and acquire bigger size. Such types of feature can only be observed when there is charge existing at the surface of the particles. Another feature observed is that fine particles interlock with bigger particles at rugged surfaces. The charging phenomenon observed on the surface of the particles further supports this theory.

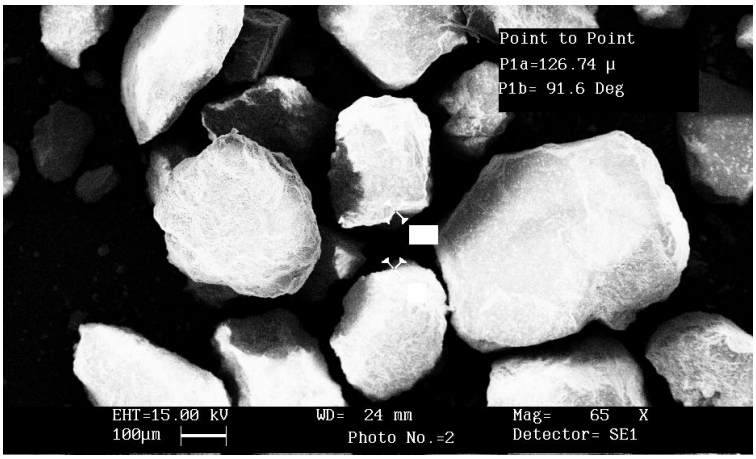

(i)

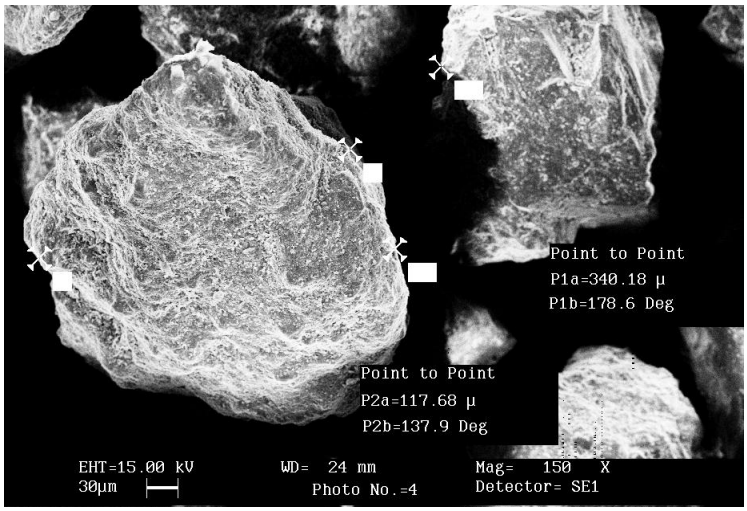

(ii)

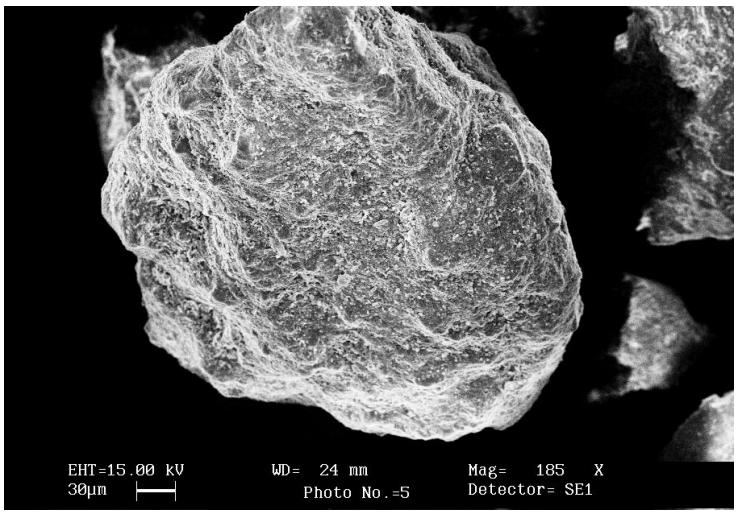

(iii)

Fig. 4.2(a) SEM pictures of clean sand

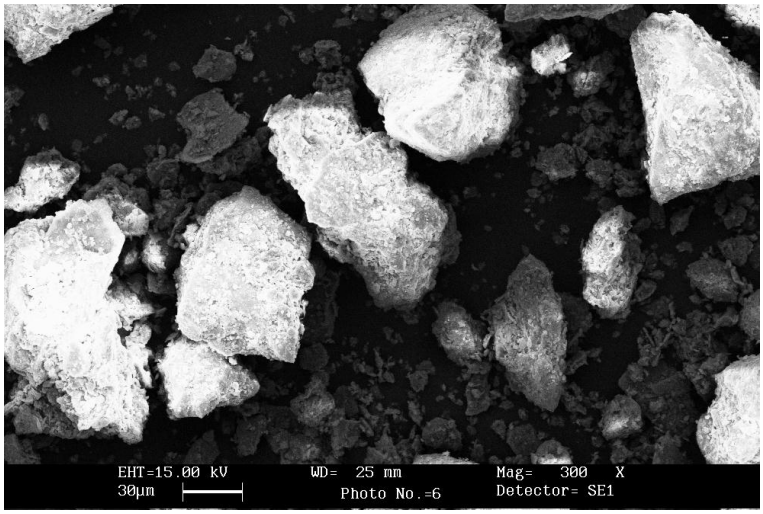

(i)

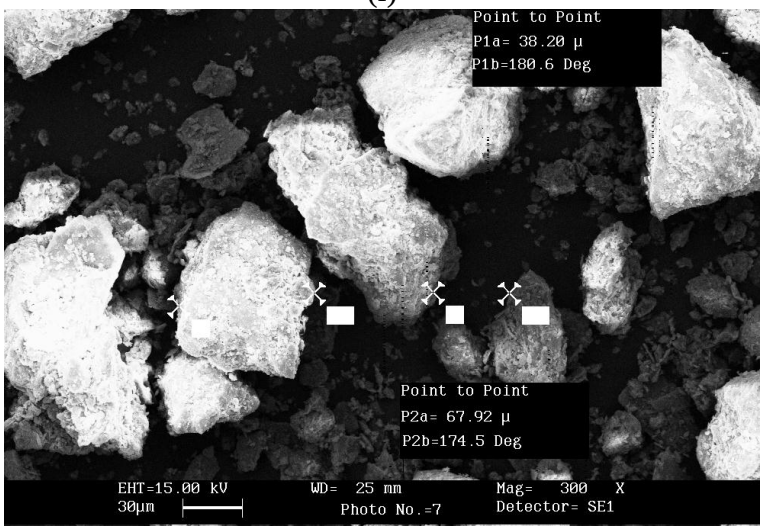

(ii)

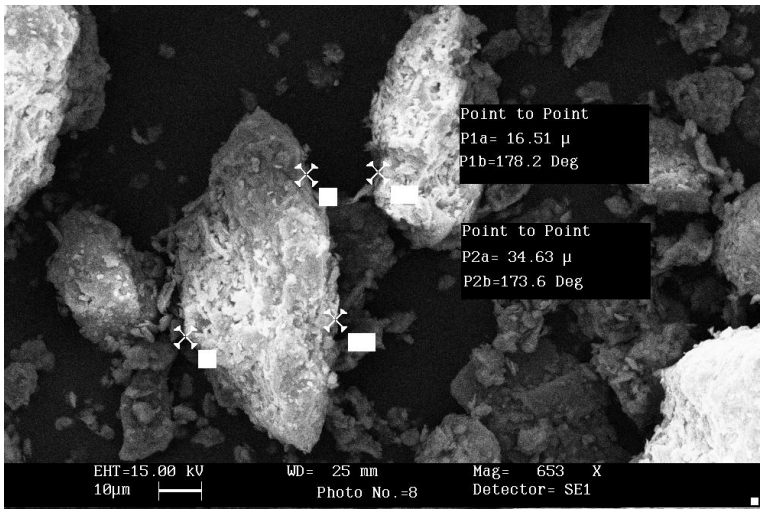

(ii)

Fig. 4.2(b) SEM pictures of fines (soil particles size less than 75 microns)

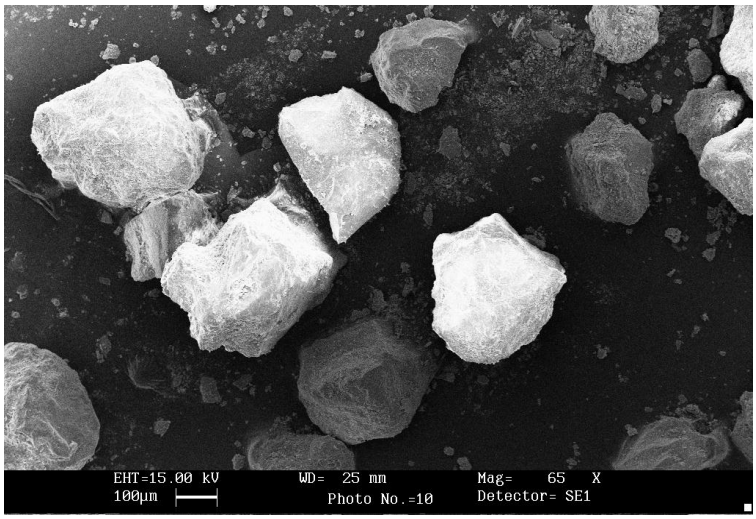

(i)

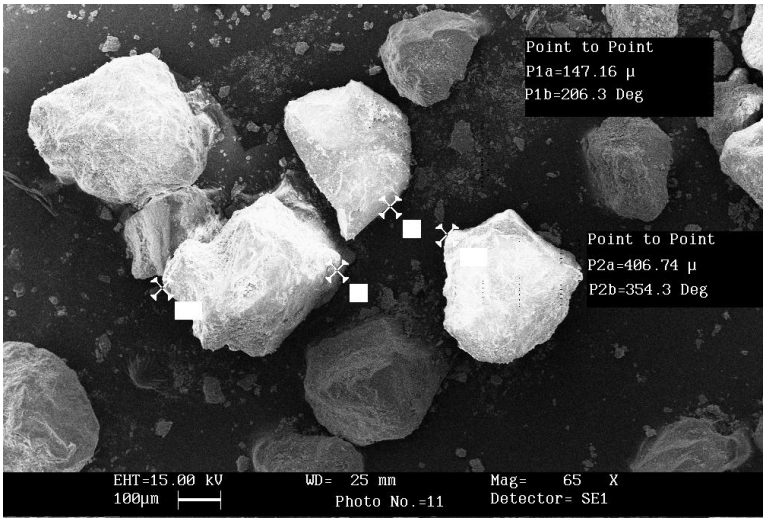

(ii)

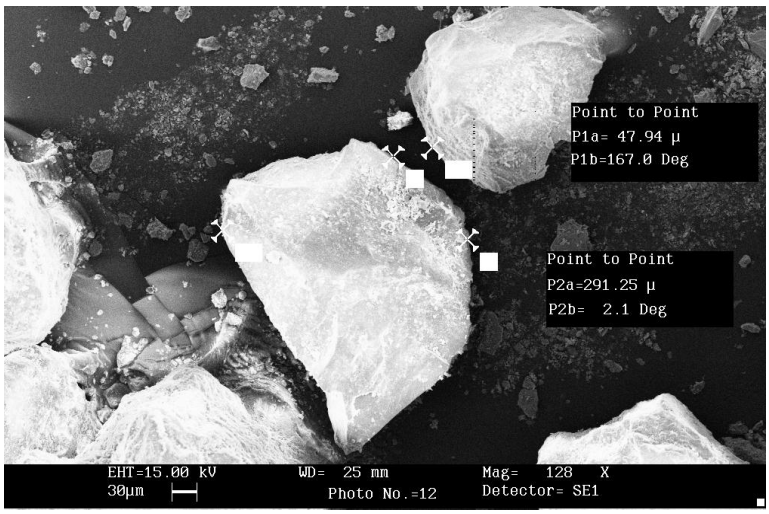

(iii)

Fig. 4.29(c) SEM pictures of sand containing 5% fines

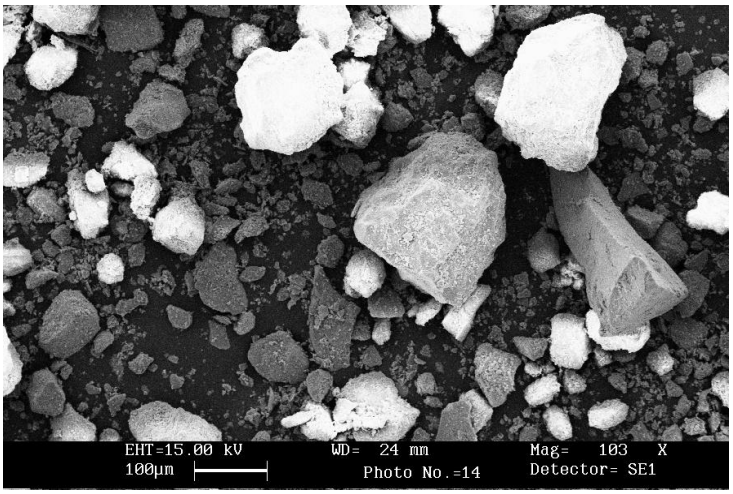

(i)

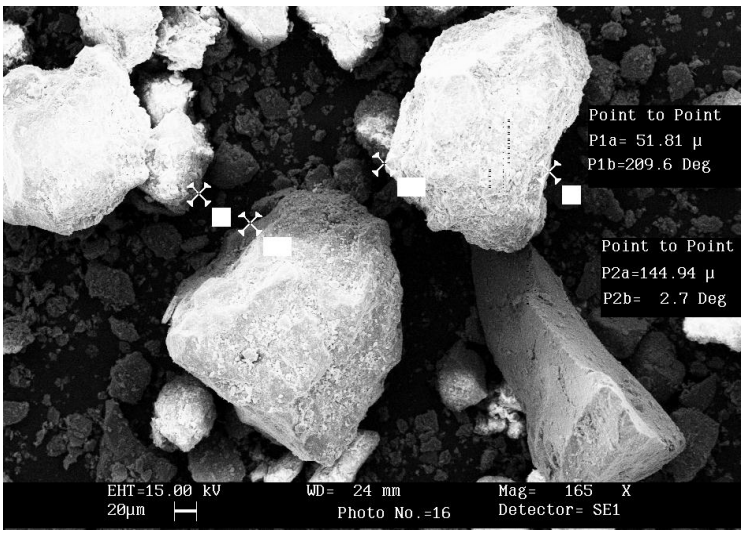

(ii)

Fig. 4.2(d) SEM pictures of sand containing 10% fines

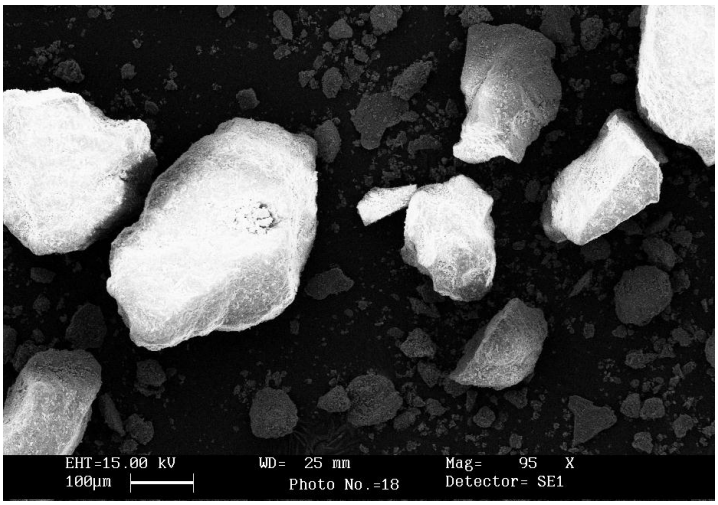

(i)

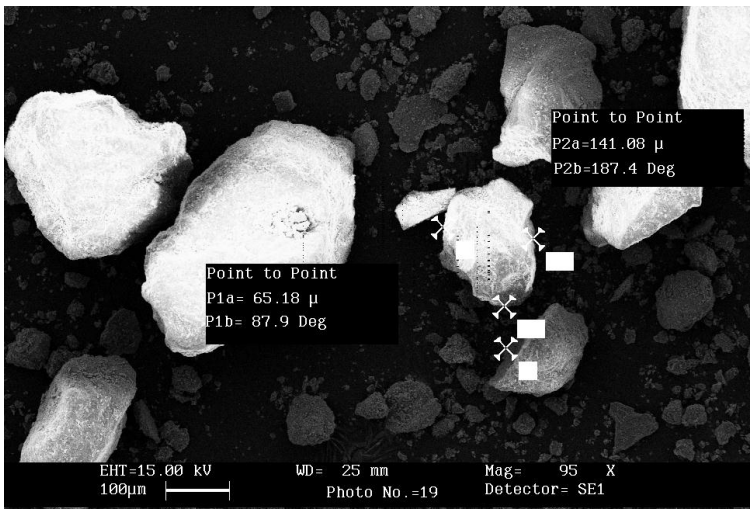

(ii)

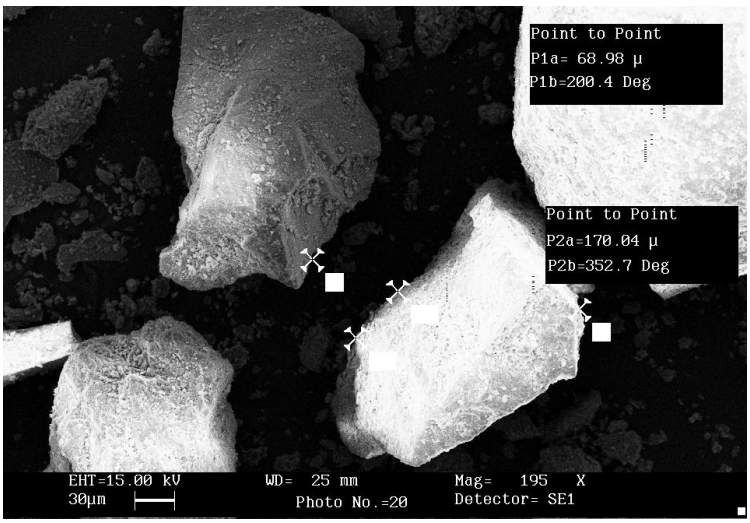

(iii)

Fig. 4.2(e) SEM pictures of sand containing 15% fines

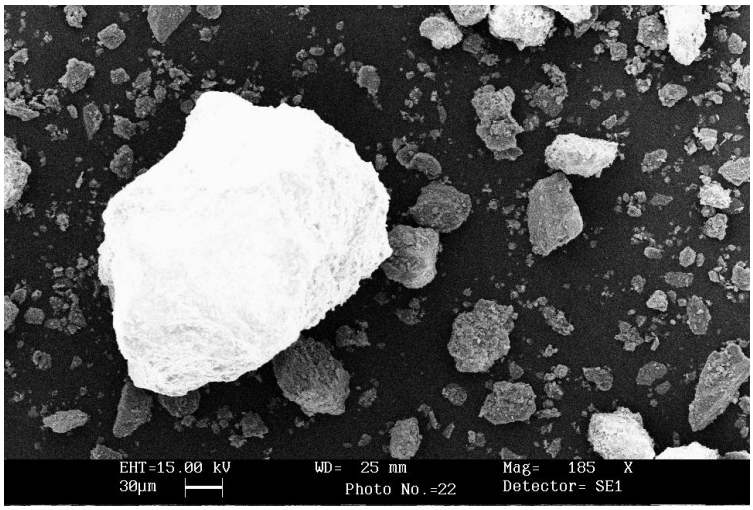

(i)

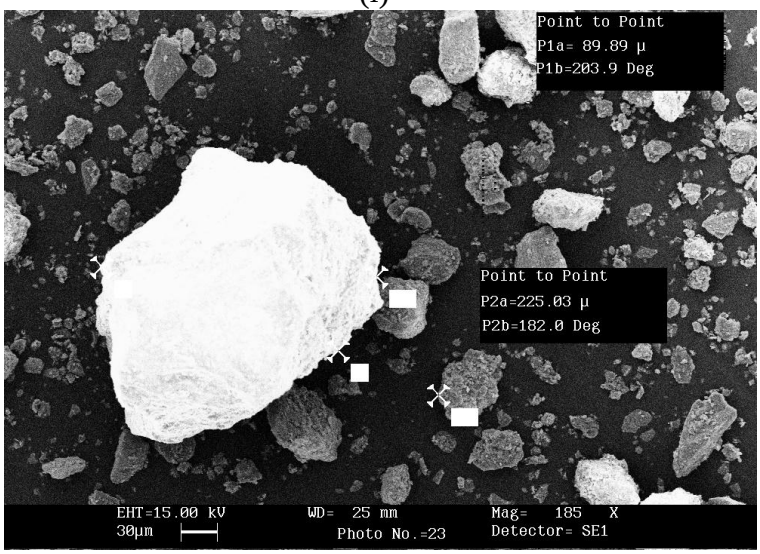

(ii)

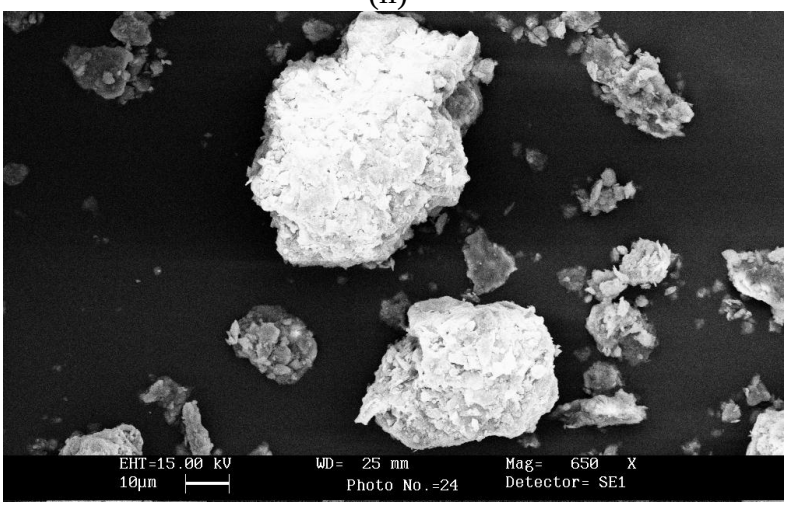

(iii)

Fig. 4.2(f) SEM pictures of sand containing 20% fines

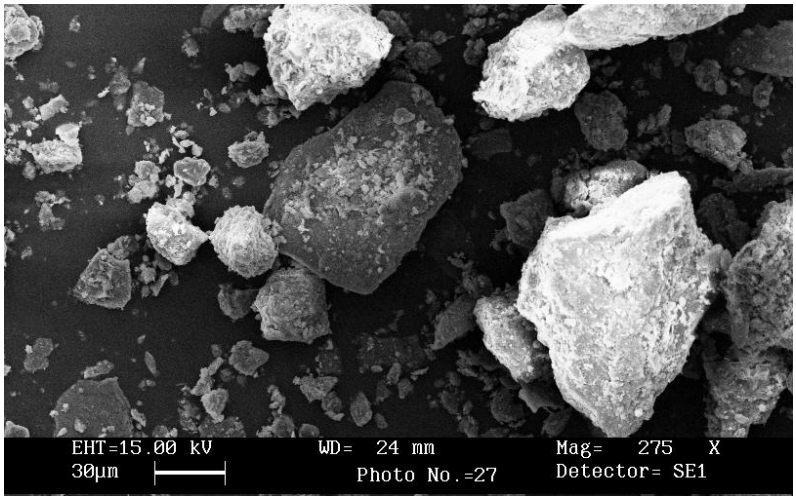

(i)

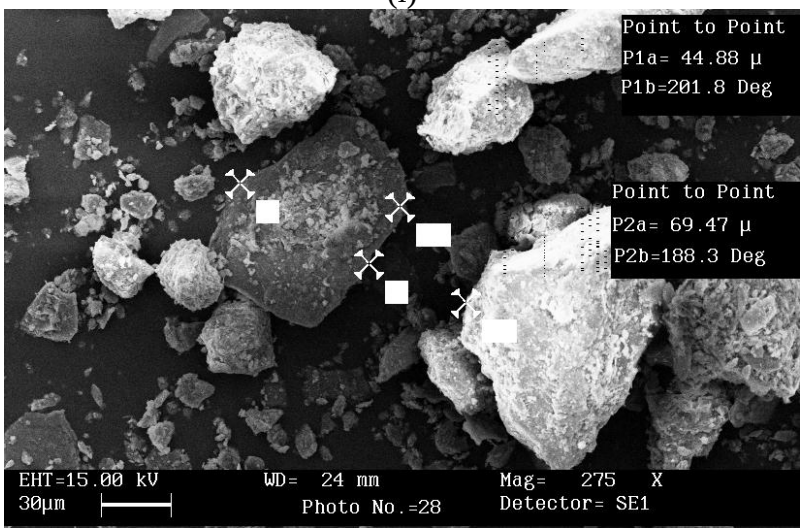

(ii)

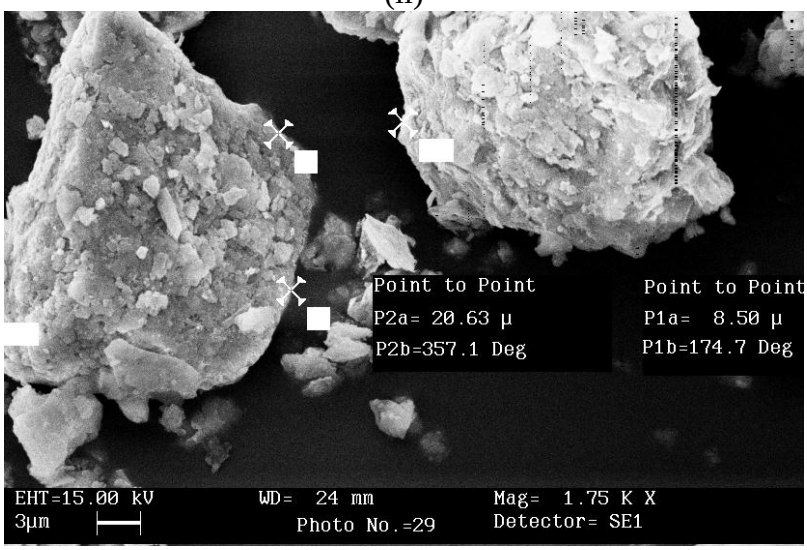

(iii)

Fig. 4.2(g) SEM pictures of sand containing 25% fines

4.1.3 Grain Size Distribution

The grain size distribution of clean sand and sand with varying amount of fines is shown in Fig (4.3). The clean sand contains particle sizes in the range of coarse sand to fine sand as shown in Fig (4.3).

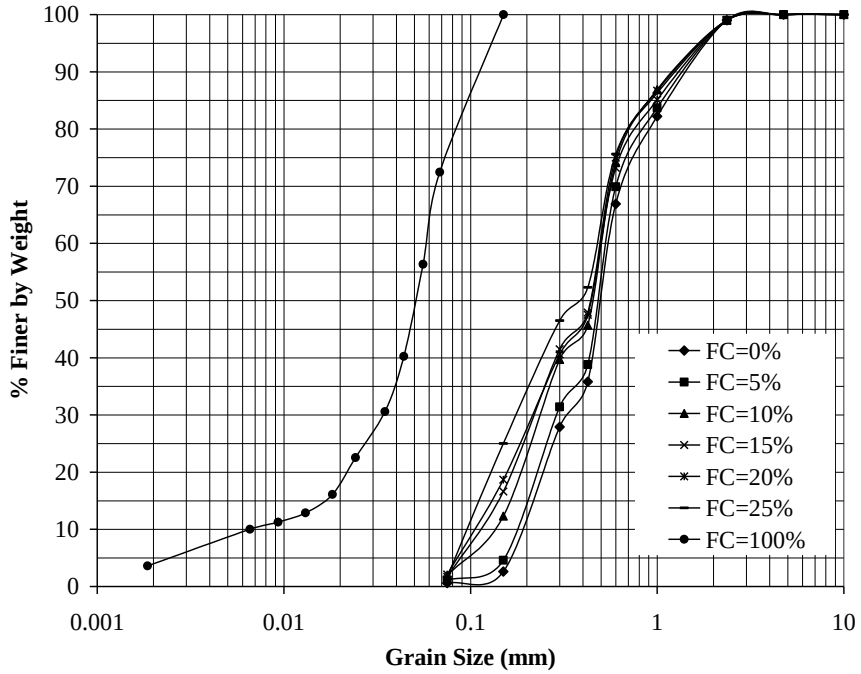

Fig. 4.3 Grain size distribution of the sand, silt and their combinations

However, the maximum frequency of particles is in the range of coarse sand to medium sand. The clean sand which was examined for bearing capacity behavior contains 60-65% of particles in coarse and medium sand size, 30-35% in fine sand size and 1-2 % of particles in the range of silt. Hydrometer analysis was also carried out on silt in order to plot grain size distribution curves as shown in Fig (4.3) along with clean sand. Table (4.1) presents the details of gradation of particles in clean sand and sand with varying amount of fines.

Table 4.1 Details of gradation of clean sand and sand with varying amount of fines

Fine Content (%)	D_{10}	D_{30}	D_{50}	D_{60}	C_c	C_u
0	0.19	0.33	0.50	0.56	1.007	2.90
5	0.18	0.29	0.488	0.54	0.87	3.02
10	0.11	0.24	0.45	0.51	1.17	4.70
15	-----	0.23	0.438	0.50	---	---
20	-----	0.22	0.44	0.51	---	---
25	------	0.18	0.37	0.48	---	---

It can be seen from the Fig (4.3) that the clean sand is poorly graded soil and the coefficient of uniformity increases with addition of fines.

4.1.4 Specific Gravity

The specific gravity of soil grains is an important property and is used in calculating the other basic parameters. Its value helps to some extent in identification and classification of soils. It gives idea about the suitability of the soil as a construction material, higher value of specific gravity give more strength for foundations. The specific gravity of clean sand and that of fines was determined and is as shown in Table (4.2). The specific gravity of clean sand was found to be 2.67. Form the table it is clear that the value of specific gravity decreases on the addition of fines and thereafter follows a constant value of 2.63.It can be concluded that there is not much effect of fines on the value of specific gravity of clean sands.

4.1.5 Relative Density

The results of relative density tests were analyzed for clean sand and sand with varying proportion of fines. It can be seen from the Table (4.2) that the minimum void ratios of silty sand decrease with increase in fines from 0 to 20%. If the fines are added beyond 20%, the maximum and minimum void ratio of silty sands increases. Similar trends were observed by Lade and Yamamuro (1997) for Navada and Ottawa sands mixed with non-plastic fines.

Table 4.2 Values of relative density, unit weight, maximum and minimum void ratios with fines content

FC (%)	γ_{min} (kN/m^3)	γ_{max} (kN/m^3)	γ_{nat} (kN/m^3)	RD (%)	e_{min}	e_{max}	e_{nat}	e_{sk}	G	ϕ (degrees)
0	15.60	17.70	16.60	50.77	0.51	0.71	0.61	0.61	2.67	42.50
5	15.60	18.50	16.95	50.80	0.44	0.71	0.57	0.66	2.63	41.00
10	15.50	19.00	17.15	51.98	0.40	0.72	0.55	0.73	2.63	39.02
15	15.60	19.30	17.32	51.80	0.38	0.71	0.54	0.81	2.63	38.01
20	15.70	19.50	17.58	54.87	0.37	0.70	0.52	0.89	2.63	37.14
25	15.40	19.20	17.15	51.88	0.39	0.73	0.56	1.07	2.63	36.12
100	8.80	13.30	10.62	50.65	1.00	2.03	1.47	-	2.63	28.38

Lade and Yamamuro (1997) explained the pattern of decrease in the maximum and minimum void ratios of silty sand with increase in fines content. With increase in the percentage of fines in a dense or loose sand matrix, most of the fine particles initially occupy the voids among the sand particles. This represents the reduction in void ratio with increase in the amount of fines. Some silt particles, however, end up between the surfaces of adjacent sand

particles. Such particles would tend to cause an increase in void ratio, as they do not occupy the natural void space left by the sand matrix. This process pushes sand particles apart.

For a given overall void ratio, they completely (or almost completely) separate adjacent sand particles. An easy way to determine the fines content for which this happens is based on the concept of skeleton void ratio e_{sk} [Kuerbis et al. (1988)], which is the void ratio of the silty sand calculated as if fines were voids

$$e_{sk} = \frac{(1+e)}{(1-f)} - 1 \qquad (4.1)$$

Where e = overall void ratio of soil; and f =ratio of weight of fines to the total weight of solids. Whenever e_{sk} is greater than the maximum void ratio $(e_{max})_{f=0}$ of clean sand, the sand matrix exists with a void ratio higher than it could achieve in the absence of fines. It means that the sand particles are, on average, not in contact and the mechanical behavior is no longer controlled by the sand matrix.

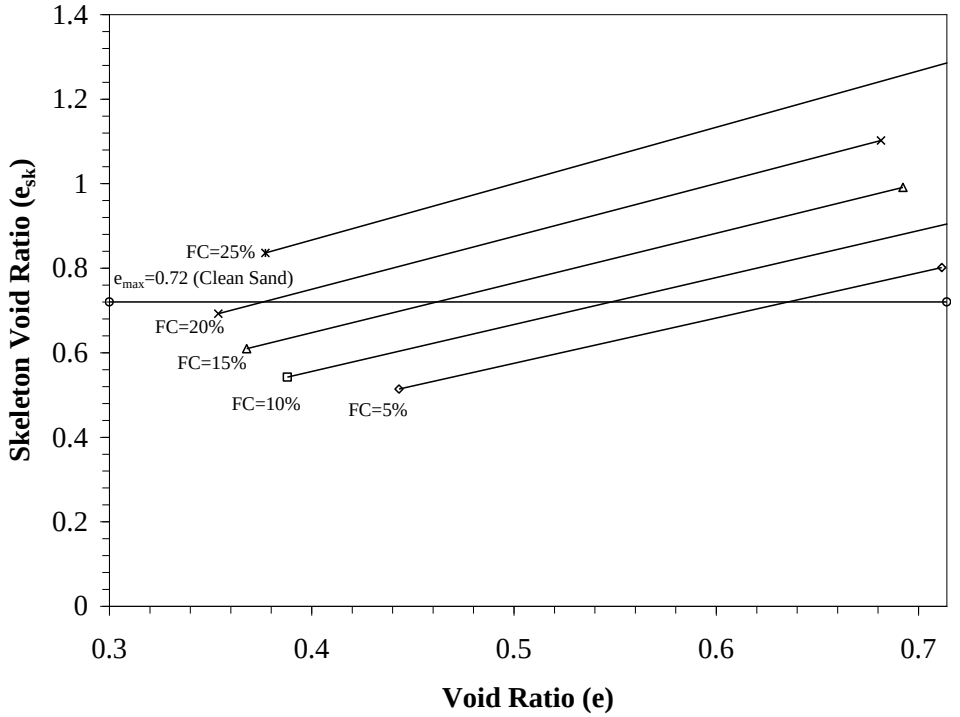

Fig.4.4 Limiting void ratio for 5, 10, 15, 20 and 25% silt content

Fig (4.4) shows the skeleton void ratio as a function of void ratio for 5, 10, 15, 20 and 25% fines. For each gradation, a limit void ratio (and a corresponding limit relative density) can be defined. For Ghaggar clean sand, with e_{max} = 0.72, these relative densities are 28.52% for 5% fines, 50.96% for 10% fines, 70.98% for 15% fines and 93.23% for 20% fines. From Fig

(4.4), it is also clear that the calculation of the limit void ratio is not possible for fine content of 25%. For relative densities lower than the limit relative density, the fines control and the behavior becomes that of a sandy silt or sandy clay, depending on the nature of the fines. For soils denser than the limit relative density, the behavior is as that of sand, modified by the presence of fines.

Fig (4.5) shows the variation of different types of void ratios with fines content. From the graph it has been seen that skeleton void ratio increases on addition of the fines whereas natural, minimum and maximum void ratios decrease when fine content is increased up to 20%.When fines are increased further the void ratios increase.

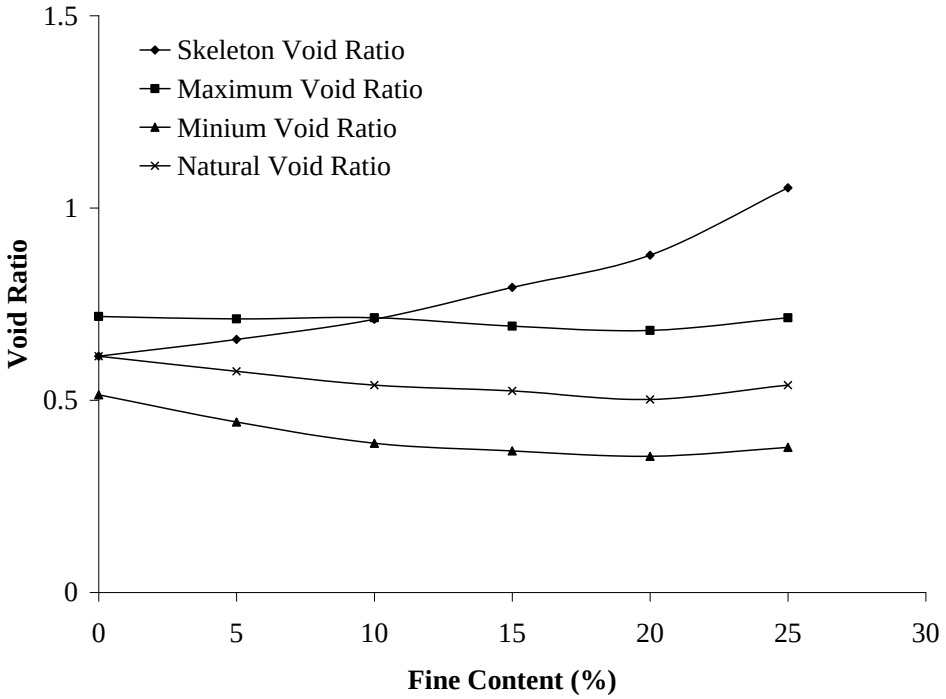

Fig. 4.5 The Skeleton, minimum, maximum and natural void ratio vs. fine content.

It has also been seen that skeleton void ratio is higher than maximum void ratio when fines content is increased beyond 10%. Skeleton void ratio (e_{sk}) is greater than the maximum void ratio $(e_{max})_{f=0}$ of clean sand corresponding to a fines content of 10%. It means that the sand particles are, on average ,not in contact and the mechanical behavior is no longer controlled by the sand matrix.

4.1.6 Shear Strength

The shear strength of clean sand and sand with varying amount of fines was determined in direct shear test at a constant density in order to know the effect of fines on the angle of

internal friction. Typical results of direct shear tests for clean sand and sand with varying proportions of fine content are presented in Fig (4.6) to Fig 4.8.

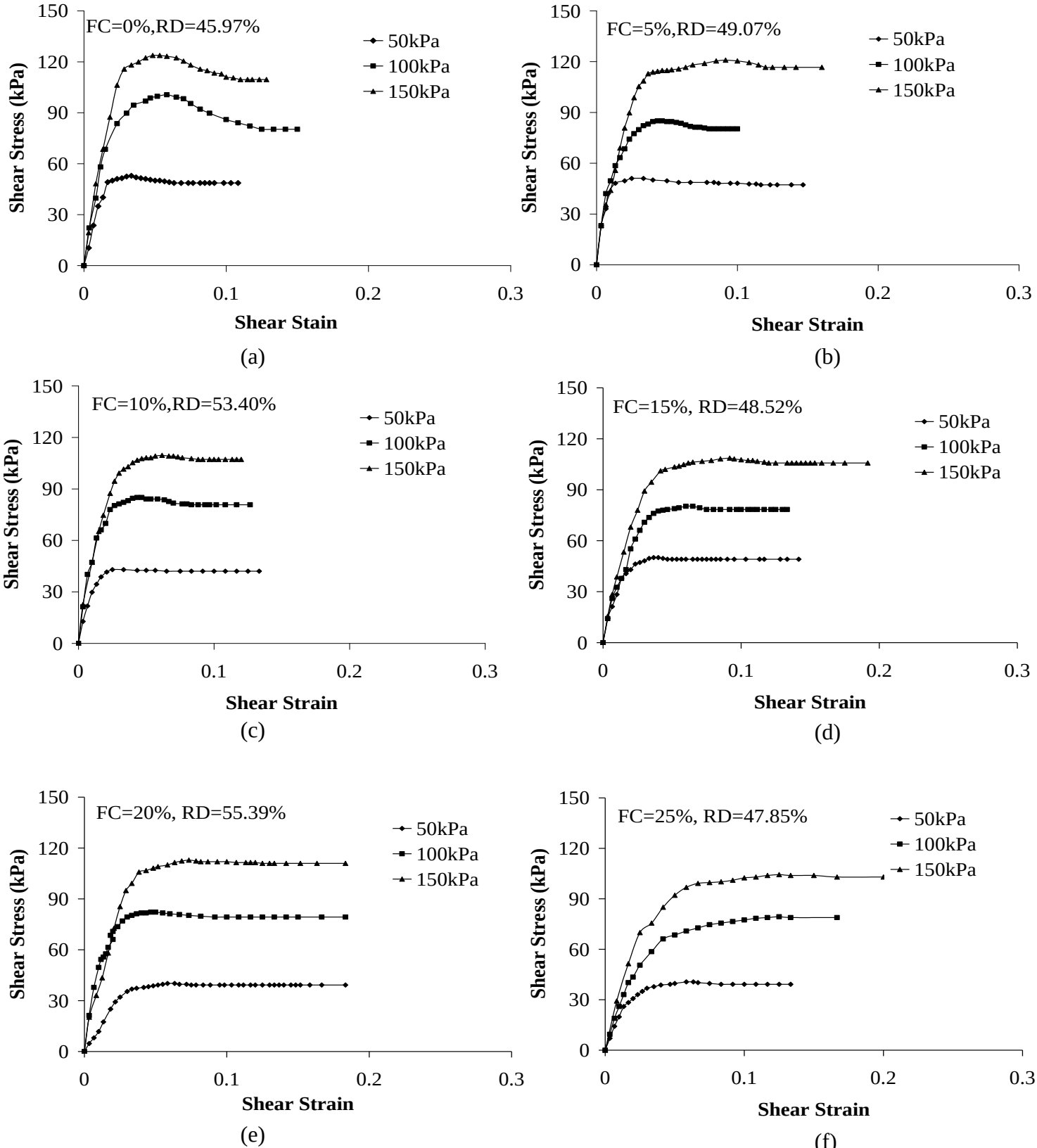

Fig.4.6 Results of direct shear tests for samples of: (a)clean sand and sand with varying proportions of fines;(a)0%; (b) 5%; (c) 10%; (d) 15%;(e) 20%; (f)25%

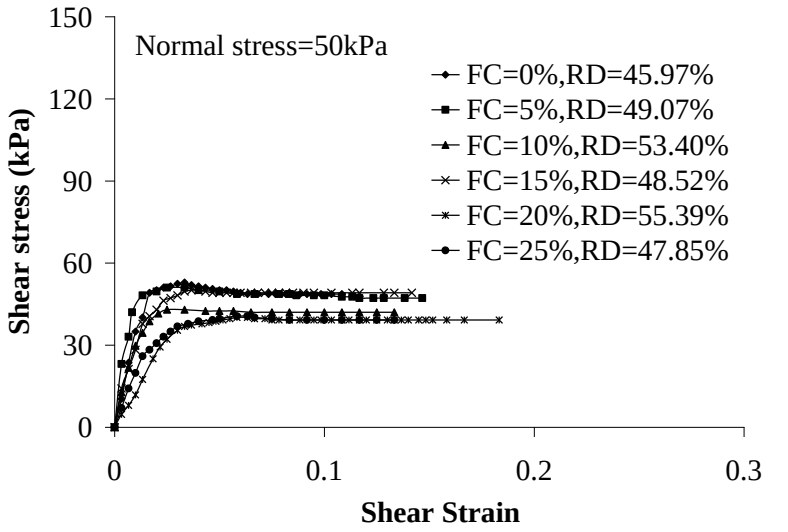

(a)

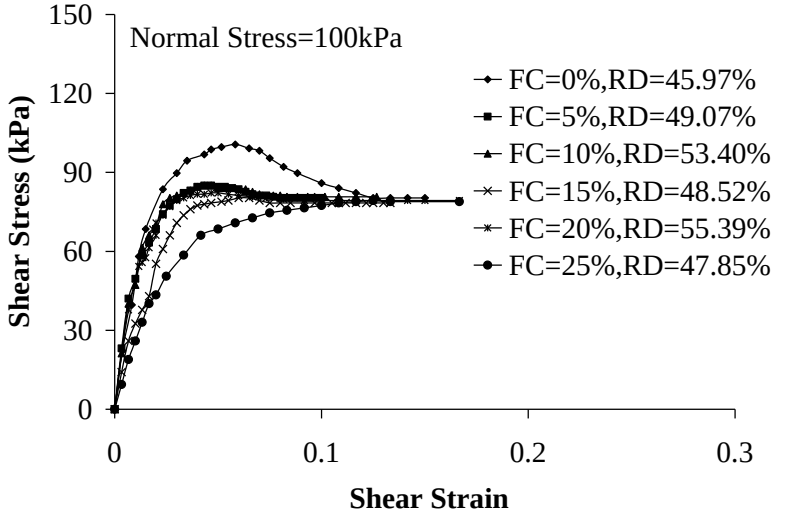

(b)

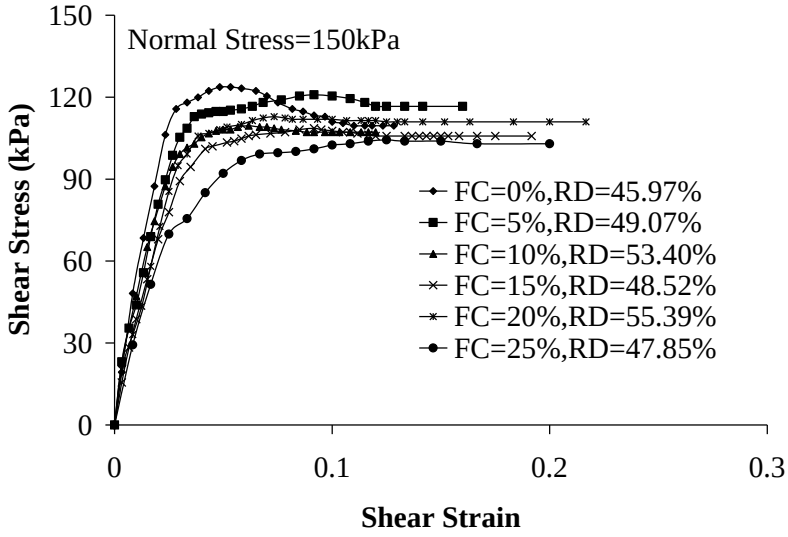

(c)

Fig.4.7 Direct shear test of clean sand with different proportions of fines under a normal stress of: (a) 50 kPa; (b) 100 kPa and (c) 150 kPa

It has been seen that with increase in fines content, failure shear stress decreases. The stress-strain curve for the clean sand shows a definite peak occurring at a relatively low strain. The peak stress decreases sharply with increasing strain and the shear stress becomes more or less constant, if the soil is continued to be sheared. When a clean sand with fines of different proportion is sheared, the stress increases with strain more gradually as compared to clean sand and maximum shear stress finally approaches a value very close to the value as obtained in case of clean sand [Fig (4.7].

Fig. 4.8 indicates a plot of shear stress and normal stress. It has been observed that the slope of failure envelope decreases with increase in fines content i.e. angle of internal friction decreases with increase in fines content. The values of ϕ are 42.5^0 for clean sand, 41° for 5%, 39° for 10%, 38.01° for 15%, 37.14° for 20% and 36.12° for 25% fines content. This may be because, although density increases with increase in the amount of fines but at the same time, compressibility increases and may have a more pronounced influence in comparison to density and it leads to the plastic type of behavior. At a fine content of 20%, the soil looks like a fine-grained soil and it seems that the coarse-grained matrix is missing in the soil mass matrix.

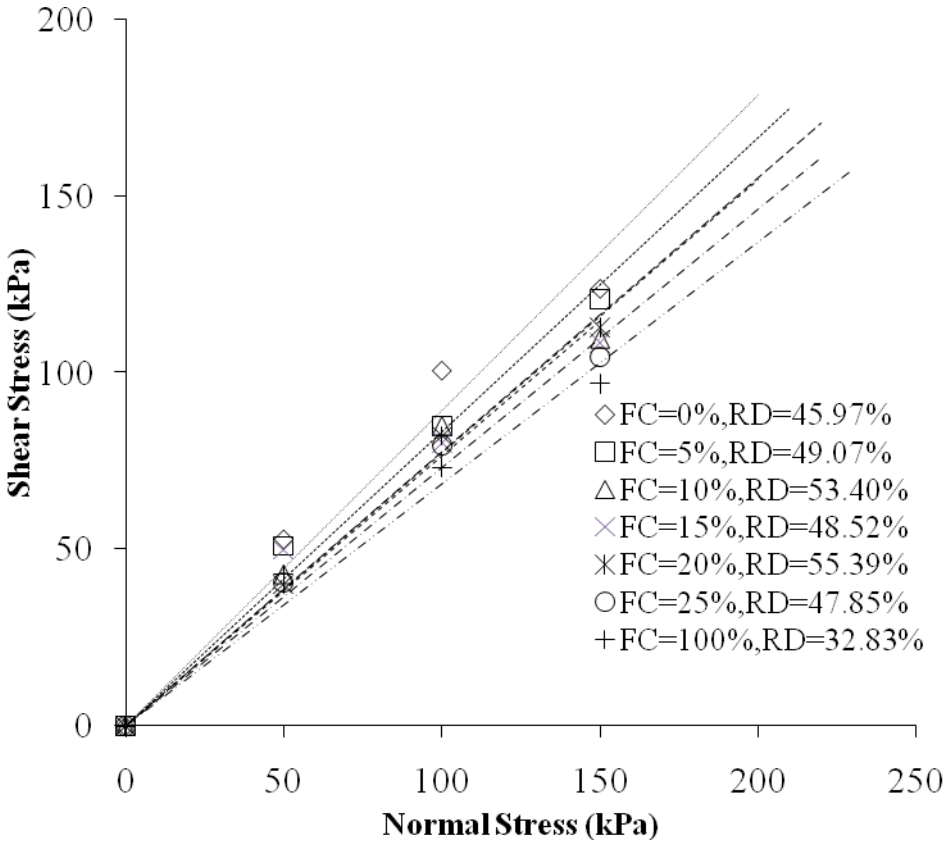

Fig. 4.8 Variation of shear stress with normal stress for different proportions of fines

4.2 Model Plate Load Test

Significant improvements in ultimate bearing capacity and settlement characteristics of footings occur when they are placed on a confined soil. The diameter of the cell, height of the cell, proportions of fines are the most important influencing factors although size of footing, type of soil and soil density also have important secondary effect on the behavior of footings resting on confined soil below the footings.

The effect of confinement and fine content on the bearing capacity and settlement characteristics of circular footings have been observed and analyzed for static loading conditions by conducting model tests on dry sand. Initially, the response of an unconfined case was determined and then compared with that of confined soil. The effect of fines on bearing capacity and settlement characteristics have been studied by varying the proportions of fines. The pressure- settlement curves have been plotted for unconfined and confined cases for different proportions of fines.

In the present chapter, the results obtained from experiments for ultimate bearing capacity and settlement of confined and un-confined cases for different diameter footings have been analyzed and discussed. The results for clean sand and sand with varying proportions of fines have also been analyzed and discussed.

The improvements in bearing capacity and settlement reduction due to confinement have been discussed in terms of non-dimensional factors.

4.2.1 Ultimate Bearing Capacity of Circular Unconfined Footings

The circular footings on clean sand and sand with varying proportions of fines have been tested with and without confinement. A series of laboratory model tests were conducted in a test box loading frame assembly. The soil beds were prepared in a test tank with inside dimensions of 0.60m X 0.60m X 0.60m and 1.5m X 1.5m X 1.0m. The sand particles were deposited in the tank-box by rainfall method. The model tests were conducted for footings of 0.1, 0.15, 0.3 and 0.45m diameters in dry condition for different proportions of fines. After the soil surface was set up, the footing was placed in position and the load was applied on it by a hydraulic jack. The load was applied in increments. The displacement of the plate was monitored using pre-calibrated settlement gauges of least count 0.01mm. Each load increment was maintained constant until the footing settlement is less than 0.02mm/min. The total assembly including hydraulic jack, proving ring and the plate were aligned with the help of plumb bob to attain verticality [Trivedi and Sud (2005)].

A typical sketch of the apparatus is illustrated in Fig.4.9. The pressure settlement curves of circular footings of 0.1m, 0.15m, 0.3m and 0.45m diameters at a relative density of ~52% have been shown in Fig (4.10) to Fig (4.13) respectively. The pressure settlement plots have varying stages of implicit failure at each data point. At a low settlement ratio (*S/B*), only limited failure is initiated. The settlement ratio is defined as a ratio of settlement (S) to the width of the footing (B) [Trivedi and Sud (2005)]. In the present study the ultimate capacity is evaluated as the bearing pressure, which produced a relative settlement of 10% of diameter of footing (i.e. *S*/*D*=0.1). Although selecting to define q_{ult} at a relative settlement of *S/D* is completely arbitrary but it has been chosen because it (i) is convenient and easy to remember, (ii) may actually be close to the average soil strain at failure, (iii) forces a fixed value at q_{ult}, and (iv) treats the displacement of all footing sizes at the same strain level. [Trivedi and Sud (2005); Lutenegger and Adams (2007)].

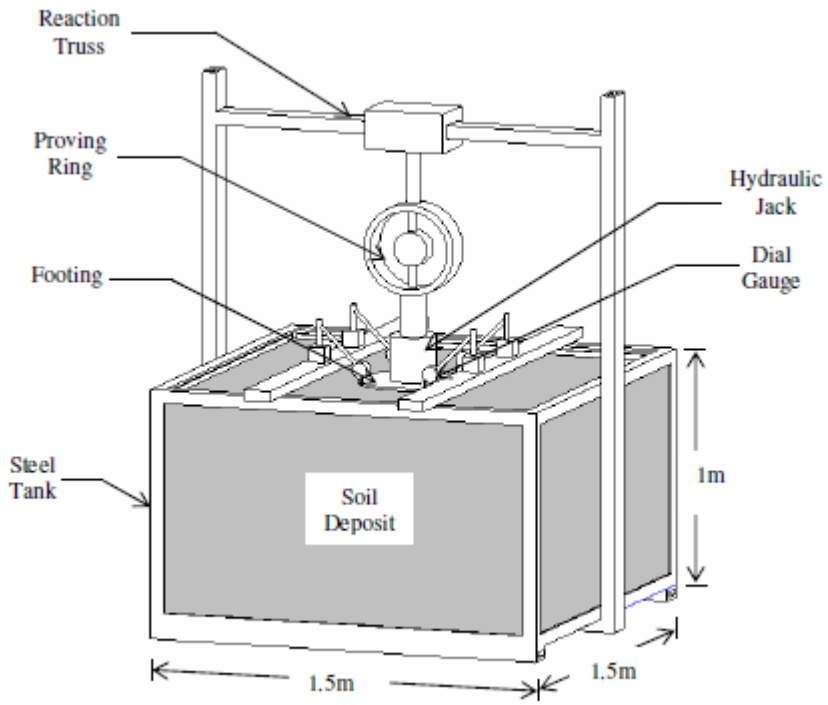

Fig. 4.9 Line sketch of plate load test (free scale)

4.2.2 Interpretation of Bearing Capacity

The bearing capacity of footings on a geomaterial is evaluated at shallow depths using the bearing capacity factors N_c and N_q proposed by Prandtl (1921) and Reisner (1924) respectively. However, substantial differences have been reported in the semi-empirical bearing capacity factors for shallow foundations N_γ in numerous studies [Brinch Hasen

(1970); Meyerhof (1965); Meyerhof (1963); Trivedi and Sud (2005); Reissner (1924)]. ***Muhs (1963)*** observed that the angle of shearing resistance estimated in direct shear test may not play relevant role in estimation of bearing capacity because of the fact of existence of progressive failure on the basis of two effects of non-linear strength behavior i.e. (1) strain restraining conditions in small scale and large scale data (2) strain dilatancy concept suggest that the difference between peak & critical angle of friction are related to dilatancy characteristics of the soil. It suggests that the shearing strength is not mobilized at all the points of slip surface. Shearing strength is first mobilized at points where shear strains are greatest, with strength mobilization progressing to other regions as shear strains develop and advance through the soil body. The consequence of this phenomenon is that when the peak load-carrying capacity of the foundation is reached, only a percentage of the material along the slip plane may be contributing a shear strength that is dependent on the soil's peak friction angle, whereas the remaining regions contribute shear strength dependent on a residual shear strength critical friction angle.

Yamaguchi et al. (1976, 1977), Perkin and Madson (2000), Trivedi and Sud (2005), Trivedi and Sud (2007), Trivedi and Arora (2007), Trivedi (2010) presented results that indicating evidence of progressive failure. It becomes more prominent with increasing footing width, and increasing confinement. ***Yamaguchi et al. (1976, 1977),*** studied clean sand of a given relative density. Since the concept of relative density applied to the silty soils has certain unanswered ambiguities due to which ASTM code does not permit extension of this work to the silty soils. However, in the absence of any criteria for the density index of the silty soil, the RD criterion was extended in the present case with certain references to Skelton void ratio. Competing with the notion of progressive failure offered by Yamaguchi et al. (1976) is the observation from shear tests that dense sands subjected to low levels of confinement have a more marked difference between peak and residual strength as compared to the same sand subjected to a much higher level of confinement. This suggests that the potential for progressive failure is more acute for low confinement conditions or for smaller footing widths. Thus it appears that two counteracting mechanisms occur: (1) The physical observation that progressive failure, being defined in terms of the non-uniformity of shear strain and mobilized friction angle in the soil at peak footing load, is more significant as footing width increases; and (2) the potential for progressive failure, being defined by the difference between the peak and residual strength of the soil, is more significant as the

footing width decreases. It is difficult to predict the point at which one effect predominates over the other.

The classical bearing capacity equation for strip foundations, popularly known as Terzaghi formula, is given by

$$q_{ult} = cN_c + qN_q + 0.5BN_\gamma \qquad (4.2)$$

where c = cohesion of soil; γ = unit weight of soil; q = γ D_f ; D_f = depth of footing embedment (m); B = width of footing (or diameter of footing); and N_c, N_q, N_γ are the bearing capacity factors which are non-dimensional and were given by Terzaghi (1943) as a function of angle of internal friction ϕ.

For cohesionless material the above equation becomes

$$q_{ult} = qN_q + 0.5BN_\gamma \qquad (4.3)$$

$$N_q = \tan^2\left(\frac{\pi}{4} + \frac{\phi}{4}\right)e^{\pi \tan\phi} \qquad (4.4)$$

The bearing capacity does not increase linearly with the width of the footing or overburden contrary to that obtained from the equation (4.3).This phenomenon is called the scale effect as defined by deBeer (1965) who attributed this to the nonlinear shape of the soil failure envelope resulting in the secant measure of the friction angle, which decreases with the mean effective confining stresses.

Equation (4.2) may be expressed for a footing of any shape as

$$q_{ult} = qN_qS_q + 0.5BN_\gamma S_\gamma \qquad (4.5)$$

S_q and S_γ is the empirical shape factors.

For the surface footing equation (4.5) may be rewritten as

$$q_{ult} = 0.5BN_\gamma S_\gamma \qquad (4.6)$$

Using the concept proposed by Vesic (1973), N_γ may be put forward as

$$N_\gamma = 2(1 + N_q)\tan\phi \qquad (4.7)$$

Experimentally it is obtained as,

$$N_\gamma = q_{ult} / 0.5B\gamma S_\gamma \qquad (4.8)$$

Using the shape factor (S_γ = 0.6) proposed for circular footings by deBeer (1970) and the values of the bearing capacity factor N_γ from Vesic (1973), the theoretical bearing capacities for clean sand and sand with different proportions of fines are listed in Table (4.3).The data in Table (4.3) shows a close agreement both between the theoretical values and experimental results for footings of 0.1m and 0.15m diameter.

Table 4.3 Model-scale footing test results (Un-confined case)

FC (%)	***D*** **(mm)**	**RD (%)**	ϕ (Peak)	**Vesic** N_γ *	$q_{experimental}$ **(kPa)**	ϕ (Critical)	**Vesic** N_γ *	**Back–calculated** N_γ
0	100	50.77	46.45	318.84	101.25	31	27.52	203.32
5		50.80	45.95	302.60	73.12	29	20.09	144.24
10		51.98	44.85	266.88	48.21	28.5	18.94	93.44
15		51.80	43.90	236.043	42.63	28	17.79	82.61
20		54.87	42.20	136.41	37.80	27.5	16.64	72.01
25		51.88	39.45	102.45	30.56	27	15.48	59.58
0	150	50.77	46.45	318.84	202.11	31	27.52	270.56
5		50.80	45.95	302.60	131.70	29	20.09	173.19
10		51.98	44.85	266.88	112.84	28.5	18.94	145.79
15		51.80	43.90	236.043	81.60	28	17.79	105.44
20		54.87	42.20	136.41	67.43	27.5	16.64	85.62
25		51.88	39.45	102.45	40.29	27	15.48	52.36
0	300	50.77	46.45	318.84	44.46	31	27.52	29.76
5		50.80	45.95	302.60	31.13	29	20.09	20.84
10		51.98	44.85	266.88	29.07	28.5	18.94	19.46
0	450	50.77	46.45	318.84	60.64	31	27.52	40.59
5		50.80	45.95	302.60	45.85	29	20.09	30.69
10		51.98	44.85	266.88	44.32	28.5	18.94	29.67

* Vesic's bearing capacity factor N_γ based on friction angle

For footings of 0.3m and 0.45m diameter, the experimental tests give smaller values N_γ as compared to theoretical values. From the results obtained for clean sand and sand with

increased proportions of fines, it can be seen that N_γ decreases on addition of fines for all the footing sizes.

The results of experiments conducted for estimation of bearing capacity for varying fines content have been plotted and shown in Fig (4.14). Best-fit trend lines were drawn through the different footing diameter test results. These results show a decrease in bearing capacity the addition of fines for all footing sizes. This may be due to the fact that although density increases on increase in amount of fines but at the same time compressibility increases which has a more pronounced influence in comparison to the overall density of the soils .The ultimate bearing capacity for all the cases is presented in Table (4.3).

All the tests were performed with a soil layer of sufficient thickness (3B), which has been found to be adequate for rigid boundary effect below the footing [Cerato and Lutenegger (2006)]. The tank wall was kept at distance of 2.5B to avoid any lateral pressure interference. N_γ values were back calculated using Eq. (4.8).

For model scale footing of 0.1m diameter tests gave good agreement between theoretical and experimental values whereas for model-scale footing of 0.15m diameter tests gave higher value of N_γ when compared with theoretical values [Vesic (1973)]. Care need to be taken while extending model-scale footing test results to the behavior of full-scale foundations. It was observed that results of tests on actual model scale footings produced higher values of N_γ than theoretical equations and therefore should not be used for the design of full-scale footings without a reduction. The footings of 0.3m and 0.45m diameter, tests gave smaller values of N_γ. Cerato and Lutenegger (2006) investigated sandy soils have also observed similar results as shown Fig 4.16. This effect becomes more acute in case of silty soils as found in the present investigation. The author interpreted that the behavior of a model scale test may not represent the behavior of a full-scale footing. It was seen that with addition of fines, N_γ follows a set pattern for various footing sizes.

The angle of shearing resistance interpreted using Mohr-Coulomb linear envelop from shear test does not play useful role in estimation of bearing capacity because of the progressive failure on account of argument offered by Muhs (1963) indicating two effects of non-linear strength behavior i.e. (1) strain restraining conditions in small scale and large scale data (2) stress dilatancy concept suggest that the difference between peak & critical angle of friction are related to dilatancy characteristics of the soil. It suggests that the shearing strength is not mobilized at all the points of slip surface. Shearing strength is first mobilized at points where shear strains are greatest, with strength mobilization progressing to other regions as shear

strains develop and advance through the soil body. The consequence of this phenomenon is that when the peak load-carrying capacity of the foundation is reached, only a percentage of the material along the slip plane may be contributing a shear strength that is dependent on the soil's peak friction angle, whereas the remaining regions contribute shear strength dependent on a residual shear strength critical friction angle. Yamaguchi et al. (1976, 1977) presented results that indicate that progressive failure becomes more prominent with increasing footing width, or increasing soil confinement, for a clean sand of a given relative density. Since the concept of relative density applied to the silty soils has certain unanswered ambiguities due to which ASTM code does not permit extension of this concept to the silty soils.

However, in the absence of any criteria for the density index of the silty soil, the RD criterion was extended in the present case with certain references to skeleton void ratio. Competing with the notion of progressive failure offered by Yamaguchi et al. (1976) is the observation from shear tests that dense sands subjected to low levels of confinement have a more marked difference between peak and residual strength as compared to the same sand subjected to a much higher level of confinement. This suggests that the potential for progressive failure is more acute for low confinement conditions or for smaller footing widths as appeared in the cases of 100mm & 150mm footing at medium RD.

Thus, it appears that two counteracting mechanisms occur: (1) The physical observation that progressive failure, being defined in terms of the non-uniformity of shear strain and mobilized friction angle in the soil at peak footing load, is more significant as footing width increases; and (2) the potential for progressive failure, being defined by the difference between the peak and residual strength of the soil, is more significant as the footing width decreases. It is difficult to predict the point at which one effect predominates over the other (Perkin and Madson, 2000) as becomes apparent for footing sizes of 300mm & 450mm.Wheres the similar observations were made by the present study and the work of Cerato and Lutenegger (2006).

Since ϕ varies as the state of stress, density and material characteristics of the soil, the concept of stress dilatancy enunciated by Rowe (1962) advanced by de Josselin de Jong (1976) and Bolton (1986) is utilized. Bolton proposed the empirical equation

$$\phi_{peak} = \phi_{cr} + AIr \qquad (4.9)$$

$$\text{where } Ir = RD(Q - \ln p) - r$$

where A is an empirical constant and has the value of 3 for axisymmetrical and 5 for plane strain case; Ir is the relative dilatancy index; p is the mean confining pressure in kPa; RD is

relative density; and Q and r are empirical material fitting constants with values of 10 and 1, respectively, for clean silica sand. The dilatancy increases with increasing Q and decreases with increasing r (Salgado et al, 2000). Incorporating Billam's (1972) triaxial test data, Bolton (1986) suggested that progressive crushing suppresses dilatancy in the soils with weaker grains, Salgado et al (2000) found that it is easier to compare the dilatancy of sand with 0, 5, 10, 15 and 20% silt by comparing the values of Q obtained if a single r value is used, for which the coefficient of correlation is satisfactory for all the gradations. A value of r = 0.5 works relatively well for all gradations. Producing Q values equal to 10, 11, 10.6, 10.3, 9.5 and 8% for 0, 5, 10, 15, 20 and 25% silt contents respectively.

As per Bolton, in the triaxial test conditions a relation among the peak and the critical angles of friction exists. It is conveniently expressed as

$$Q.\mathrm{RD} - r = 0.33\,(\phi_{\mathrm{peak}} - \phi_{\mathrm{critical}}) + \mathrm{R\,D.\ln}\,(p) \qquad (4.10)$$

The critical state friction angle was considered as per Sadannand (2011). The critical state friction angle (ϕ_{critical}), for clean sand and sand with 0, 5,10,15,20 and 25% silt content observed by Sadannand (2011) was 31,29,28.5,28,27.5 and 27 respectively for Yamuna sand. The value of parameter Q for sand with 0,5,10,15,20 and 25% silt content was 10,11,10.6,10.3,9.5 and 8 respectively (Salgado et al 2000). Therefore the knowledge of ϕ_{critical}, RD, and p is utilized to interpret the peak angle of internal friction of silty sand from Eq. (4.10).

The mobilized peak effective angle of internal friction that is a function of mean confining pressure (p) and relative density was evaluated as per Eq. (4.10). Based on knowledge of peak angle of internal friction, constant volume friction angle, the value of $N\gamma$ was computed (by Vesic 1973).Fig. 4.17 shows the comparison of bearing capacity factor for peak mobilized friction at corresponding relative density, experimental, and at constant volume friction with variation of silt content. The bearing capacity factor for the clean sand and sand with 0, 5,10,15,20 and 25% fine content was observed to fall between the estimates by the use of the peak friction and the constant volume or critical angles. Trivedi and Sud (2005) suggested the concept of index of progressive failure. They observed that if index of progressive failure takes a value of one, it implies that the constant volume friction governs the ultimate bearing capacity of soil fill while a value of zero indicates that the peak angle of friction is mobilized. It may be identified here that various factors that influence the progressive failure are settlement ratio, relative density, size, depth of the footing, constant volume, peak friction and soil material properties represented by parameters Q and r.

In fact, different sized tank, skirt, plate sizes produce varied magnitude of progressive failure. Cerato and Lutenegger (2006) have reported that for all the tests, smaller footing always has a higher N_γ value than the larger footing and increases according to increase in density. The actual test results (For D=0.3m & 0.45m) produce lower values of N_γ than theoretical values [Vesic (1973)] as shown in Fig (4.15).

The settlement of foundations under working load conditions is an important design consideration. The settlement of footings in cohesionless soil is often estimated based on the results of in situ tests, particularly the standard penetration test (SPT). In the present investigation the settlement is estimated from model plate load tests and measured resistance in terms of SPT below count N.

The Standard penetration test was conducted in field on silty sand strata having a fines content of 5% and a value of four (N=4) was observed in the field at a depth of 1.5m.Based on SPT value the settlements were calculated as per Teng (1962).The plots are drawn as shown in Fig.4.16 from predicted settlement for 0.3m and 0.45m diameter footing by Terzaghi and Peck (1948) and based on SPT value as per Teng (1962).

The settlements of 0.3m and 0.45m diameter footings have been under estimated by 50.58% and 10.58%, respectively by the estimates based on SPT value [Fig. (4.18)]. The predicted settlement based on actual settlement of 0.3m diameter footing gives more conservative results. Therefore, the results of 0.45m diameter footings should be used to extrapolate the bearing capacity of full-scale footings instead of 0.3m diameter footing for loose silty sands.

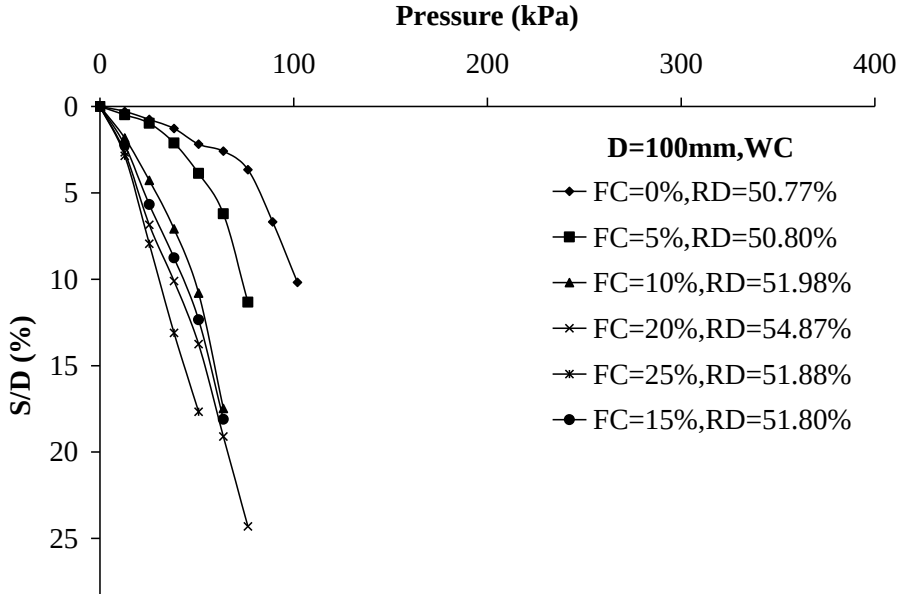

Fig. 4.10 Pressure vs. settlement ratio (*S*/*D*) for a circular plate of 100 mm without lateral confinement.

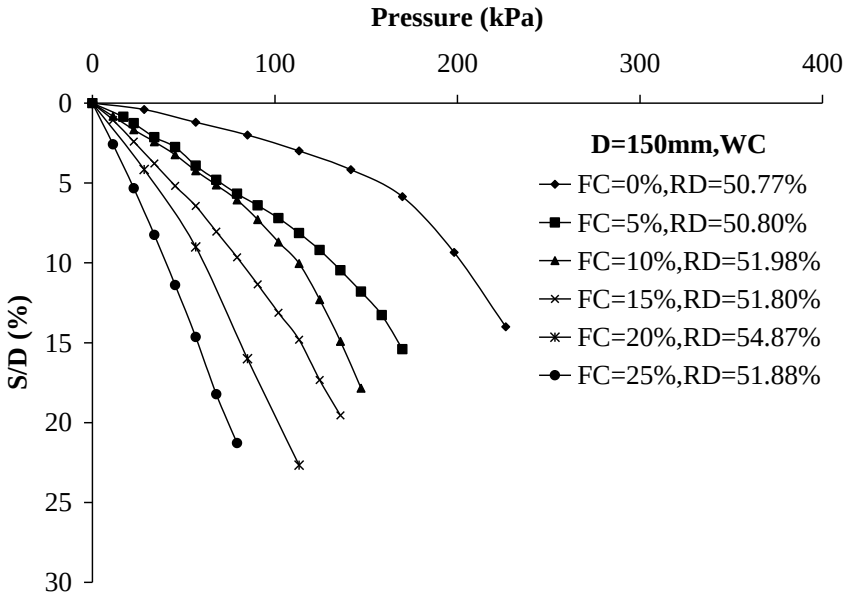

Fig. 4.11 Pressure vs. settlement ratio (*S*/*D*) for a circular plate of 150 mm without lateral confinement.

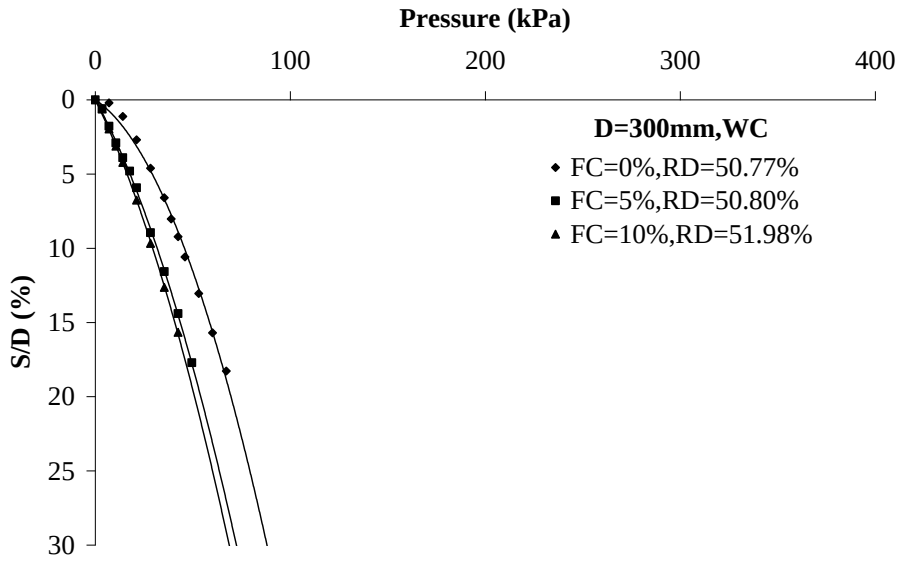

Fig. 4.12 Pressure vs. settlement ratio (*S*/*D*) for a circular plate of 300 mm without lateral confinement

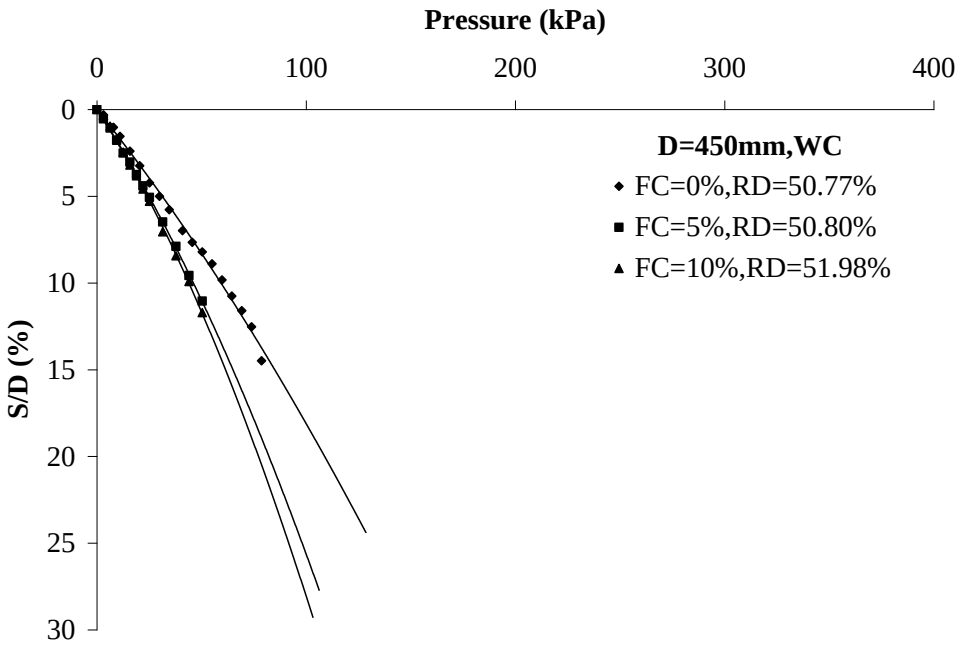

Fig.4.13 Pressure vs. settlement ratio (*S*/*D*) for a circular plate of 450 mm without lateral confinement

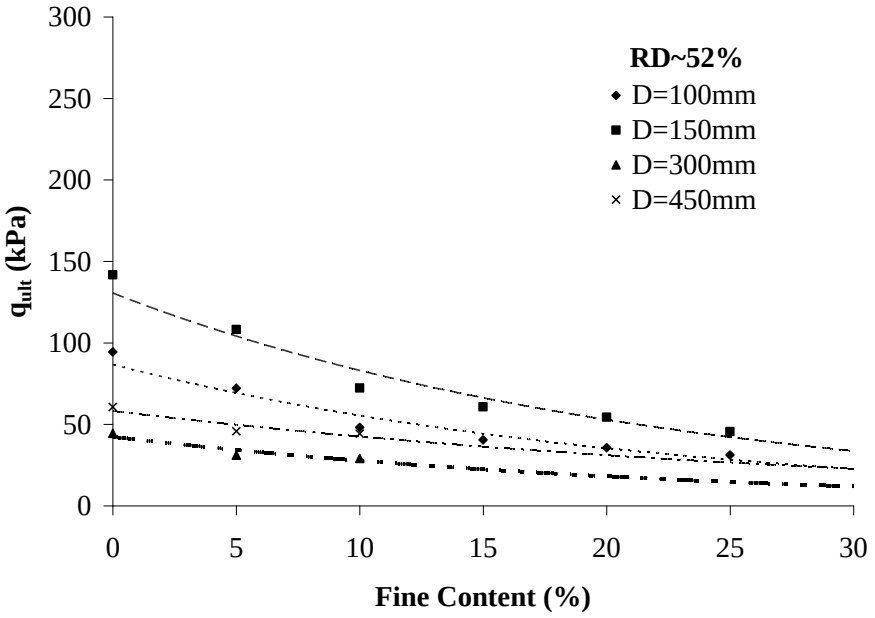

Fig. 4.14 Variation of ultimate bearing capacity with different proportions of fines for different footing diameters

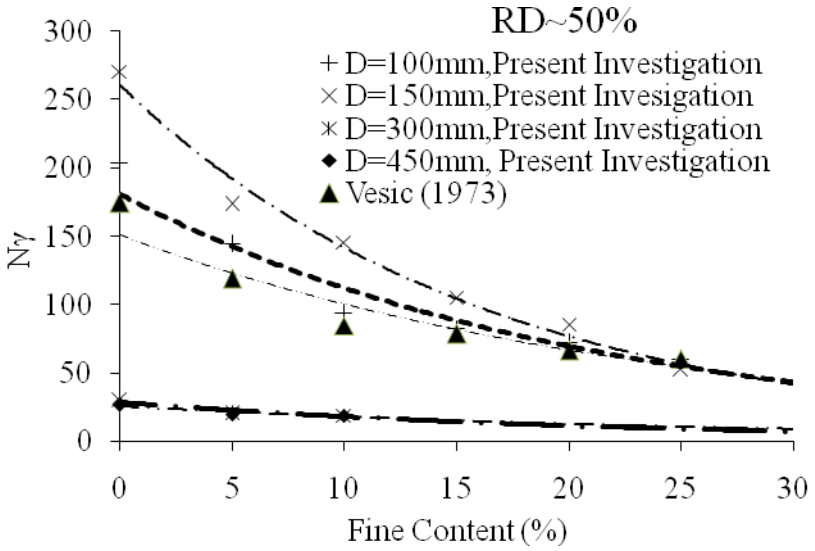

Fig.4.15 Bearing capacity factor vs. fines content

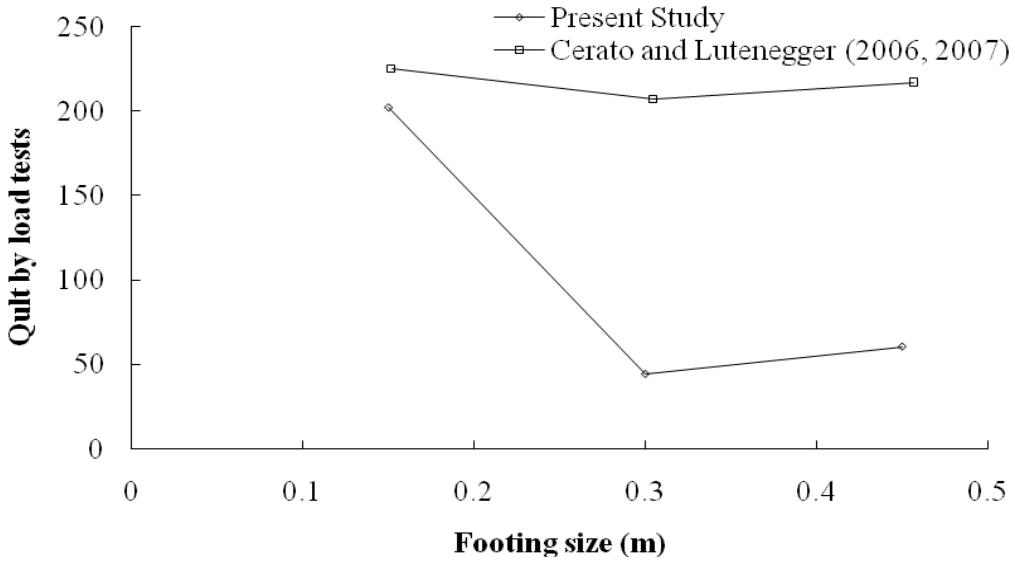

Fig.4.16 Ultimate load capacity predicted by Cerato and Luteneger (2006, 2007) and present study vs footing size.

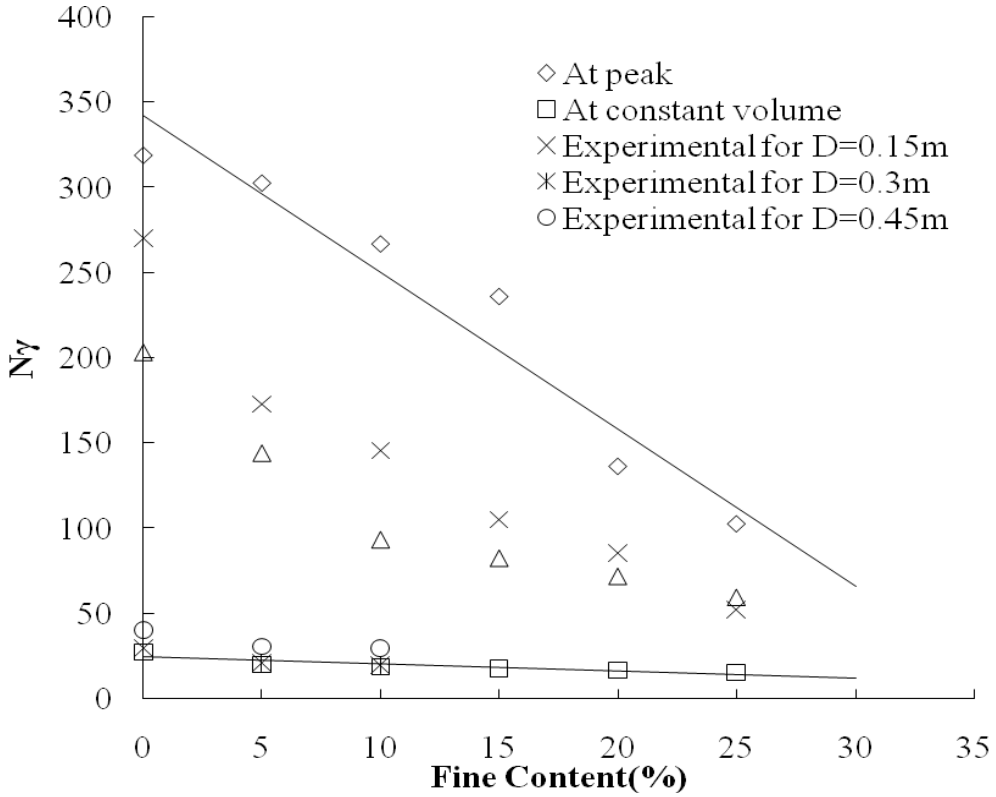

Fig.4.17 Comparison of bearing capacity factor for peak, experimental and constant volume friction angle.

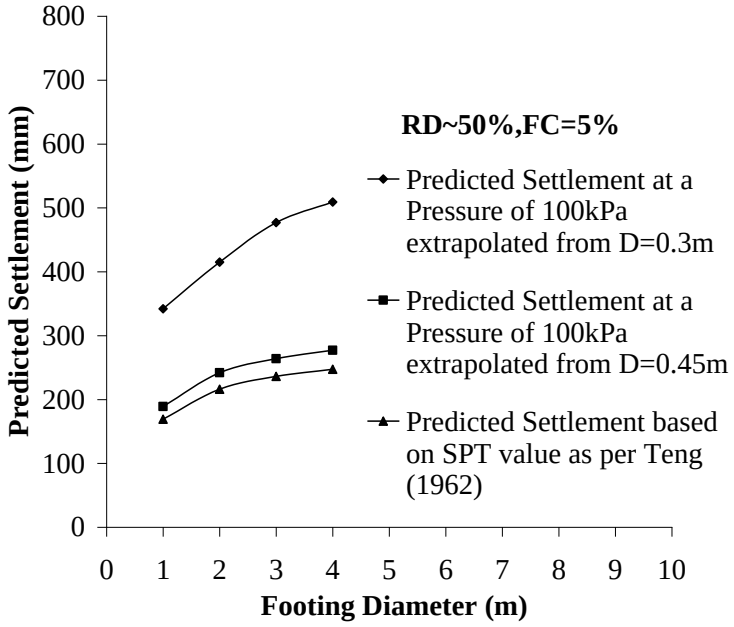

Fig. 4.18 Predicted settlement from plate load test as per Terzaghi and Peck Criteria and based on SPT value (as per Teng 1962) vs. footing diameter at 100 kPa for loose silty sands

4.2.3 Ultimate Capacity of Model Circular Confined Footings

In the present research work a detailed experimental investigation was carried out to develop an understanding of the performance of the model footings with cellular supports.

A few model cells with different diameters and heights were used to confine the silty sand. The effect of the cell diameter, cell height and fines on bearing capacity and settlement were investigated with the help of an experimental programme using circular footings of 0.1, 0.15 and 0.3m diameter. Initially, the response of the footing without confinement was determined and then compared with that of footing with confinement as shown in Fig (4.19). Model cells were manufactured in the laboratory for different normalized d/D (i.e. diameter of cell to the diameter of the footing) ratio varying from 0 to 2.0 and different normalized h/D (i.e. height of the cell to the diameter of the footing) ratio varying from 0 to 1.5. Tests were also performed for different values of normalized embedded depth i.e. z/h [Fig (4.20a)].

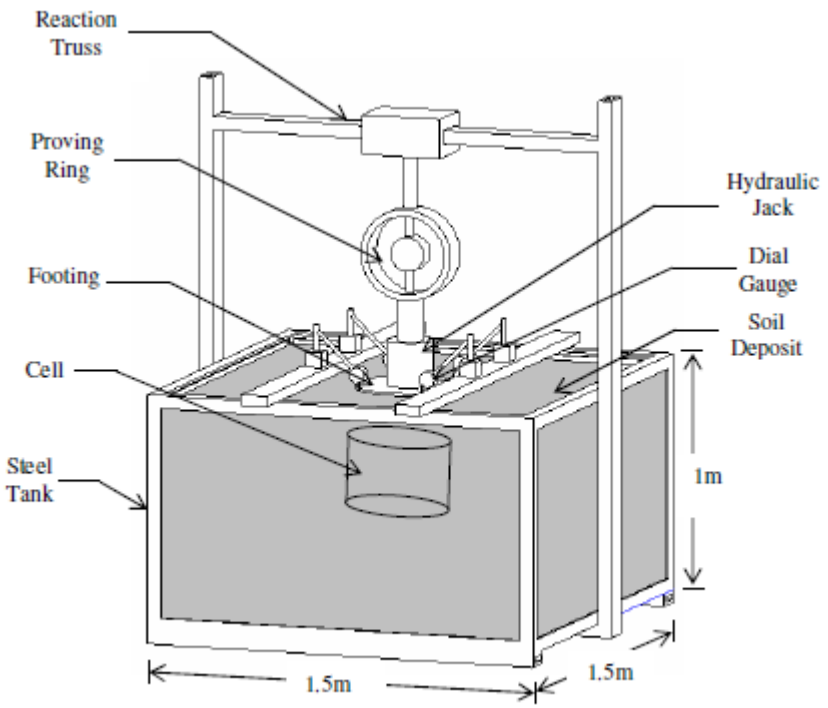

Fig 4.19 Line sketch of plate load test with cell below the footing (free scale)

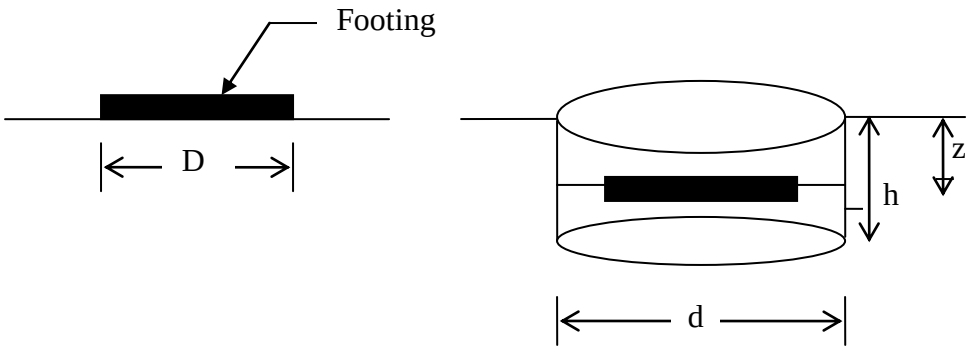

Fig 4.20a Geometric parameters of confined soil-foundation model

There are varied engineering possibilities of placement of a footing on the soil confined by a skirt i.e.

1) Un-confined case (skirt at infinite distance from the centre of the footing

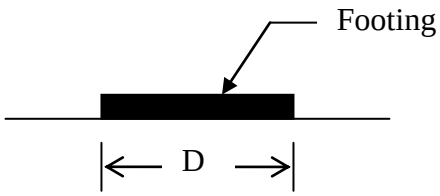

2) Confining the footing by a skirt
Changing the depth of confinement

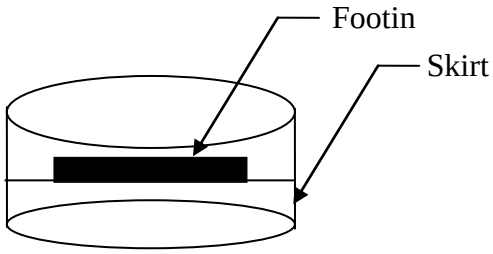

3) Confining the footing by a skirt
Changing the diameter of confinement relative to the footing

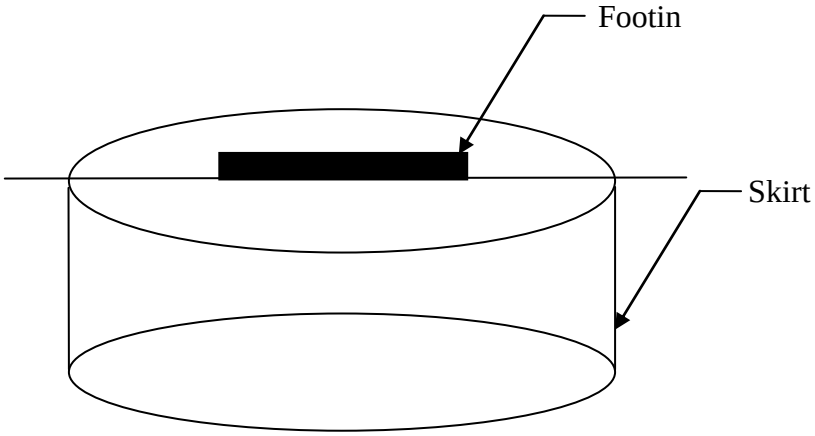

4) Placing the confinement below the footing

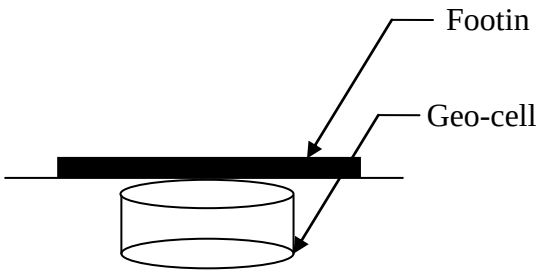

Fig.4.20b Varied engineering possibilities of placement of a footing on the soil confined by a skirt

The results indicate that the bearing capacity of the circular footings decreases on addition of fines and can be appreciably improved by soil confinement below the footing. It was interpreted that such confinement provides lateral displacement of soil underneath the footing which leads to a significant improvement in the response of the footing. The improvement due to the soil confinement is represented by using a non-dimensional improvement factor (I_f), which is defined as the ratio of the footing ultimate load with cellular support to the footing ultimate load in tests without cellular support.

The results also indicate that the settlement of circular footings can be appreciably decreased by soil confinement. The reduction in settlement due to the soil confinement is represented by using a non-dimensional factor, called the settlement reduction factor (S_f) which is defined as the ratio of the settlement with confinement to the settlement without confinement corresponding to a constant stress intensity of 100 kPa. The study was carried out for clean sand and the sand with varying proportions of fines.

4.3 Effect of Cell Diameter

In order to investigate the effect of cell diameter on the behavior of footings, a few cells with normalized d/D ratio of 1.0, 1.5 and 2.0 were used for three different footing diameters i.e. 0.1, 0.15 and 0.3m. The typical pressure settlement responses observed from different series of tests have been presented in Fig (4.21) to Fig (4.31).

The pressure settlement responses show that there is no pronounced peak in the unconfined case of silty sand bed but the slope of the pressure settlement curve tends to become almost vertical beyond some point, indicating the failure. With the provision of cellular support below the footing clear failure is not noticed even up to a settlement as high as 20% of the footing diameter. In addition, the pressure settlement responses with cellular support are

found to be much stiffer than those of footings without cellular support which indicates that the cellular support can reduce the footing settlement substantially.

The results in Table (4.4) to (4.6) show that the load carrying capacity of the footing with confinement can be increased by 6.51times (FC=0%, d/D=1.5, h/D=1.5) in case of 0.1m diameter footing, 3.94 times (FC=0%, d/D=1.5,h/D=1.0) in case of 0.15m diameter footing and 1.86 times (FC=0%,d/D=1.5,h/D=0.5) in case of 0.3m diameter footing. Fig (4.32) to Fig (4.42) represents the improvement factor vs. normalized cell diameter for different proportions of fines. The value of improvement factor for circular footings on confined silty sands increases up to 1.5. If *d*/*D* ratio is increased beyond 1.5, improvement factor decreases. While conducting the model tests, it was observed that as failure approached in the tests carried out with small cell diameters, the inside soil and the cell behaved as one unit (when the load was increased, the cell, soil and footing settled altogether) as shown in Plate (4.1) to 4.3). During the tests carried out with large cell diameters, this behavior was noticed for the initial part of loading but as the load was increased it could no longer be observed (the footing settled down while the cell was unaffected with the increase of the load) as shown in Plate (4.4) & (4.5). It is clear that the best benefit of cellular confinement could be obtained with a (*d*/*D*) ratio between 1.5 to 2.0 with the maximum improvement in the bearing capacity at a ratio of about 1.5 for different heights of confining cells. This observation confirmed the observation made by Sawwaf (2005) that the maximum benefit can be achieved when d/D lies between 1 and 2.

For *d*/*D* = 2.0 and *h*/*D* =1.5, the bearing capacity (I_f = 7.13) is more in comparison to *d*/*D* = 1.0 and 1.5 for *h/D* values equal to 0.5, 1.0 and 1.5. It is due to the increased height of cellular supports by which the surface area increases and failure plane moves in the downward direction

From the Fig (4.21) to Fig (4.31), it can also be seen that installation of confining cell appreciably reduces the settlement of the footings corresponding to constant pressure intensity. In order to study the settlement characteristics of the footings on silty sands, settlements corresponding to a constant pressure intensity of 100kPa are compared. Fig (4.43) to Fig (4.53) represents the settlement reduction factor (S_f) vs. normalized cell diameter (d/D) for different values of h/D ratio. A significant decrease in the settlement of the model footings supported on confined silty sand with increase of normalized cell diameter (d/D) is observed up to 1.5 for all footing sizes, after which the settlement reduction factor (S_f) increases with an increase in this ratio. It is clear that the best benefit of soil confinement

could be obtained with a d/D ratio between1.0 to 2.0 with the maximum reduction in settlement at a d/D ratio of about 1.5 for different footing sizes.

This increase in the bearing capacity and reduction in settlement of the footing can be explained with the help of Fig (4.54). When the footing is loaded, such cells resist the lateral displacements of soil particles underneath the footing and confines the soil leading to a significant decrease in vertical settlement and hence improvement in bearing capacity. For small cell diameters, as the pressure is increased, the plastic state is developed initially around the edges of the footing and then spreads downward and outward. The mobilized vertical frictions between the sand and the inside wall of the cell increase with increase of the acting active earth pressure until the point when the system (the cell, the soil, and the footing) behaves as one unit as shown in Plate (4.2). The behavior is similar to that observed in deep foundations in which the bearing capacity increases due to the shear resistance of cell surface. This explains the increase of the bearing capacity with the increase of the cell diameter and cell height.

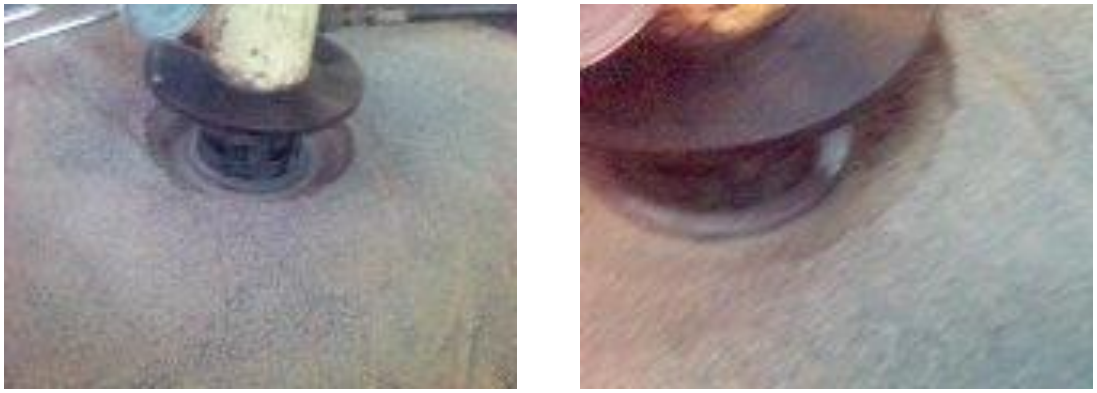

(a) **(b)**

Plate 4.1 Photograph indicating cell, soil, and footing settled together (a) for D=100mm; (b) D=150mm.

Plate 4.2 Photograph indicating cell, soil, and footing settled together for D=150mm (d/D=1.0)

Plate 4.3 Photograph indicating cell, soil, and footing settled together for D=150mm (d/D=1.5)

Plate 4.4 Photograph indicating the settlement of the plate while the cell is unaffected for D=150mm

Plate 4.5 Photograph indicating the settlement of the plate while the cell is unaffected for D=100mm

Table 4.4 Results of model footing on confined silty sands (D=100mm)

FC (%)	RD (%)	D (mm)	d/D	h/D	$q_{experimental}$ (kPa)	Improvement Factor (I_f)
0	50.77	100	1.0	0.5	314.34	3.10
0		100	1.5	0.5	352.44	3.48
0		100	2.0	0.5	300.37	2.96
0		100	1.0	1.0	395.35	3.90
0		100	1.5	1.0	542.10	5.35
0		100	2.0	1.0	497.38	4.91
0		100	1.0	1.5	460.63	4.54
0		100	1.5	1.5	659.49	6.51
0		100	2.0	1.5	721.94	7.13
5	50.80	100	1.0	0.5	140.33	1.91
5		100	1.5	0.5	256.16	3.50
5		100	2.0	0.5	83.39	1.14
5		100	1.0	1.0	171.48	2.34
5		100	1.5	1.0	352.54	4.82
5		100	2.0	1.0	308.36	4.21
5		100	1.0	1.5	219.18	2.99
5		100	1.5	1.5	383.12	5.23
5		100	2.0	1.5	493.95	6.75
10	51.98	100	1.0	0.5	129.51	2.68
10		100	1.5	0.5	159.99	3.31
10		100	2.0	0.5	65.38	1.35
10		100	1.0	1.0	143.23	2.97
10		100	1.5	1.0	219.69	4.55
10		100	2.0	1.0	197.12	4.08
10		100	1.0	1.5	169.64	3.51
10		100	1.5	1.5	244.79	5.07
10		100	2.0	1.5	306.71	6.36
20	54.87	100	1.0	0.5	44.58	1.17
20		100	1.5	0.5	73.16	1.93
20		100	2.0	0.5	43.63	1.15
20		100	1.0	1.0	74.30	1.96
20		100	1.5	1.0	166.58	4.40
20		100	2.0	1.0	137.95	3.64
20		100	1.0	1.5	90.16	2.38
20		100	1.5	1.5	206.87	5.74
20		100	2.0	1.5	235.09	6.21
25	51.88	100	1.0	0.5	38.59	1.26
25		100	1.5	0.5	45.18	1.47
25		100	2.0	0.5	36.71	1.20
25		100	1.0	1.0	40.60	1.32
25		100	1.5	1.0	80.78	2.64
25		100	2.0	1.0	59.06	1.93
25		100	1.0	1.5	45.75	1.49
25		100	1.5	1.5	69.93	2.28
25		100	2.0	1.5	79.68	2.60

Table 4.5 Results of model footing on confined silty sands (D=150mm)

FC(%)	RD (%)	D(mm)	d/D	h/D	$q_{experimental}$ (kPa)	Improvement Factor(I_f)
0	50.77	150	1.0	0.5	358.02	1.77
0		150	1.5	0.5	383.33	1.89
0		150	2.0	0.5	213.91	1.05
0		150	1.0	0.75	400.36	1.98
0		150	1.5	0.75	456.25	2.25
0		150	2.0	0.75	400.54	1.98
0		150	1.0	1.0	505.66	2.50
0		150	1.5	1.0	797.63	3.94
0		150	2.0	1.0	665.95	3.29
5	50.80	150	1.0	0.5	209.83	1.59
5		150	1.5	0.5	224.62	1.70
5		150	2.0	0.5	146.48	1.11
5		150	1.0	0.75	226.76	1.72
5		150	1.5	0.75	301.81	2.29
5		150	2.0	0.75	223.14	1.69
5		150	1.0	1.0	262.04	1.98
5		150	1.5	1.0	447.27	3.39
5		150	2.0	1.0	375.21	2.84
10	51.98	150	1.0	0.5	153.62	1.36
10		150	1.5	0.5	173.58	1.53
10		150	2.0	0.5	127.49	1.12
10		150	1.0	0.75	170.29	1.50
10		150	1.5	0.75	214.52	1.90
10		150	2.0	0.75	190.16	1.68
10		150	1.0	1.0	193.17	1.71
10		150	1.5	1.0	344.52	3.05
10		150	2.0	1.0	303.43	2.68
20	54.87	150	1.0	0.5	94.90	1.56
20		150	1.5	0.5	104.50	1.72
20		150	2.0	0.5	87.22	1.43
20		150	1.0	0.75	100.28	1.65
20		150	1.5	0.75	128.37	2.11
20		150	2.0	0.75	96.78	1.59
20		150	1.0	1.0	106.57	1.75
20		150	1.5	1.0	169.08	2.78
20		150	2.0	1.0	113.94	1.87
25	51.88	150	1.0	0.5	55.86	1.38
25		150	1.5	0.5	67.56	1.67
25		150	2.0	0.5	52.75	1.30
25		150	1.0	0.75	62.22	1.54
25		150	1.5	0.75	82.71	2.05
25		150	2.0	0.75	76.14	1.88
25		150	1.0	1.0	80.47	1.99
25		150	1.5	1.0	112.71	2.79
25		150	2.0	1.0	106.34	2.63

Table 4.6 Model footing results on confined silty sands (D=300mm).

FC (%)	RD (%)	D (mm)	d/D	h/D	$q_{experimental}$ (kPa)	Improvement Factor (I_f)
0	50.77	300	1.0	0.5	60.94	1.37
0		300	1.5	0.5	82.61	1.86
0		300	2.0	0.5	51.40	1.56
5	50.80	300	1.0	0.5	46.82	1.50
5		300	1.5	0.5	55.32	1.77
5		300	2.0	0.5	41.82	1.34
10	51.98	300	1.0	0.5	41.26	1.42
10		300	1.5	0.5	47.68	1.64
10		300	2.0	0.5	33.15	1.14

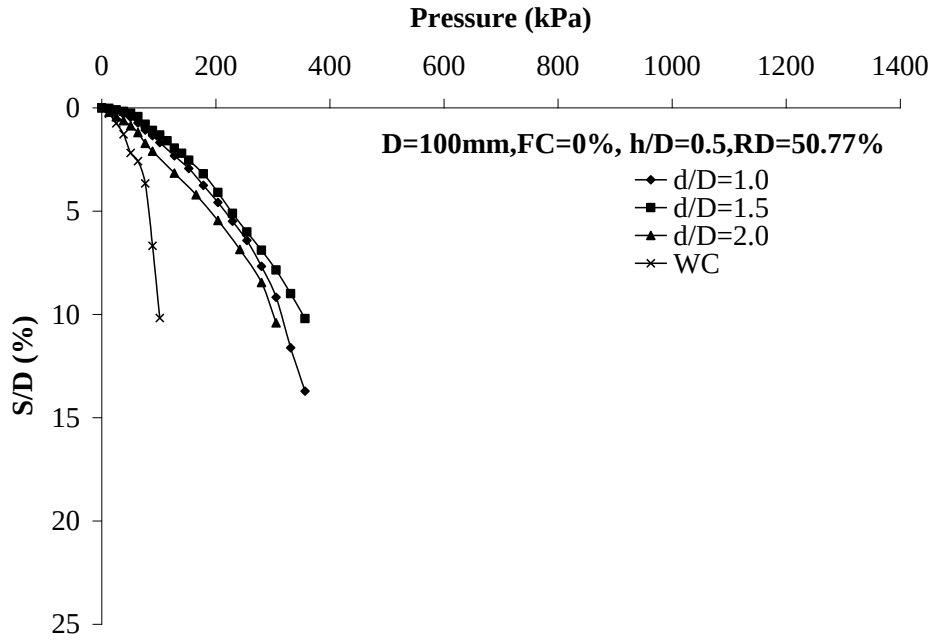

Fig. 4.21 (a) Pressure vs. S/D for different values of d/D ratios for h/D=0.5

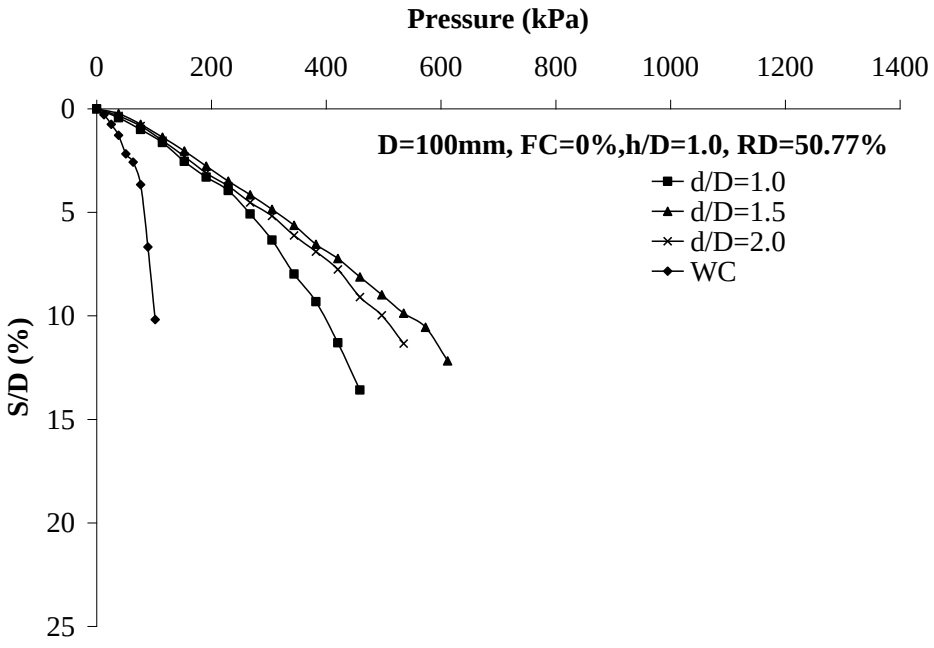

Fig. 4.21(b) Pressure vs. S/D for different values of d/D ratios for h/D=1.0

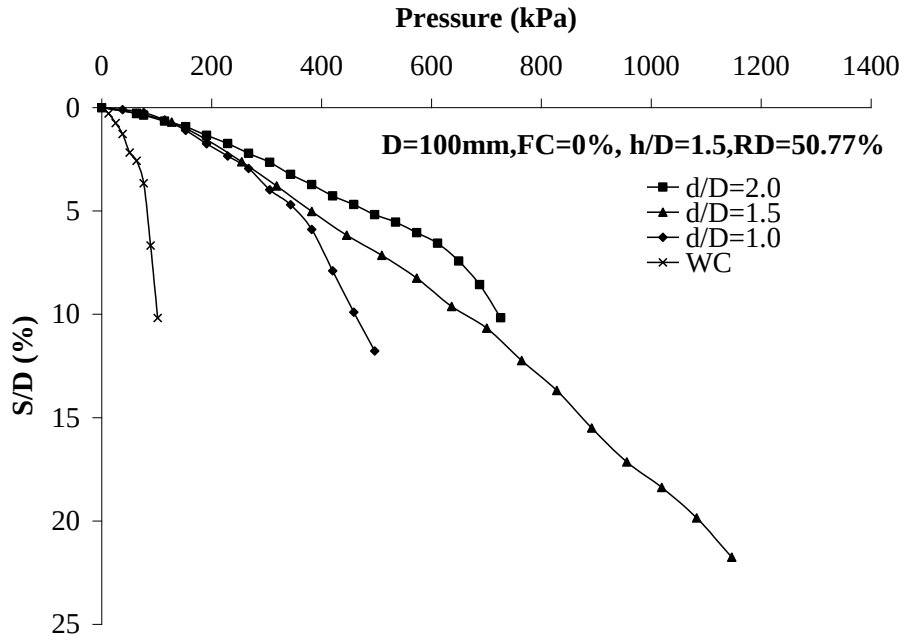

Fig. 4.21(c) Pressure vs. S/D for different values of d/D ratios for h/D=1.5

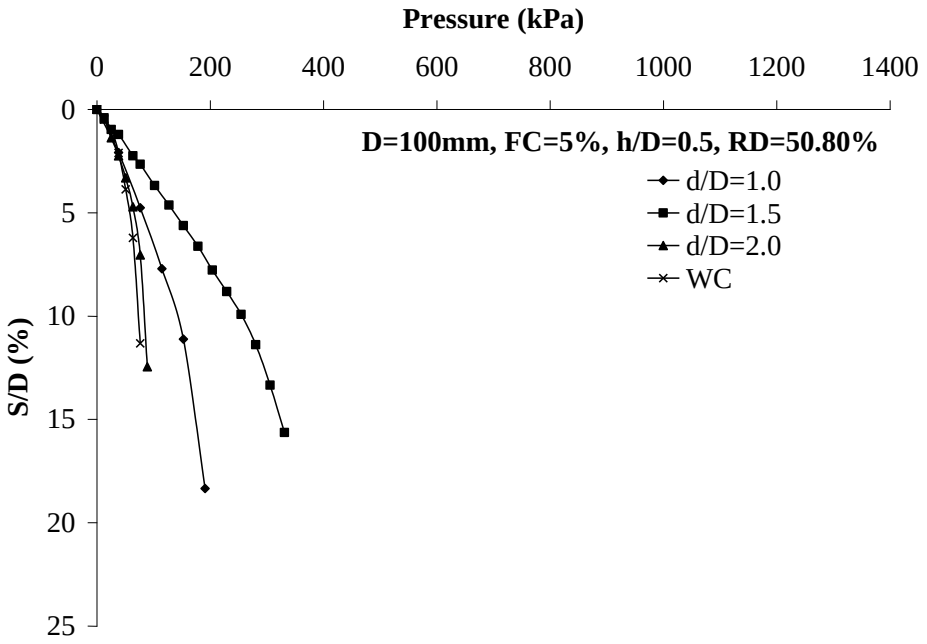

Fig. 4.22(a) Pressure vs. S/D for different values of d/D ratios for h/D=0.5

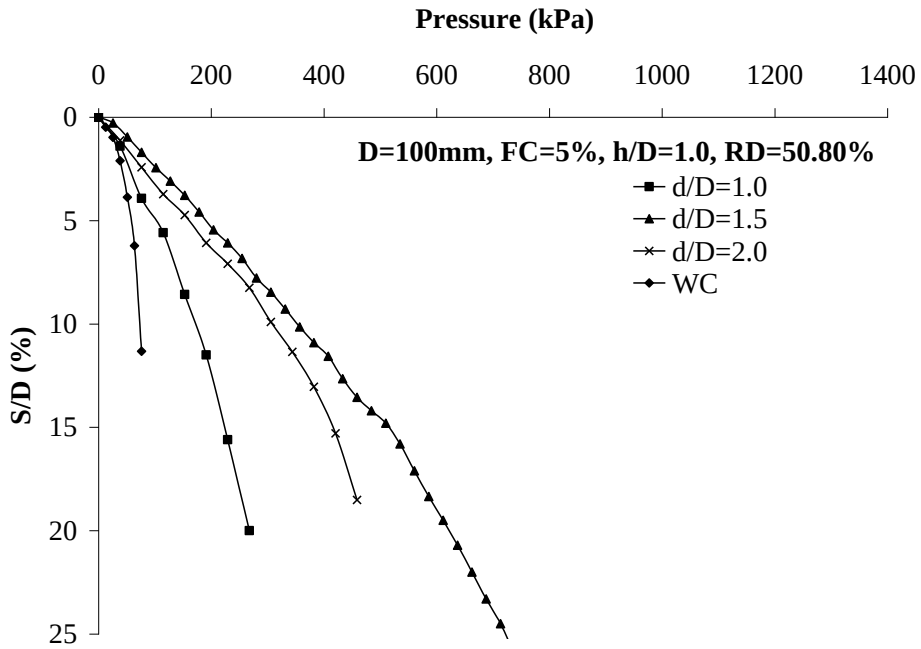

Fig. 4.22(b) Pressure vs. S/D for different values of d/D ratios for h/D=1.0

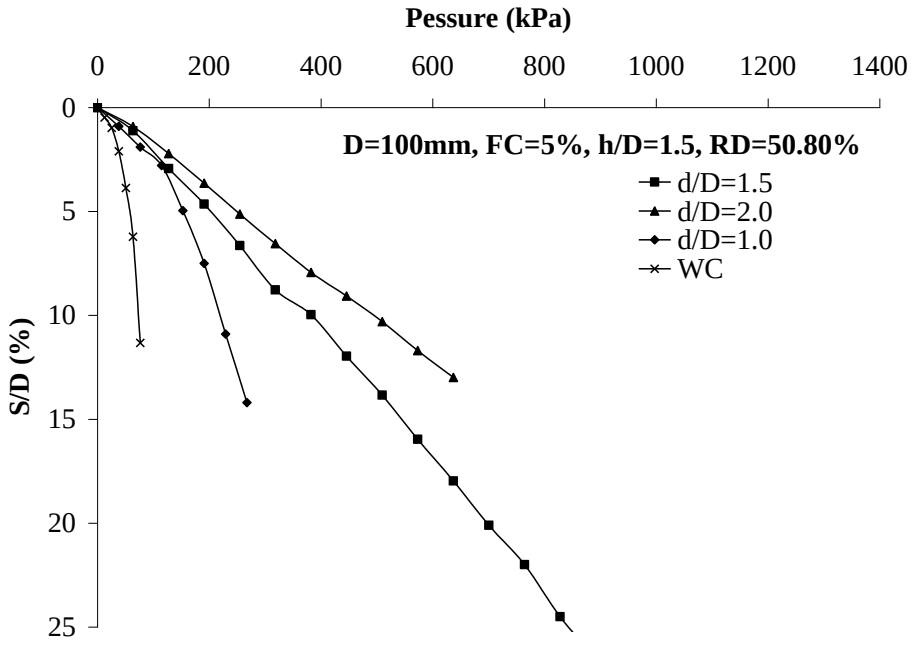

Fig. 4.22(c) Pressure vs. S/D for different values of d/D ratios for h/D=1.5

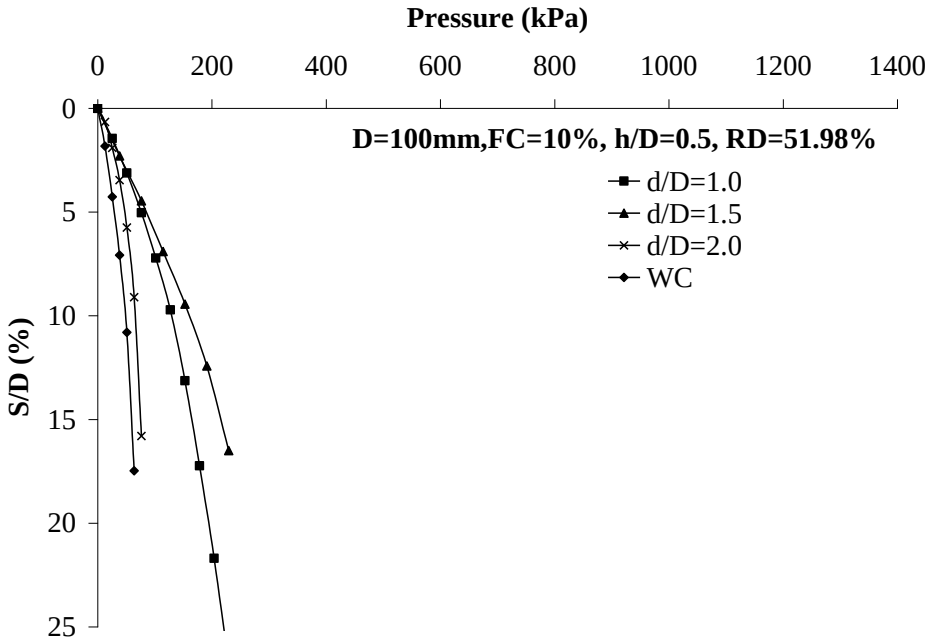

Fig. 4.23(a) Pressure vs. S/D for different values of d/D ratios for h/D=0.5

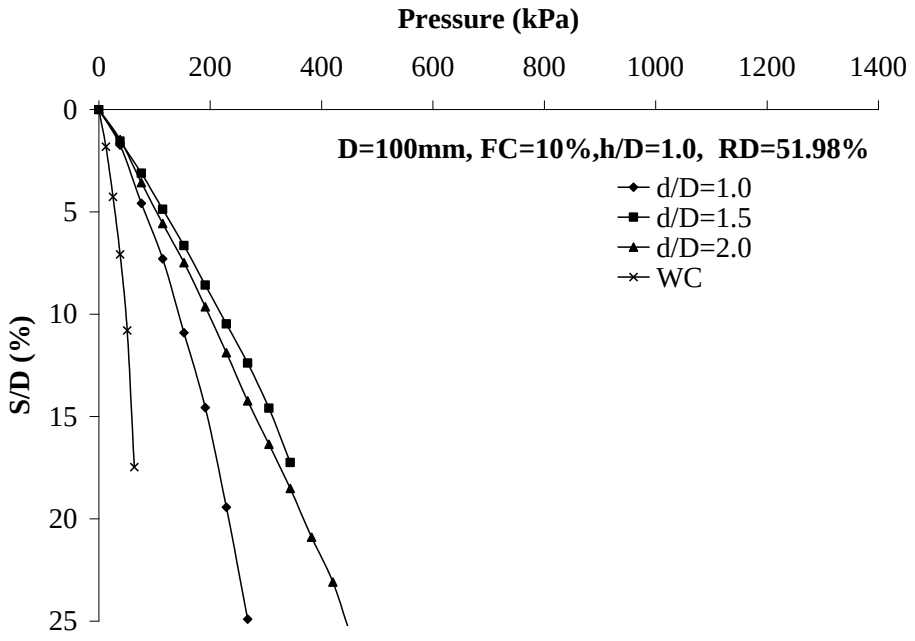

Fig. 4.23(b) Pressure vs. S/D for different values of d/D ratios for h/D=1.0

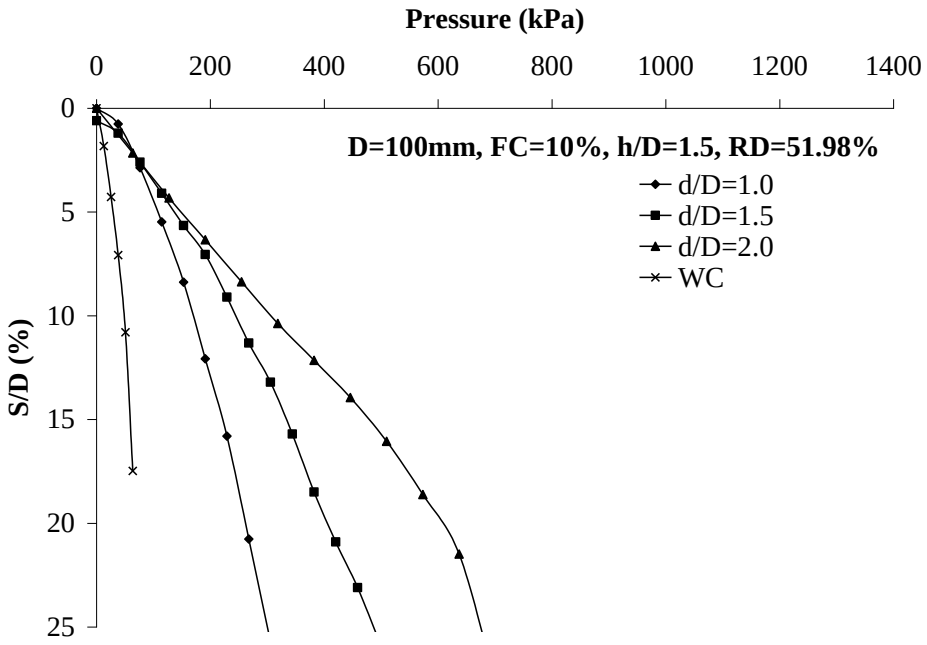

Fig. 4.23(c) Pressure vs. S/D for different values of d/D ratios for h/D=1.5

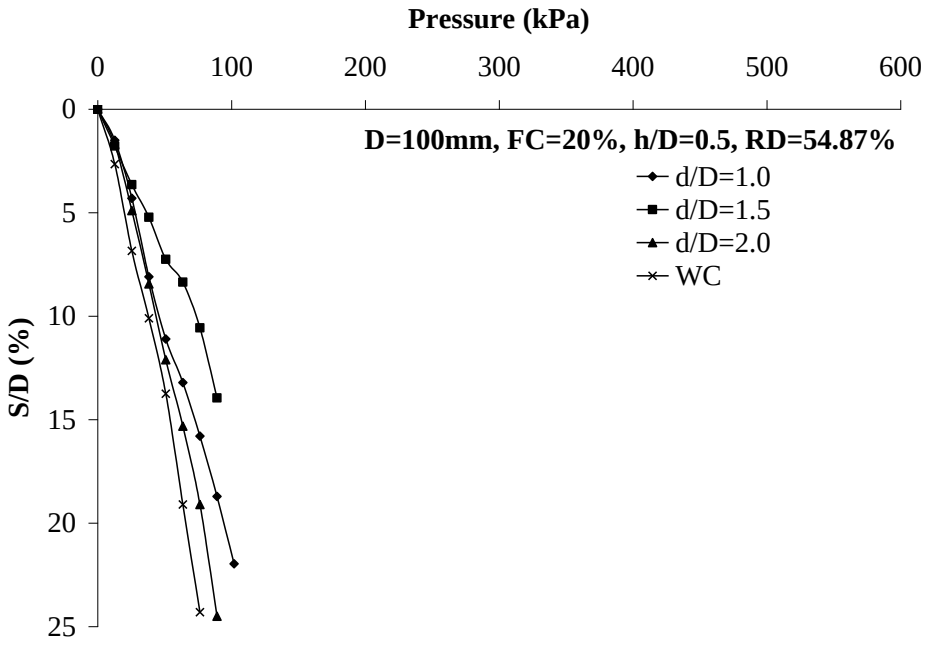

Fig. 4.24(a) Pressure vs. S/D for different values of d/D ratios for h/D=0.5

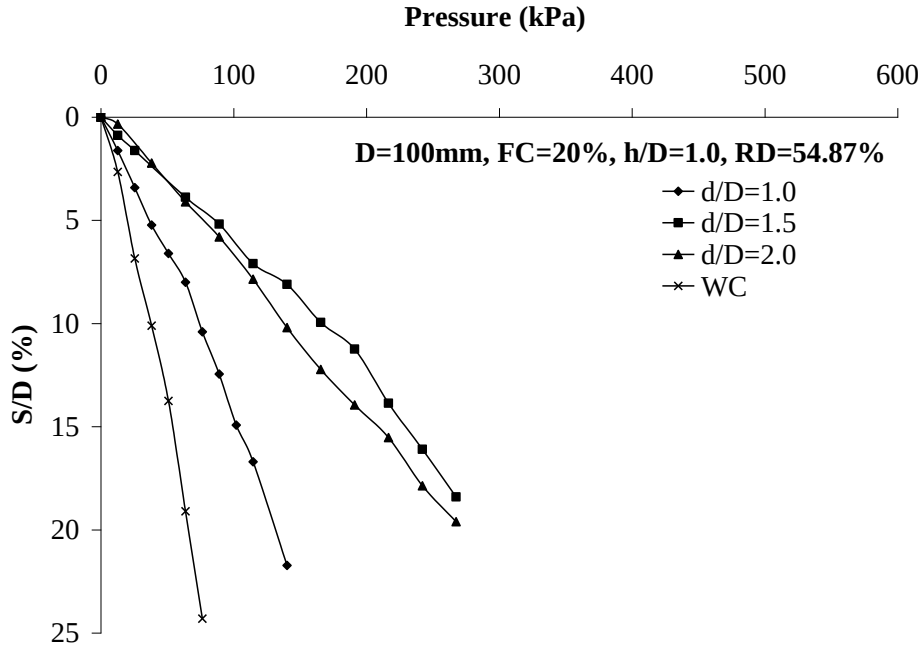

Fig. 4.24(b) Pressure vs. S/D for different values of d/D ratios for h/D=1.0

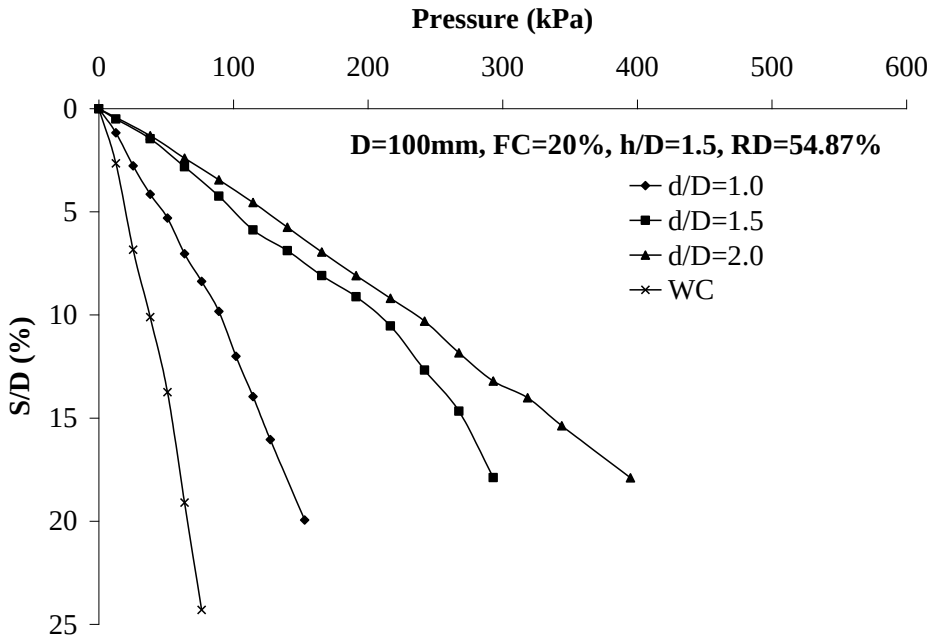

Fig. 4.24(b) Pressure vs. S/D for different values of d/D ratios for h/D=1.5

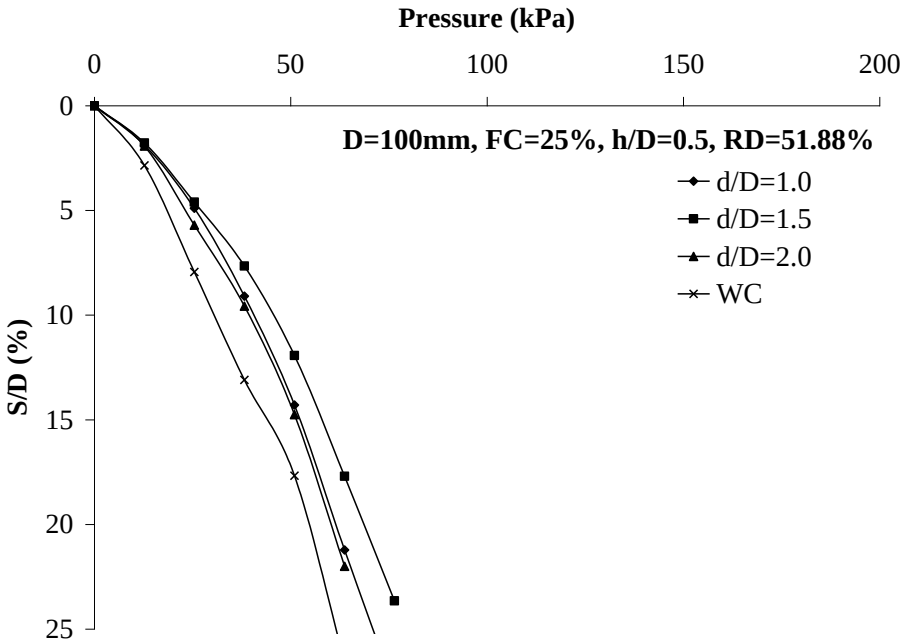

Fig. 4.25(a) Pressure vs. S/D for different values of d/D ratios for h/D=0.5

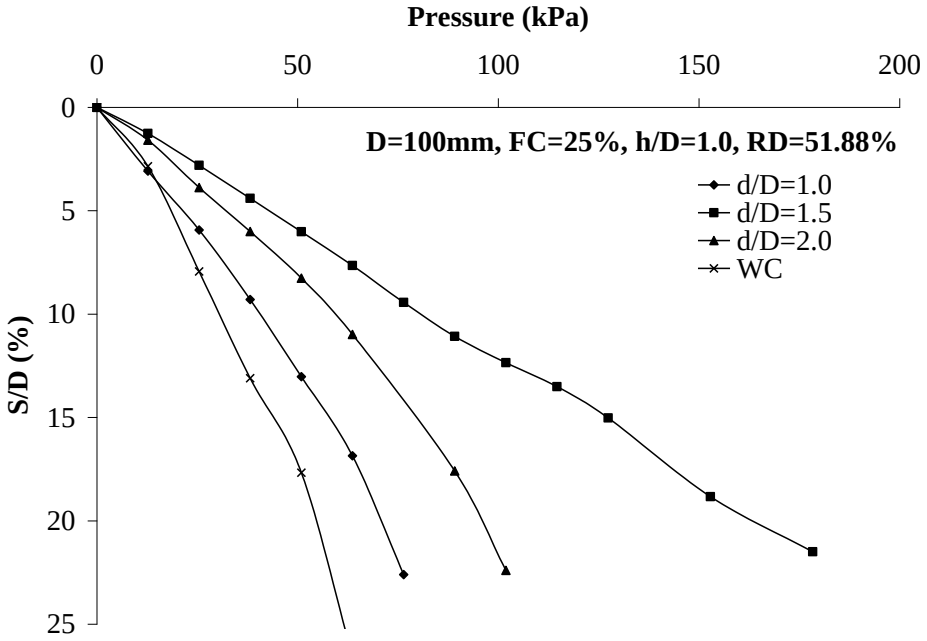

Fig. 4.25(b) Pressure vs. S/D for different values of d/D ratios for h/D=1.0

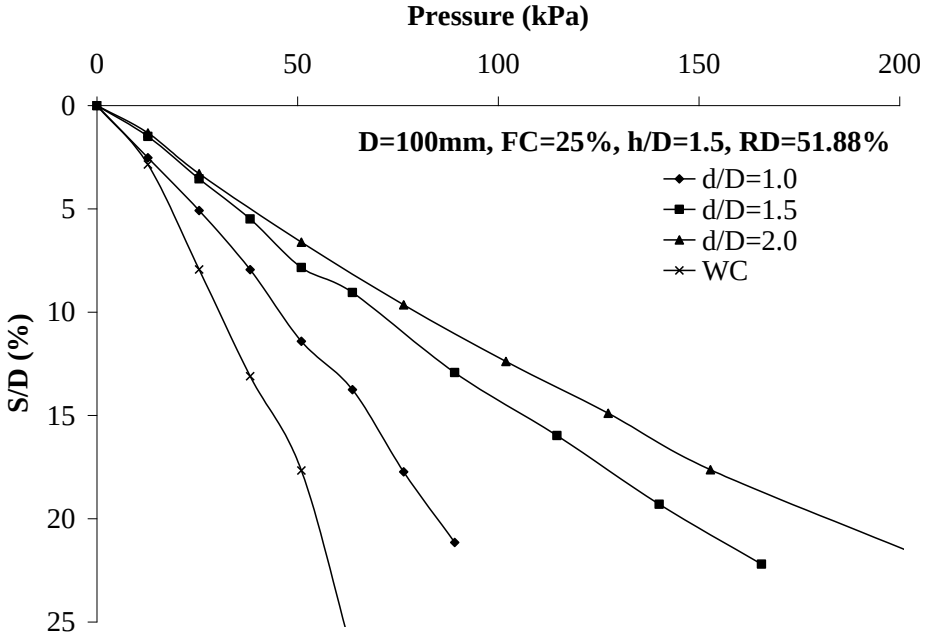

Fig. 4.25(c) Pressure vs. S/D for different values of d/D ratios for h/D=1.5

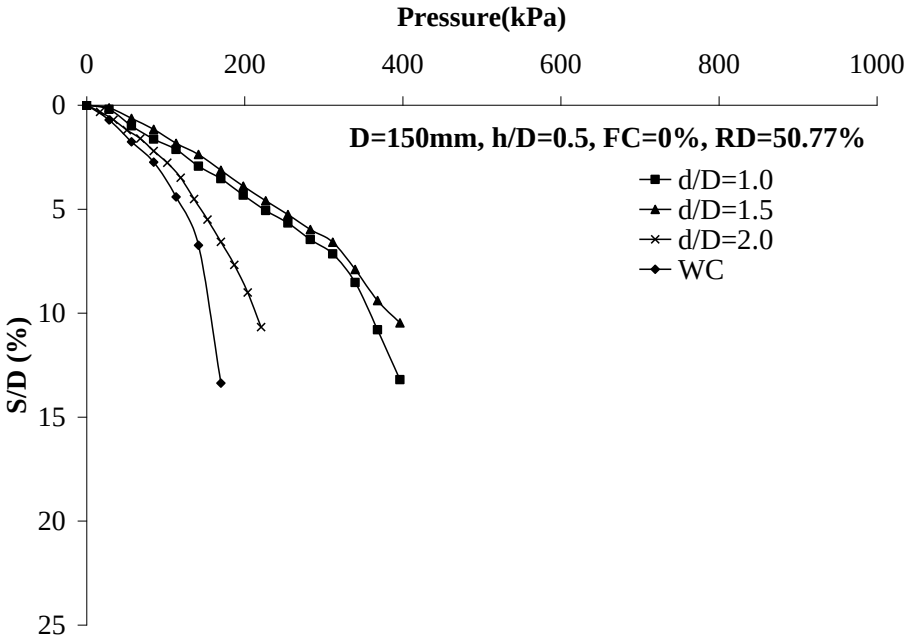

Fig. 4.26(a) Pressure vs. S/D for different values of d/D ratios for h/D=0.5

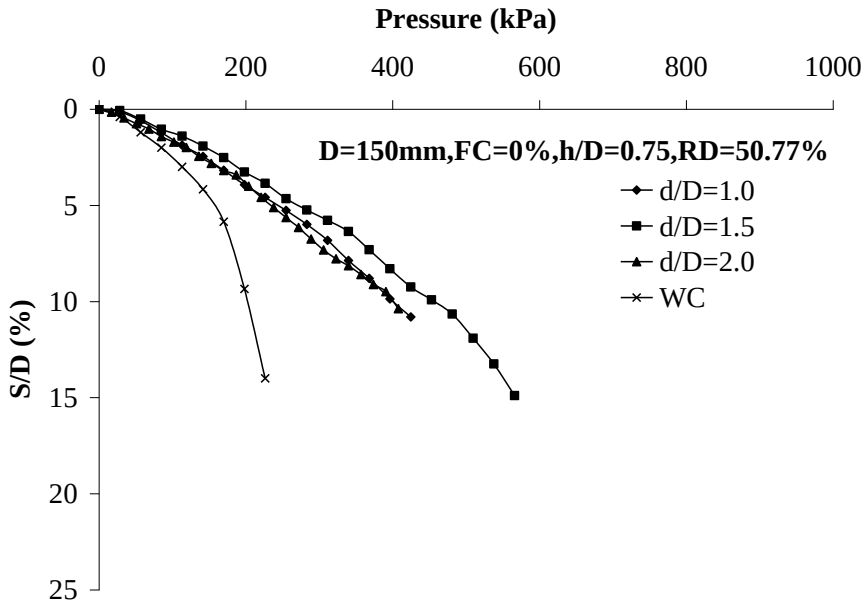

Fig. 4.26(b) Pressure vs. S/D for different values of d/D ratios for h/D=0.75

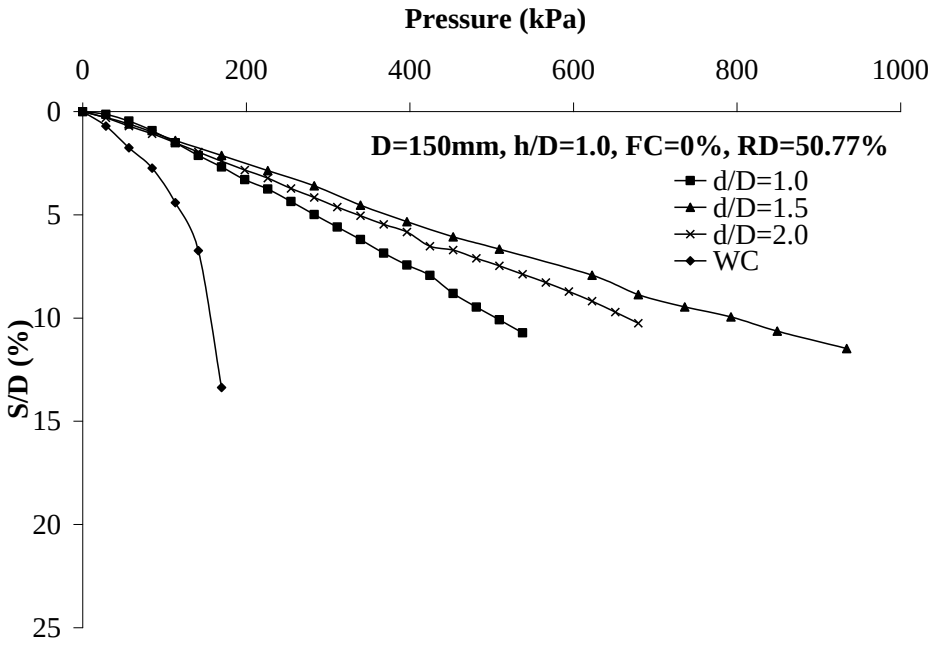

Fig. 4.26(c) Pressure vs. S/D for different values of d/D ratios for h/D=1.0

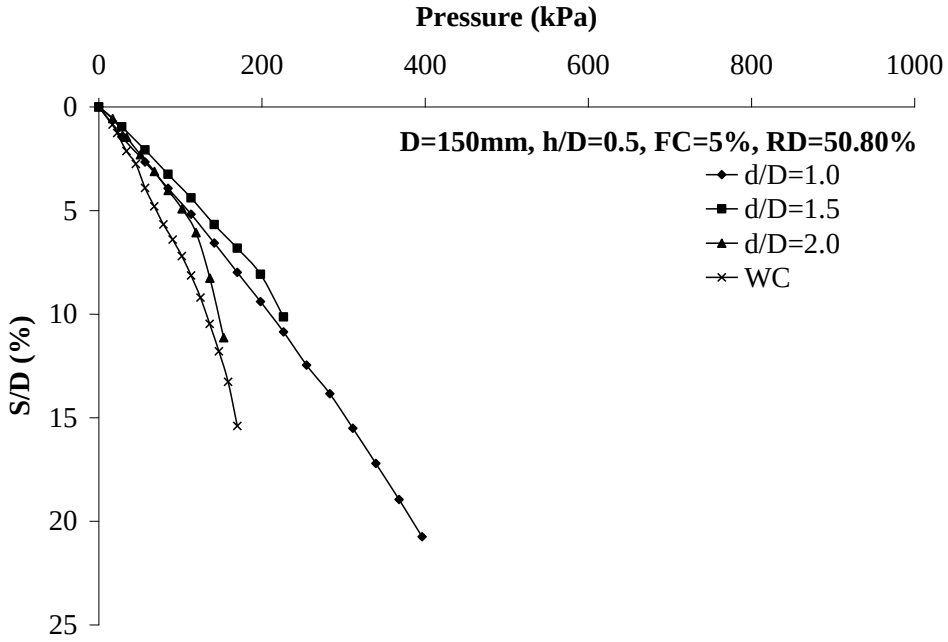

Fig. 4.27(a) Pressure vs. S/D for different values of d/D ratios for h/D=0.5

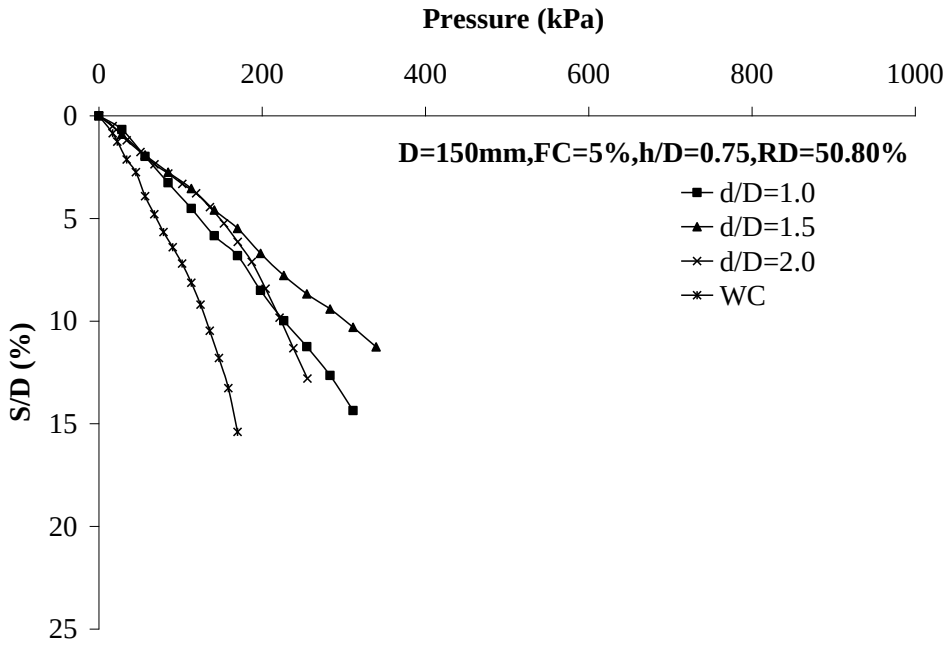

Fig. 4.27(b) Pressure vs. S/D for different values of d/D ratios for h/D=0.75

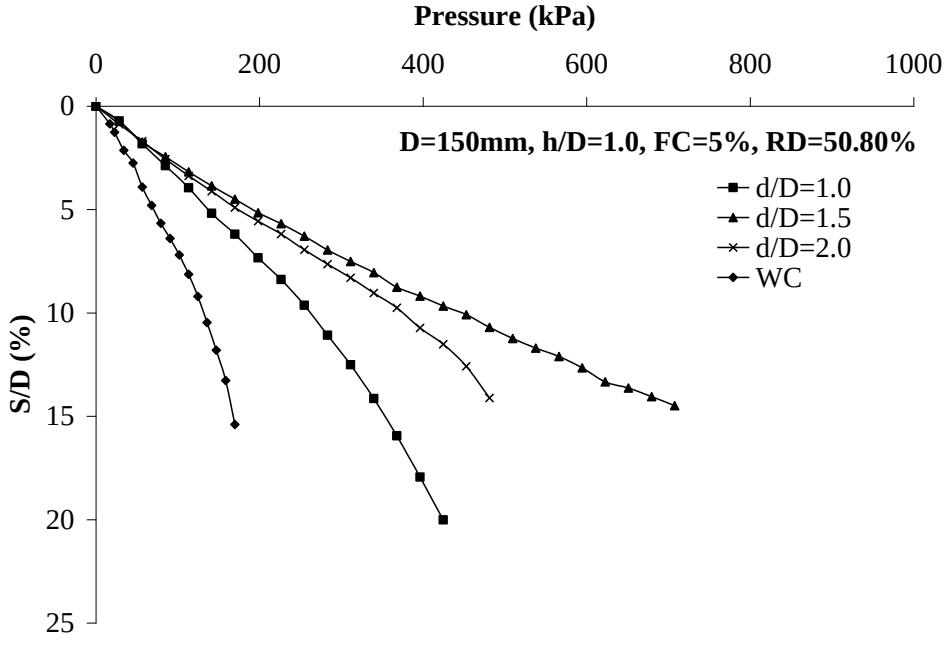

Fig. 4.27(c) Pressure vs. S/D for different values of d/D ratios for h/D=1.0

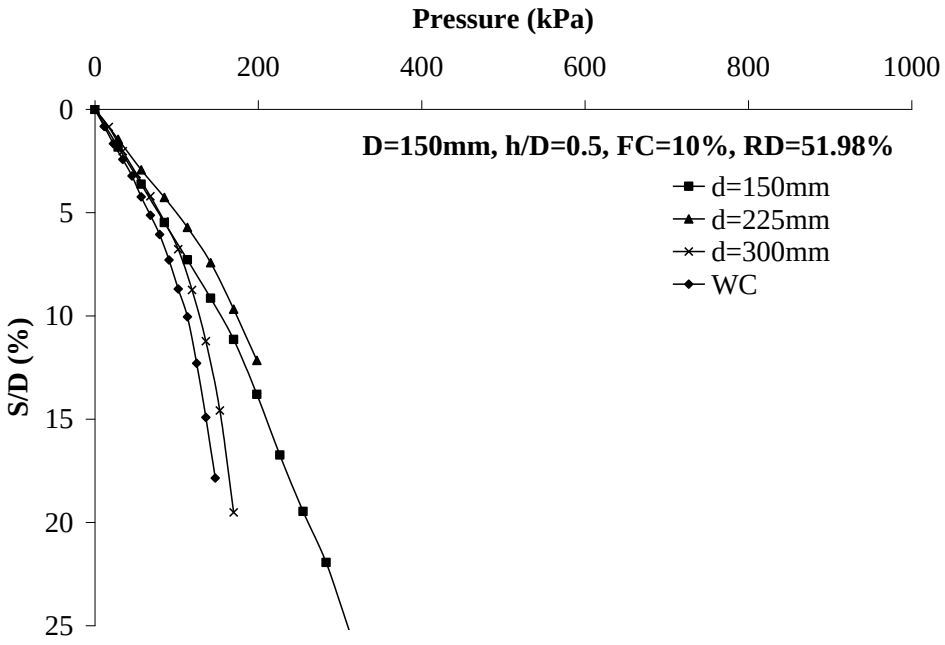

Fig. 4.28(a) Pressure vs. S/D for different values of d/D ratios for h/D=0.5

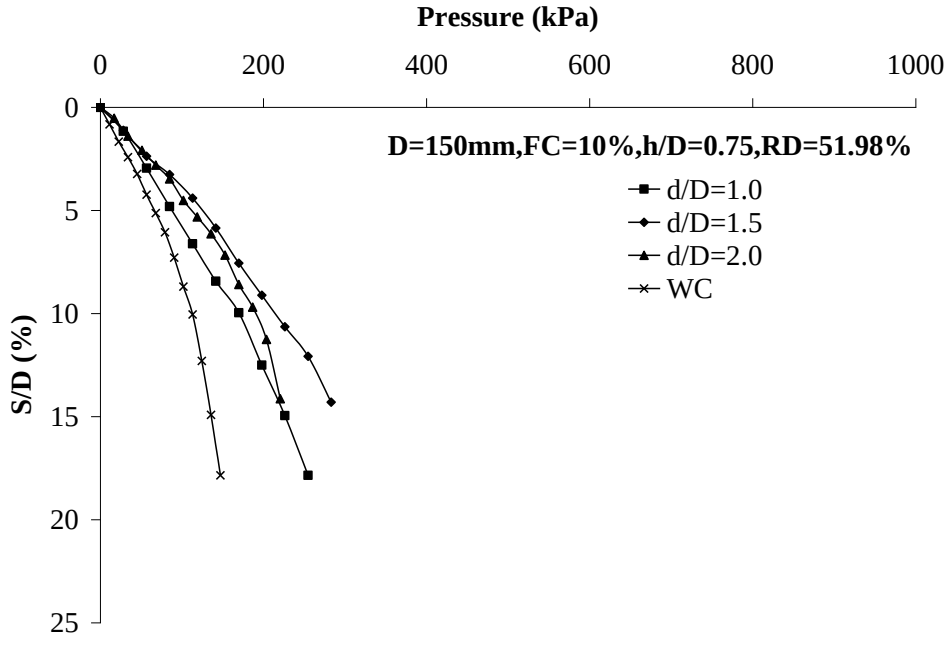

Fig. 4.28(b) Pressure vs. S/D for different values of d/D ratios for h/D=0.75

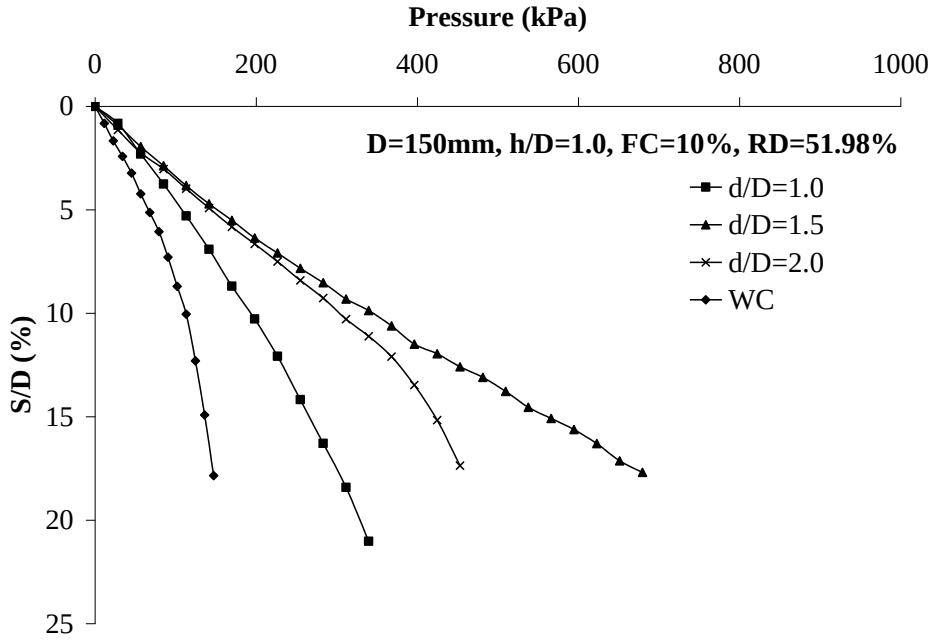

Fig. 4.28(c) Pressure vs. S/D for different values of d/D ratio for h/D=1.0

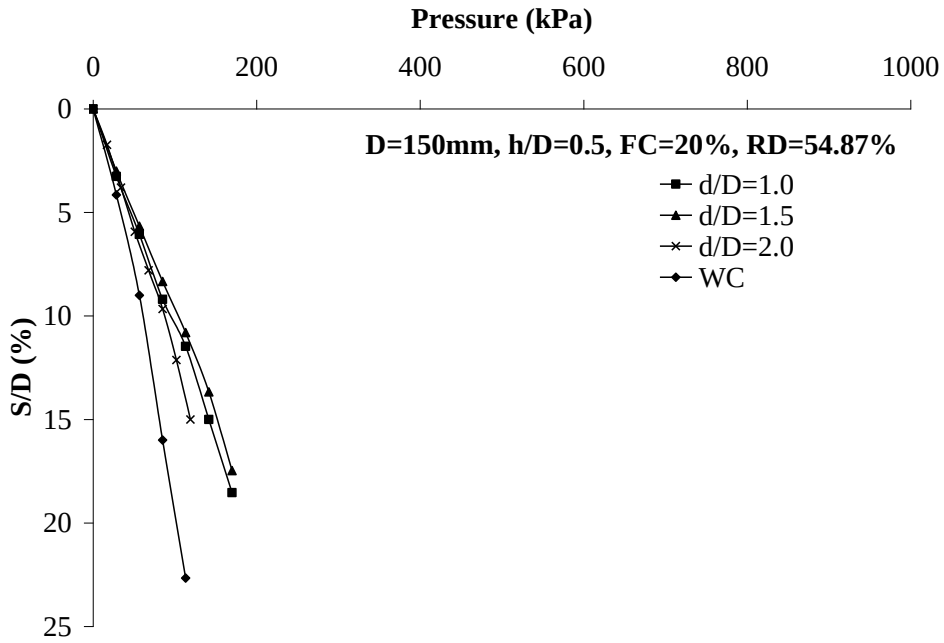

Fig. 4.29(a) Pressure vs. S/D for different values of d/D ratios for h/D=0.5

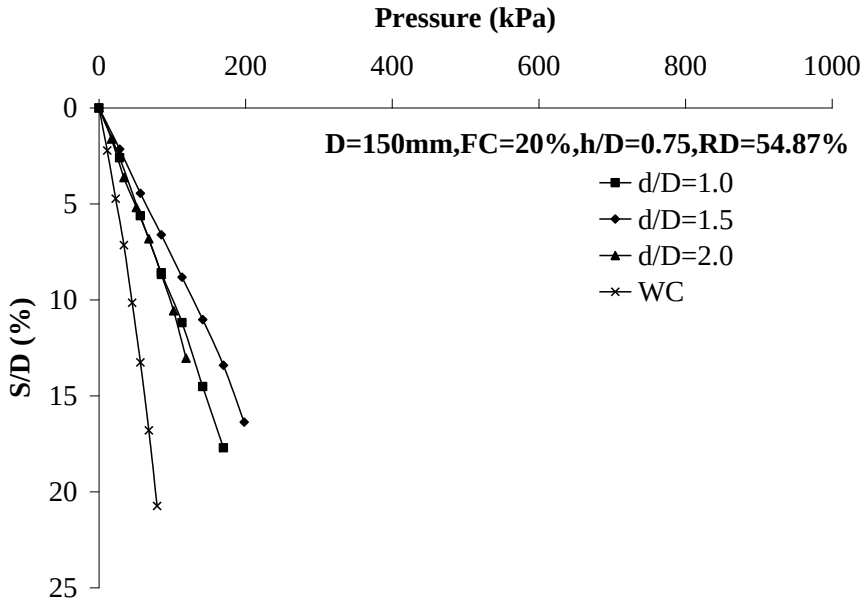

Fig. 4.29(b) Pressure vs. S/D for different values of d/D ratios for h/D=0.75

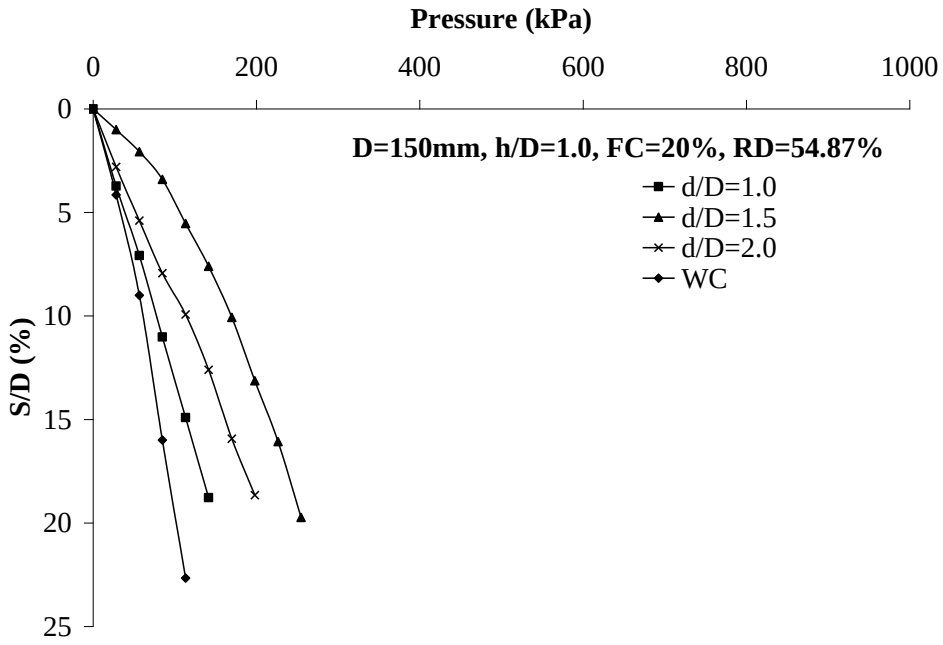

Fig. 4.29(c) Pressure vs. S/D for different values of d/D ratios for h/D=1.0

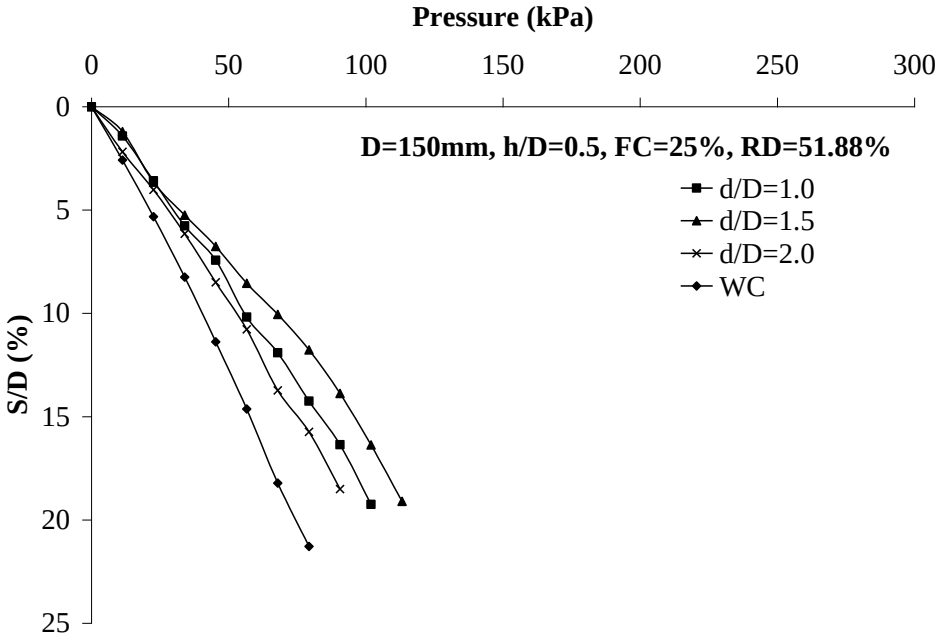

Fig. 4.30(a) Pressure vs. S/D for different values of d/D ratios for h/D=0.5

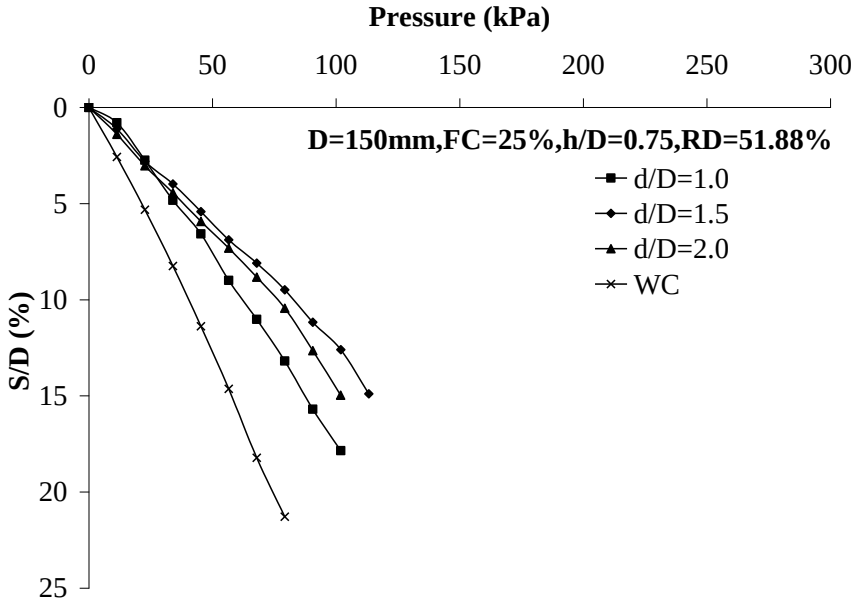

Fig. 4.30 (b) Pressure vs. S/D for different values of d/D ratios for h/D=0.75

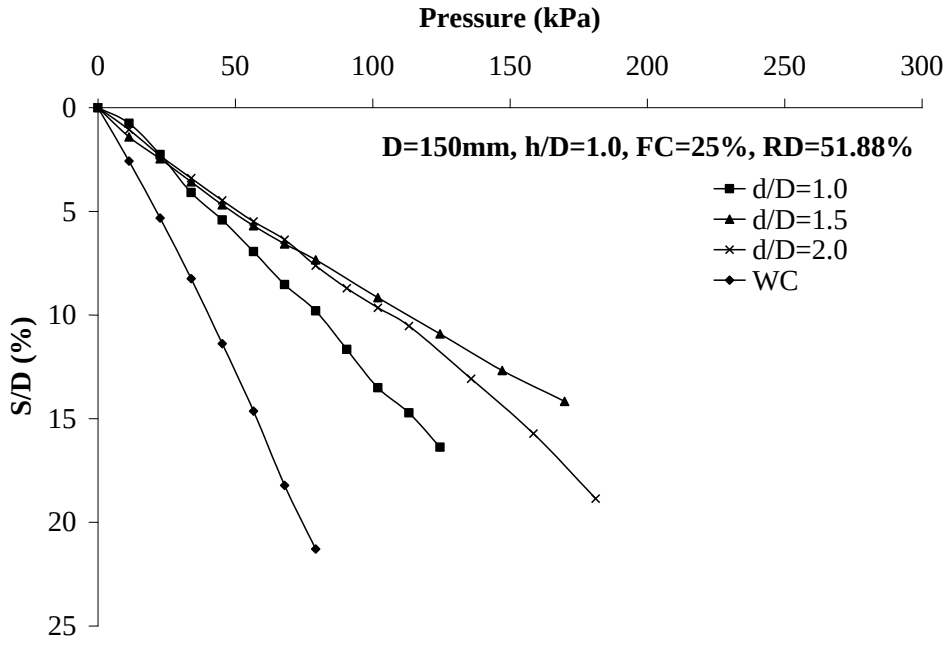

Fig. 4.30 (c) Pressure vs. S/D for different values of d/D ratios for h/D=1.0

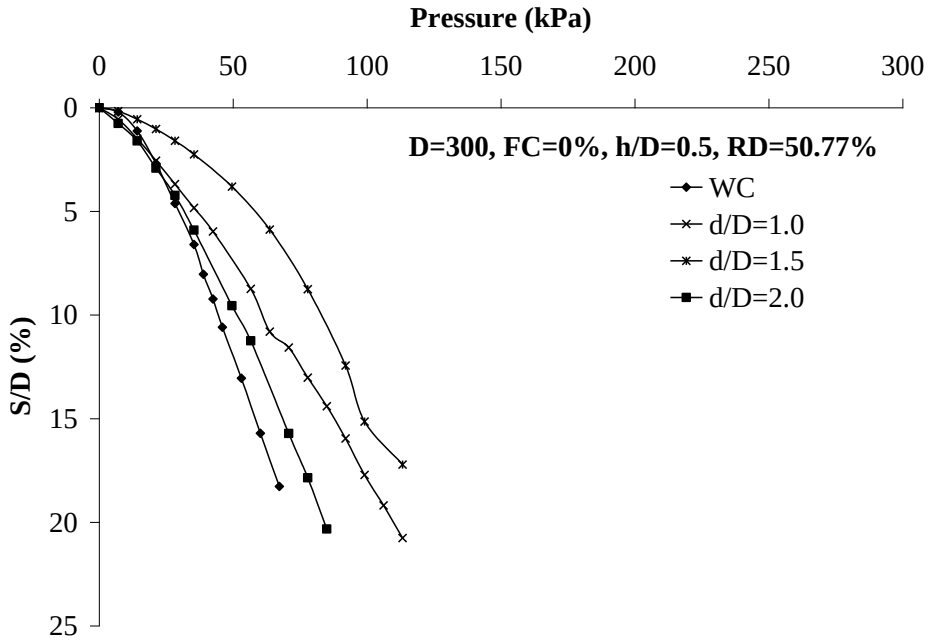

Fig. 4.31(a) Pressure vs. S/D for different values of d/D ratios for h/D=0.5 and FC=0%

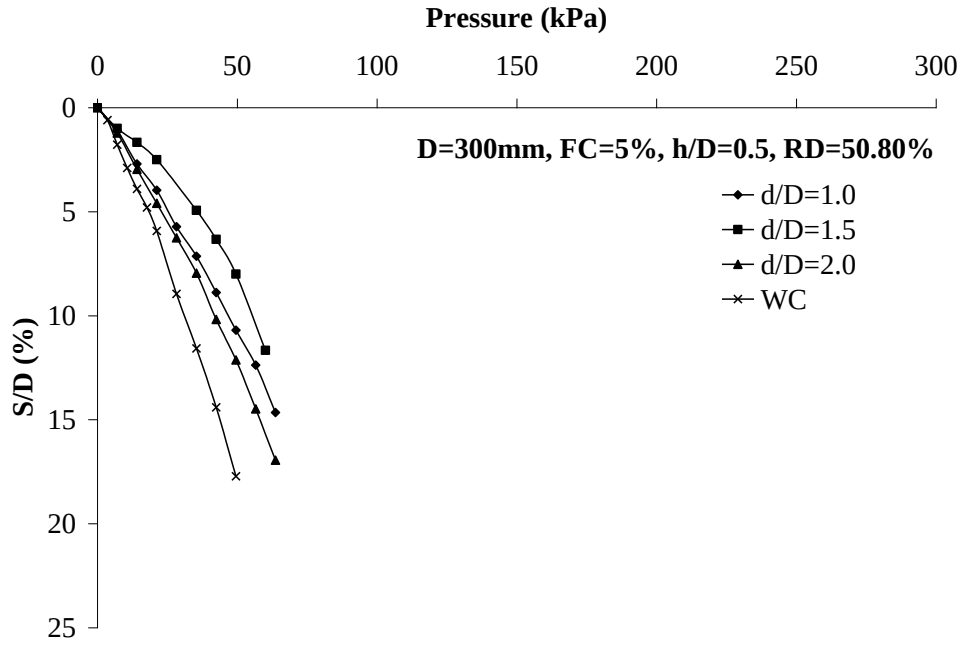

Fig. 4.31(b) Pressure vs. S/D for different values of d/D ratios for h/D=0.5 and FC=5%

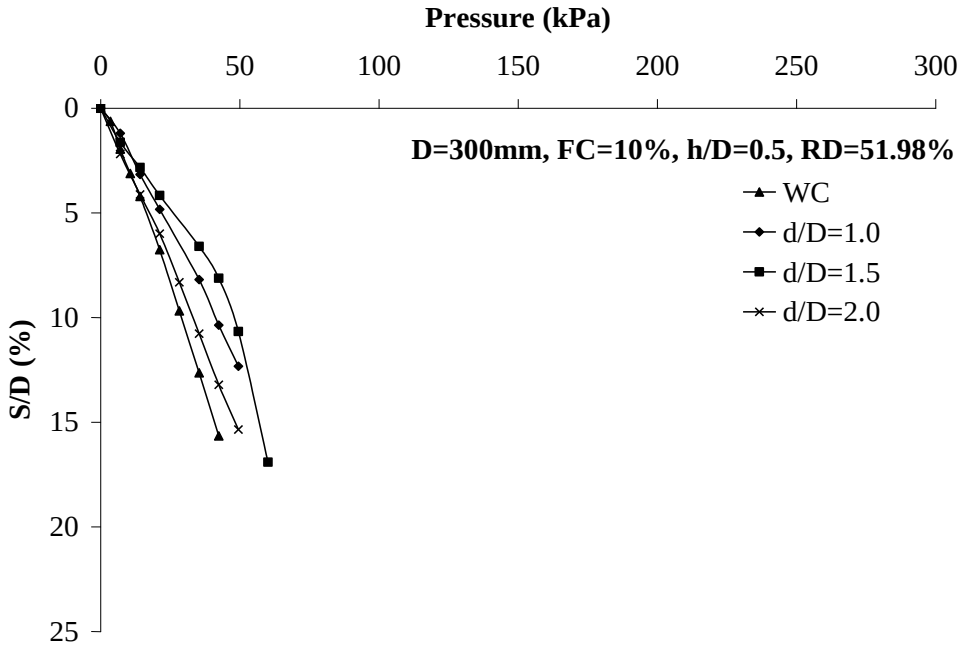

Fig. 4.31(c) Pressure vs. S/D for different values of d/D ratios for h/D=0.5 and FC=10%

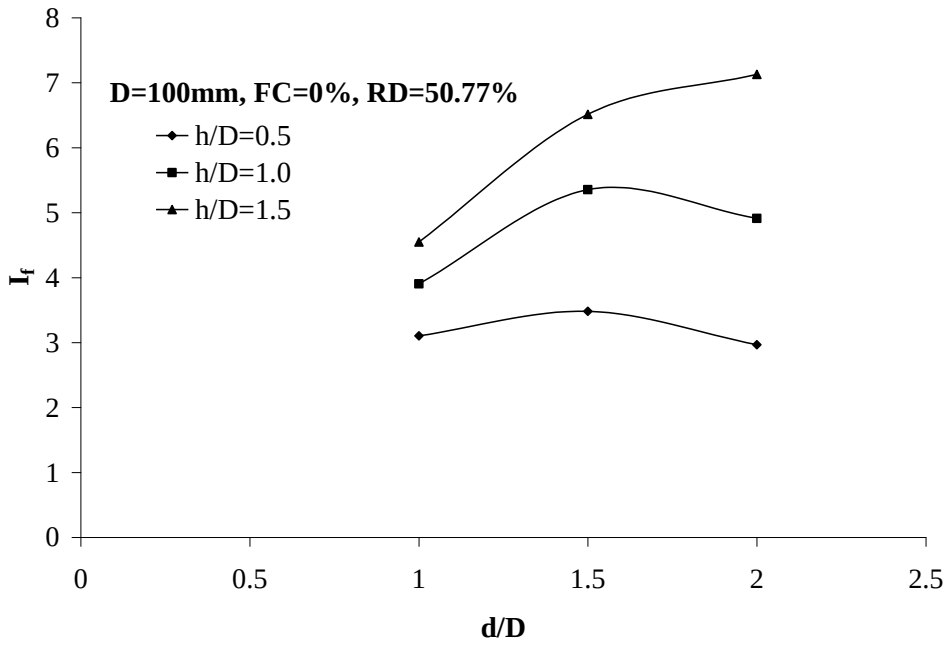

Fig. 4.32 Improvement factor vs. normalized cell diameter (d/D) for different cell heights for D=100mm and FC=0%

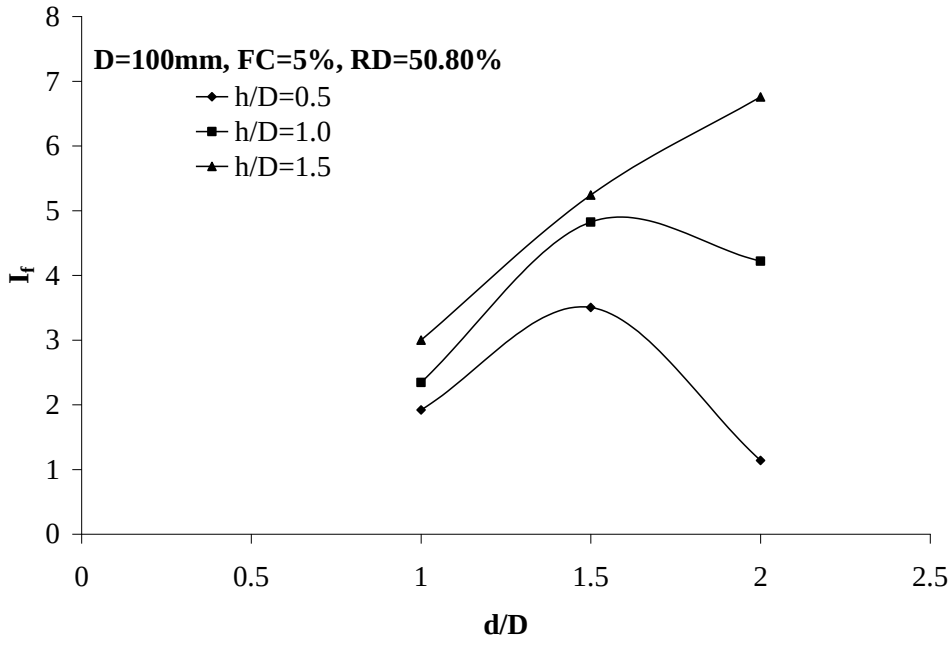

Fig. 4.33 Improvement factor vs. normalized cell diameter (d/D) for different cell heights for D=100mm and FC=5%

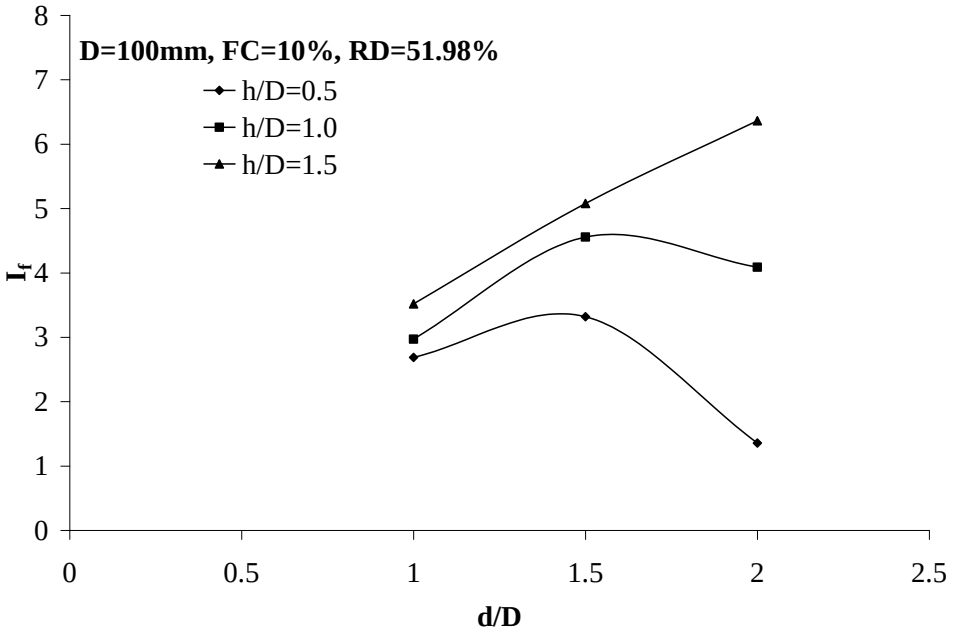

Fig. 4.34 Improvement factor vs. normalized cell diameter (d/D) for different cell heights for D=100mm and FC=10%

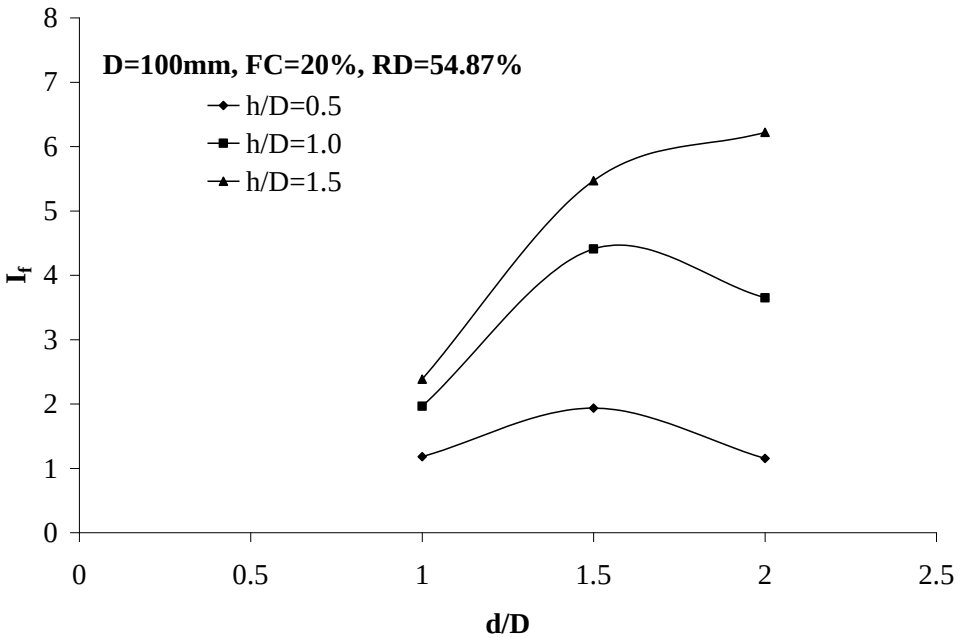

Fig. 4.35 Improvement factor vs. normalized cell diameter (d/D) for different cell heights for D=100mm and FC=20%

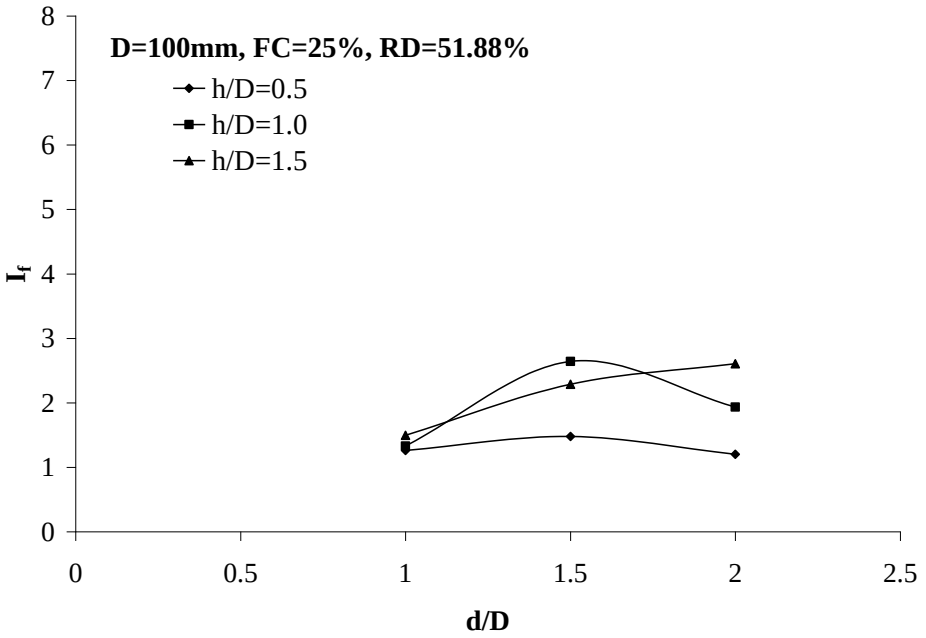

Fig. 4.36 Improvement factor vs. normalized cell diameter (d/D) for different cell heights for D=100mm and FC=25%

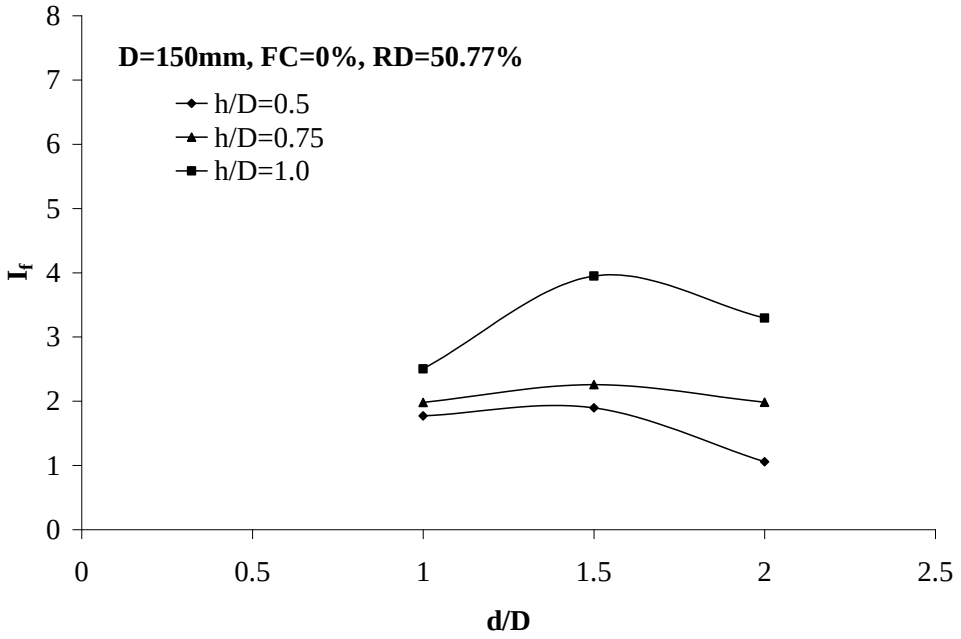

Fig. 4.37 Improvement factor vs. normalized cell diameter (d/D) for different cell heights for D=150mm and FC=0%

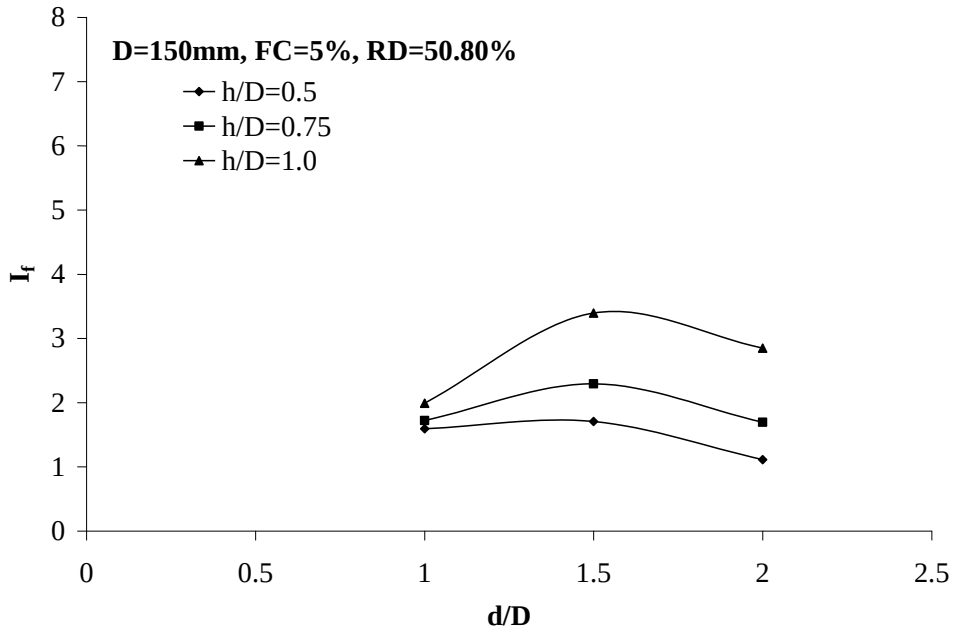

Fig. 4.38 Improvement factor vs. normalized cell diameter (d/D) for different cell heights for D=150mm and FC=5%

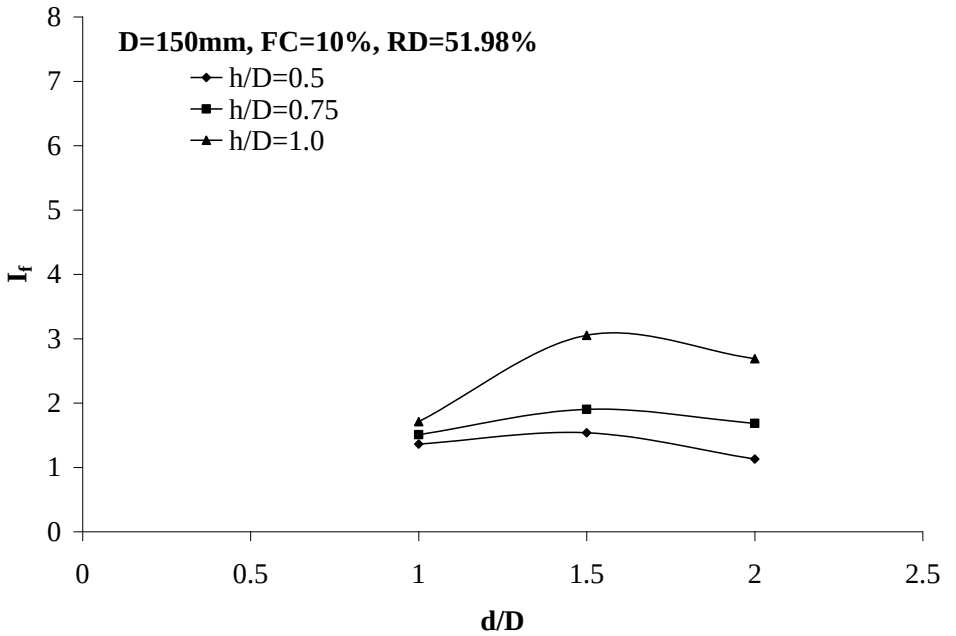

Fig. 4.39 Improvement factor vs. normalized cell diameter (d/D) for different cell heights for D=150mm and FC=10%

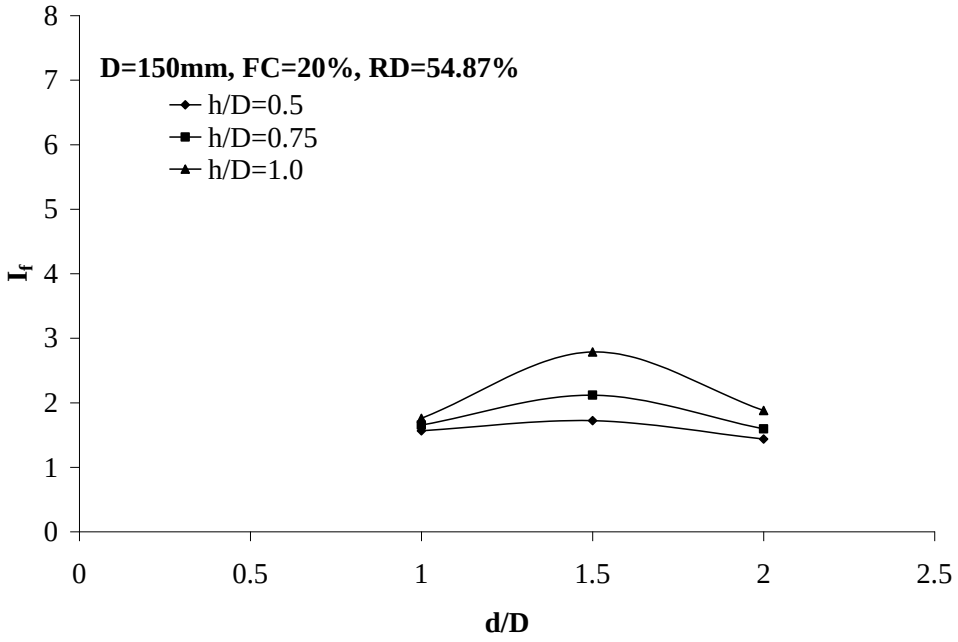

Fig. 4.40 Improvement factor vs. normalized cell diameter (d/D) for different cell heights for D=150mm and FC=20%

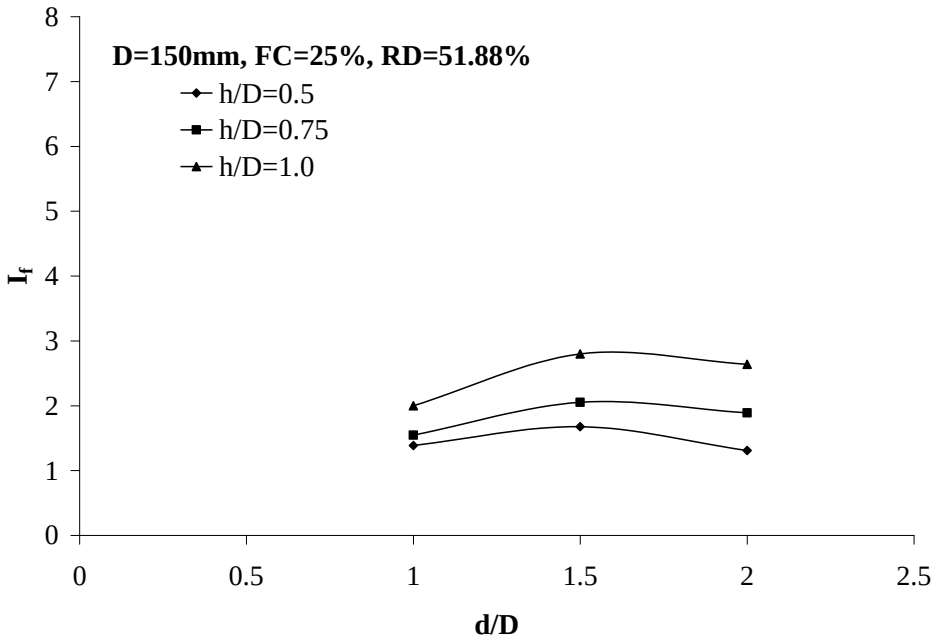

Fig. 4.41 Improvement factor vs. normalized cell diameter (d/D) for different cell heights for D=150mm and FC=25%

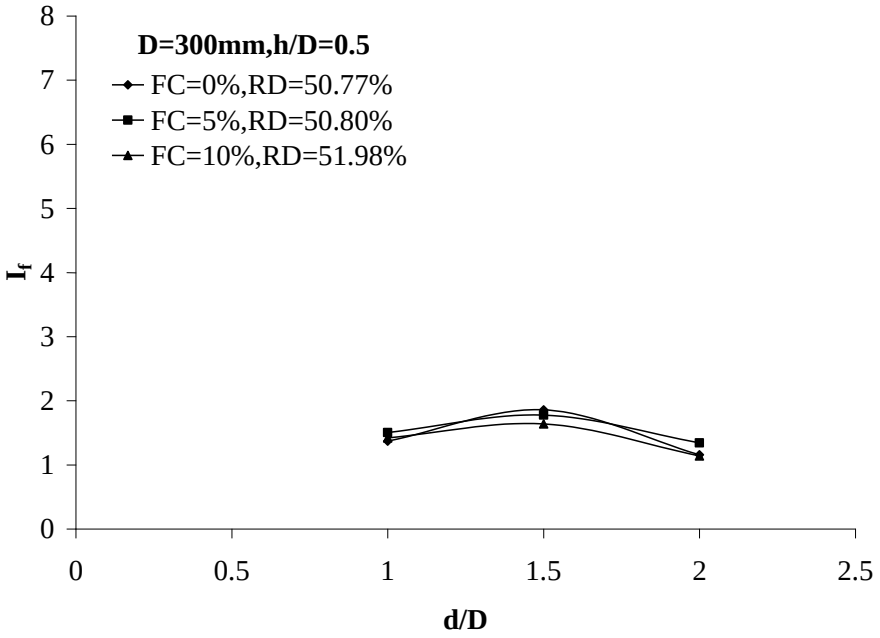

Fig. 4.42 Improvement factor vs. normalized cell diameter (d/D) for h/D=0.5

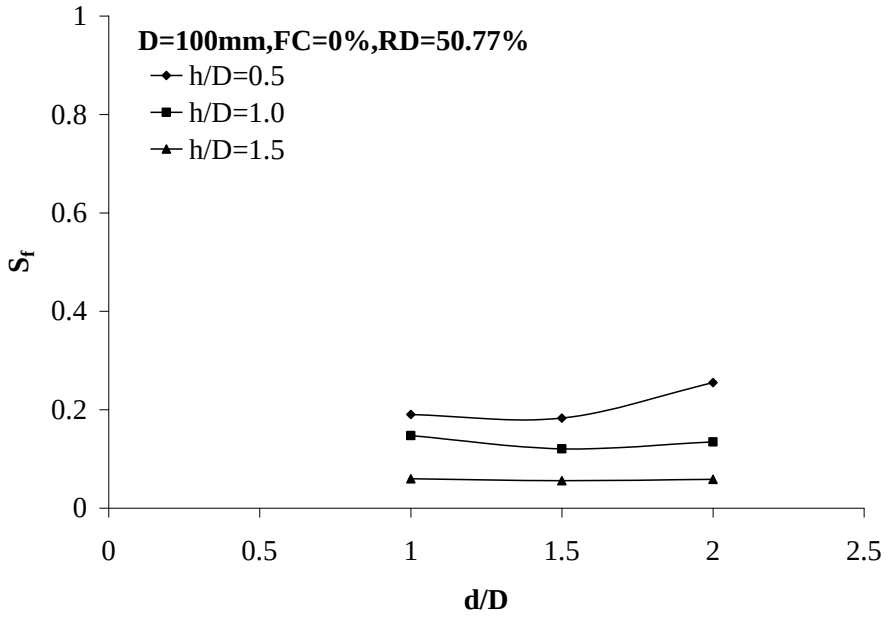

Fig. 4.43 Settlement reduction factor vs. normalized d/D ratio for different (h/D) ratios for D=100mm and FC=0%

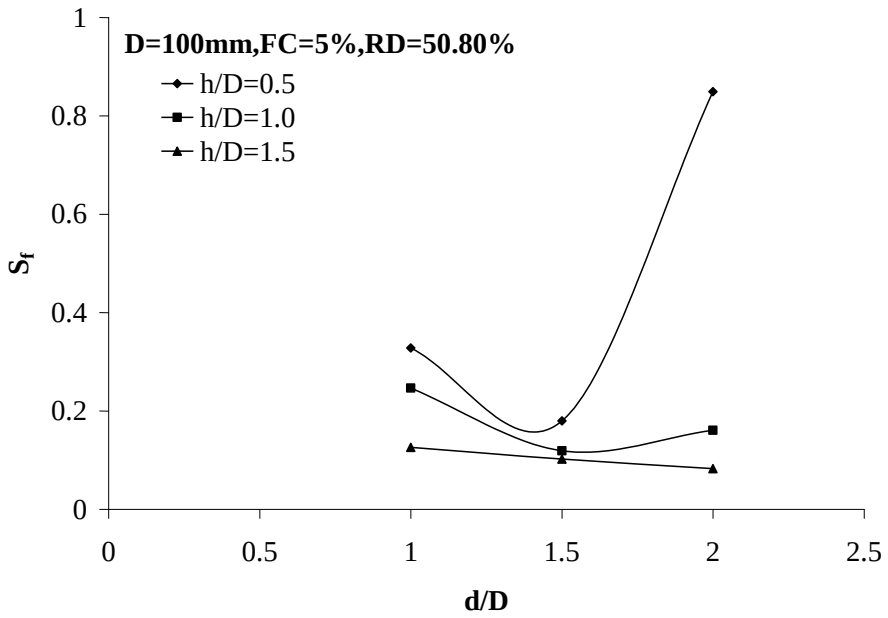

Fig. 4.44 Settlement reduction factor vs. normalized d/D ratio for different (h/D) ratios for D=100mm and FC=5%

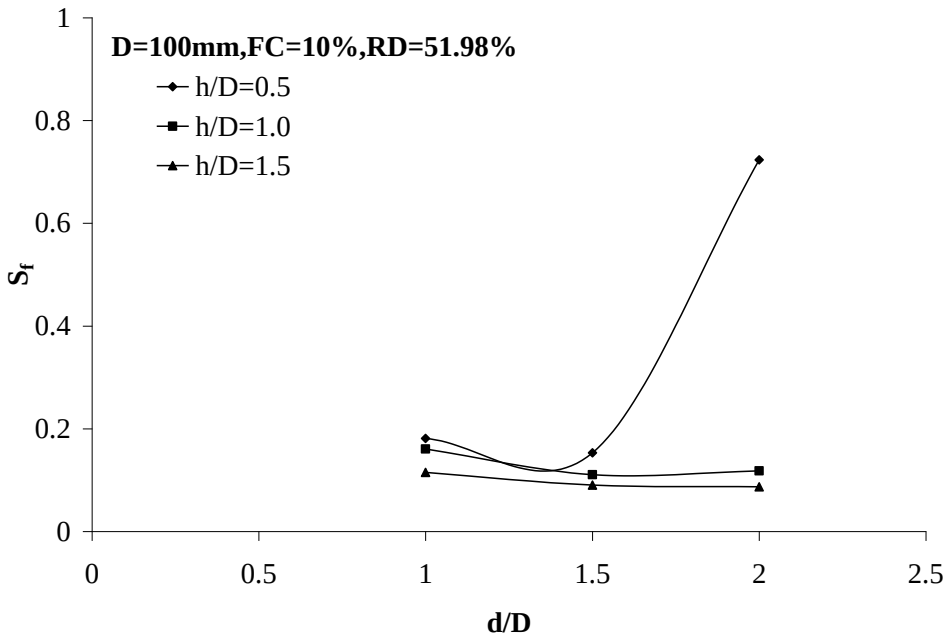

Fig. 4.45 Settlement reduction factor vs. normalized d/D ratio for different (h/D) ratios for D=100mm and FC=10%

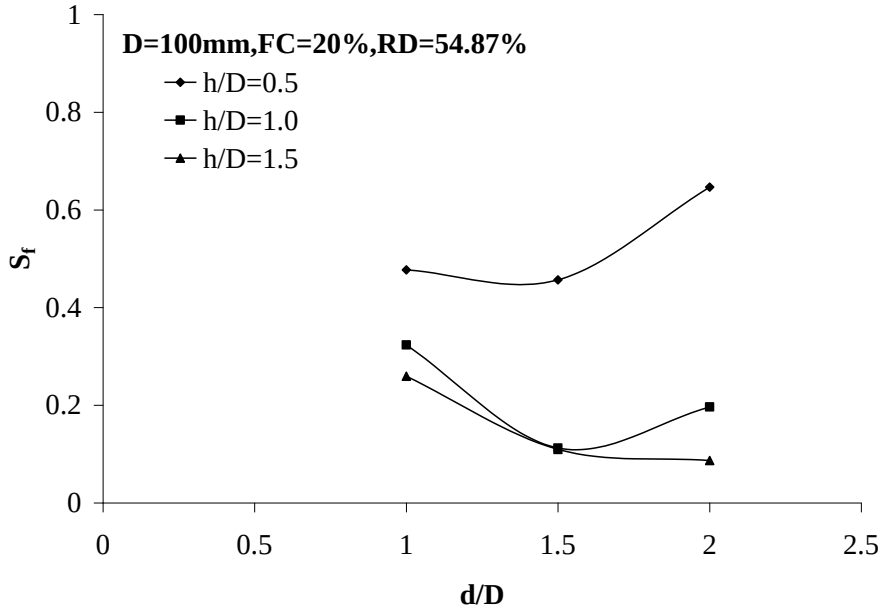

Fig. 4.46 Settlement reduction factor vs. normalized d/D ratio for different (h/D) ratios for D=100mm and FC=20%

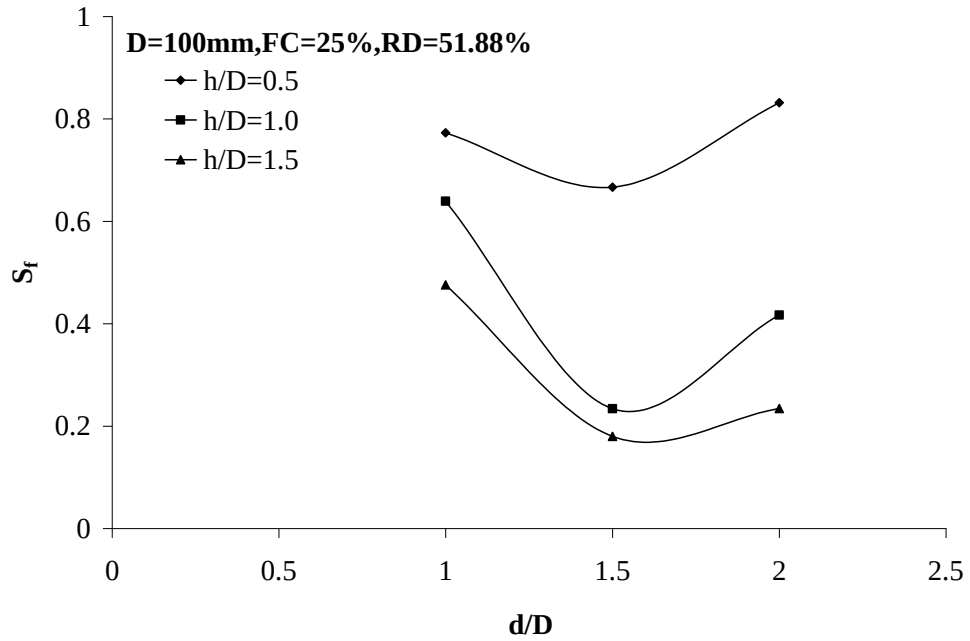

Fig. 4.47 Settlement reduction factor vs. normalized d/D ratio for different (h/D) ratios for D=100mm and FC=25%

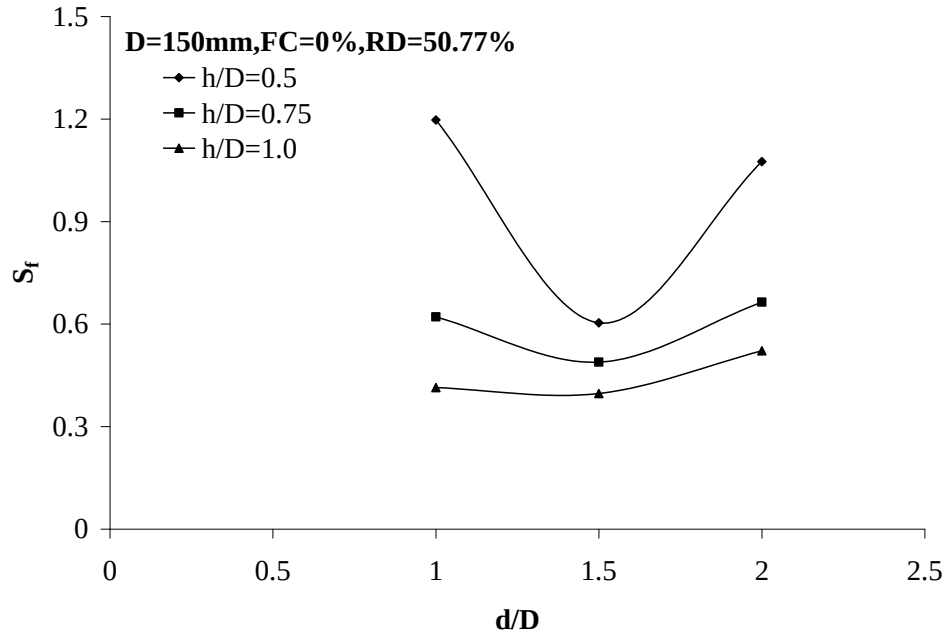

Fig. 4.48 Settlement reduction factor vs. normalized d/D ratio for different (h/D) ratios for D=150mm and FC=0%

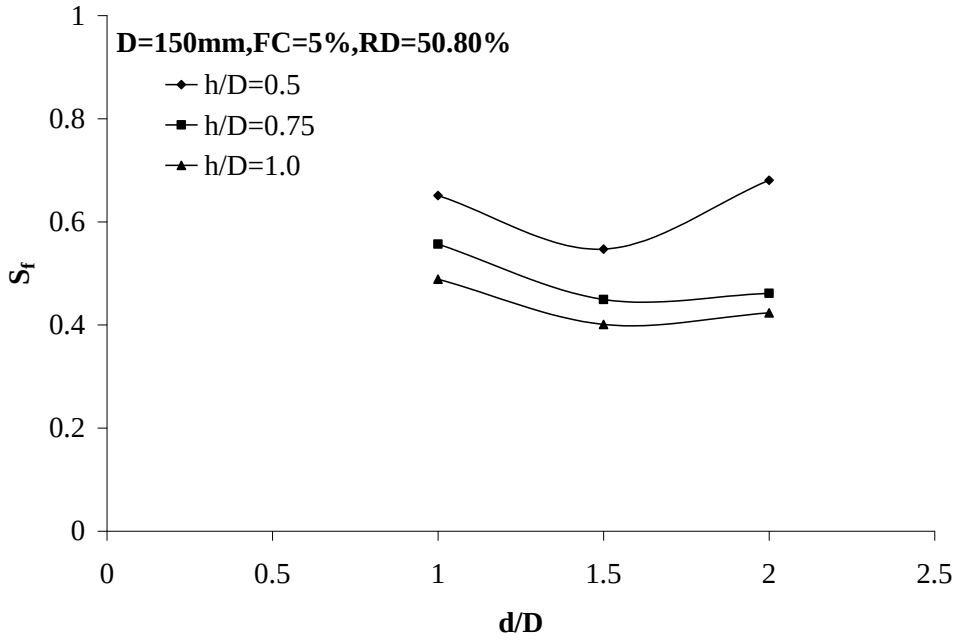

Fig. 4.49 Settlement reduction factor vs. normalized d/D ratio for different (h/D) ratios for D=150mm and FC=5%

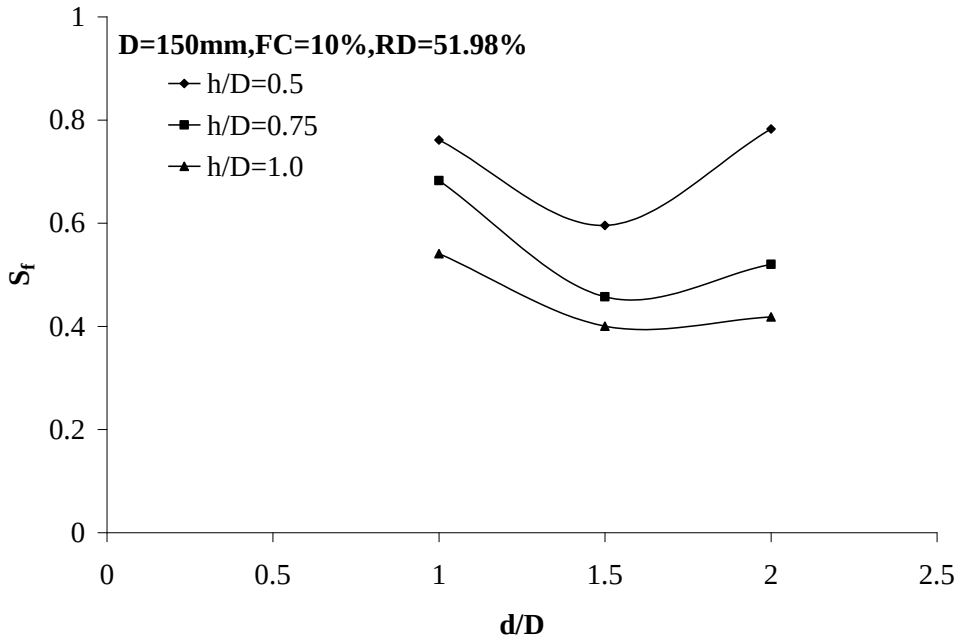

Fig. 4.50 Settlement reduction factor vs. normalized d/D ratio for different (h/D) ratios for D=150mm and FC=10%

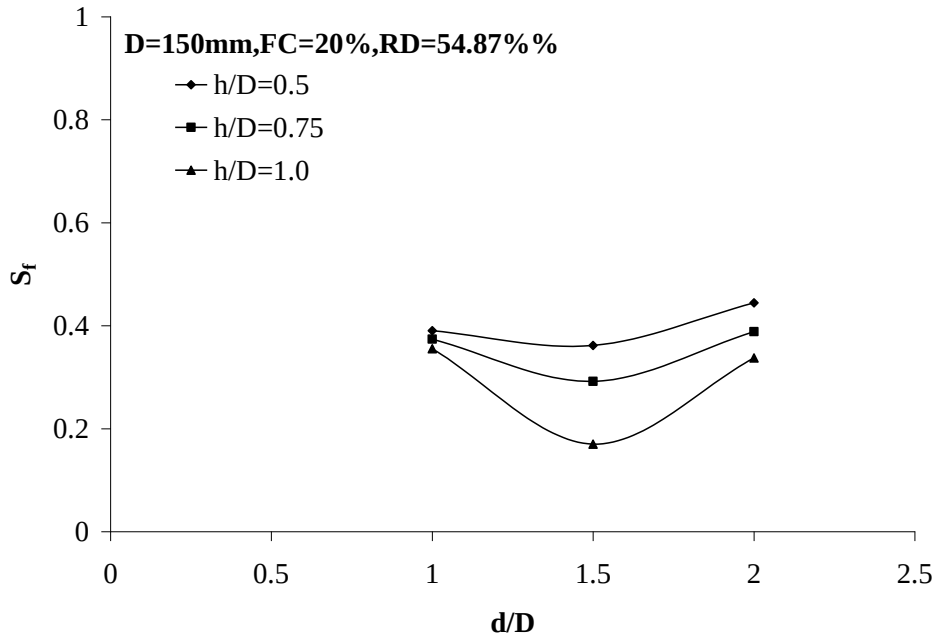

Fig. 4.51 Settlement reduction factor vs. normalized d/D ratio for different (h/D) ratios for D=150mm and FC=20%

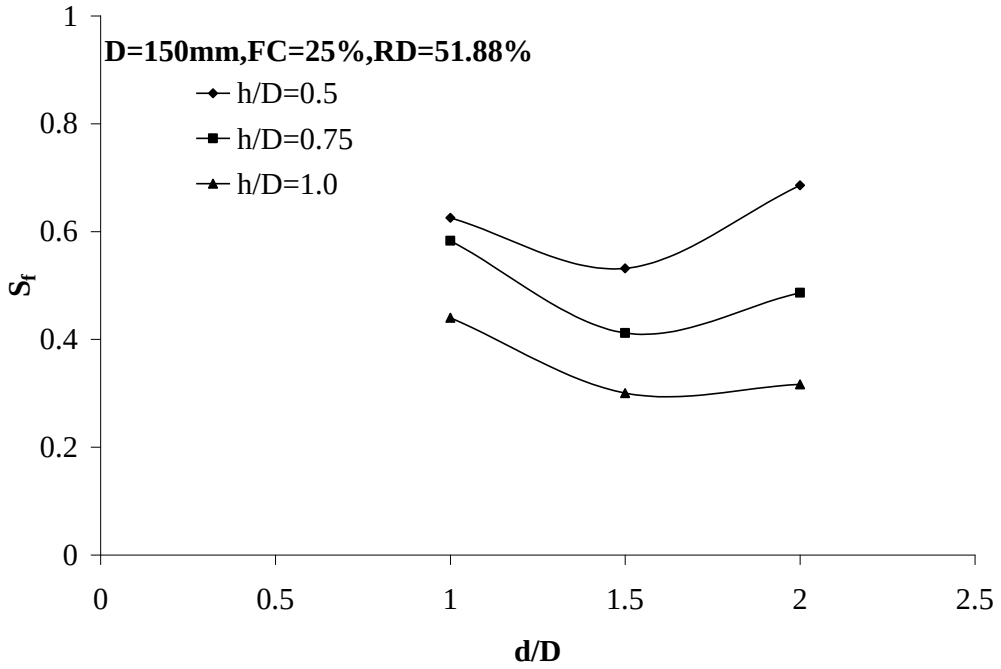

Fig. 4.52 Settlement reduction factor vs. normalized d/D ratio for different (h/D) ratios for D=150mm and FC=25%

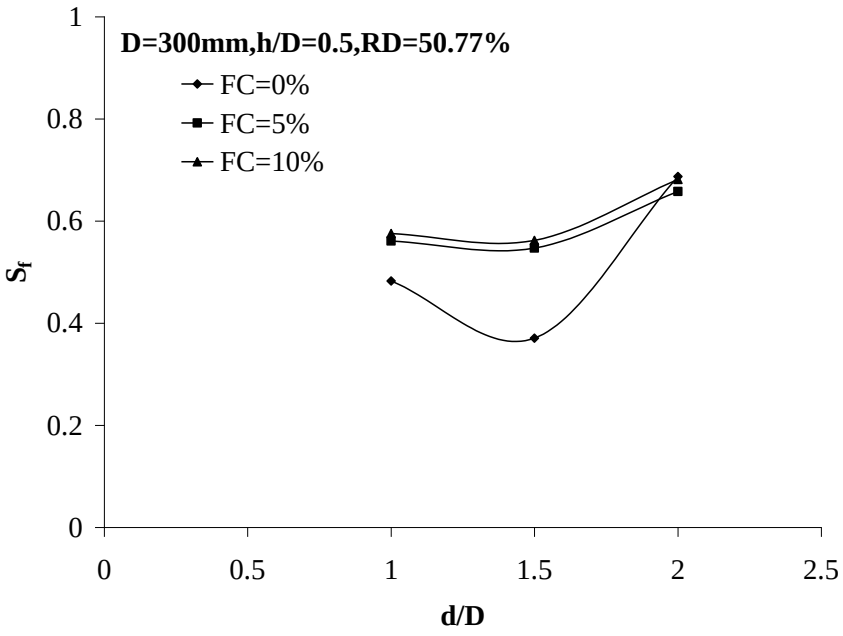

Fig. 4.53 Settlement reduction factor vs. normalized d/D ratio for (h/D) of 0.5

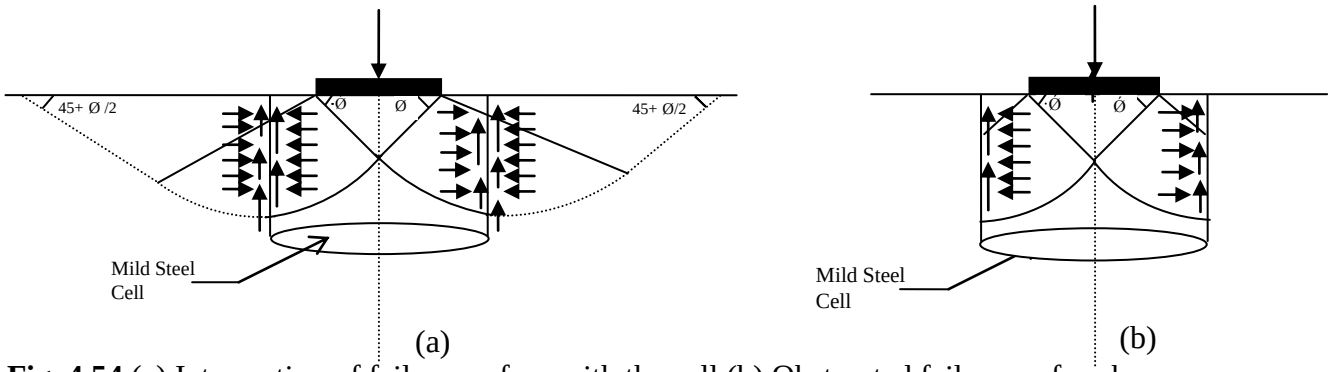

Fig. 4.54 (a) Intersection of failure surface with the cell (b) Obstructed failure surface by a cell

4.4 Effect of Cell Height

In order to investigate the effect of cell height on the footing response of silty soil, tests were carried out using h/D ratio of 0.5,1.0,1.5m for 0.1m diameter footing and 0.5,0.75 and 1.0 for 0.15m diameter footing and 0.5 for 0.3m diameter footing for each cell diameter for different percentages of fines. Fig (4.55) to Fig (4.64) shows the bearing pressure vs. S/D ratio for different values of h/D ratio. On comparing the curves of pressure vs. S/D ratio with and without confinement using different values of h/D ratios, it has been observed that the footing with higher h/D ratio gives higher bearing capacity. The improvement factor vs. normalized cell height (*h*/*D*) is shown in Fig (4.65) to Fig (4.74) for different normalized cell diameters (*d*/*D*) for different footing diameters. The figure shows the same pattern of behavior for the different cell diameters. Increase in cell heights results in a greater improvement in the bearing capacity. The increase in cell height results in the enlargement in the surface area of the cell–model footing leading to a higher bearing capacity.

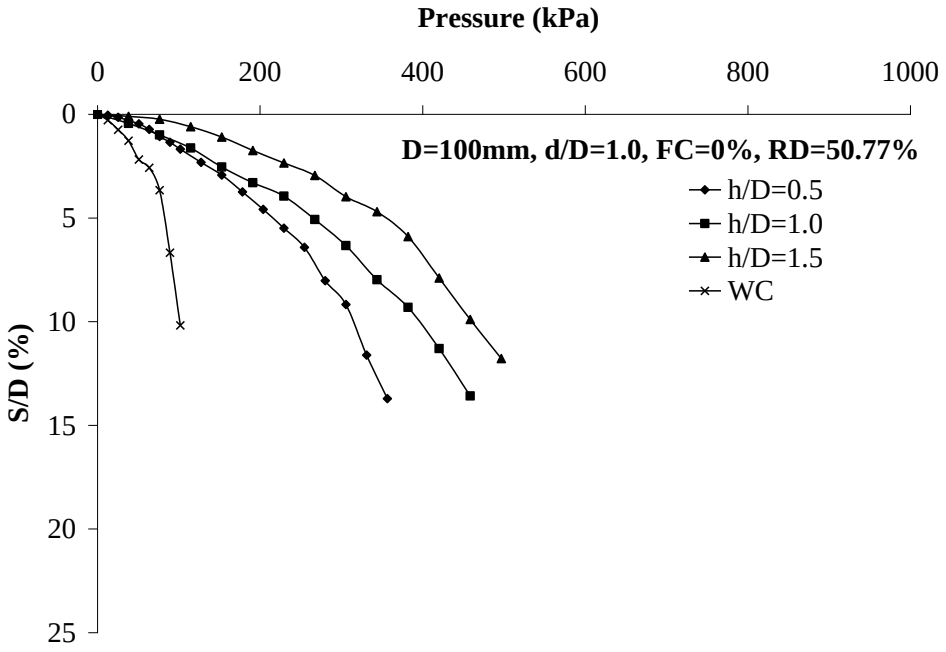

Fig. 4.55(a) Pressure vs. S/D for different values of h/D ratios for D=100mm, d/D=1.0 and FC=0%

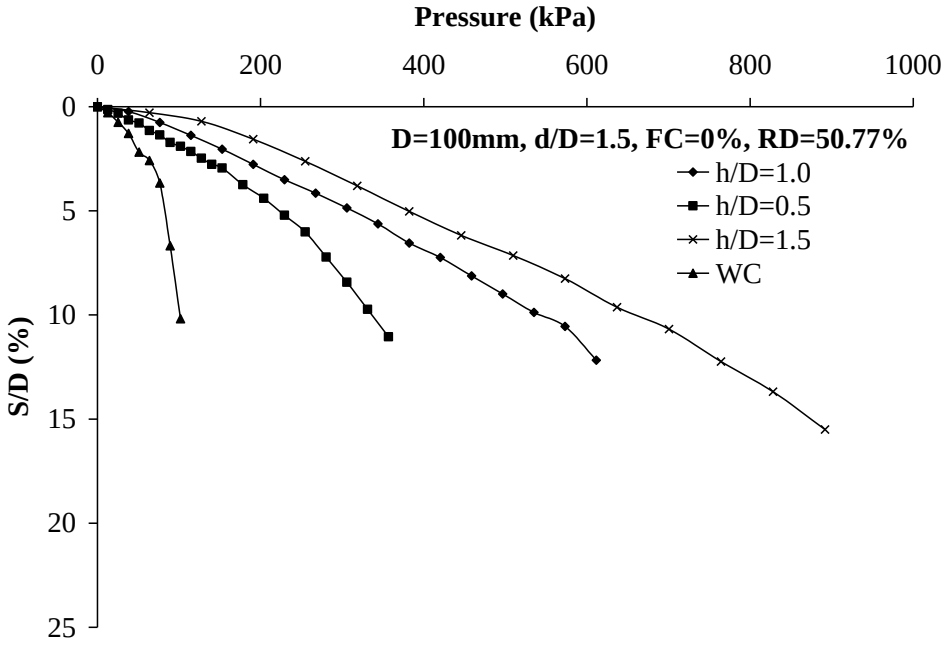

Fig. 4.55(b) Pressure vs. S/D for different values of h/D ratios for D=100mm, d/D=1.5 and FC=0%

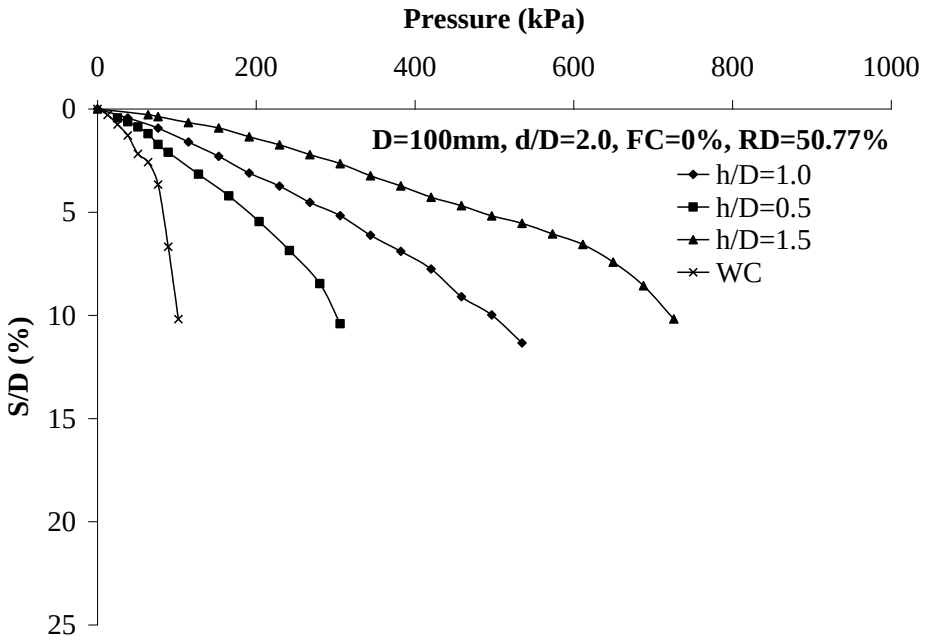

Fig. 4.55(c) Pressure vs. S/D for different values of h/D ratios for D=100mm, d/D=2.0 and FC=0%

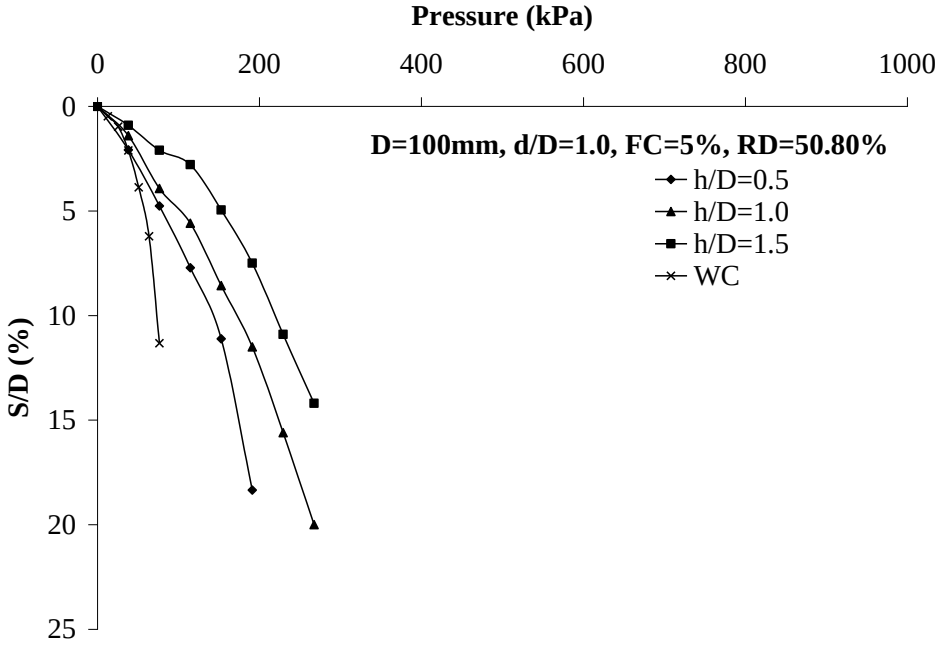

Fig. 4.56(a) Pressure vs. S/D for different values of h/D ratios for D=100mm, d/D=1.0 and FC=5%

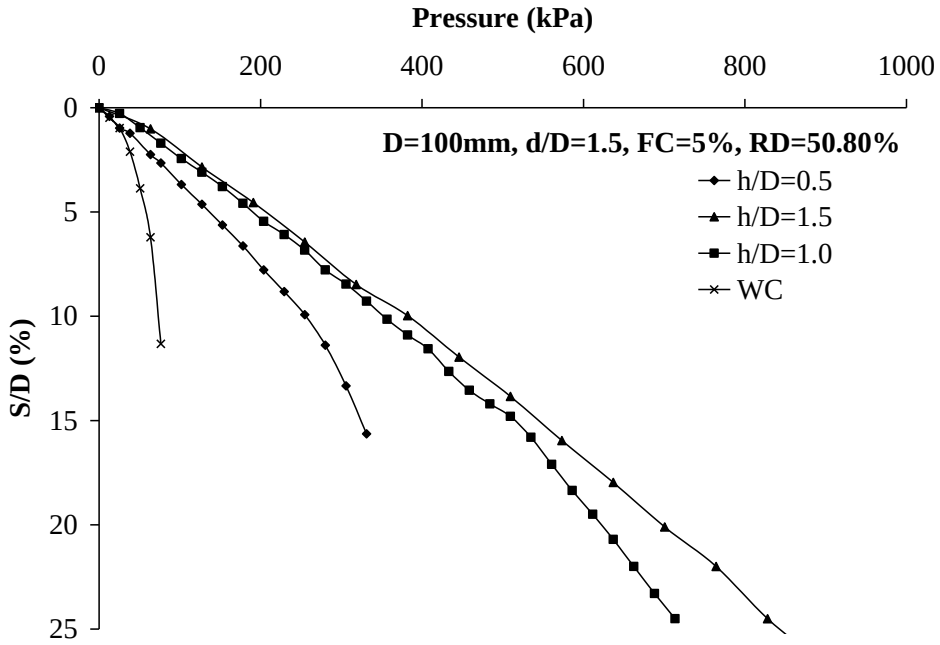

Fig. 4.56(b) Pressure vs. S/D for different values of h/D ratios for D=100mm, d/D=1.5 and FC=5%

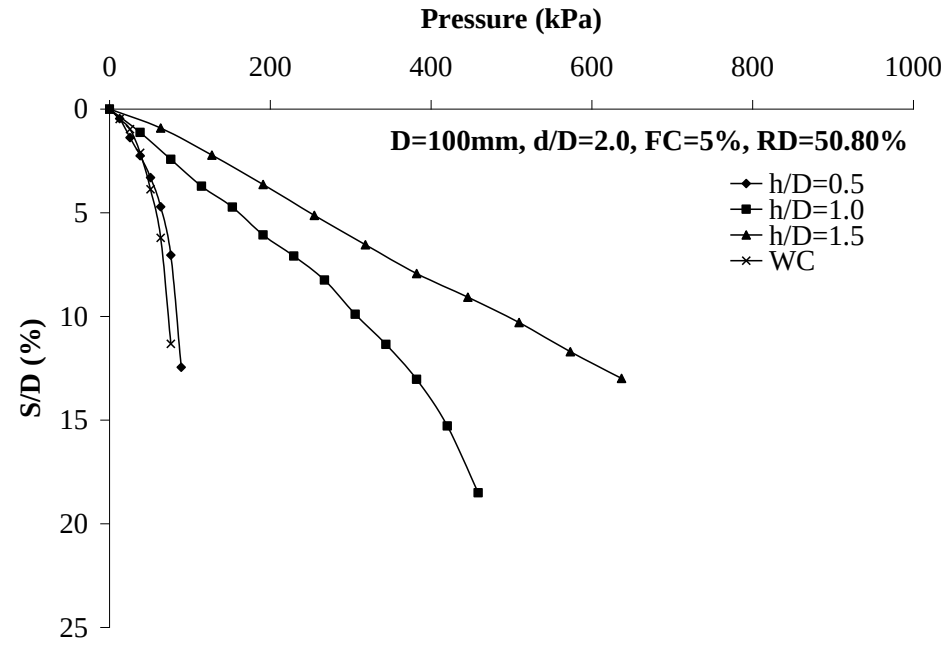

Fig. 4.56(c) Pressure vs. S/D for different values of h/D ratios for D=100mm, d/D=2.0 and FC=5%

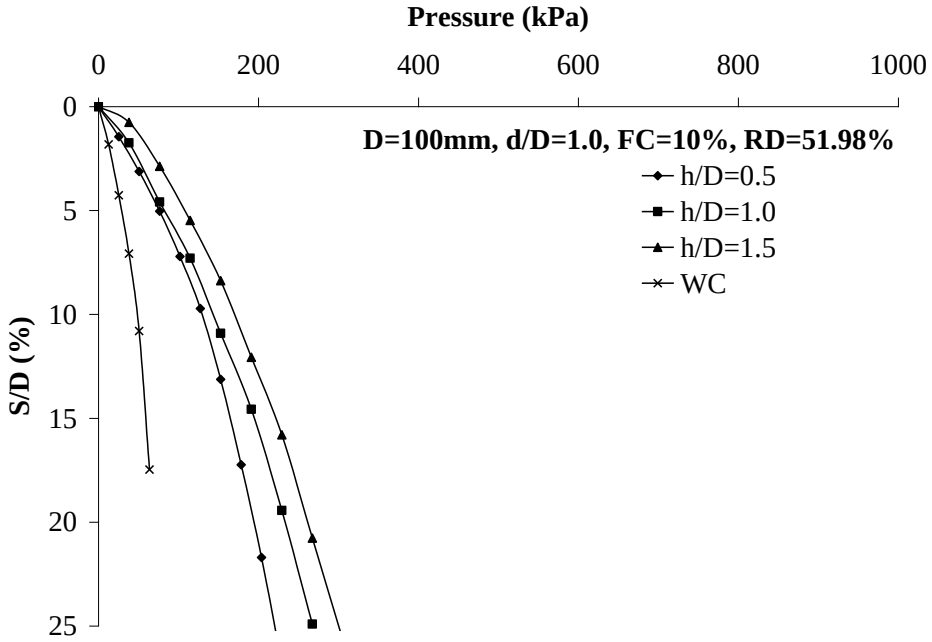

Fig. 4.57(a) Pressure vs. S/D for different values of h/D ratios for D=100mm, d/D=1.0 and FC=10%

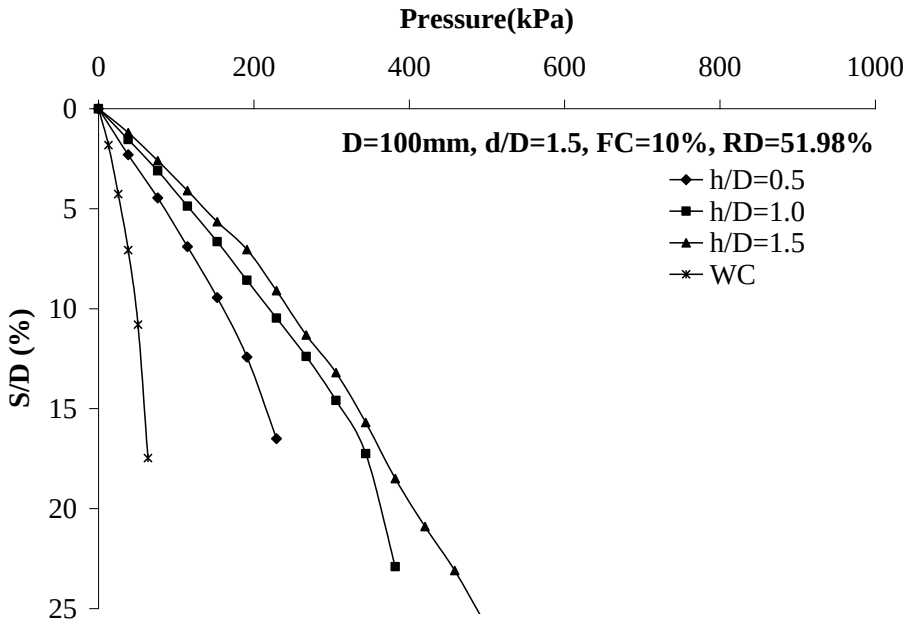

Fig. 4.57(b) Pressure vs. S/D for different values of h/D ratios for D=100mm, d/D=1.5 and FC=10%

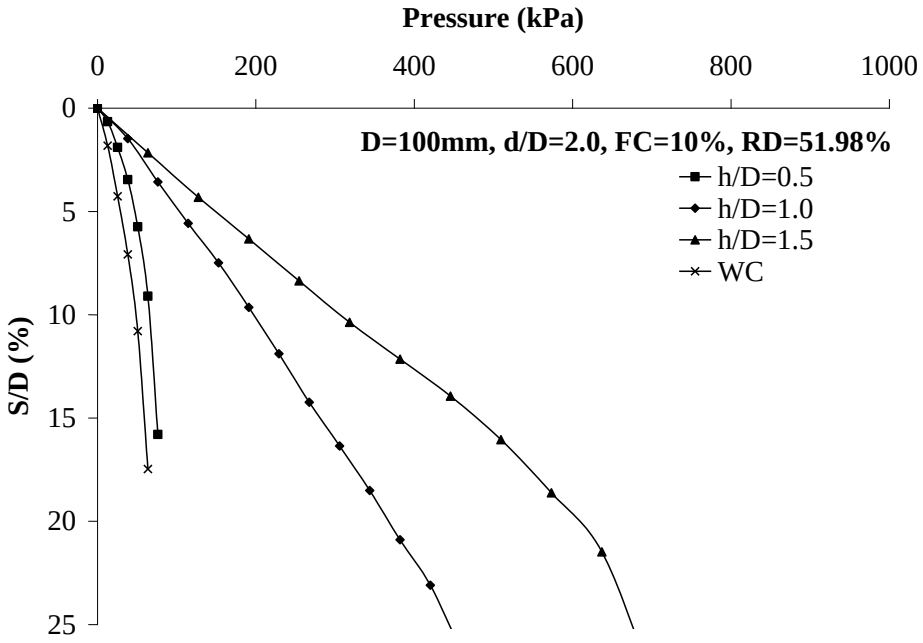

Fig. 4.57(c) Pressure vs. S/D for different values of h/D ratios for D=100mm, d/D=2.0 and FC=10%

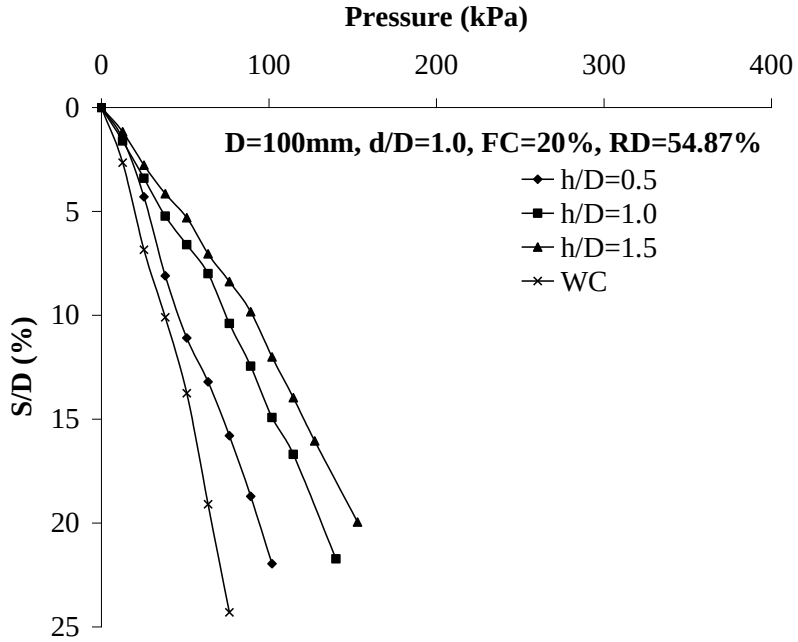

Fig. 4.58(a) Pressure vs. S/D for different values of h/D ratios for D=100mm, d/D=1.0 and FC=20%

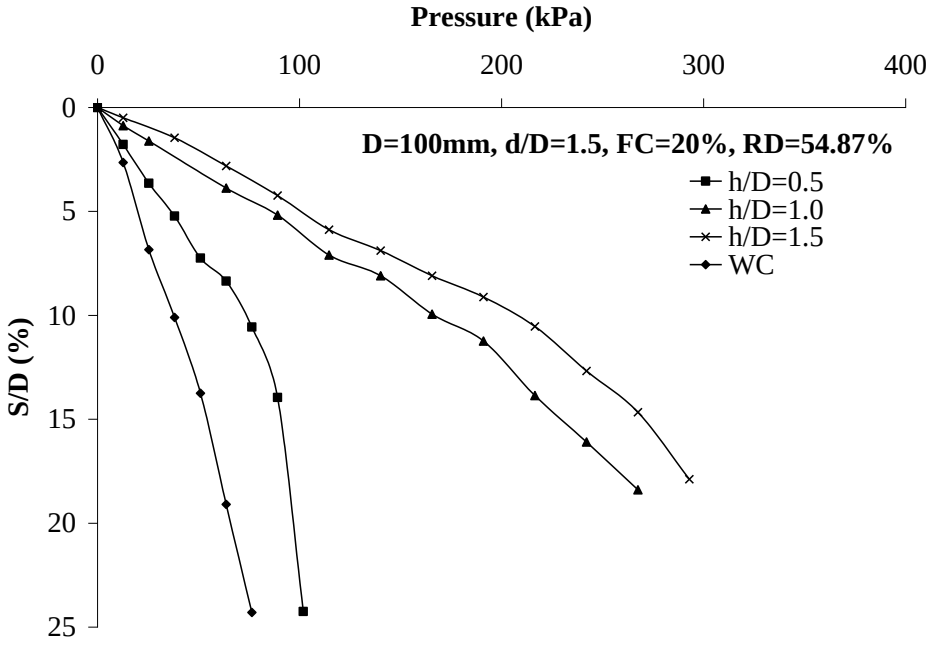

Fig. 4.58(b) Pressure vs. S/D for different values of h/D ratios for D=100mm, d/D=1.5 and FC=20%

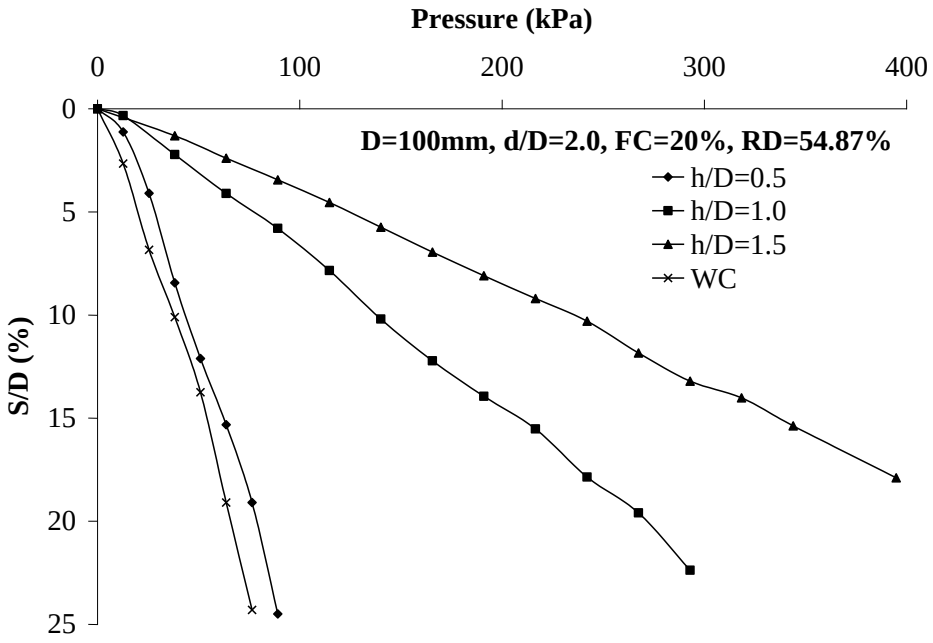

Fig. 4.58(c) Pressure vs. S/D for different values of h/D ratios for D=100mm, d/D=2.0 and FC=20%

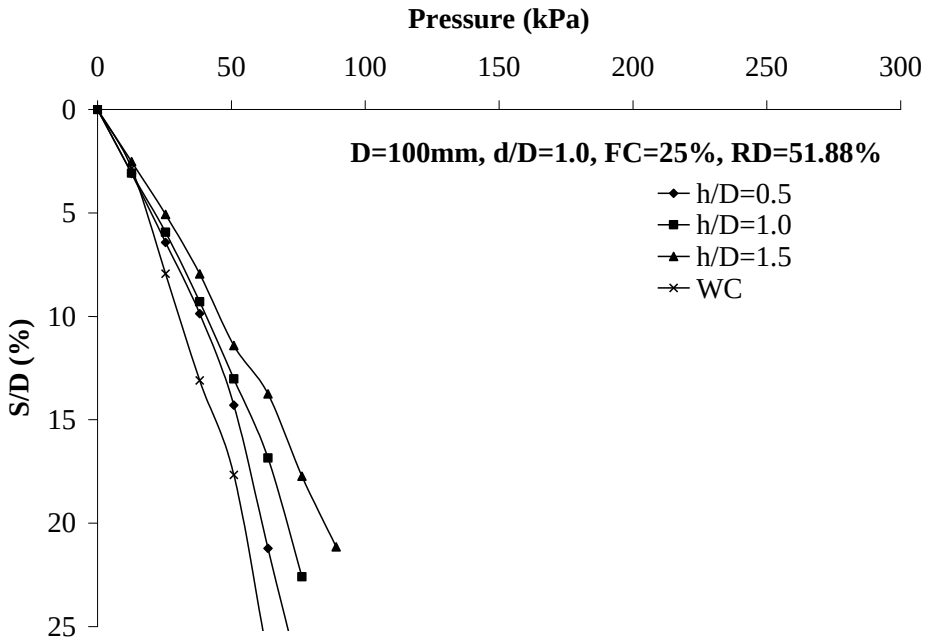

Fig. 4.59(a) Pressure vs. S/D for different values of h/D ratios for D=100mm, d/D=1.0 and FC=25%

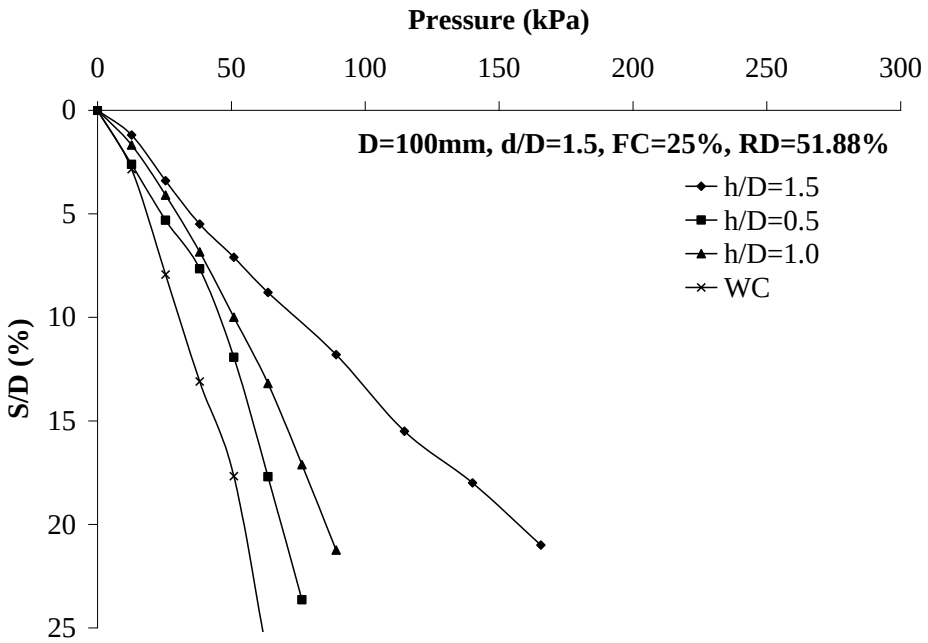

Fig. 4.59(b) Pressure vs. S/D for different values of h/D ratios for D=100mm, d/D=1.5 and FC=25%

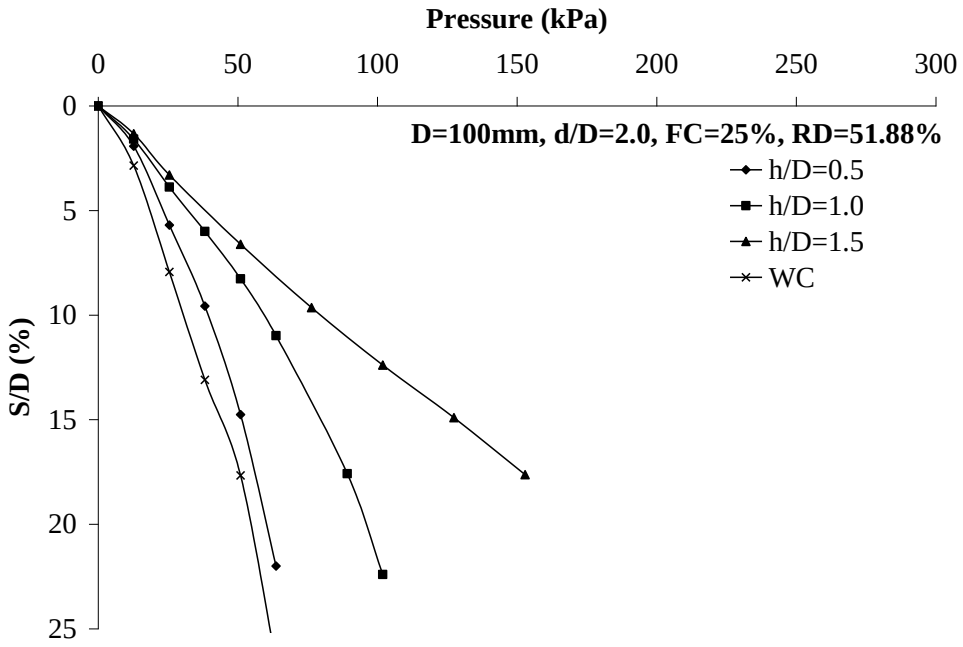

Fig. 4.59(c) Pressure vs. S/D for different values of h/D ratios for D=100mm, d/D=2.0 and FC=25%

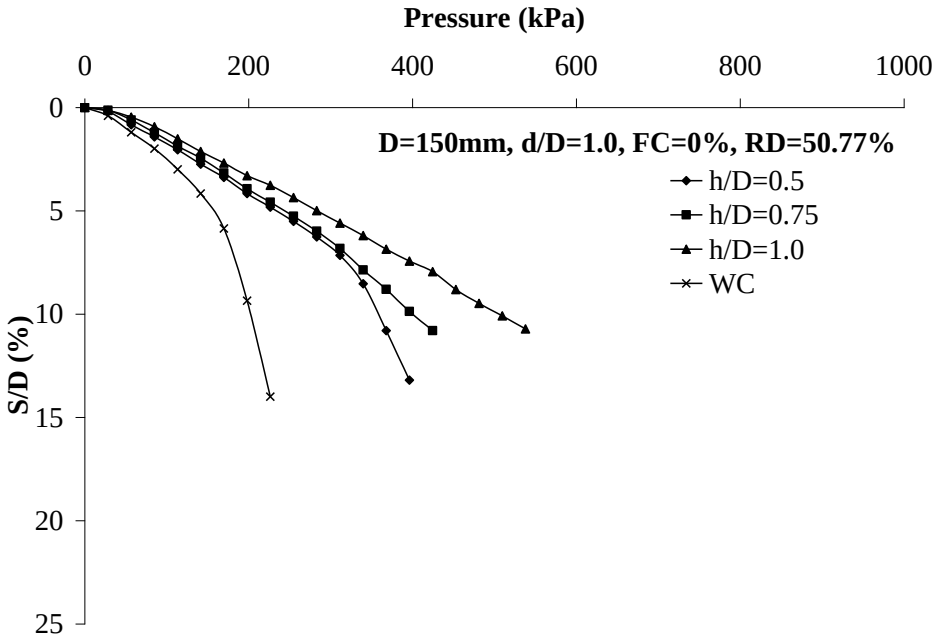

Fig. 4.60(a) Pressure vs. S/D for different values of h/D ratios for D=150mm, d/D=1.0 and FC=0%

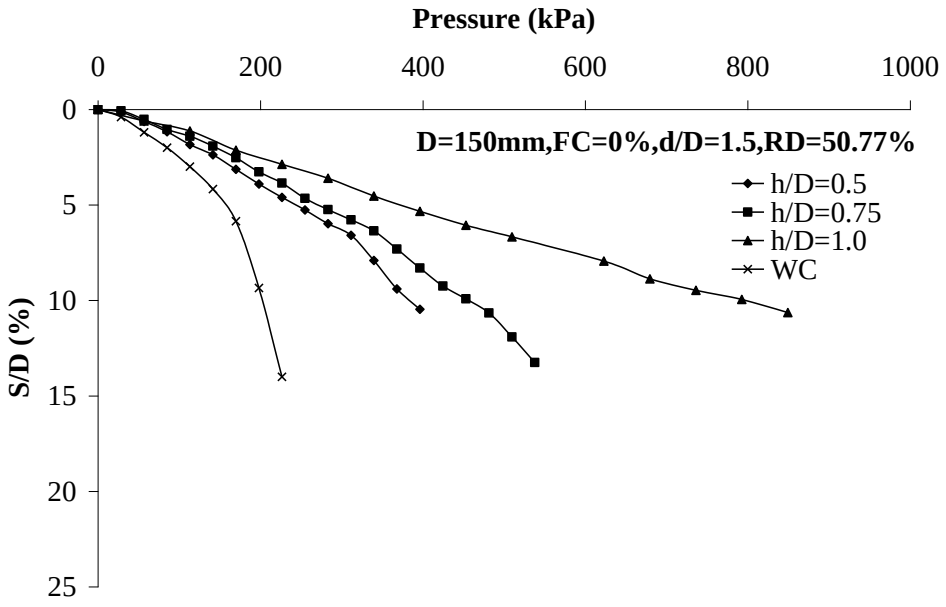

Fig. 4.60(b) Pressure vs. S/D for different values of h/D ratios for D=150mm, d/D=1.5 and FC=0%

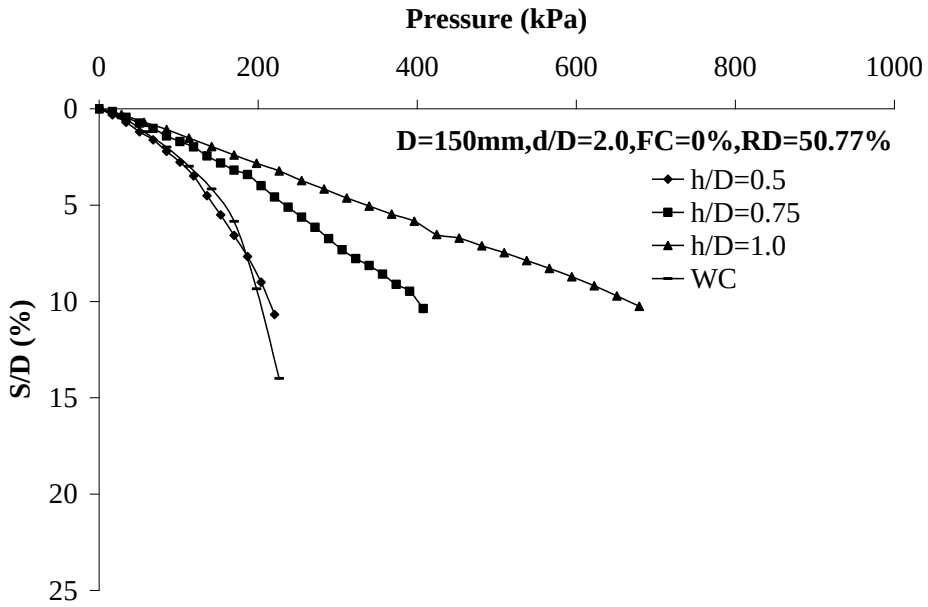

Fig. 4.60(c) Pressure vs. S/D for different values of h/D ratios for D=150mm, d/D=2.0 and FC=0%

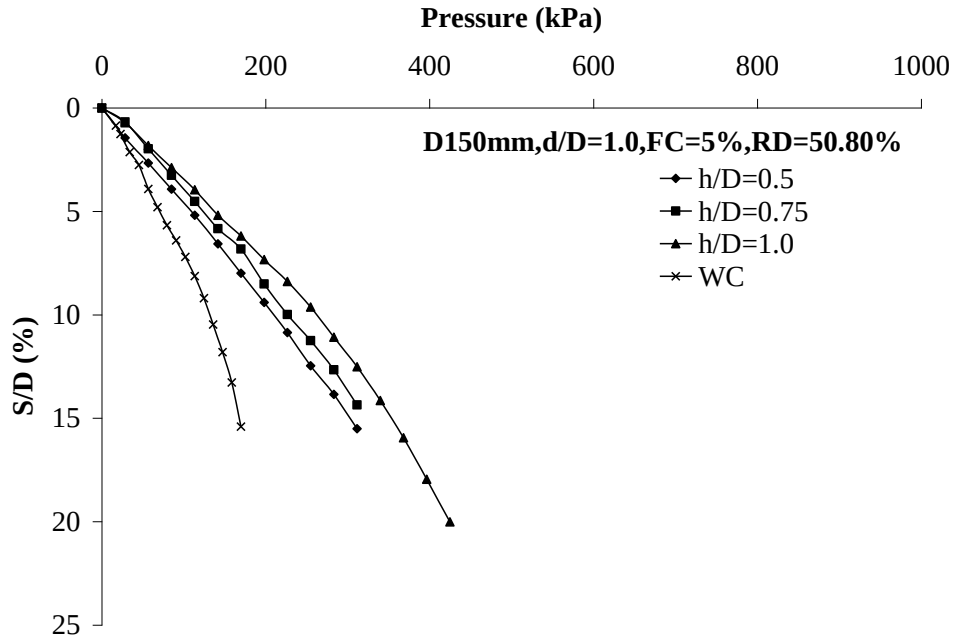

Fig. 4.611(a) Pressure vs. S/D for different values of h/D ratios for D=150mm, d/D=1.0 and FC=5%

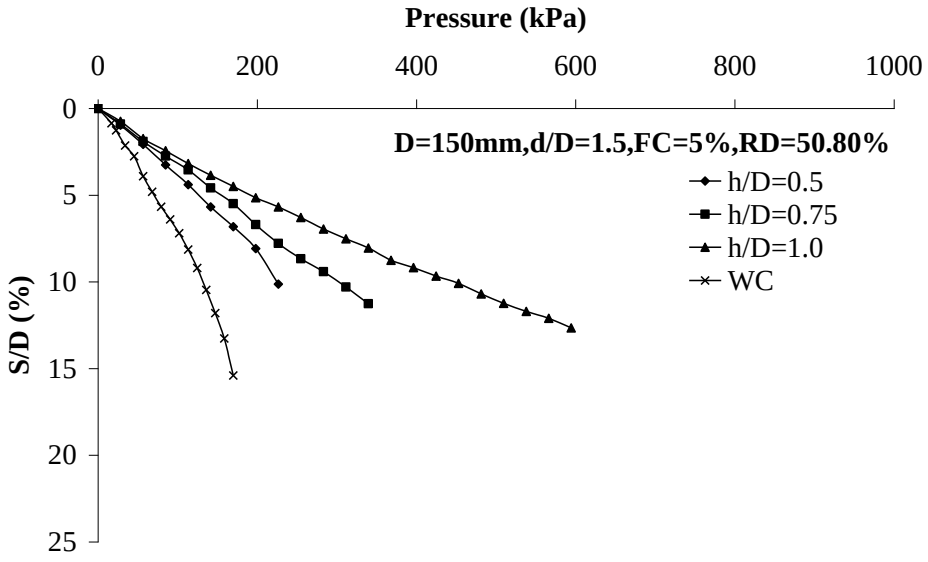

Fig. 4.61(b) Pressure vs. S/D for different values of h/D ratios for D=150mm, d/D=1.5 and FC=5%

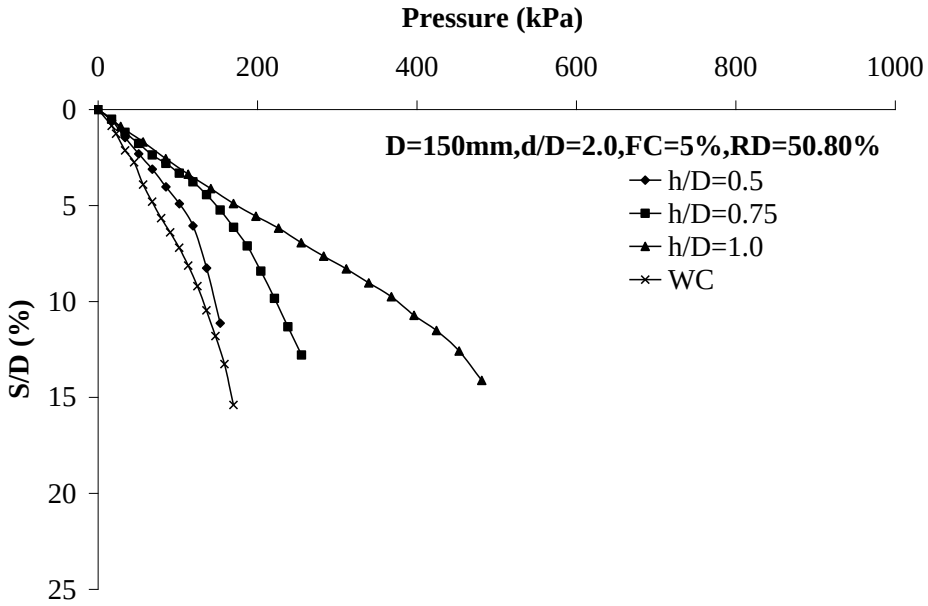

Fig. 4.61(c) Pressure vs. S/D for different values of h/D ratios for D=150mm, d/D=2.0 and FC=5%

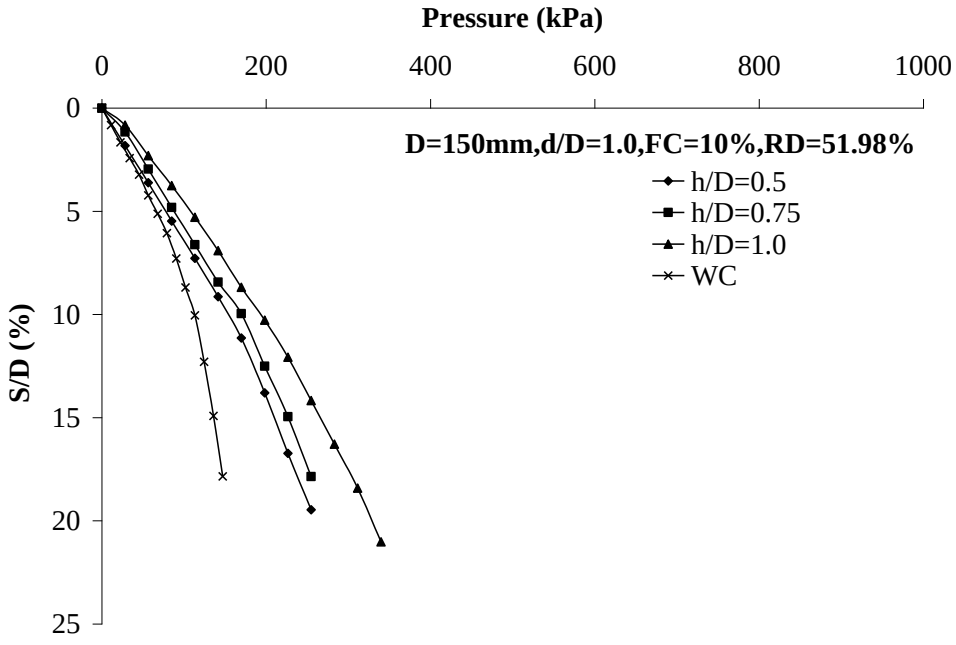

Fig. 4.62(a) Pressure vs. S/D for different values of h/D ratios for D=150mm, d/D=1.0 and FC=10%

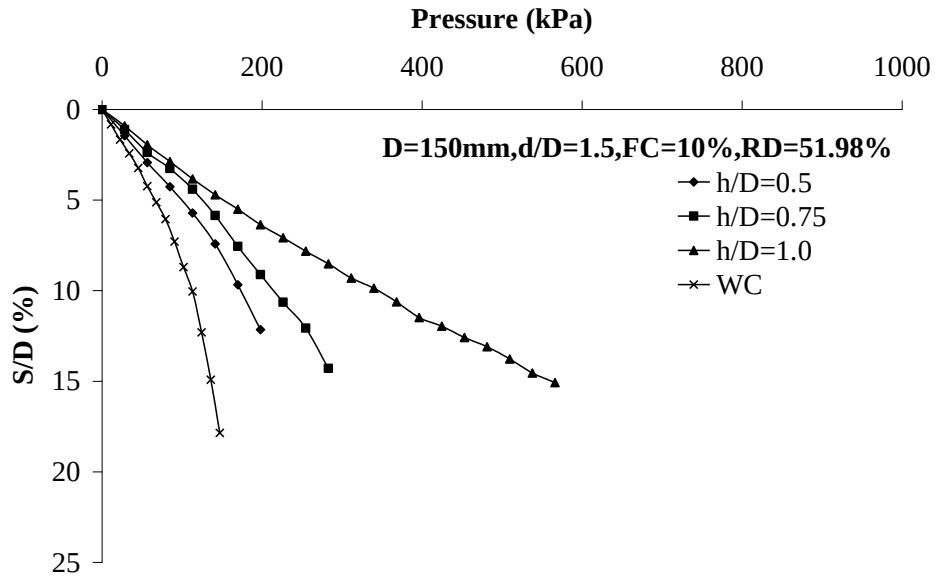

Fig. 4.62(b) Pressure vs. S/D for different values of h/D ratios for D=150mm, d/D=1.5 and FC=10%

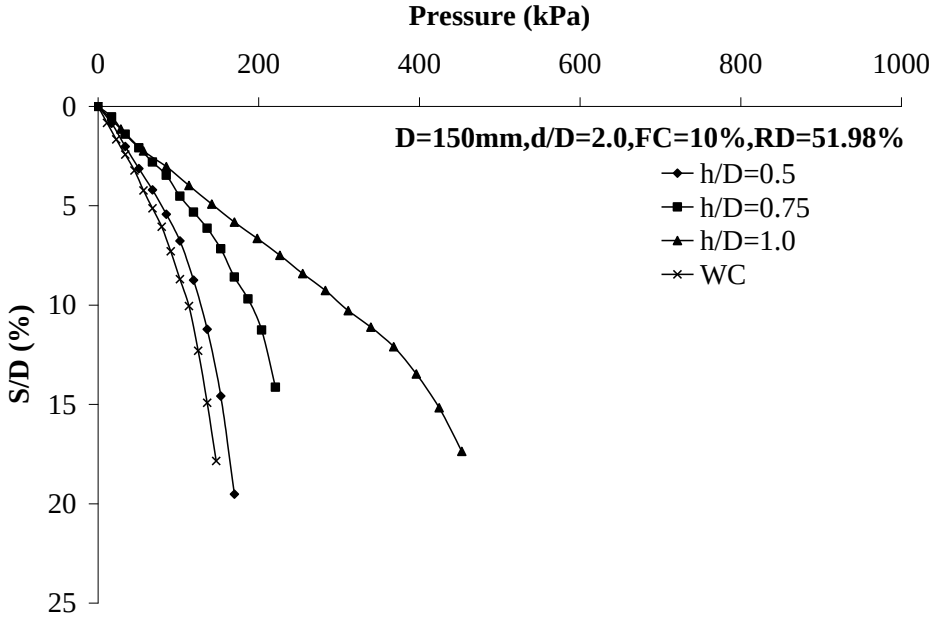

Fig. 4.62(c) Pressure vs. S/D for different values of h/D ratios for D=150mm, d/D=2.0 and FC=10%

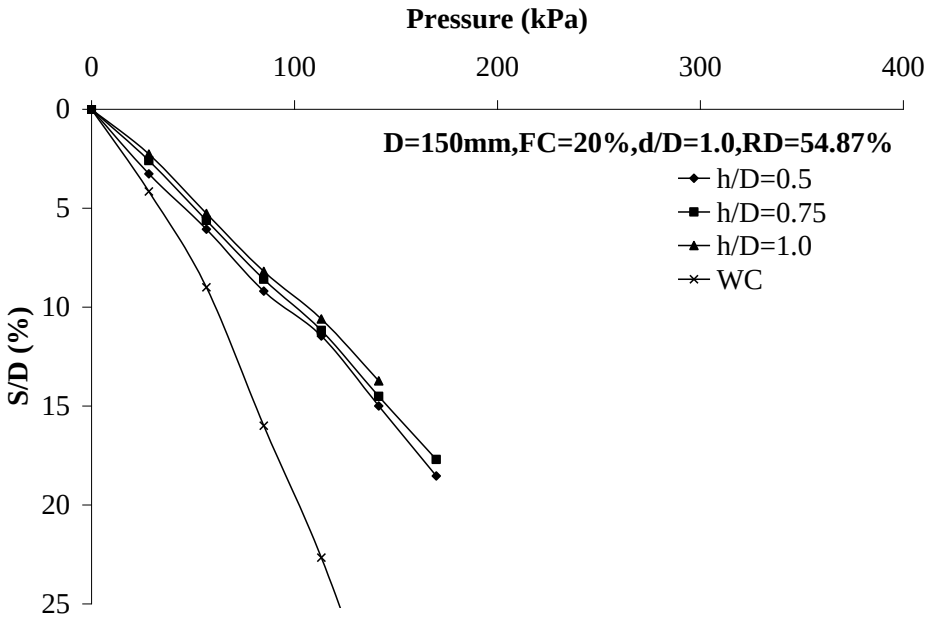

Fig. 4.63(a) Pressure vs. S/D for different values of h/D ratios for D=150mm, d/D=1.0 and FC=20%

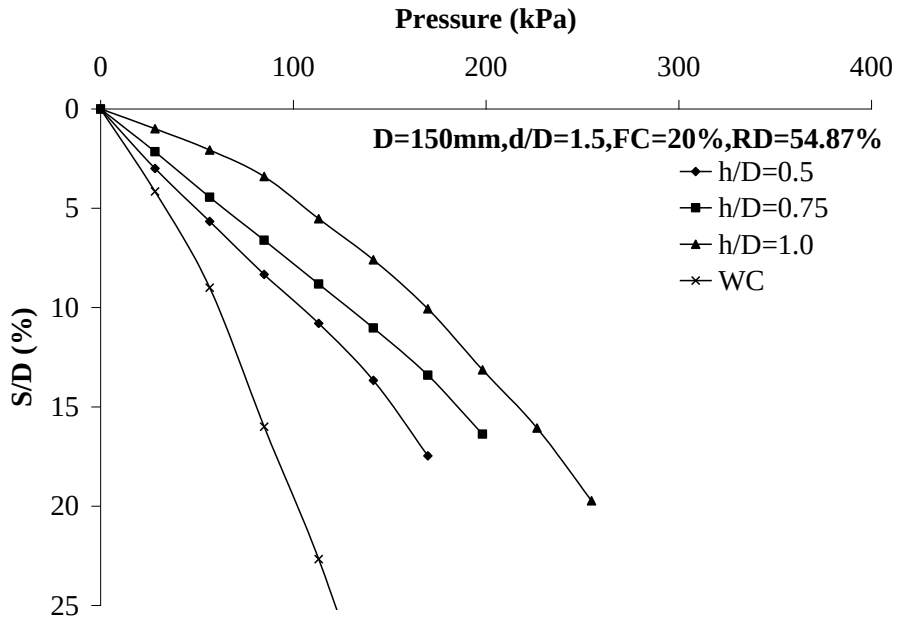

Fig. 4.63(b) Pressure vs. S/D for different values of h/D ratios for D=150mm, d/D=1.5 and FC=20%

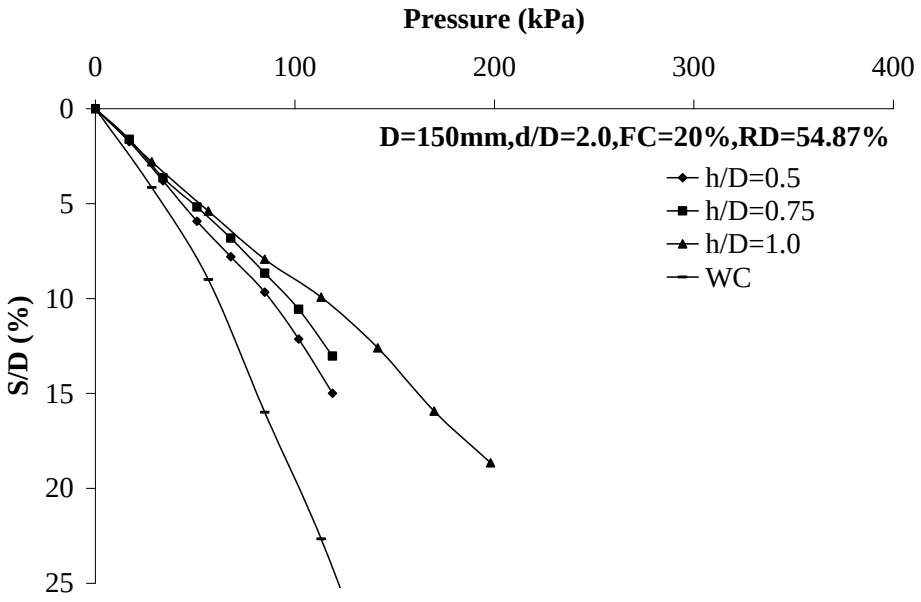

Fig. 4.63(c) Pressure vs. S/D for different values of h/D ratios for D=150mm, d/D=2.0 and FC=20%

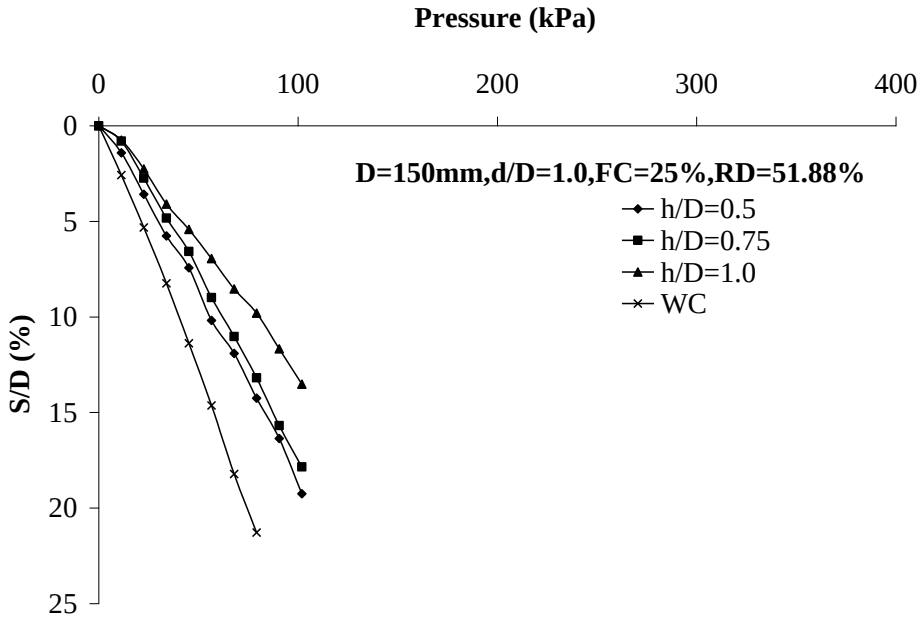

Fig. 4.64(a) Pressure vs. S/D for different values of h/D ratios for D=150mm, d/D=1.0 and FC=25%

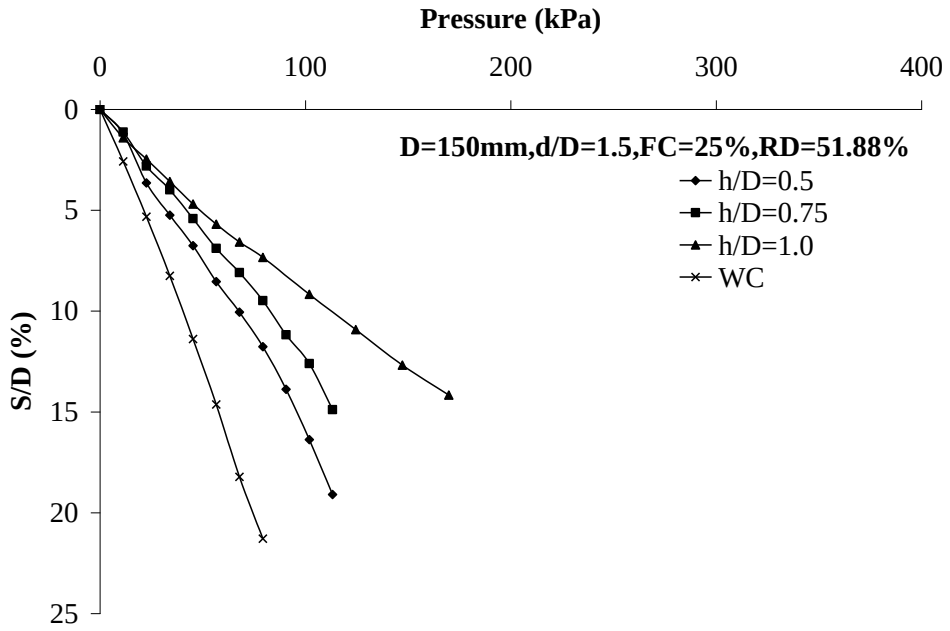

Fig. 4.64(b) Pressure vs. S/D for different values of h/D ratios for D=150mm, d/D=1.5 and FC=25%

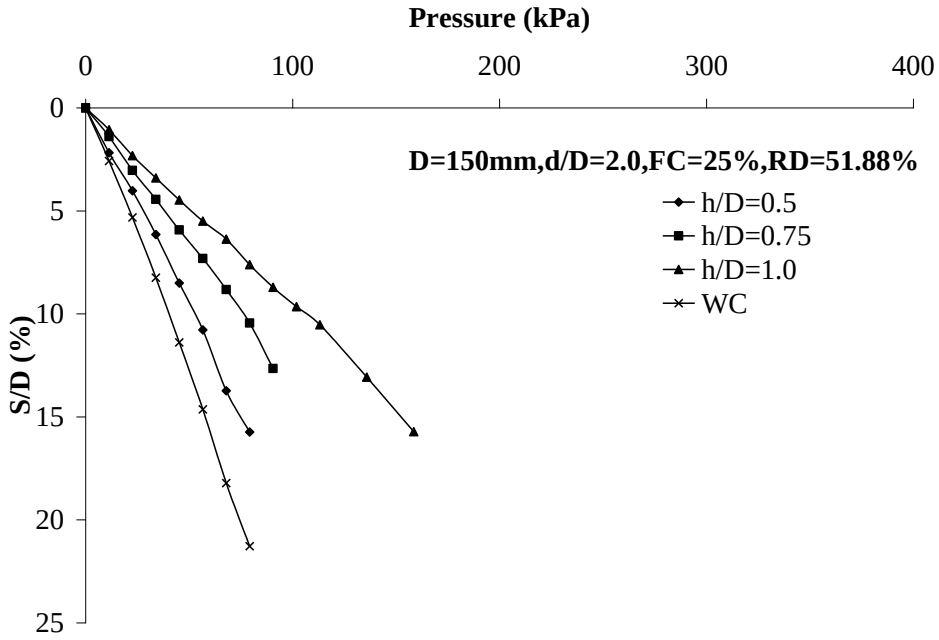

Fig. 4.64(c) Pressure vs. S/D for different values of h/D ratios for D=150mm, d/D=2.0 and FC=25%

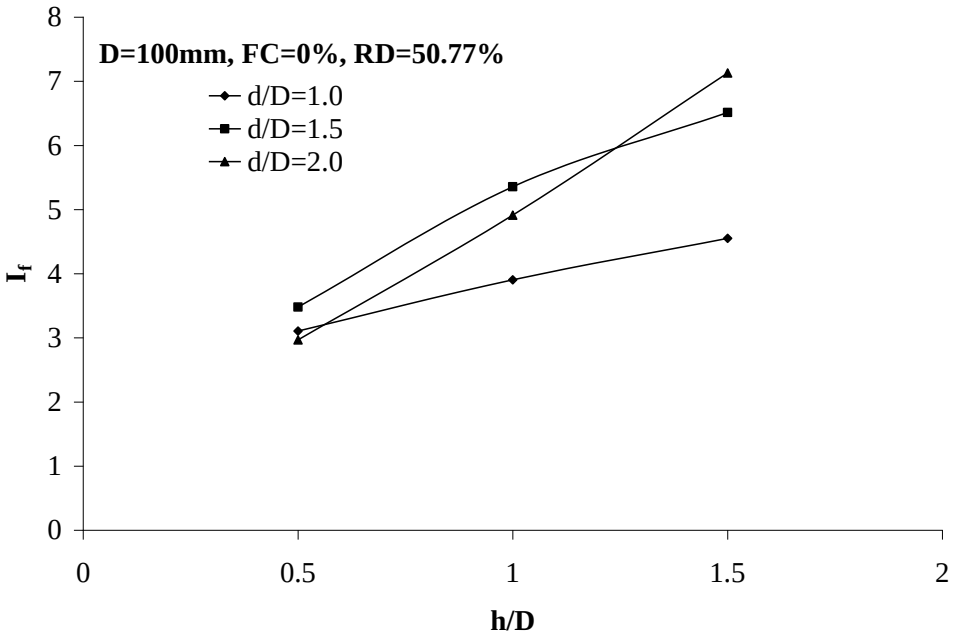

Fig.4.65 Improvement factor vs. normalized cell height (h/D) for different cell diameters for D=100mm and FC=0%

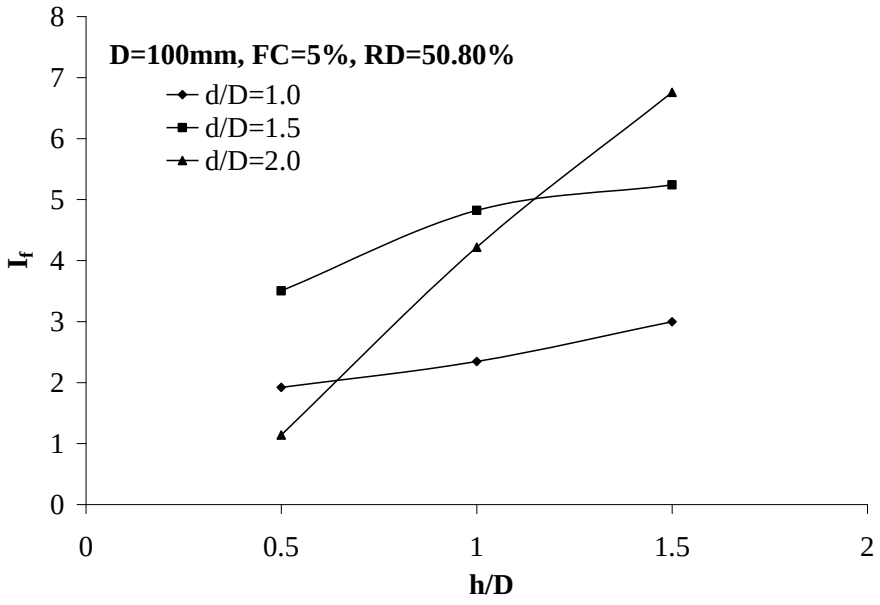

Fig.4.66 Improvement factor vs. normalized cell height (h/D) for different cell diameters for D=100mm and FC=5%

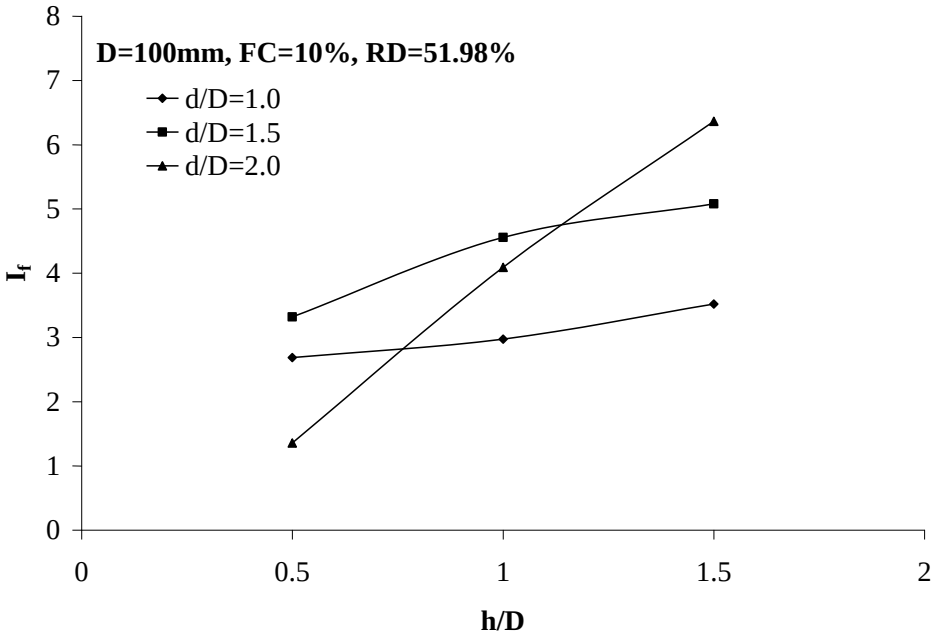

Fig. 4.67 Improvement factor vs. normalized cell height (h/D) for different cell diameters for D=100mm and FC=10%

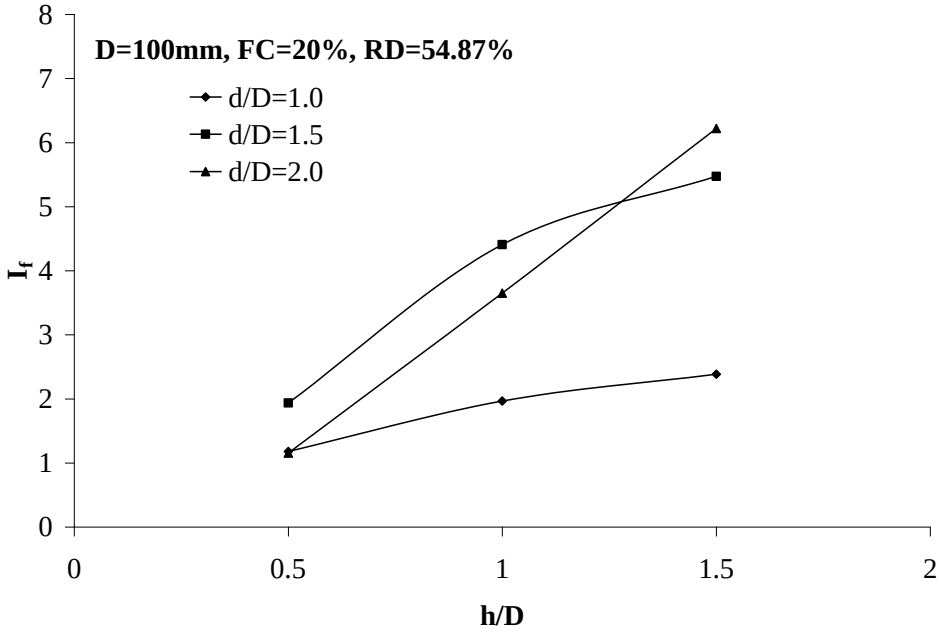

Fig. 4.68 Improvement factor vs. normalized cell height (h/D) for different cell diameters for D=100mm and FC=20%

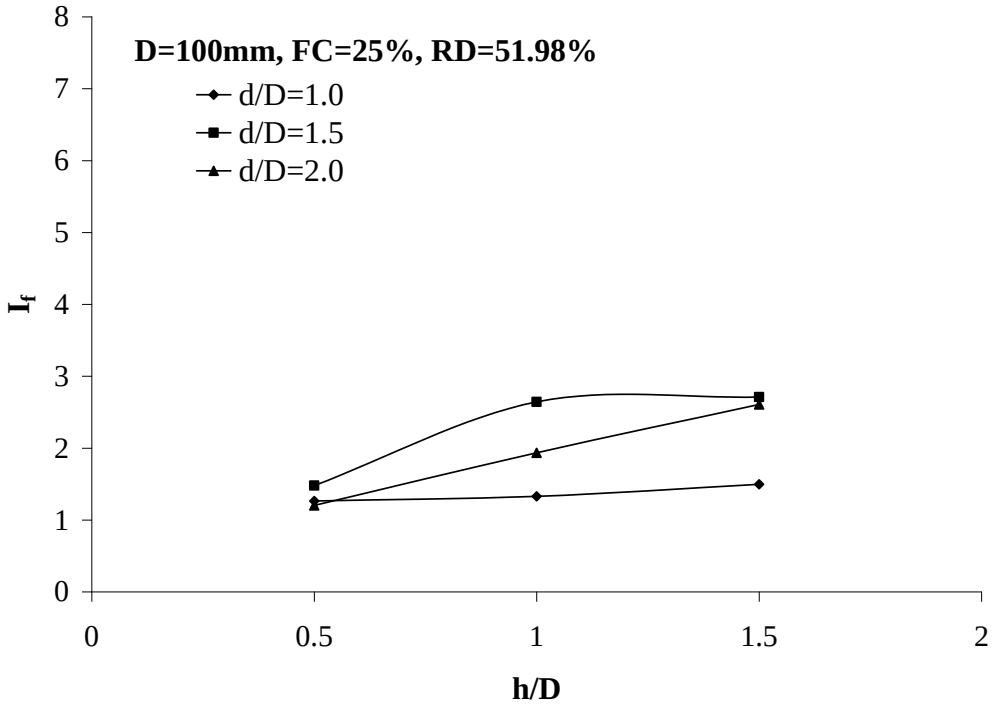

Fig. 4.69 Improvement factor vs. normalized cell height (h/D) for different cell diameters for D=100mm and FC=25%

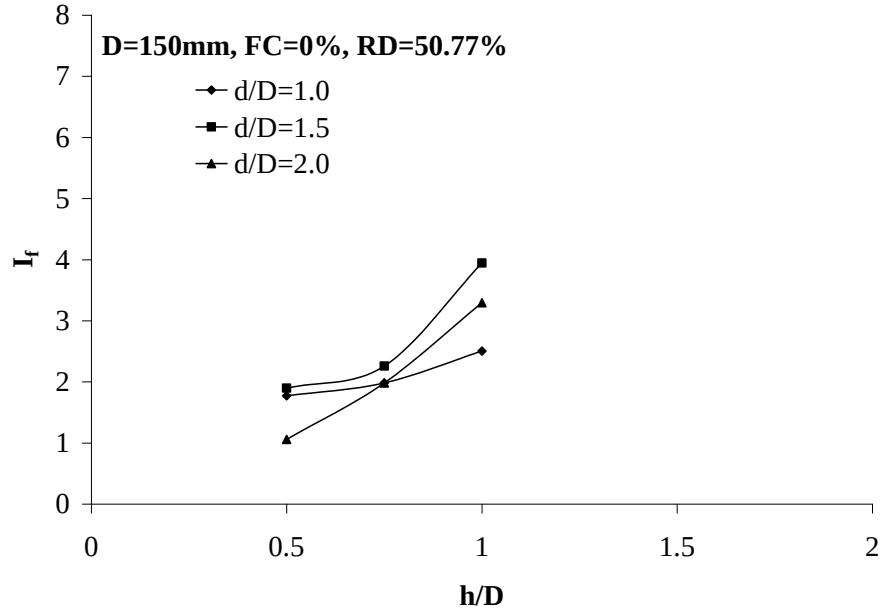

Fig. 4.70 Improvement factor vs. normalized cell height (h/D) for different cell diameters for D=150mm and FC=0%

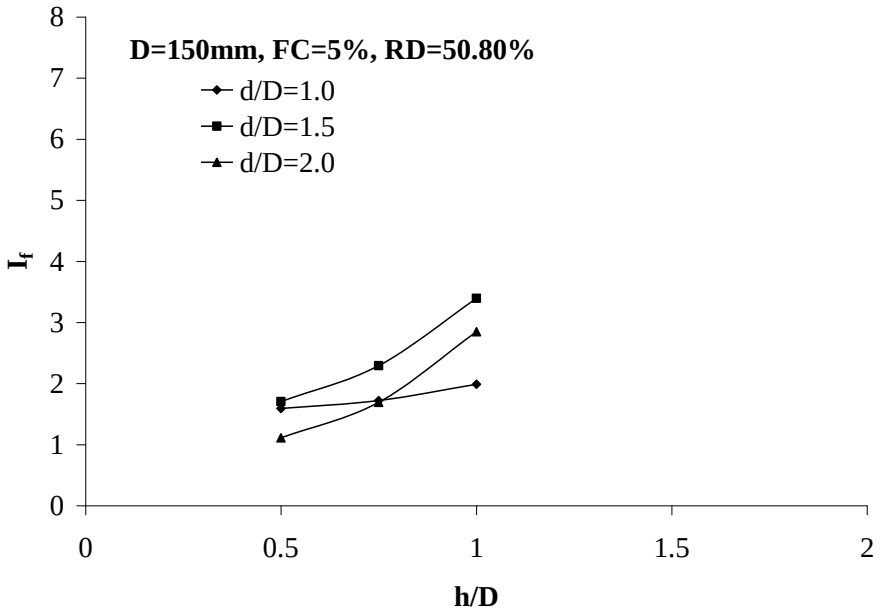

Fig. 4.71 Improvement factor vs. normalized cell height (h/D) for different cell diameters for D=150mm and FC=5%

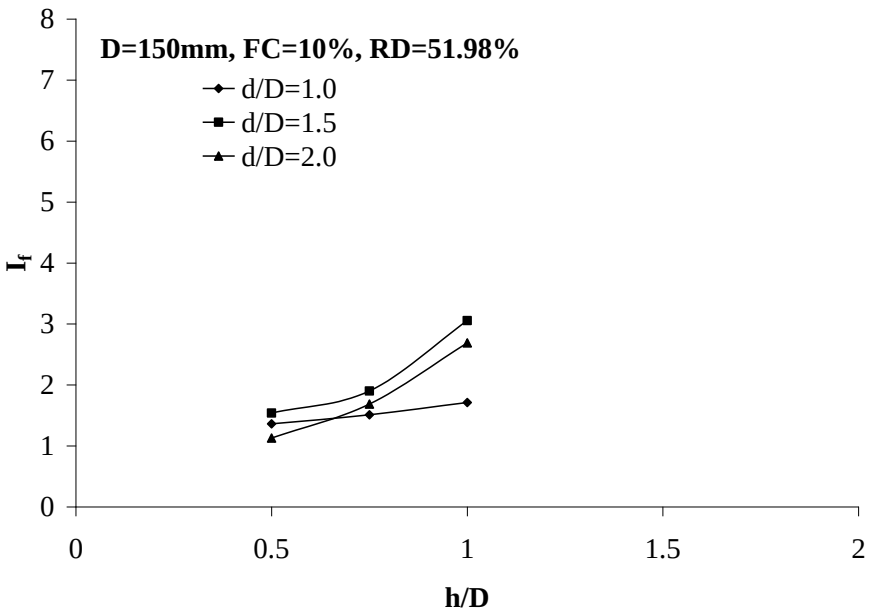

Fig. 4.72 Improvement factor vs. normalized cell height (h/D) for different cell diameters for D=150mm and FC=10%

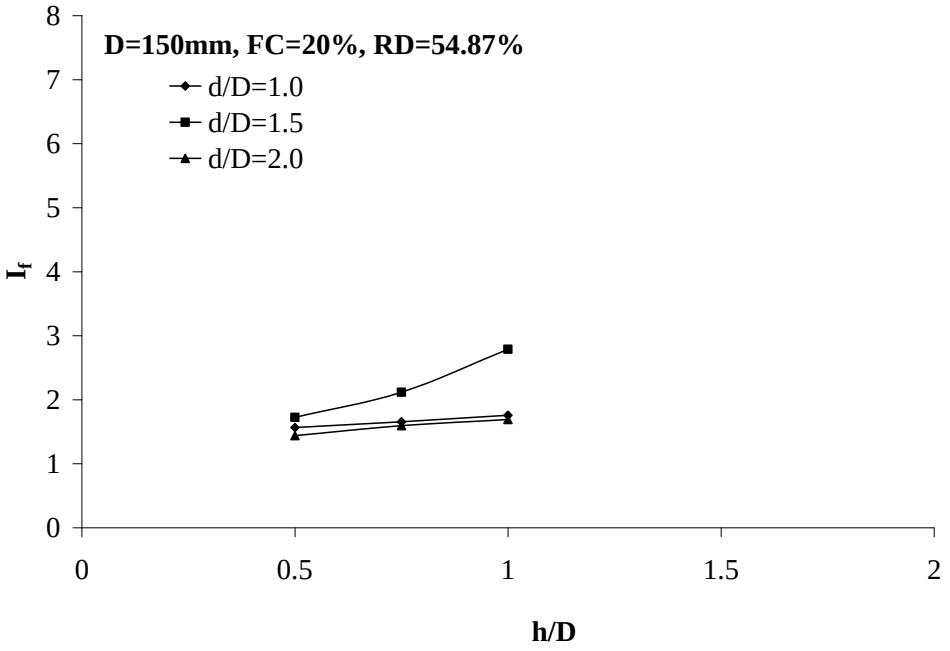

Fig. 4.73 Improvement factor vs. normalized cell height (h/D) for different cell diameters for D=150mm and FC=20%

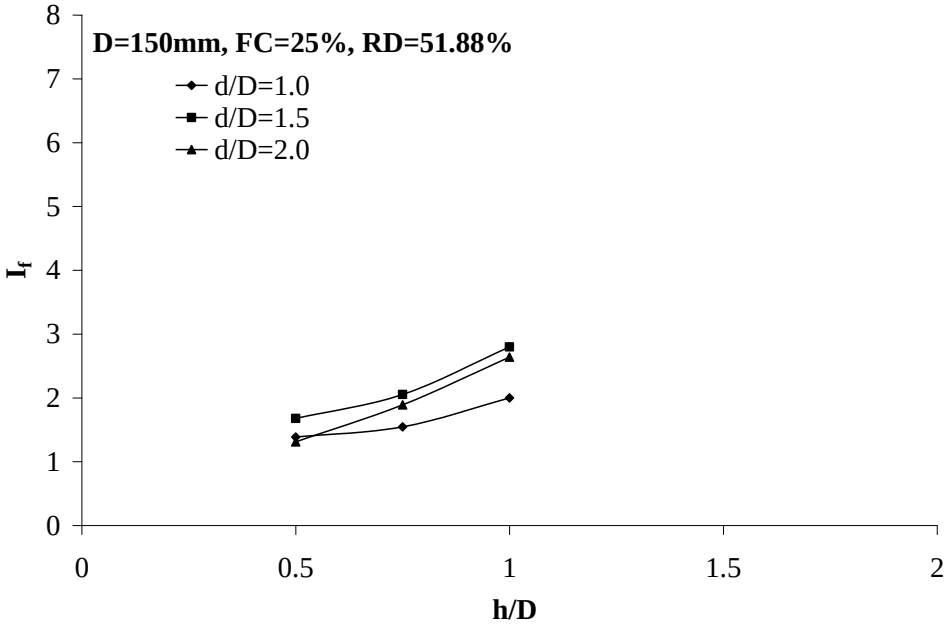

Fig. 4.74 Improvement factor vs. normalized cell height (h/D) for different cell diameters for D=150mm and FC=25%

4.5. Effect of Depth of Embedment

In order to investigate the effect of side supports constructed to support the soil cuts on the behavior when the foundation level is low, a series of tests were carried out (i.e. some times the footing is placed at a low depth relative to top of the side support). All the parameters i.e. diameter of the cell, height of the cell and proportion of fines were held constant except the depth of the footing relative to the top of the cell (*z*) for two footing sizes of 0.1m and 0.15m. To precisely model the site conditions, two cases were evaluated in this series of tests. The two cell diameters with *d*/*D* ratio equal to 1 & 2 for 0.1m diameter footing and one cell diameter with d/D ratio equal to 1.5 for 0.15m diameter footing were used. The normalized depth of the footing to the cell height (*z*/*h*) values varied from 0 to 0.8 for *d*/*D* equal 1 & 2 for 0.1m footing and for d/D equal to 1.5 for 0.15m footing were used. The improvement factor vs. normalized embedded depth (*z*/*h*) for cells with d/D equal to 1.0 & 2.0 and *h*/*D* of 0.5 and d/D equal to 1.5 and h/D of 0.5 have been shown in Fig (4.75). It is clear that variation in the footing depth relative to the cell top has no effect on the behavior of cell–model footing.[Table (4.7)]

Table 4.7 Results of model embedded footing on confined silty.

FC (%)	RD (%)	D (mm)	d/D	h/D	z/h	$q_{experimental}$ (kPa)	Improvement Factor (I_f)
10	51.98	100	1.0	0.5	00	129.51	2.68
10		100	1.0	0.5	0.20	133.67	2.77
10		100	1.0	0.5	0.40	132.40	2.74
10		100	1.0	0.5	0.60	131.49	2.72
10		100	1.0	0.5	0.80	130.08	2.69
10		100	1.5	0.5	00	159.99	3.31
10		100	1.5	0.5	0.20	152.22	3.15
10		100	1.5	0.5	0.40	150.28	3.11
10		100	1.5	0.5	0.60	148.99	3.09
10		100	1.5	0.5	0.80	148.38	3.07
10		100	2.0	0.5	00	65.38	1.35
10		100	2.0	0.5	0.20	67.67	1.40
10		100	2.0	0.5	0.40	71.92	1.49
10		100	2.0	0.5	0.60	72.12	1.49
10		100	2.0	0.5	0.80	69.23	1.43
10		150	1.5	0.5	00	111.01	0.98
10		150	1.5	0.5	0.20	113.90	1.00
10		150	1.5	0.5	0.40	109.27	0.96
10		150	1.5	0.5	0.60	102.17	0.90
10		150	1.5	0.5	0.80	119.01	1.05

The difference between the maximum improvement factor (2.77 & 1.49) and the minimum value (2.68, 1.35) is 0.09 and 0.14 respectively for 0.1m footing and the difference between the maximum improvement factor (1.05) and the minimum value (0.90) is 0.15 for 0.15m footing, which is caused by the slight disturbance that occurred in sand beds while placing the footing within the cell. This can be explained as follows. For ordinary footings (without cellular support), increase in the foundation depth results in increase in the overburden pressure and hence increase in the bearing capacity. However, footing with cellular support the effect of overburden pressure is not significant. When the footing is loaded, it settles and the plastic state is developed until the point at which the system behaves as one unit. Therefore, increase in the embedment affects only the initial part of the behavior until that point after which the ultimate load depends on the surface area of the cell, which is constant. Hence, it can be concluded that the embedment of a footing in confined granular soil has no effect on the response of the footing–cell system.

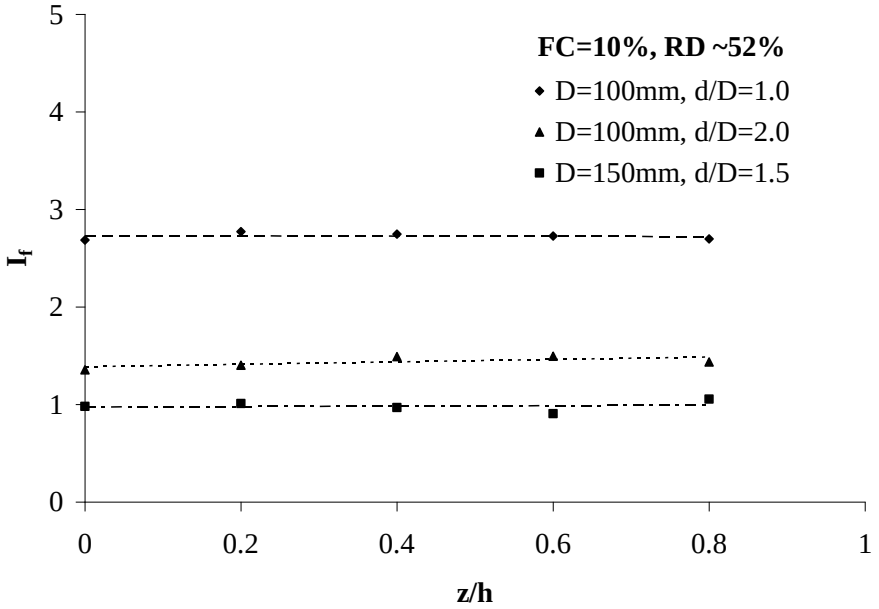

Fig. 4.75 Improvement factor vs. normalized embedded depth (z/h)

4.6. Effect of Fines

In order to analyze the effect of fines, a series of tests were carried out with all parameters i.e. diameter of cylinder, height of cylinder except the percentage of fines content which was held constant [Fig (4.76) to (4.96)]. Fig (4.97) to Fig (4.103) represent the variation in bearing capacity with different percentages of fines content for varying cells with *d*/*D* of 1.0, 1.5 and 2 for different h/D ratios. It is clear that with increase in the percentage of fines for different values of *d*/*D* and *h*/*D* ratios, the slope of pressure versus settlement curve increases i.e. the bearing capacity decreases. It is due to the fact that as we increase the proportions of fine

content the density increases along with the compressibility. The effect of compressibility offsets the improvement due increase in density. In other words, with addition of fines, settlement increases and the ultimate bearing carrying capacity decrease. Hence in the presence of fines the failure criterion is governed by allowable settlement and the bearing capacity of the footing decreases.

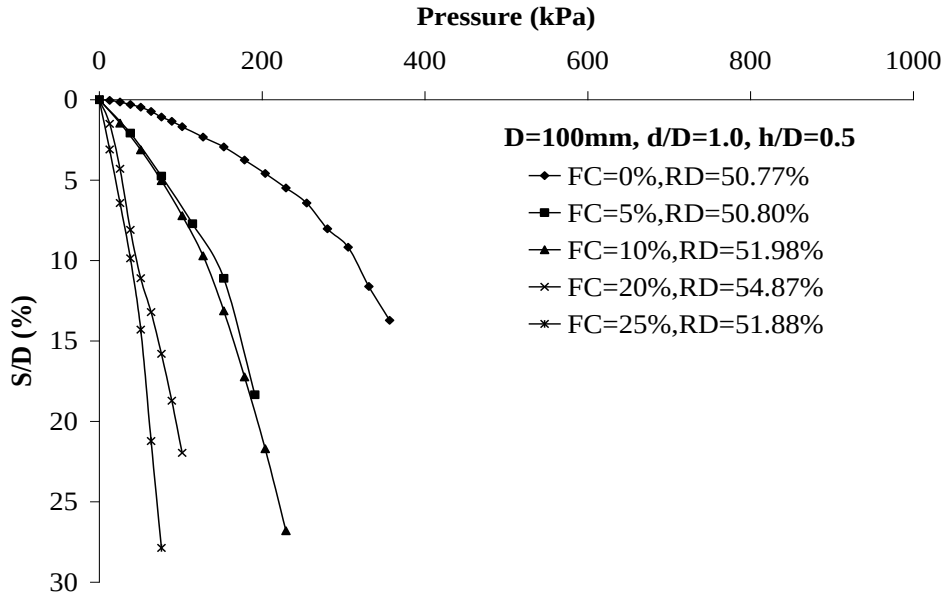

Fig. 4.76 Bearing pressure vs. settlement ratio (*S*/*D*) for a confined circular plate for different proportions of fines for D=100mm, d/D=1.0 and h/D=0.5

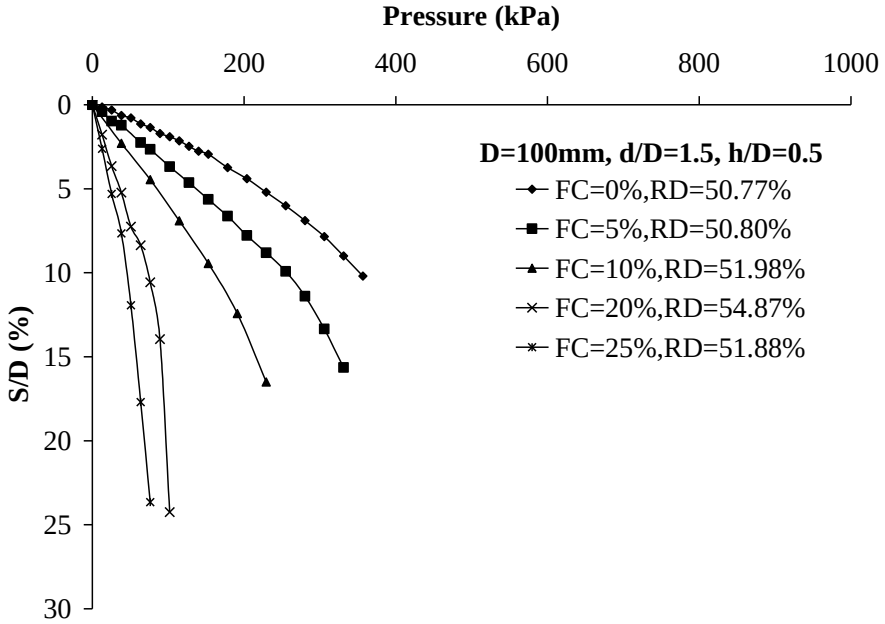

Fig. 4.77 Bearing pressure vs. settlement ratio (*S*/*D*) for a confined circular plate for different proportions of fines for D=100mm, d/D=1.5 and h/D=0.5

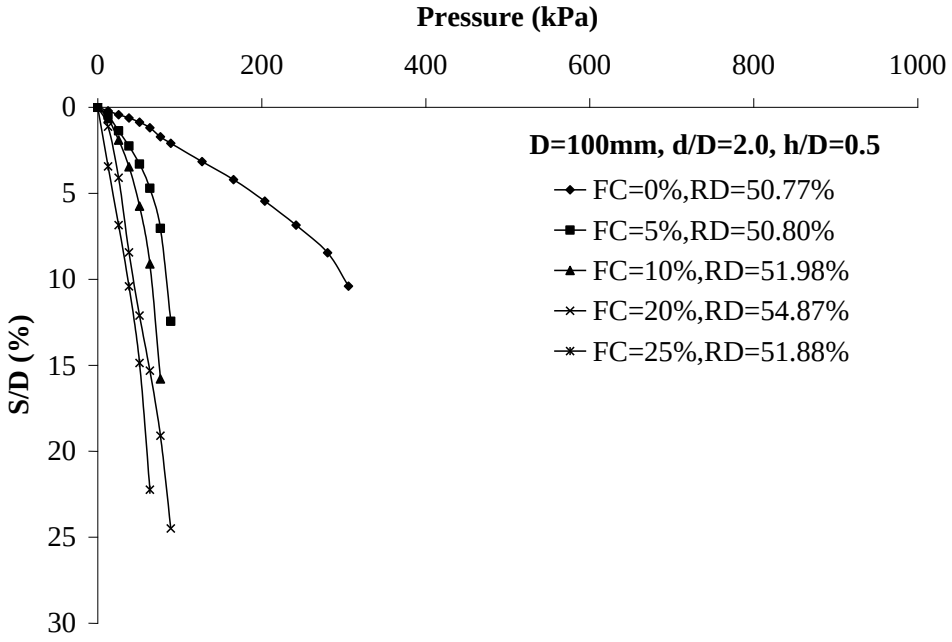

Fig. 4.78 Bearing pressure vs. settlement ratio (*S*/*D*) for a confined circular plate for different proportions of fines for D=100mm, d/D=2.0 and h/D=0.5

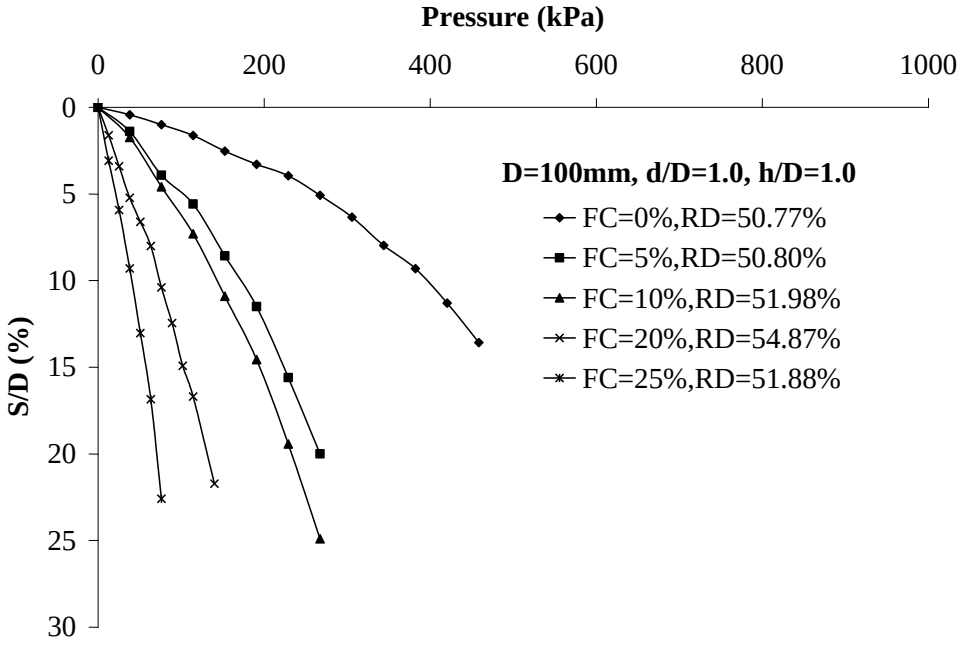

Fig. 4.79 Bearing pressure vs. settlement ratio (*S*/*D*) for a confined circular plate for different proportions of fines for D=100mm, d/D=1.0 and h/D=1.0

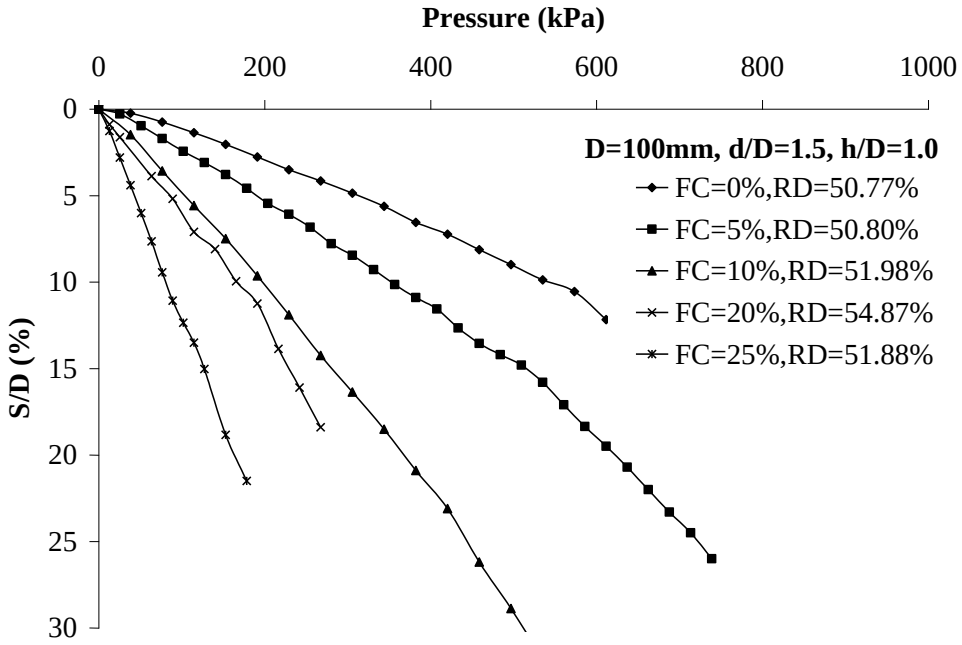

Fig. 4.80 Bearing pressure vs. settlement ratio (*S*/*D*) for a confined circular plate for different proportions of fines for D=100mm, d/D=1.5 and h/D=1.0

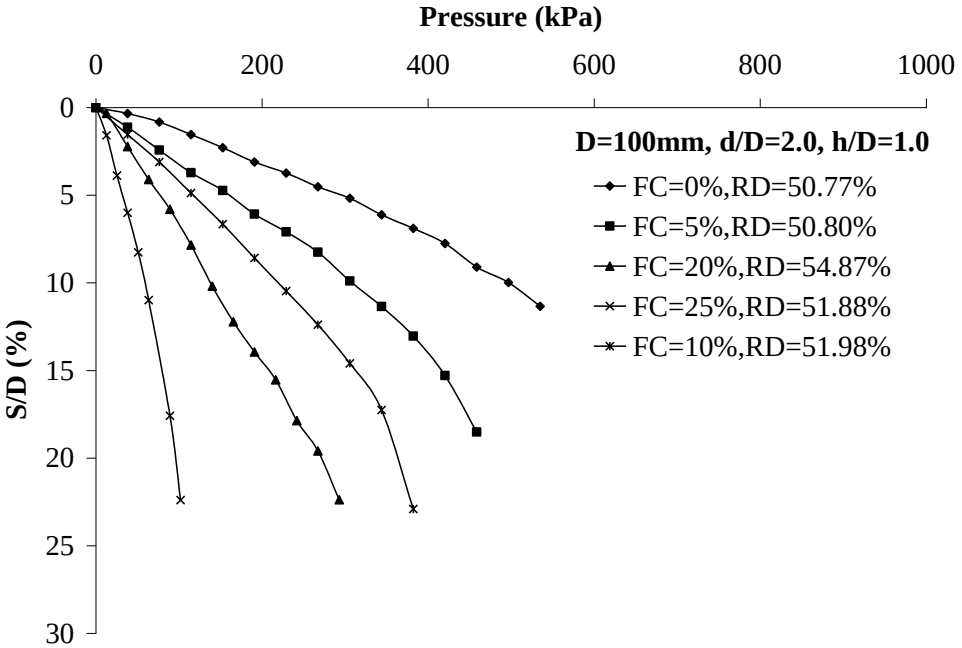

Fig. 4.81 Bearing pressure vs. settlement ratio (*S*/*D*) for a confined circular plate for different proportions of fines for D=100mm, d/D=2.0 and h/D=1.0

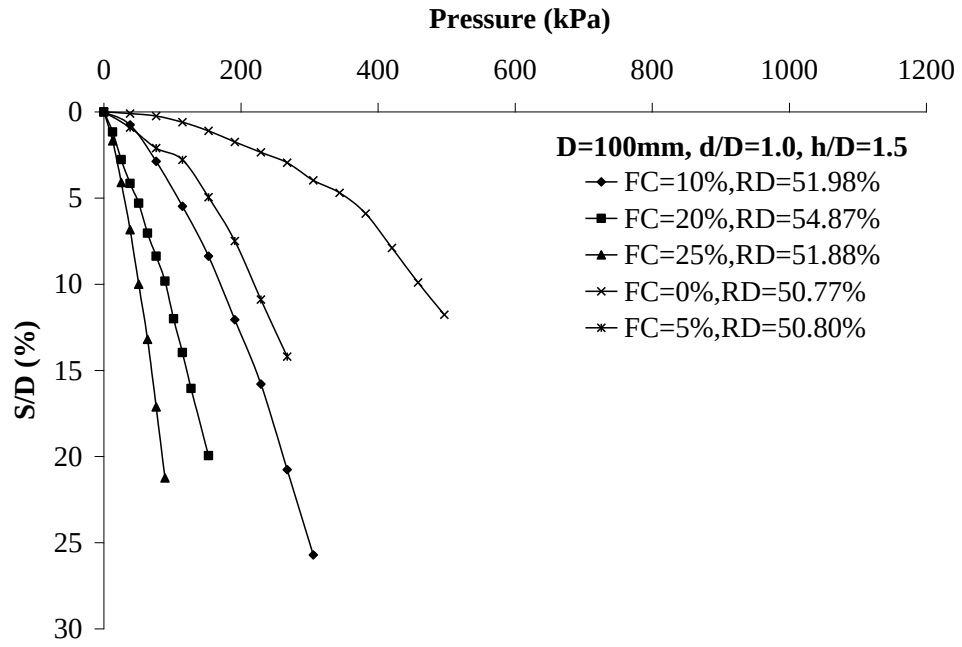

Fig. 4.82 Bearing pressure vs. settlement ratio (*S*/*D*) for a confined circular plate for different proportions of fines for D=100mm, d/D=1.0 and h/D=1.5

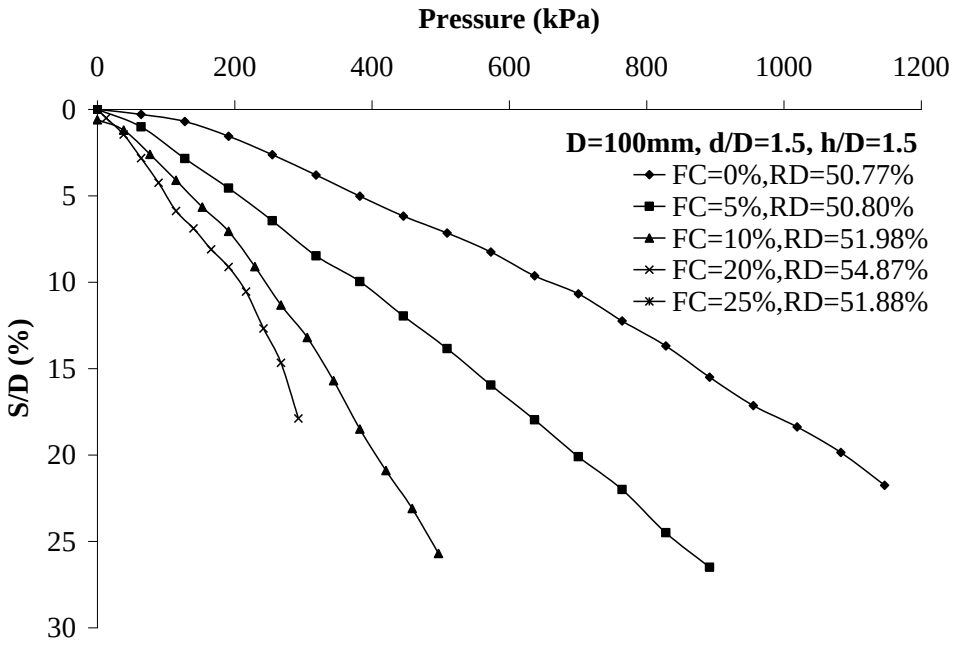

Fig. 4.83 Bearing pressure vs. settlement ratio (*S*/*D*) for a confined circular plate for different proportions of fines for D=100mm, d/D=1.5 and h/D=1.5

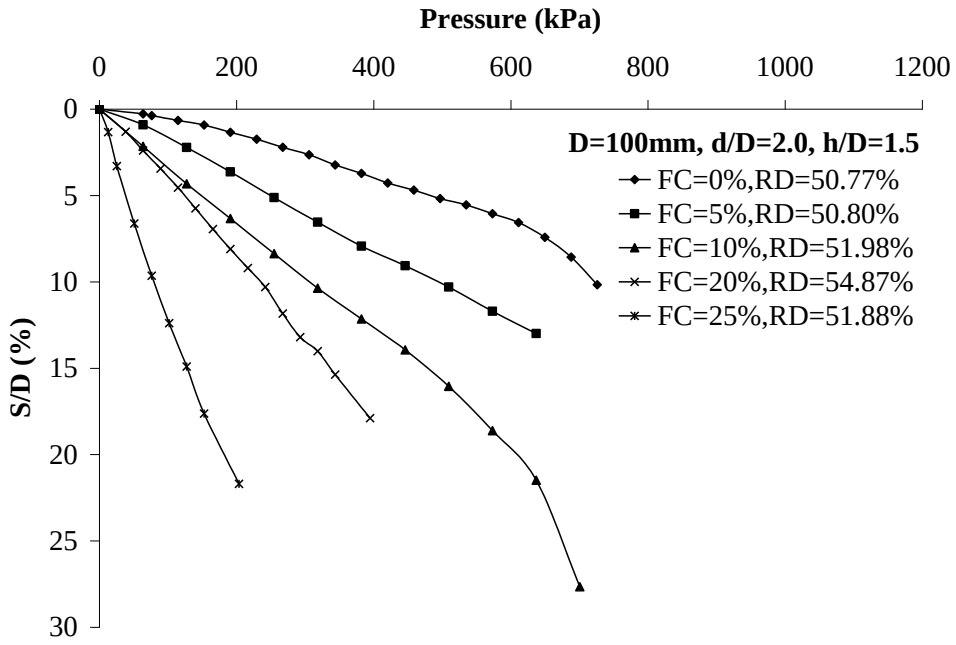

Fig. 4.84 Bearing pressure vs. settlement ratio (*S*/*D*) for a confined circular plate for different proportions of fines for D=100mm, d/D=2.0 and h/D=1.5

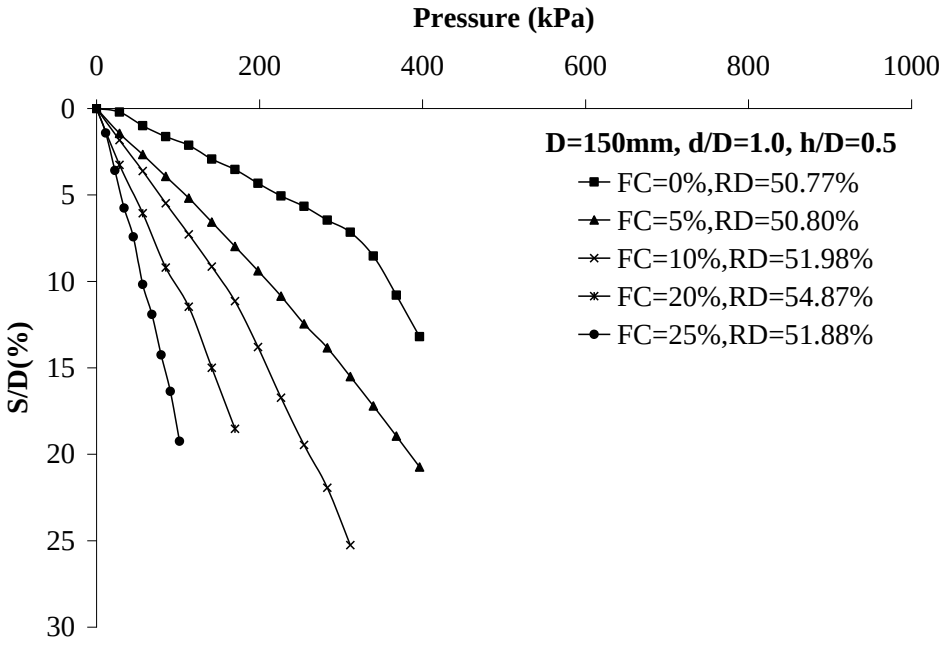

Fig. 4.85 Bearing pressure vs. settlement ratio (*S*/*D*) for a confined circular plate for different proportions of fines for D=150mm, d/D=1.0 and h/D=0.5

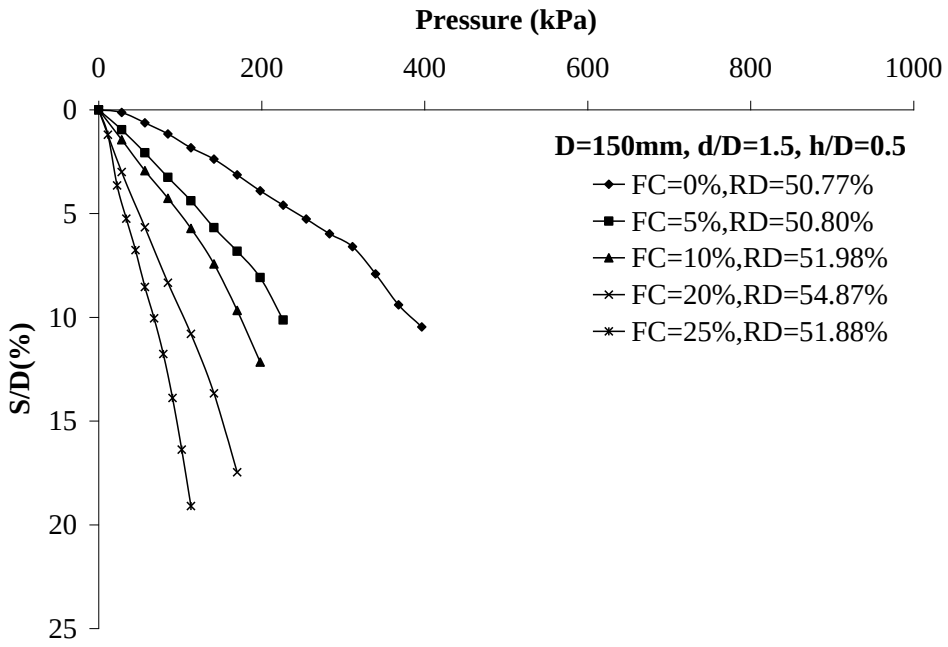

Fig. 4.86 Bearing pressure vs. settlement ratio (*S*/*D*) for a confined circular plate for different proportions of fines for D=150mm, d/D=1.5 and h/D=0.5

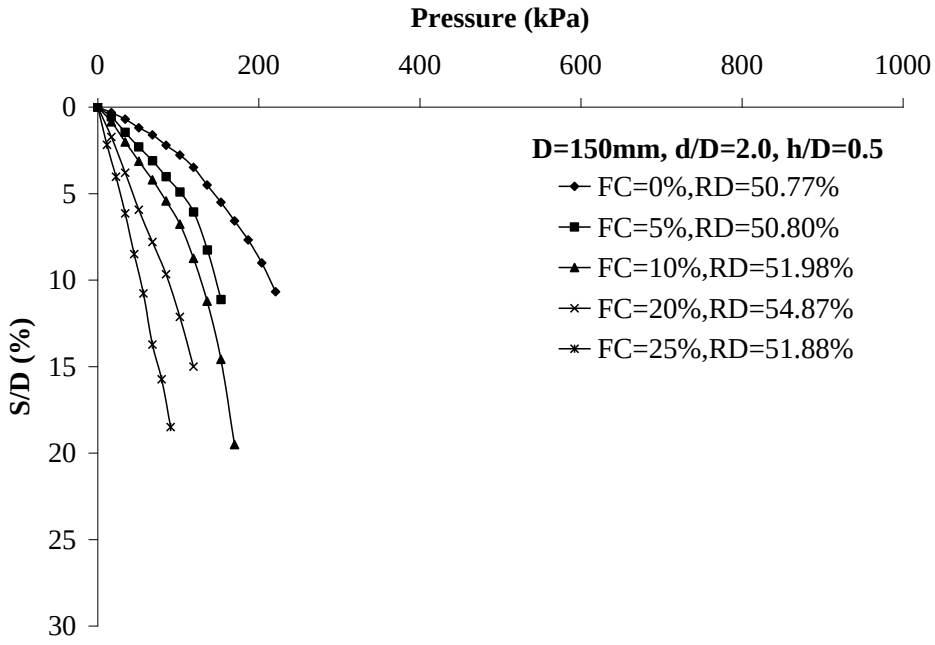

Fig. 4.87 Bearing pressure vs. settlement ratio (*S*/*D*) for a confined circular plate for different proportions of fines for D=150mm, d/D=2.0 and h/D=0.5

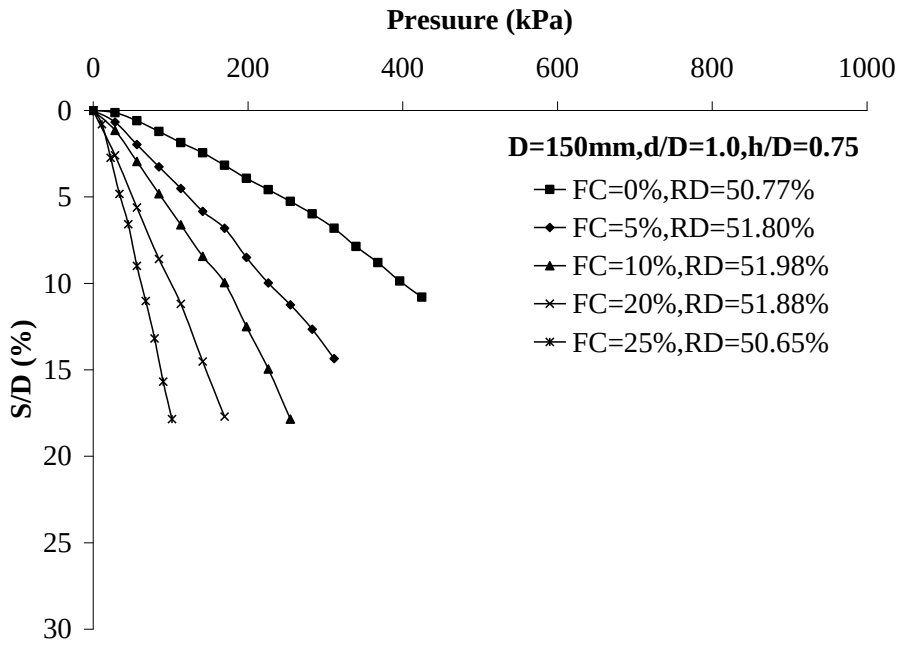

Fig. 4.88 Bearing pressure vs. settlement ratio (*S*/*D*) for a confined circular plate for different proportions of fines for D=150mm, d/D=1.0 and h/D=0.75

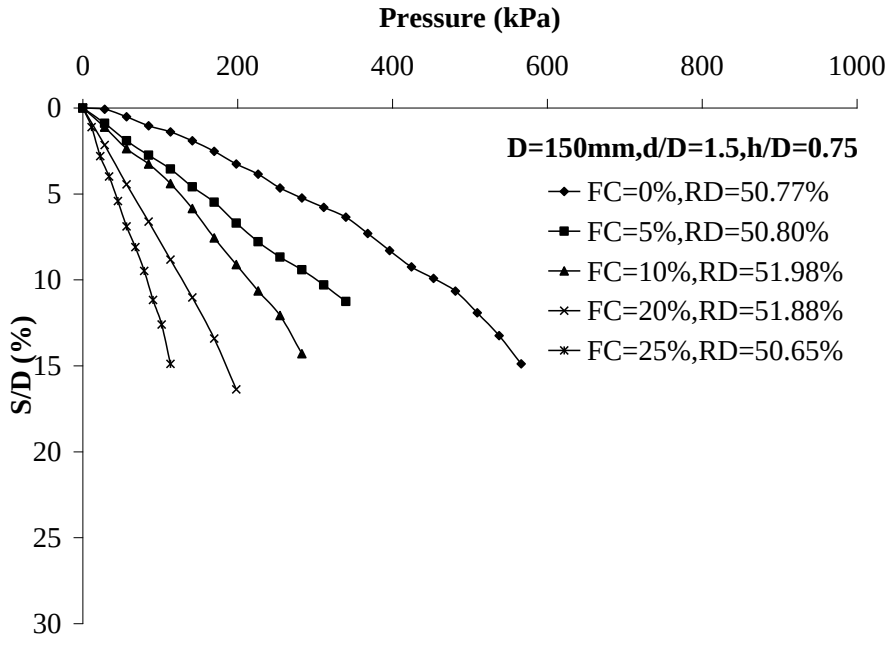

Fig. 4.89 Bearing pressure vs. settlement ratio (*S*/*D*) for a confined circular plate for different proportions of fines for D=150mm, d/D=1.5 and h/D=0.75

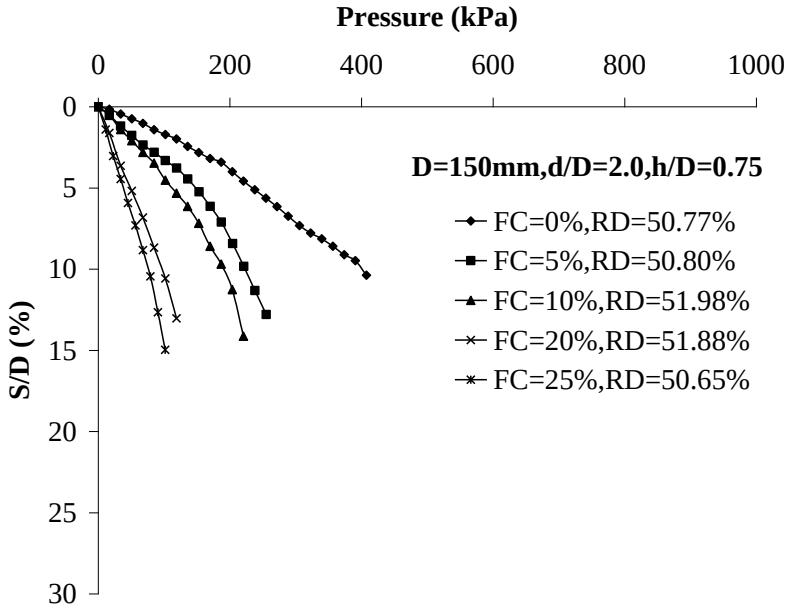

Fig. 4.90 Bearing pressure vs. settlement ratio (*S*/*D*) for a confined circular plate for different proportions of fines for D=150mm, d/D=2.0 and h/D=0.75

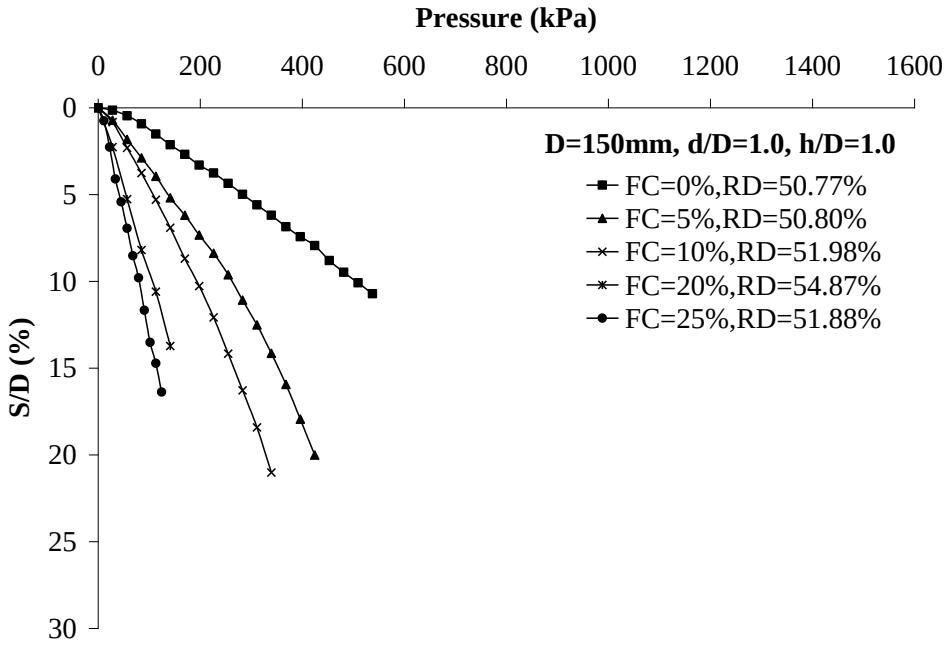

Fig. 4.91 Bearing pressure vs. settlement ratio (*S*/*D*) for a confined circular plate for different proportions of fines for D=150mm, d/D=1.0 and h/D=1.0

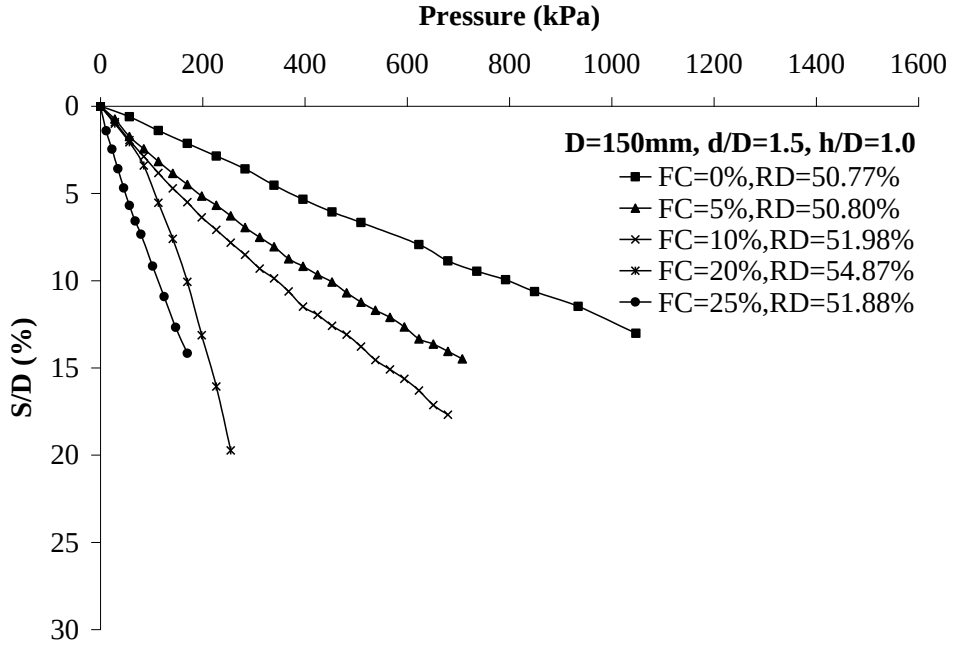

Fig. 4.92 Bearing pressure vs. settlement ratio (*S*/*D*) for a confined circular plate for different proportions of fines for D=150mm, d/D=1.5 and h/D=1.0

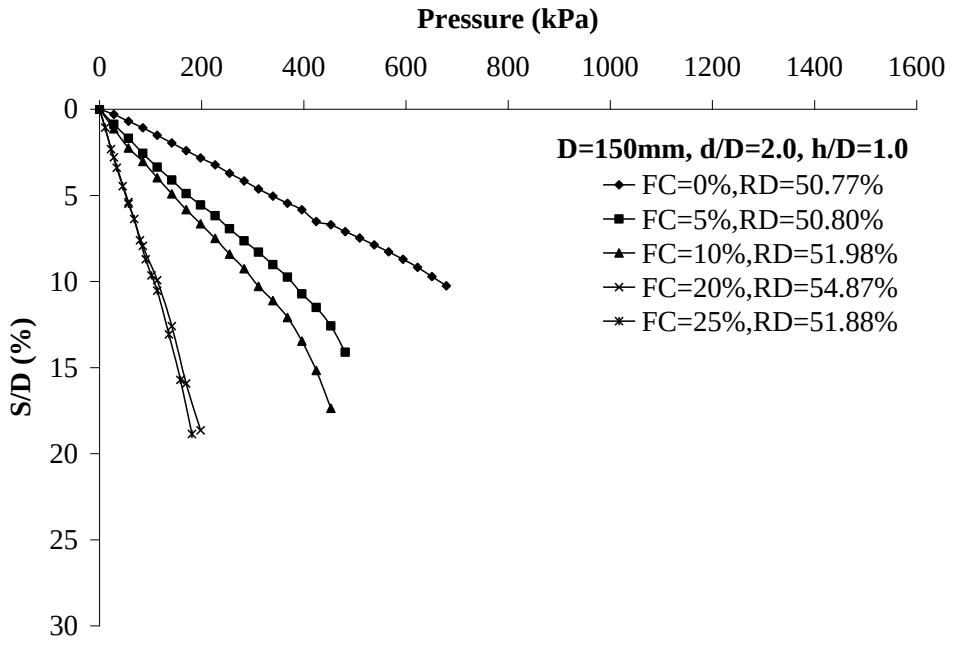

Fig. 4.93 Bearing pressure vs. settlement ratio (*S*/*D*) for a confined circular plate for different proportions of fines for D=150mm, d/D=2.0 and h/D=1.0

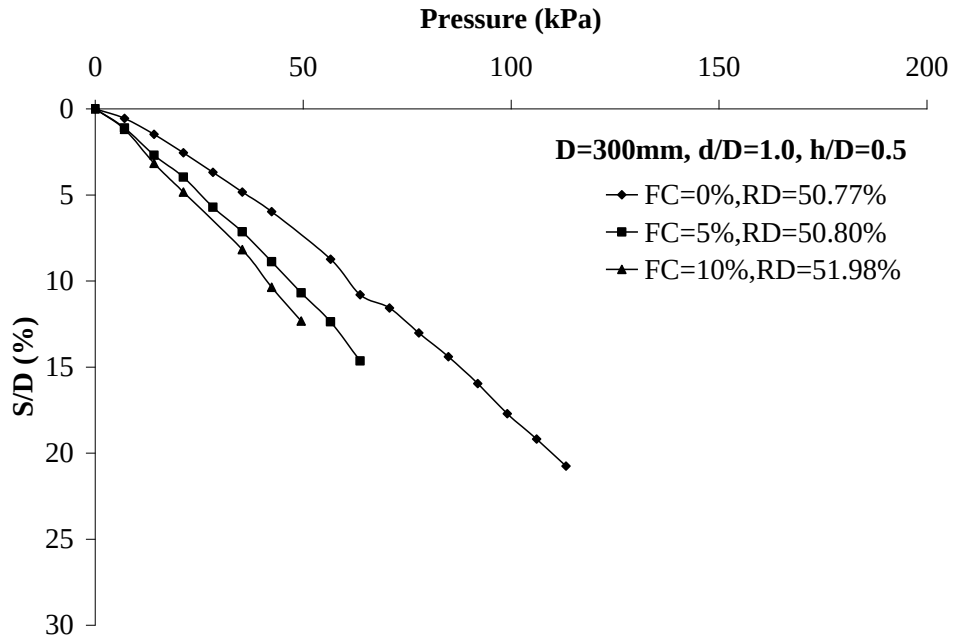

Fig. 4.94 Bearing pressure vs. settlement ratio (*S*/*D*) for a confined circular plate for different proportions of fines for D=300mm, d/D=1.0 and h/D=0.5

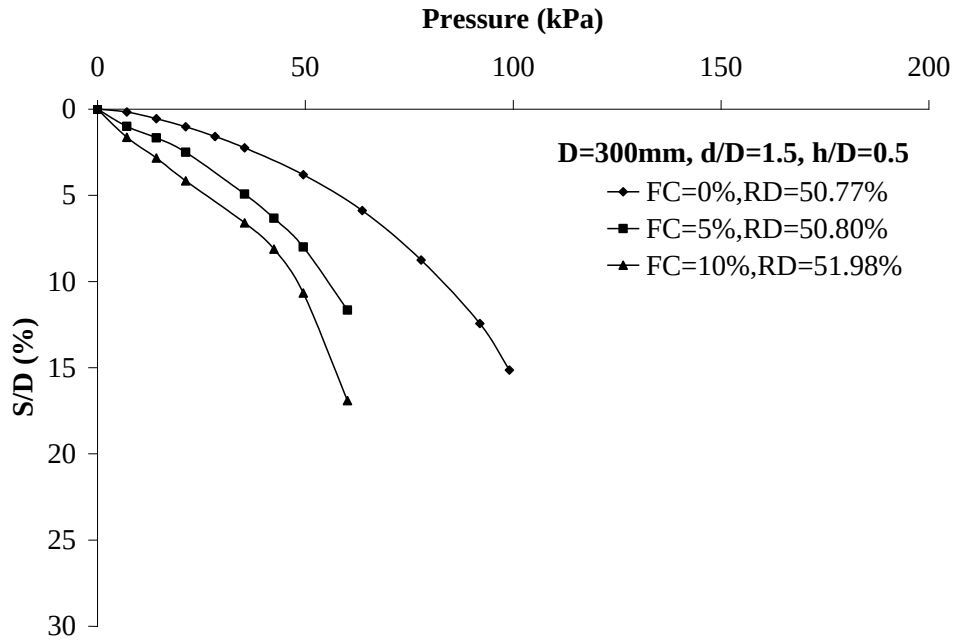

Fig. 4.95 Bearing pressure vs. settlement ratio (*S*/*D*) for a confined circular plate for different proportions of fines for D=300mm, d/D=1.5 and h/D=0.5

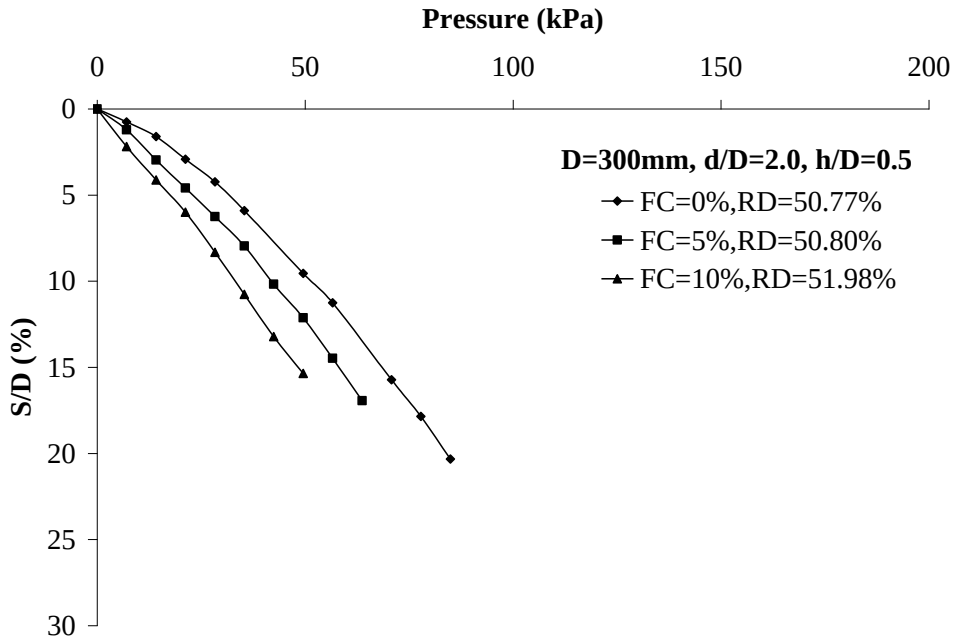

Fig. 4.96 Bearing pressure vs. settlement ratio (*S*/*D*) for a confined circular plate for different proportions of fines for D=300mm, d/D=2.0 and h/D=0.5

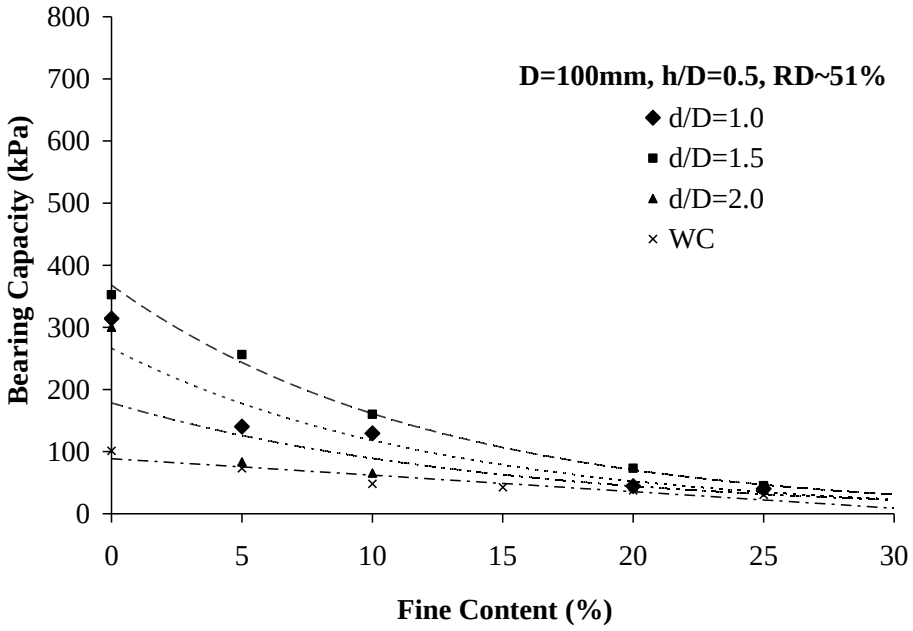

Fig. 4.97 Variation of bearing capacity with different proportions of fines for D=100mm, h/D=0.5

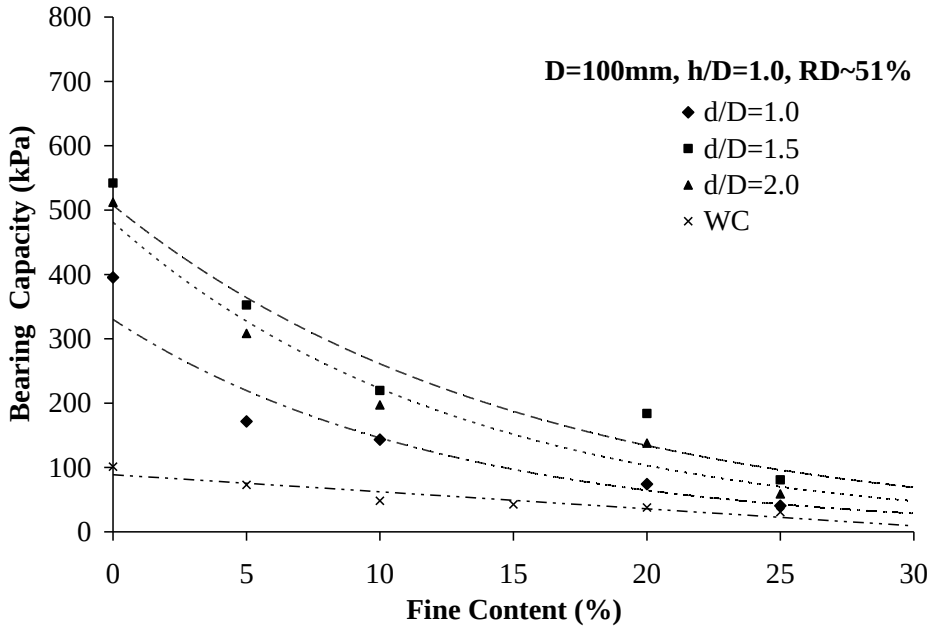

Fig. 4.98 Variation of bearing capacity with different proportions of fines for D=100mm, h/D=1.0

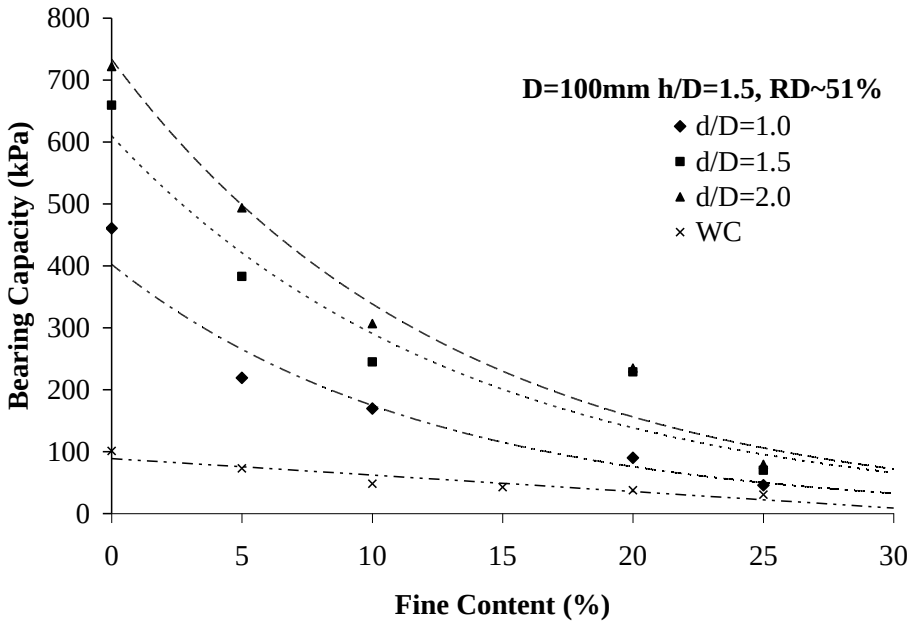

Fig. 4.99 Variation of bearing capacity with different proportions of fines for D=100mm, h/D=1.5

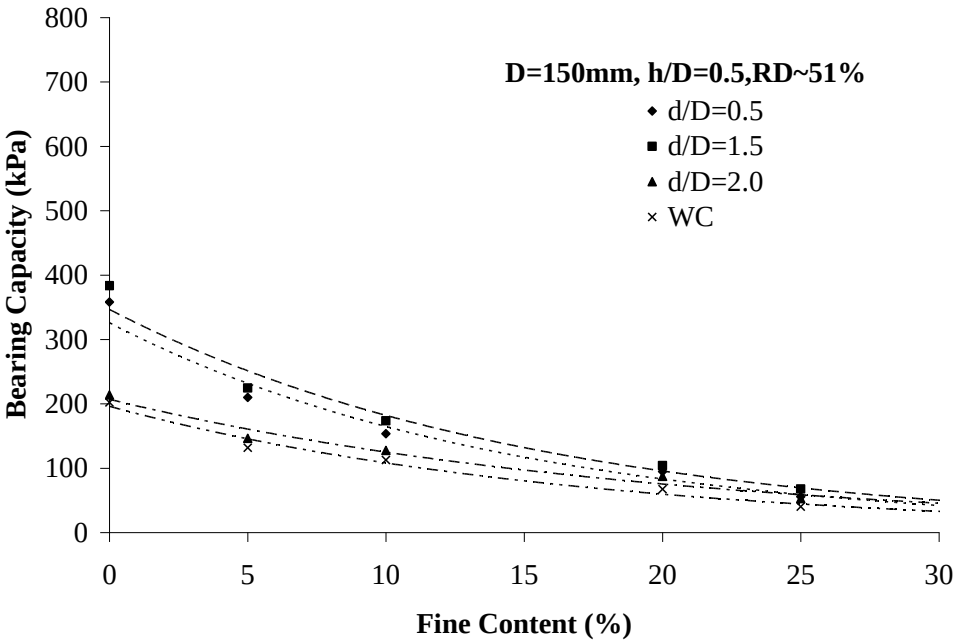

Fig. 4.100 Variation of bearing capacity with different proportions of fines for D=150mm, h/D=0.5

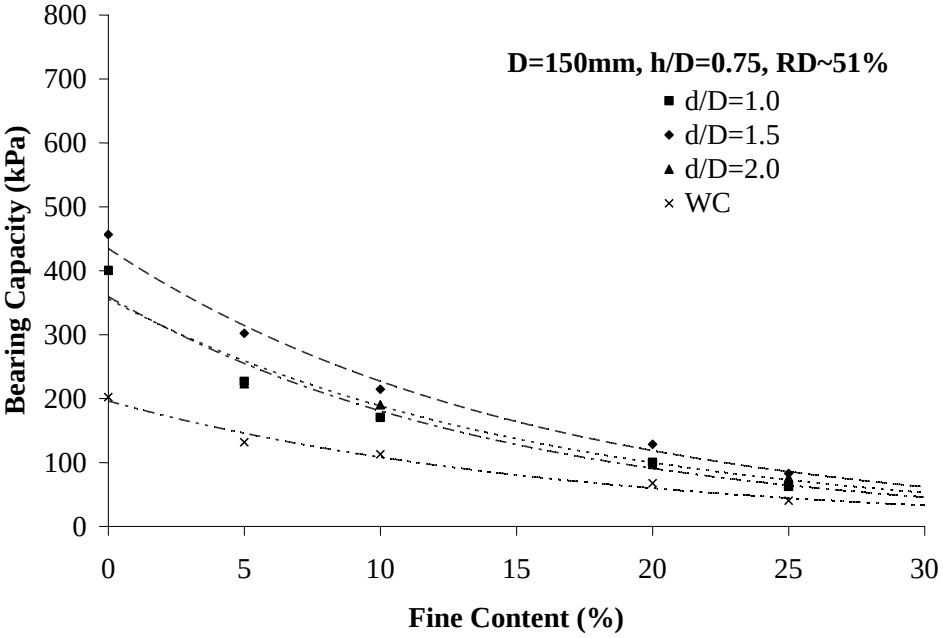

Fig. 4.101 Variation of bearing capacity with different proportions of fines for D=150mm, h/D=0.75

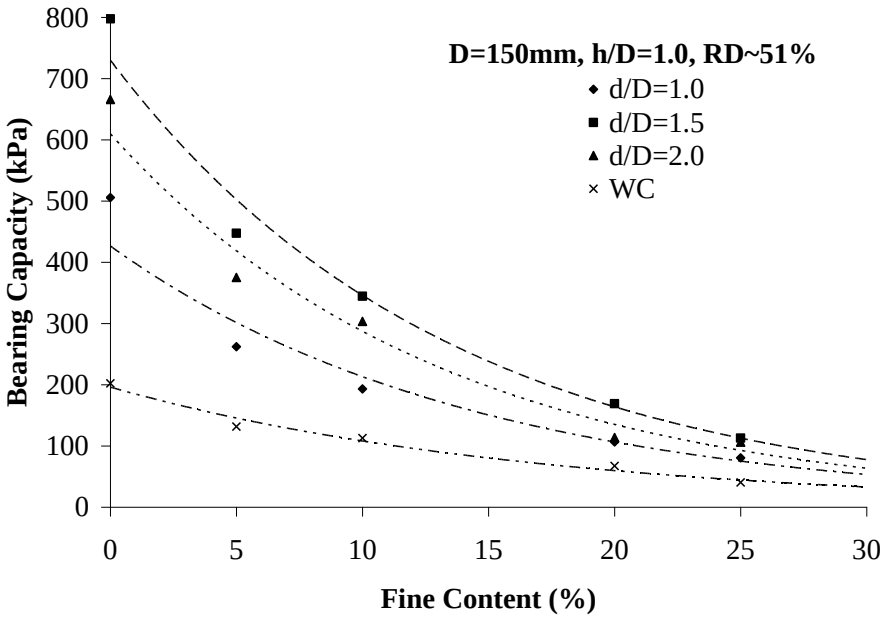

Fig. 4.102 Variation of bearing capacity with different proportions of fines for D=150mm, h/D=1.0

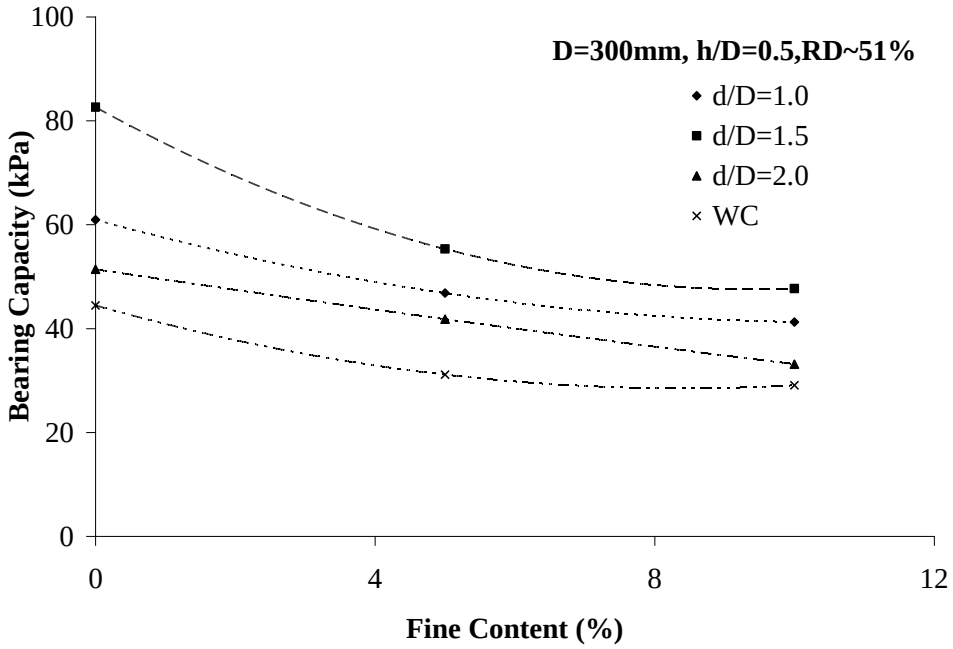

Fig. 4.103 Variation of bearing capacity with different proportions of fines for D=300mm, h/D=0.5

4.7. Effect of Soil Pressure on the Cell

One of the parameters to be investigated was the thickness of the cell wall in order to study the effect of the cell rigidity on the footing–cell system behavior and also to study the hoop tension in the cell wall due to the pressure under the footing. The cell used in the present study was made up of 0.94mm thick mild steel sheet and the cells were instrumented in the laboratory. The cells were open at both the ends. It was modeled as a circular footing supported on silty soil, which was surrounded by a mild steel cell having same soil outside. The internal pressures which the cell can withstand without yielding was estimated to be 4700 MPa. In the model tests, the maximum pressure which was applied on the cell was 762 kPa. The horizontal pressure acting on the sidewalls of the cell was approximated by the vertical pressure and the coefficient of lateral earth pressure. It can be seen that the maximum estimated horizontal earth pressures on the sidewalls of the cell are relatively insignificant in comparison to the allowable internal pressure. The given allowable value is the net inside pressure while the cell in the model is subjected to both internal and external pressures. The checks were performed after each test to observe any deformation in the cell wall features and measurements were made to check the internal diameter as well as the thickness of the cell wall. No change was noticed in the cell features or its dimensions. Therefore, for the given model and dimensions, the footing pressures have no effect on the cell wall. Therefore, the same cellular support was used for all the varied model test setups.

CHAPTER-V
CONCLUSIONS

5.0 General

An experimental study on the effect of silt and influence of cell confinement on the bearing capacity of circular footings on silty sands was carried out. The laboratory tests on clean sand and sand containing silt up to 25% were performed. The cells with different heights and diameters were used to confine the silty sand. The effect of proportion of silt in sand, cell diameter, cell height and the embedded depth of footing was studied. Conclusions reported are based on the results obtained during this research investigation. On the basis of the present study, the following conclusions have been drawn:

5.1 Effect of Fines

(1) The Skeleton void ratio (e_{sk}) is greater than the maximum void ratio $(e_{max})_{f=0}$ of clean sand corresponding to a fines content of 10% indicating that the sand particles are on an average, not in contact and the mechanical behavior is no longer controlled by the sand matrix.

(2) The increase of fines in clean sand significantly alters the settlement and bearing capacity characteristics of a footing as supported by the variation in angle of internal friction. The effect of fines has a more pronounced influence in case of smaller diameter footings.

5.2 Effect of Confinement

(1) The soil confinement has a significant influence on the behavior of circular footings leading to bearing capacity enhancement and settlement reduction for systems supported on granular soils.

(2) For small diameters of cells relative to footing size (d/D = 1.0), the cell-soil-footing system acts as one unit i.e. the cell, soil, and footing settle all together.

(3) For large diameter cells relative to footing size (d/D >1.0), the cell–soil–footing system behaves initially as one unit but as the failure approaches, the footing only settles while the cell remains unaffected.

(4) The improvement in the ultimate bearing capacity depends on the d/D (cell diameter/footing diameter) and h/D (cell height/footing diameter) ratio. The optimum

value of this ratio is 1.5 beyond which the improvement decreases as the ratio for *h*/*D* increases from 0.5 to 1. Whereas if *d*/*D* =2, the improvement factor (I_f) increases for all the values of *h/D*.

(5) The increase in the height of the confining cell transfers footing loads to the deeper locations and increases the improvement factor due to an increase in the surface area of the cell–model footing.

(6) The embedded depth of footing relative to the top of confining cell has insignificant effect on the response of footing–cell systems.

(7) The soil confinement could be considered as a method to reduce the settlement of isolated footings on loose to medium density silty sands. These type of cells with different diameters could be easily manufactured and placed around the individual footings leading to a significant improvement in their response. In cases where structures are very sensitive to settlement, soil confinement can be used to obtain the same allowable bearing capacity at a much lower settlement

(8) The settlement reduction factor (S_f) is a function of d/D (cell diameter/footing diameter) ratio. The optimum value of this ratio is 1.5 beyond which the reduction in settlement increases with increase in this ratio.

5.3 Effect of Footing Diameter

(1) The bearing capacity factor, $N_{\gamma,}$ depends on the absolute diameter of the circular footings and fine content.

(2) For model-scale footings of diameter 0.15m, tests gave higher value of $N_{\gamma.}$ A care should be taken while extending model-scale footing test results to the behavior of full-scale foundations. Since small scale footing tests produce higher values of N_γ than theoretical equations, therefore, should not be used for the design of full-scale footings. For footings of diameter 0.3m and 0.45m, tests gave smaller and comparable values of $N_{\gamma.}$ The actual test results produced lower values of N_γ than the theoretical values.

(3) It is recommended that the experimental results of 0.45m diameter footing should be used to extrapolate the bearing capacity of full-scale footings instead of the normal practice of using results of 0.3m diameter footings.

CHAPTER - VI
SUGGESTIONS FOR FUTURE WORK

1. The model tests have been conducted on clean sand placed at a relative density of 52 percent. Investigations may be extended to sands compacted at different relative densities and having different angles of shearing resistance.

2. The effect of confinement has been analyzed by confining the soil below the footings by using cells which were made up of mild steel plate. Investigations may be extended by using cells of different materials.

3. The model tests have been conducted by placing the skirt around the footing. Investigations may be extended by placing the skirt below the footing.

4. The model tests have been conducted on dry silty sands. Further tests may be conducted on partially saturated and fully saturated soils under drained and undrained conditions.

5. Field investigations may be conducted to check the validity of results of laboratory investigations in the field.

6. The problem may also be analyzed theoretically and compared with the experimental results.

LIST OF PUBLICATIONS FROM THE CURRENT WORK

1. Gupta, R. and Trivedi, A. (2009) "Bearing capacity and settlement of footing resting on confined loose silty sands". *Electronic Journal of Geotechnical Engineering, Vol. 14, Bundle A.* Available on line "www.ejge.com"

2. Gupta, R. and Trivedi, A. (2010) "Behavior of Model Circular Footings on Silty Soils with Cellular Supports". *International Journal of Engineering*, 23(1),21-35.

3. Gupta, R. and Trivedi, A. (2009) "Effects of Non-Plastic Fines on the Behavior of Loose Sand-An Experimental Study". *Electronic Journal of Geotechnical Engineering.* (Accepted for publication) "www.ejge.com"

4. Gupta, R. and Trivedi, A. (2009) "Settlement Characteristics of Confined Model Circular Footings on Silty Sands". Communicated to *Journal of Testing and Evaluation,* ASTM (Under second review).

REFERENCES

1. Al-Aghbari, M.Y. and Zein, Y.E. (2004) “Bearing capacity of strip foundations with structural skirts”, Journal of Geotechnical and Geological Engineering, 22(1), 43-57.
2. Al-Aghbari, M.Y.and Zein, Y.E. (2006) “Improving the performance of circular foundations using structural skirts”, Journal of Ground Improvement, 10(3), 125-132.
3. Amini, F., and Qi, G. Z. (2000) ‘‘Liquefaction testing of stratified silty sands.’’ *J. Geotech. Geoenviron. Eng.*, 126(3), 208–217.
4. Appolonia, D.J.D., Appolonia E.D. and Brisette R.F. (1968) “Settlement of Spread Footings on Sand,” ASCE Journal of Soil Mechanics and Foundations Division, Vol. 94, No. SM3, 735-760.
5. Bathurst, R. J. and Karpurapu, R. (1993) “Large scale triaxial compression testing of geocell-reinforced granular soil”, Geotechnical Testing Journal, ASTM, 16 (3), 296-303.
6. Boushehrian, J. H. and Hataf, N. (2003) "Experimental and numerical investigation of the bearing capacity of model circular and ring footings on reinforced sand", Journal of Geotextiles and Geomembranes, 21(4), 241-256.
7. Bolton, M.D. (1986), “The strength and dilatancy of sands”, *Geotechnique*, 36(1), 65-78.
8. Billam, J. (1972), “Some aspects of the behaviour of granular material at high pressures”, *Stress strain behaviour of soils*, (ed. R.H.V.Parry), Foulis, London, 69-80.
9. Bransby, M.F. and Randolph, M.F. (1999) "The Effect of Skirted Foundation Shape on Response to Combined V-M-H Loadings," International Journal of Offshore and Polar Engineering, Vol. 9, No. 3, 214- 218.
10. Bransby, M.F. and Randolph, M.F. (1998) “ Combined loading of skirted foundation, geotechnoque, 48(5), 637-655.

11. Brinch Hasen, J. (1970) “A revised and extended formula for bearing capacity.” Bulletin No. 28, Danish Tech. Inst., Copenhagen, 5-11.
12. Brown, G. (1961) “X-ray diffraction and crystal structure of clay minerals” (Ed), Mineralogical Society, London, 2nd Ed., 554.
13. Burmister, D. (1948) “The importance and practical use of relative density in soil mechanics”, Spec.Publ.No.48, ASTM, West Conshohocken, 1-20.
14. Bush, D.I., Jenner, C. G. and Bassett, R. H. (1990) “The design and construction of geocell foundation mattresses supporting embankments over soft ground”, Geotextiles and Geomembranes, 9, 83-98.
15. Casagrande, A. (1975) “Liquefaction and cyclic mobility of sands. A critical review”, *Proc., 5th Pan American Conf. on Soil Mech. And Found. Engrg.*, Vol. 5, 80–133.
16. Cerato, A.B., and Lutenegger, A.J. (2006) “Bearing capacity of square and circular footings on a finite layer of granular soil underlain by a rigid base”, Journal of Geotech. Geoenviron. Engg., ASCE, 132(11), 1496-1501.
17. Chaney, R. C., and Pamukcu, S. (1991) ‘‘Earthquake effects on soil foundation systems. Part II. Prior to 1975.’’ *Foundation engineering handbook*, 2nd Ed., H.-Y. Fang, ed., Van Nostrand Reinhold, New York, 623–672.
18. Chang, N. Y., Yeh, S. T., and Kaufman, L. P. (1982) “Liquefaction potential of clean and silty sands” *Proc., 3rd Int. Earthquake Microzonation Conf.*, Vol. 2, 1017–1032.
19. Cowland, J. W. and Wong, S.C.K. (1993) “Performance of road embankment on soft clay supported on a geocell mattress foundation”, Geotextiles and Geomembranes, 12, 687-705.
20. Dash, S. K., Sireesh, S., and Sitharam, T. G. (2003) “Behavior of geocell reinforced sand beds under circular footing”, Ground Improvement, 7, 111-115.
21. Dash, S., Krishnaswamy, N., and Rajagopal, K. (2001) “Bearing capacity of strip footing supported on geocell-reinforced sand.” Geotextiles and Geomembranes, 19, 235–256.
22. deBeer, E. E. (1965) “Bearing capacity and settlement of shallow foundations on sand”, Symposium on Bearing Capacity and Settlement of Foundations, Duke Univ. 15-33.
23. deBeer, E. E. (1970) “Experimental determination of the shape factor and the bearing capacity factors of sand”, Geotechnique, 20, 387-411.

24. Dezfulian, H., (1982) “Effects of Silt Content on Dynamic Properties of Sandy Soils”, *Proceedings of the Eighth World Conference on Earthquake Engineering*, San Francisco, USA, 63-70.
25. El Hosri, M. S., Biarez, J., and Hicher, P.Y. (1982) “Liquefaction Characteristics of Silty Clay”, *Proceedings. of the Eighth World Conference on Earthquake Engineering,* San Francisco, USA, 277-284.
26. Emersleben, A. and Meyer, N. (2008) “Bearing capacity improvement of gravel base layer in road construction using geocells”, 12th International Conference of International Association for Computer Methods and Advances in Geomechanics, Goa, 3538-3545.
27. Feda, J. (1961) “Research on bearing capacity of loose soil”, Procs. 5th Int. Conf. Soil Mech. Found. Eng., Paris, 1, 635-642.
28. Fei, H.C. (1991) “The Characteristics of Liquefaction Of Silt Soil”, Soil Dynamics and Earthquake Engineering V, Computational Mechanics Publications, Southhampton, 293-302.
29. Finn, W. D. L., Ledbetter, R. H., and Wu, G. (1994) “Liquefaction in silty soils: Design and analysis”, *Ground failures under seismic conditions, Geotech. Spec. Publ. No. 44*, ASCE, New York, 51–76.
30. Florin, V.A., and Ivanov, P.L. (1961) “Liquefaction Of Saturated Sandy Soils”, *Proceedings of the Fifth International Conference on Soil Mechanics and Foundation Engineering*, Paris, France, Vol. 1, 107-111.
31. Garga, V., and McKay, L. (1984) “Cyclic Triaxial Strength of Mines Tailings”, *Journal of Geotechnical Engineering*, ASCE, Vol. 110(8), 1091- 1105.
32. Giri, P. (1994) “Performance of Skirted Foundation in Sand Subjected to Vibrations,” Proc. 13th ICSMFE, New Delhi, India, 787- 790.
33. Gourvenec, S. (2002) “Combined Loading of Skirted Foundations,” Proc. 5th ANZYGPC Rotorua, New Zealand, 105- 110.
34. Gourvenec, S. (2003) “Alternative Design Approach for Skirted Footings Under General Combined Loading,” Proc. International Conference on Foundations (ICOF), Dundee, Scotland, 341- 349.
35. Ghosh, C. and Madhav, M. R. (1994) “Reinforced Granular Fill - Soft Soil System: Confinement Effect”, Geotextiles and Geomembranes, Vol. 13, 727-741.

36. Hanzawa, H. (1980) “Undrained strength and stability analysis for a quick sand”, Soils and Found., Tokyo, 20(2), 17-19.
37. Holzer, T. L., Youd, T. L., and Hanks, T. C. (1989) “Dynamics of Liquefaction During the 1987 Superstition Hills, California, Earthquake”, *Science*, Vol. 244, 56-59.
38. IS: 2720 (Part 13)-1986 Methods of test for soils: Part 13 Direct shear test.
39. IS: 2720(Part14)-1983 Methods of test for soils: Part 14 determination of density index (relative density) of cohesion less soils.
40. IS: 2720(Part3/Sec 2)-1980 Methods of tests for soils: Part 3 Determination of specific gravity, Section 2 Fine, medium and coarse grained soils.
41. IS: 2720(Part4)-1985 Methods of test for soils: Part 4 Grain size analysis.
42. Ishihara, K., and Koseki, (1989) “Discussion On The Cyclic Shear Strength Of Fines- Containing Sands”, Earthquakes Geotechnical Engineering, *Proceedings of the Eleventh International Conference on Soil Mechanics and Foundation Engineering*, Rio De Janiero, Brazil, 101-106.
43. Ishihara, K., Sodewkawa, M., and Tanaka, Y. (1977) “Effects of Overconsolidation On Liquefaction Characteristics Of Sands Containing Fines” Dynamic Geotechnical Testing, ASTM STP 654, American Society for Testing and Materials, pp. 246-264.
44. Ishihara, K. (1993) “Liquefaction and flow failure during earthquakes”, *Geotechnique*, 43(3), 351–415.
45. Ishihara, K., Troncoso, J., Kawase, Y., and Takahashi, Y. (1980) “Cyclic strength characteristics of tailings materials”, *Soils Found.*, 20(4), 127–142.
46. Klug, H.P., and Alexander, L.E. (1974) “X-ray diffraction procedures for polycrystalline and amorphous materials”, John Wiley, New York.
47. Koester, J. P. (1994) “The influence of fine type and content on cyclic resistance”, *Ground failures under seismic conditions, Geotech. Spec. Publ. No. 44*, ASCE, New York, 17–33.
48. Krishnaswamy, N.R., Rajagopal, K., and Madhavi Latha, G. (2000) “Model studies on geocell supported embankments constructed over soft clay foundation”, Geotechnical Testing Journal, ASTM, 23, 45-54.
49. Kuerbis, R., Negussey, D., and Vaid, V. P. (1988) “Effect Of Gradation And Fines Content On The Undrained Response Of Sand” *Proceedings. Hydraulic Fill Structures*, Fort Collins, USA, 330-345.

50. Lade, P. V., and Yamamuro, J. A. (1997) “Effects of non-plastic fines on static liquefaction of sands”, Canadian Geotechnical Journal, 34, 905-917.
51. Laman, M. and Yildiz, A. (2003) "Model studies of ring foundations on geogrid-reinforced sand", International Journal of Geosynthetics, 10(5), 142-152.
52. Law, K. T., and Ling, Y. H. (1992) “Liquefaction of granular soils with non-cohesive and cohesive fines” *Proc., 10th World Conf. on Earthquake Engrg.*, 1491–1496.
53. Lee, K. L., and Seed, H. B. (1967) “Cyclic stress conditions causing liquefaction of sand”, *J. Soil Mech. and Found. Div.*, ASCE, 93(1), 47–70.
54. Lee, K.L., and Albaisa, A. (1974) “Earthquake Induced Settlements In Saturated Sands”, *Journal of the Geotechnical Engineering Division*, ASCE, Vol. 100(4), 387 - 406.
55. Lee, K.L., and Fitton, J.A. (1968) “Factors Affecting The Cyclic Loading Strength Of Soil”, Vibration Effects of Earthquakes on Soils and Foundations, ASTM STP 450, American Society for Testing and Materials, 71-95.
56. Lee, K.L., and Seed, H.B. (1967a) “Cyclic Stress Conditions Causing Liquefaction Of sand”, *Journal of the Soil Mechanics and Foundations Division*, ASCE, Vol. 93, SM1, 47-70.
57. Lutenegger, A.J, and Cerato Amy B. (2007) “Scale effects of shallow foundation bearing capacity on granular material”, Journal of Geotech. Geoenviron. Engg., ASCE, 133 (10), 1192-1202
58. MacEwan, D.C.M. (1946) “Identification and estimation of the montmorillonite group of minerals with special Reference to clay soils”, Chem. Ind., London, 68, 278.
59. Mahiyar, H. and Patel, A.N. (2000) “Analysis of angle shaped footing under eccentric loading”, Journal of Geotech. Geoenviron. Engg., ASCE, 126(12), 1151- 1156.
60. Mandal, J.N., and Manjunath, V.R. (1995) “Bearing capacity of strip footing resting on reinforced sand subgrades”, Journal of Construction and Building Material, 9(1), 35-38.
61. Martin, C.M. (2001) “Vertical bearing capacity of skirted circular foundations on Tresca soil”, Proc. 15th ICSMGE, 1, 743-746.

62. McCaleb, S. B. (1966) “X-ray diffraction automation and its use in clay mineralogy”, Clays and Clay minerals, Paragamon Press, London, 25, 123-130.
63. Meyerhof, G.G. (1963) “Some recent research on the bearing capacity of foundations”, Canadian Geotechnical Journal, 1(1), 16-26.
64. Meyerhof, G.G. (1965) “Shallow foundations”, J. Soil Mech. Founda. Div., ASCE, 91(2), 21-31.
65. Mhaiskar, S.Y. and Mandal, J. N. (1992) “Soft clay subgrade stabilization using geocells”, Grouting, Soil Improvement and Geosynthetics, New Orleans, Louisiana, ASCE, 2(30), 1092-1103.
66. Mhaiskar, S.Y. and Mandal, J.N. (1996) “Investigation on soft clay subgrade strengthing using geocells”, Construction and Building Materials, 10(4), 281-286.
67. Mogami, T., and Kubo, K. (1953) “The behaviour of soil during vibration”, *Proc., 3rd Int. Conf. on Soil Mech. and Found. Engrg.,* Vol. 1, 152–153.
68. Muhs, E. (1963). ‘‘Uber die Zulassige Belastung nichtibindiger Boden’’, *Mitteilungen der Deutschen Forschungsgesellshaft Fur Bodenmechanik (Degebo),* Berlin, Heft 16, 102–121 (in German).
69. Nasser M. Saleh, Ahmed E. Alsaied, and Azza M. Elleboudy (2008) “Performance of skirted Strip Footing subjected to eccentric inclined load”, Electronic Journal of Geotechnical Engineering, 13, Bund. F.
70. Okashi, Y. (1970) “Effects Of Sand Compaction on Liquefaction During Tokachioki Earthquake”, *Soils and Foundations*, JSSMFE, Vol. 10(2), 112-128.
71. Okusa, S., Anma, S., and Maikuma, H. (1980) “Liquefaction of Mine Tailings In The 1978 Izu-Oshima-Kinkai Earthquake, Central Japan”, *Proceedings. of the Seventh World Conference on Earthquake Engineering,* Istanbul, Turkey, Vol. 3, 89-96.
72. Oner, M. (1972) “Bearing capacity under combined inclined and eccentric loading”, Research Report, Norwegian Institute of Technology.
73. Ortiz, J.M.R. (2001) "Strengthening of foundations through peripheral confinement", Proc. 15th Int. Conf. on Soil Mech. and Geotech. Eng., Netherlands, 1, 779-782.

74. Perkins, S.W. and Madson, C.R. (2000), "Bearing capacity of shallow foundations on sand: A relative density approach", *J. Geotech. and Geoenv. Eng., ASCE,* 126 (6), 521-529.

75. Pitman, T.D., Robertson, P. K. and Sego, D. C. (1994) "Influence of fines on collapse of loose sands". Canadian Geotechnical Journal, 31, 728-739.
76. Prandtl, L. (1921) "Uber die Eindrigungsfestigkeit plastischer Baustoffe und die Festigkeit von Schneiden", Zeitschrift far Angewandte Mathematik und Mechanik Berlin, 1(1), 15-20 (in German).
77. Rajagopal, K., Krishnaswamy, N., and Latha, G. (1999) "Behavior of sand confined with single and multiple geocells", Geotexiles and Geomembranes, 17, 171-184.
78. Ranjan, G. and Rao, B. G. (1985) "Settlement analysis of skirted granular piles", Journal of Geotechnical Engineering Division, ASCE, 111(11), 1264-1280.
79. Rao, B.G. and Narhari, D.R. (1979) "Skirted Soil Plug Foundation", Proc. 6th Asian Regional Conf. on Soils, Singapore, 319-322.
80. Rea, C. and Mitchell, J. K. (1978) "Sand reinforcement using paper grid cells", *Reprint 3130*, SpringC and Exhibit., Pittsburgh, ASCE, 24-28.
81. Reissner, H. (1924) "Zum Erddrukproblem", Proc., Ist Int. Conf. App. Mech., Delft, The Netherlands, 295-311 (in German).
82. Robertson, P.K., and Campanella, R.G., (1985). "Liquefaction Potential of Sands Using CPT", *Journal of Geotechnical Engineering*, ASCE, Vol. 111(3), 384-403.
83. Sadannand Ojha (2011) " Non linear behavior of silty sands", Un-published PhD thesis , Deptt of civil engineering , University of Delhi.
84. Salgado, R., Bandini, P., and Karim, A. (2000) "Shear strength and stiffness of silty sand", Journal of Geotech. Geoenviron. Engg., ASCE, 126(5), 451-462.
85. Sawwaf, M. EI, and Nazer, A. (2005) "Behavior of circular footings on confined granular soil", Journal of Geotech. and Geoenviron. Eng., ASCE, 131(3), 359-366.

86. Seed, H. B., and Lee, K. L. (1966) ‘‘Liquefaction of saturated sands during cyclic loading”, *J. Soil Mech. and Found. Div.*, ASCE, 92(6), 105–134.
87. Seed, H. B., Chaney, R. C., and Pamukcu, S.(1991) ‘‘Earthquake effects on soil-foundation systems. Part I. Prior to 1975,’’ *Foundation engineering handbook*, 2nd Ed., H.-Y. Fang, ed., Van Nostrand Reinhold, New York, 594–623.
88. Seed, H.B., and Idriss, I.M. (1971) “Simplified Procedure For Evaluation Soil Liquefaction Potential”, *Journal of the Soil Mechanics and Foundations Division*, ASCE, Vol. 97(9), 1249-1273.
89. Seed, H.B., Idriss, I.M., and Arango, I. (1983) “Evaluation Of Liquefaction Potential Using Field Performance Data”, *Journal of Geotechnical Engineering*, ASCE, Vol. 109(3), 458-482.
90. Seed, H.B., Tokimatsu, K., Harder, L., and Chung, R. (1985) “Influence of SPT Procedures in Soil Liquefaction Resistance Evaluations”, *Journal of Geotechnical Engineering*, ASCE, Vol. 111(12), 1425-1445.
91. Selig, E.T. and Ladd, R.S. (1973) “Evaluation of relative density measurement and applications”, Evaluation of Relative Density and its Role in Geotechnical Projects Involving Cohessionless Soils, (ASTMSTP 523), ASTM, West Conshohocken, Pa., 487-504.
92. Shen, C. K., Vrymoed, J. L., and Uyeno, C. K. (1977) “The effects of fines on liquefaction of sands”, *Proc., 9th Int. Conf. on Soil Mech. And Found. Engrg.*, Vol. 2, 381–385.
93. Singh, S. (1994). “Liquefaction Characteristics Of Silt”, Ground Failures Under Seismic Conditions, Geotechnical Special Publication No. 44, ASCE, 105-116.
94. Singh, V.K., Prasad, A., Aggarwal, R.K. (2008) “Effect of soil confinement on ultimate bearing capacity of square footing under eccentric-Inclined load”, Electronic Journal of Geotechnical Engineering, 12, Bund. E.
95. Sitharam, T. G., Sireeesh, S. (2005) “Behavior of embedded footings supported on geogrid cell reinforced foundation beds”, Geotechnical Testing Journal, ASTM, 28(5), 1-12.
96. Sladen, J. A., D’Hollander, R. D., and Krahn, J. (1985) “The liquefaction of sands, a collapse surface approach”, *Can. Geotech. J.*, 22, 564– 578.

97. Tatsuoka, F., Iwasaki, T., Tokida, K., Yasuda, S., Hirose, M., Imai, T., and Kon-No, M. (1980). "Standard Penetration Tests And Soil Liquefaction Potential Evaluation", *Soils and Foundations*, JSSMFE, Vol. 20, No. 4, 95-111.
98. Teng, W.C. (1962) "Foundation Design", Willey, New York.
99. Terzaghi, K. (1943) "Theoretical soil mechanics", Wiley, New York.
100. Terzaghi, K. (1956) "Varieties of submarine slope failure", Procs., 8th Texas Conf. on soil Mech. And Found. Engrg., Tokyo, 26(3), 23-41.
101. Terzaghi, K., and Peck R.B. (1948) "Soil mechanics in engineering practice", Willey, New York.
102. Thevanayagam, S. (1998) ''Effect of fines and confining stress on undrained shear strength of silty sands.'' *J. Geotech. Geoenviron. Eng.*, 124(6), 479–491.
103. Thevanayagam, S., and Nesarajah, S. (1998) "Fractal model for flow through saturated soils", Journal of Geotech. and Geoenvir. Engrg., ASCE, 124(1), 53-66.
104. Thevanayagam, S., Ravishankar, K., and Mohan, S. (1996a) "Steady state strength, relative density and fines content relationship for sands", Trans. Res. Record, 1547, 61-67.
105. Thevanyagam, S., Wang, C. C., and Ravishankar, K. (1996b) "Determination post liquefaction strength of sands: Steady state versus residual strength", Geotech. Spec. Publ., ASCE, 58(2), 1210-1224.
106. Tokimatsu, K., and Yoshimi, Y. (1983) "Empirical Correlation Of Soil Liquefaction Based On SPT N-Value And Fines Content", *Soils and Foundations*, JSSMFE, Vol. 23, No. 4, 56-74.
107. Trivedi A., and Arora V.K. (2007). "Discussion of bearing capacity of shallow foundations in anisotropic non-Hoek–Brown rock masses". J Geotech Geoenv Eng., ASCE, 133(2):238-240.
108. Trivedi, A. (2010) "Strength and dilatancy of jointed rocks with granular fill." Acta Geotechnica, 5(1), 15-31.
109. Trivedi, A., and Sud, V. K. (2002) "Grain characteristics and engineering properties of coal ash", Granular Matter, 4 (3), 93-101.
110. Trivedi, A., and Sud, V.K., (2005) "Ultimate bearing capacity of footings on coal ash", Granular Matter, 7 (4), 203-212.

111. Tronsco, J.H., and Verdugo, R., (1985) “Silt Content And Dynamic Behavior of Tailing Sands”, *Proceedings. Twelfth International Conference on Soil Mech. and Found. Eng.,* San Francisco, USA, 1311-1314.
112. Tyagi, S (2007) Bearing Capacity of Skirted Circular Footings on Sand, ME Thesis, Civil Engineering, University of Delhi.
113. Vaid, V. P. (1994) “Liquefaction of silty soils”, *Ground failures under seismic conditions, Geotech. Spec. Publ. No. 44*, ASCE, New York, 1–16.
114. Verdugo, R., and Ishihara, K. (1996) ‘‘The steady state of sandy soils.’’ *Soils Found.,* 36(2), 81–91.
115. Vesic, A. S. (1973) “Analysis of loads of shallow foundations.” J. Soil Mech. Found. Div., ASCE, 99 (1), 45-73.
116. Watson, P.G. and Randolph, M.F. (1998) “ Skirted foundation in calcareous soil, Geotechnical Engineering Journal, Proceedings of the Institute of Civil Engineering, 131, 171-179.
117. Yamaguchi, H., Kimura, T., and Fujii, N. (1976) ‘‘On the influence of progressive failure on the bearing capacity of shallow foundation in dense sand’’, *Soil and Found.,* Tokyo, 16(4), 11–22.
118. Yamaguchi, H., Kimura, T., and Fujii, N. (1977) ‘‘On the scale effect of footings in dense sand’’, *Proc., 9th Int. Conf. on Soil Mech. and Found. Engrg.*, Vol. 1, 795–798.
119. Yamamuro, J. A., and Covert, K. M. (2001) ‘‘Monotonic and cyclic liquefaction of very loose sands with high silt content.’’ *J. Geotech. Geoenviron. Eng.,* 127(4), 314–324.
120. Yamamuro, J. A., and Lade, P. V. (1997) ‘‘Static liquefaction of very loose sands.’’ *Can. Geotech. J.*, 34, 905–917.
121. Yamamuro, J. A., and Lade, P. V. (1999) ‘‘Experiments and modeling of silty sands susceptible to static liquefaction.’’ *Mech. Cohesive-Frict. Mater.,* 4, 545–564.
122. Yamamuro, J. A., and Lade, P.V. (1997b) “Static liquefaction of very loose sands”, Canadian Geotechnical Journal, 34(6), 905-917.
123. Yamamuro, J.A., and Lade, P.V. (1998) “Steady state concepts and static liquefaction of silty sands”. Journal of Geotech. Geoenviron. Engg., ASCE 124(9), 868-877.

124. Yasuda, S., Wakamatsu, K., Nagase, H., (1994). “Liquefaction of Artificially Filled Silty Sands” Ground Failures Under Seismic Conditions, Geotechnical Special Publication No. 44, ASCE, pp. 91-104.
125. Youd, T. L., and Bennett, M. J. (1983) ‘‘Liquefaction sites, Imperial Valley, California’’, *J. Geotech. Engrg.*, ASCE, 109(3), 440–457.
126. Yun, G.J. and Bransby, M.F. (2003) “Centrifuge Modeling of the Horizontal Capacity of Skirted Foundations on Drained Loose Sand,” Proc. International Conference on Foundations, Dundee, Scotland, 1-10.
127. Zadroga, B. (1994) “Bearing capacity of shallow foundations on non-cohesive soils”, J. Geotech. Engg. ASCE, 120(11), 1991-2008.
128. Zlatovic, S., and Ishihara, K. (1995) “On the influence of nonplastic fines on residual strength”, Proc. IS-TOKYO 95, Ist Int. Conf. on Earthquake Geotech. Engrg., A.A. Balkema, Rotterdam, The Netherlands, 239-244
129. Zlatovic, S., and Ishihara, K. (1997) “Normalized behavior of very loose nonplastic soil: Effects of fabric”, *Soils and Found.*, Tokyo, 37(4), 47–56.